



— BUREAU OF —  
RECLAMATION

Long-Term Operation – Initial Alternatives

# **Appendix I – Old and Middle River Flow Management**

Central Valley Project, California

Interior Region 10 – California-Great Basin

## **Mission Statements**

The U.S. Department of the Interior protects and manages the Nation's natural resources and cultural heritage; provides scientific and other information about those resources; honors its trust responsibilities or special commitments to American Indians, Alaska Natives, and affiliated Island Communities.

The mission of the Bureau of Reclamation is to manage, develop, and protect water and related resources in an environmentally and economically sound manner in the interest of the American public.

Long-Term Operation – Initial Alternatives

# **Appendix I – Old and Middle River Flow Management**

Central Valley Project, California

Interior Region 10 – California-Great Basin

Page Intentionally Left Blank



# Contents

	Page
1. Introduction .....	1
2. Performance Metrics.....	3
2.3 Fish Performance Metrics .....	3
2.4 Water Supply .....	3
2.5 NEPA Resource Areas .....	4
3. Methods .....	5
3.3 Datasets .....	5
3.3.1 Salvage Facilities Fish Data.....	5
3.3.2 In-Delta Fish Monitoring Datasets.....	6
3.4 Literature .....	6
3.4.1 Winter-Run and Spring-Run Chinook Salmon .....	6
3.4.2 Delta Smelt.....	8
3.4.3 Steelhead .....	8
3.4.4 Green Sturgeon .....	10
3.5 Models.....	11
3.5.1 Hydrodynamic Models.....	11
3.5.2 Fish Behavioral Models .....	13
4. Lines of Evidence .....	21
4.3 Common Components.....	21
4.3.1 First Flush .....	21
4.3.2 Turbidity Bridge.....	22
4.4 Historical, Presence-Based, and Model-Based OMR On-Ramp Analysis.....	22
4.4.1 Calendar-Based .....	22
4.4.2 Presence-based.....	22
4.4.3 Model-Based .....	24
4.5 Hydrological Footprint, Zone of Influence, Fate Mapping Analyses .....	25
4.6 Expanded Loss Autocorrelation Analysis .....	25
4.7 Historical, Environmental Surrogate, and Calendar-Based OMR Offramp Analysis....	28
4.7.1 Real-Time .....	29
4.7.2 Temperatures.....	29

4.7.3	Calendar .....	30
5.	Conclusions .....	31
6.	References .....	33
I.1.	Attachment 1: Delta Particle Tracking Modeling under Varying OMR Conditions.....	35
I.2.	Attachment 2: Zone of Influence Analysis.....	81
I.3.	Attachment 3: OMR Flow Management CalSim Analysis .....	185
I.4.	Attachment 4: Delta Passage Model: A Simulation Model of Chinook Salmon Survival, Routing, and Travel Time in the Sacramento–San Joaquin Delta. ....	215

# 1. Introduction

This appendix to the Initial Alternatives Report analyses options for the management of exports for Old and Middle River reverse flows to reduce entrainment stressors on winter-run and spring-run Chinook salmon, steelhead, and Delta smelt.

Export operations at the C.W. Bill Jones Pumping Plant and Harvey O. Banks Pumping Plant are anticipated to entrain fish into the central and south Delta. The CVP operates the Tracy Fish Collection Facility and the SWP operates the Skinner Delta Fish Protection Facility (collectively “Salvage Facilities”) to monitor entrainment and salvage fish before they reach the pumps. The effectiveness of capturing and the survival of fish through salvage (salvage efficiency) can be high for salmonids, but very low or zero for smelt. Net flows in Old and Middle Rivers provide a surrogate for how exports influence hydrodynamics in the Delta. Negative flow rates indicate a net direction towards export facilities, and positive flow rates indicate a net direction towards exiting the Delta past Chippis Island. The management of exports for Old and Middle Rivers reverse flows, in combination with other environmental variables, can minimize or avoid adverse effects to the migration of fish and reduce or avoid entrainment at the export facilities.

The flow in Old and Middle Rivers is tidally influenced, reversing twice a day with a 14-day periodicity. An index equation allows for shorter-term operational planning and real-time adjustments; therefore, a 14-day averaged Old and Middle River index [DWR 2017] hereafter referred to as “OMR”, will be used for operations. When operating to OMR criteria, Reclamation and DWR will make changes within 3 days. A 3-day response time allows for efficient power scheduling.

Reclamation’s management questions for the formulation of an alternative include:

- Should the onset of OMR management be based on real-time conditions, or does a fixed schedule based on the historical migration timing protect species with limited impacts on water supply?
- How does the magnitude of different OMR restrictions change the relative risk of species entrainment at the export facilities and in the central and/or south Delta?
- How does the duration of temporary OMR restrictions change the entrainment of species within the influence of export facilities?
- Does an offramp of OMR management based on real-time conditions protect species and improve water supply performance, or does a fixed schedule protect species with limited impacts on water supply?
- What is the effect of different levels of near- and far-field entrainment on population viability?

Old and Middle River flows, survival, and other factors depend, in part, on actions by other parties, including the State Water Board, in-Delta diverters, flood projects, and non-project upstream releases. Initial alternatives describe how Reclamation and DWR may operate for reducing entrainment in response to potential decisions by these other parties.

## 2. Performance Metrics

Performance metrics describe criteria that can be measured, estimated, or calculated relevant to informing trade-offs for alternative management actions.

### 2.1 Fish Performance Metrics

- Salmonids: Winter-run and Spring-run Chinook salmon, Steelhead
  - Routing probability into Delta Cross Channel, Georgiana Slough, Sutter/Steamboat Slough, Head of Old River, Sacramento and San Joaquin Rivers.
  - Survival probability to Chipps Island.
  - Estimated seasonal loss
  - Estimated first entrainment date (useful for on-ramping to OMR)
  - Zone of entrainment.
  - Population growth or cohort replacement rate.
- Delta smelt
  - Estimated seasonal loss.
  - Population growth ( $\lambda$ ).
  - Survival probability to the next life stage.

### 2.2 Water Supply

- South of Delta agricultural deliveries (average and critical/dry years).
- San Joaquin River Exchange and Settlement Contracts and CVPIA Refuge deliveries.
- Frequency of when OMR is controlling exports.

## **2.3 NEPA Resource Areas**

Considerations under the National Environmental Policy Act will include changes in multiple resource areas. Key resources are anticipated to include surface water supply, water quality, groundwater resources, power, aquatic resources, terrestrial biological resources, regional economics, land use and agricultural resources, recreation, cultural resources, socioeconomics, environmental justice, and climate change.

## 3. Methods

Reclamation solicited input for the knowledge base paper *Old and Middle River Reverse Flow Management – Smelt, Chinook Salmon, and Steelhead Migration and Survival*, which is included as Attachment I. Knowledge base papers compile potential datasets, literature, and models for analyzing potential effects from the operation of the CVP and SWP on species, water supply, and power generation. From the knowledge base papers, Reclamation and DWR organized the best available information for evaluating the impacts of OMR management as described below:

### 3.1 Datasets

#### 3.1.1 Salvage Facilities Fish Data

Salvage facilities are located upstream of the pumping plants and use a series of louvers or screens to capture entrained fish from the pumped water. Fish captured in this way are deemed to have been salvaged as they are eventually trucked and released back into the more downstream portion of the Sacramento–San Joaquin Delta (Delta). A subsample of fish is taken, counted, and measured over a given period—typically a 30-minute subsample over a two-hour collection period—to estimate the total number of fish “salvaged.” Because only a fraction of fish that enter the south Delta within the zone of influence of the pumping plants are actually “salvaged,” fish losses due to pumping are estimated by applying various multipliers to the salvage estimates. Salvage data are managed by Reclamation, DWR, and CDFW, and can be found at the CDFW website (<https://wildlife.ca.gov/Conservation/Delta/Salvage-Monitoring>) or through SacPAS (<https://www.cbr.washington.edu/sacramento/>). Note that races of Chinook salmon (*Oncorhynchus tshawytscha*) are identified in the database based on length-at-date (LAD) criteria (Fisher 1992) that are known to be inaccurate under many situations.

Meanwhile, larval Delta smelt (*Hypomesus transpacificus*) can often be difficult to identify due to the presence of other morphologically similar osmerids in the system: longfin smelt (*Spirinchus thaleichthys*) and wakasagi (*Hypomesus nipponensis*). Work has been done over the years to conduct genetic analysis on fish collected at the salvage facilities to confirm race and/or species identification. A list of relevant datasets can be found below:

- Data from the fish salvage facilities (Tracy Fish Collection Facility for the Central Valley Project and the Skinner Fish Facility for the State Water Project). See:
  - Genetic run assignment data for Chinook salmon caught at salvage facilities and surveys have been collected over the past few decades. A subsample of the data can be found below:
    - <https://portal.edirepository.org/nis/mapbrowse?packageid=edi.1053.1>
    - <https://portal.edirepository.org/nis/mapbrowse?packageid=edi.1054.1>
    - <https://portal.edirepository.org/nis/mapbrowse?packageid=edi.1055.1>

- <https://portal.edirepository.org/nis/mapbrowse?packageid=edi.1056.1>
- <https://portal.edirepository.org/nis/mapbrowse?packageid=edi.1049.2>

### 3.1.2 In-Delta Fish Monitoring Datasets

- U.S. Fish and Wildlife Service Delta Juvenile Fish Monitoring Program. Monitors juvenile salmonids in the Delta as well as the lower Sacramento and San Joaquin Rivers. Includes Sacramento Trawl, Chipps Island Trawl, Mossdale Trawl, and beach seine survey. Available on SacPAS and Environmental Data Initiative. See: <https://www.fws.gov/project/delta-juvenile-fish-monitoring-program>.
- U.S. Fish and Wildlife Service Enhanced Delta Smelt Monitoring Program. Monitors all life stages of Delta smelt year-round throughout the species' range. See: <https://www.fws.gov/project/enhanced-delta-smelt-monitoring-program>.
- California Department of Fish and Wildlife Spring Kodiak Trawl survey. Monitors adult Delta smelt during springtime. Available from: <https://wildlife.ca.gov/Conservation/Delta/Spring-Kodiak-Trawl>.
- California Department of Fish and Wildlife 20-mm Survey. Surveys larval and early juvenile Delta smelt during late spring to early summer. Available from: <https://www.dfg.ca.gov/delta/projects.asp?ProjectID=20mm>.
- CalFishTrack: Central Valley Enhanced Acoustic Tagging Project. Riverine and Delta survival by reach and to Chipps Island, route entrainment, and salvage of acoustically tagged juvenile salmonid from numerous release groups originating on the Sacramento and San Joaquin Rivers. Results are available for each group and seasonally here: <https://oceanview.pfeg.noaa.gov/CalFishTrack/index.html>. Raw acoustic receiver data, receiver deployment, and tag group data is stored on ERDDAP at [ERDDAP - Home Page \(noaa.gov\)](#).
- Long-term acoustic telemetry data for Green sturgeon in the Delta are available at: [cftc.metro.ucdavis.edu/biotelemetry-autonomous-real-time-database/landingmap](https://cftc.metro.ucdavis.edu/biotelemetry-autonomous-real-time-database/landingmap).

## 3.2 Literature

### 3.2.1 Winter-Run and Spring-Run Chinook Salmon

Windell et al. (2017) developed conceptual model framework for the various life stages of winter-run Chinook salmon. Although specific for winter-run Chinook salmon, Windell et al.'s (2017) Bay-Delta conceptual model can also be applied for spring-run Chinook salmon, as the environmental drivers and habitat attributes present in the Bay-Delta affect both runs in a similar manner. Delta operation of the CVP and SWP can potentially influence both the route juvenile Chinook salmon may follow and the conditions for growth and survival that juvenile Chinook salmon may experience along different routes. Central Valley Chinook salmon use the Delta as a migratory pathway between their natal tributaries and the Pacific Ocean (Moyle 2002; Williams 2006). Depending on conditions, these



juvenile Chinook salmon can also use the Delta as rearing habitat in some years. Studies have shown that juvenile outmigrants from the Sacramento River experience lower survival when they route through the central and south Delta instead of remaining in the mainstem Sacramento River, which is hypothesized to be linked to CVP and SWP diversion rates. The reversed tidal flows in the central and south Delta due to the pumping facilities is hypothesized to slow outmigration for juvenile Chinook salmon towards the ocean, which may reduce survival due to the unfavorable Delta habitat conditions (high densities of predators, lower density of food, and suboptimal water quality). In addition, it is hypothesized juvenile Chinook salmon may experience a diminished ability to navigate out of the south Delta due to confusing navigational cues from altered hydrology and water quality gradients, the highly altered channel network configuration, and impairments to sensory systems from contaminants (Windell et al. 2017). A general negative correlation between water exports and survival probabilities have been demonstrated (and often assumed) (Newman and Brandes 2010).

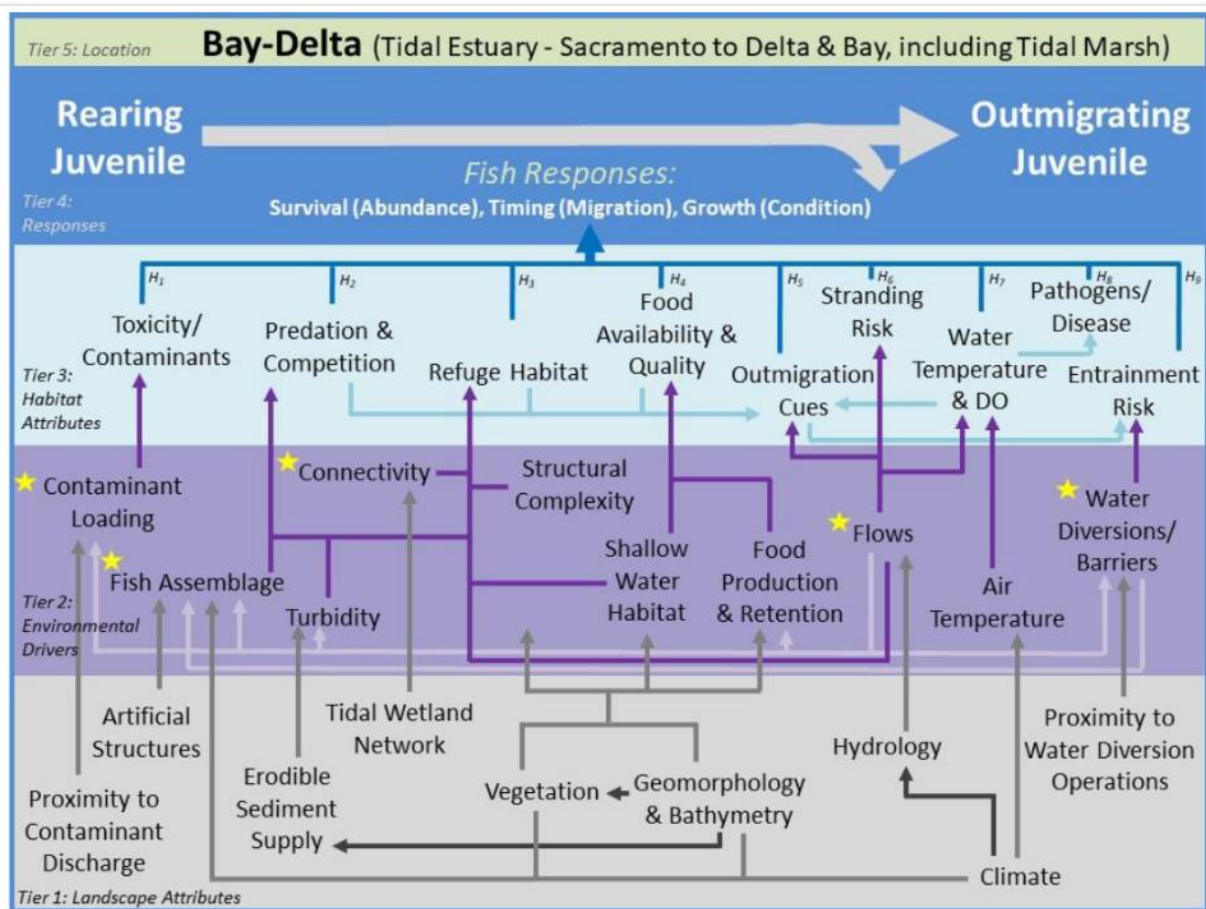


Figure 1. Conceptual Model of Juvenile Chinook Salmon in the Bay-Delta from Windell et al. (2017)

### 3.2.2 Delta Smelt

The operation of the CVP and SWP pumping plants can potentially entrain Delta smelt in all post-hatch life stages. Upon hatching, Delta smelt begin a pelagic larval life stage and are distributed primarily by water current direction due to minimal swimming ability. Flows due to the operations of the CVP and SWP may entrain these early life stages. Delta smelt become more proficient at swimming at approximately 20 mm (IEP MAST 2015) and are assumed to seek out suitable habitat with turbid water ( $>12$  FNU), suitable water temperatures ( $< 25^{\circ}\text{C}$ ), and low salinity ( $< 6$  psu). The subadult Delta smelt rear until the fall when flows and turbidity from seasonal rains would initiate a migration to the low salinity zone ( $<0.2$  ppt) where they stage until moving upstream into freshwater to spawn. The increases in flows and turbidity that initiate migration may increase the likelihood of entraining adults if they migrate into the central and south Delta toward the CVP and SWP pumping plants. After the initial migration, Delta smelt are hypothesized to remain in areas of high turbidity, and CVP and SWP operations are adjusted to minimize turbidity in the south Delta. Delta smelt adults typically do not live long after spawning and two-year-old adults are rare.

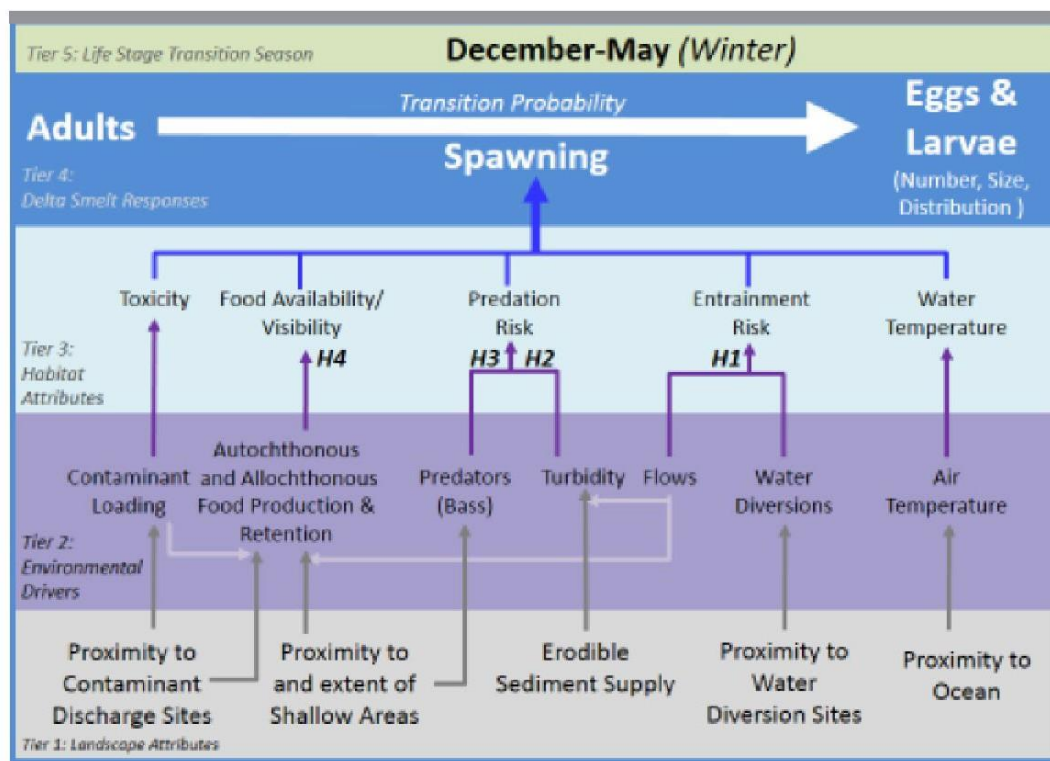


Figure 2. Conceptual Model of Delta Smelt in the Delta (Baxter et al. 2015)

### 3.2.3 Steelhead

Steelhead, or *Oncorhynchus mykiss* expressing anadromous life history, pass through the Delta as they outmigrate towards the Pacific Ocean. However, unlike Chinook salmon, the age at which steelhead conduct their outmigration may vary by multiple years. Steelhead are also iteroparous and can pass through the Delta more than twice (juvenile outmigration and return as adults) within their lifetime (Moyle 2002). Upon reaching the Delta, there are many pathways

that steelhead may take to reach the Pacific Ocean. The flows in the Delta are influenced by the complex set of water management regulations for water quality, across the Central Valley via reservoir releases and pumping in the Delta, except during large rain events. The process of pumping water from the Delta influences outmigration route selection by disrupting the natural flow of water from the San Joaquin River to the ocean (Beakes et al. 2022). These changes in flows can attract fish entering the Delta out of the San Joaquin River (with low-moderate survival) into the interior Delta (with extremely low survival) and pumping facilities (with low-moderate survival; Buchanan et al. 2021). Thus, changes in the flow regime due to water management can have large impacts on route selection and ultimately survival (Figure 3).

Additionally, the duration of the migration, and therefore timing of ocean entry, are also likely impacted by water management in the Delta through changes in the flow patterns and route selection of outmigrating juveniles. Assuming *O. mykiss* smolts travel time in the Delta is comparable to juvenile Chinook salmon, we would expect a rapid migration during periods of high flow entering the Delta and low pumping (i.e., low import/export ratio where most water is exiting the Delta via the Carquinez Strait). Oppositely, under low flow conditions and higher rates of pumping (i.e., high import/export ratio where a large fraction of water is getting pumped out of the Delta), we would expect slower outmigration for *O. mykiss* smolts.

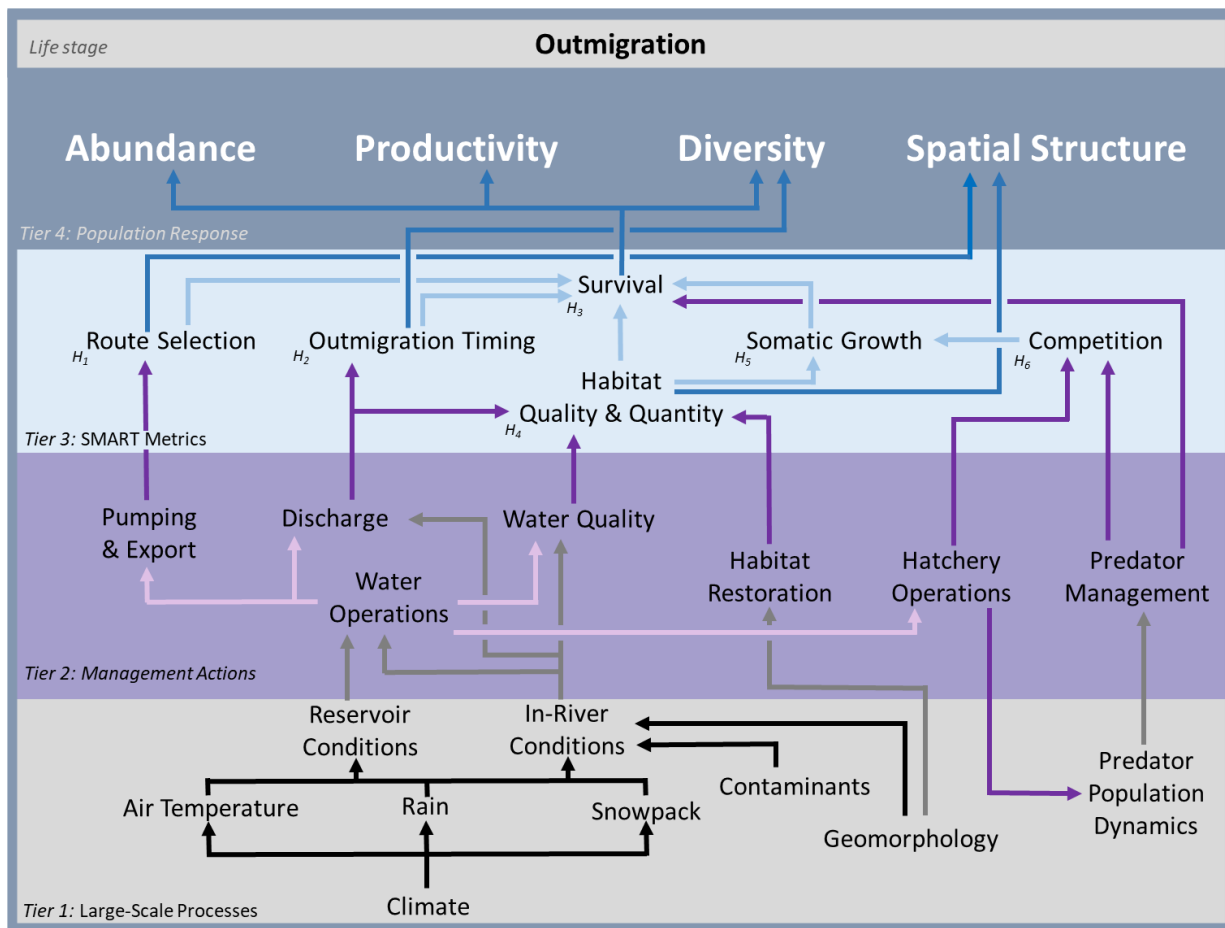


Figure 3. Steelhead Smolt Outmigration Conceptual Model Linking Large-Scale Processes to Management Actions, SMART Metrics, and Desired Population Responses (i.e., VSP criteria) from Beakes et al. (2022).

### 3.2.4 Green Sturgeon

Green sturgeon (*Acipenser medirostris*) is an anadromous species, spawning in the upper Sacramento River from January through November. Juveniles outmigrate from the Sacramento River to the Delta through San Francisco Bay starting in late August; however, juveniles are present in the central Delta in all months, except January (Miller et al. 2020). Subadults are in the Delta and San Francisco Bay in all months, with greater presence from April through October (Miller et al. 2020; Colborne et al. 2022).

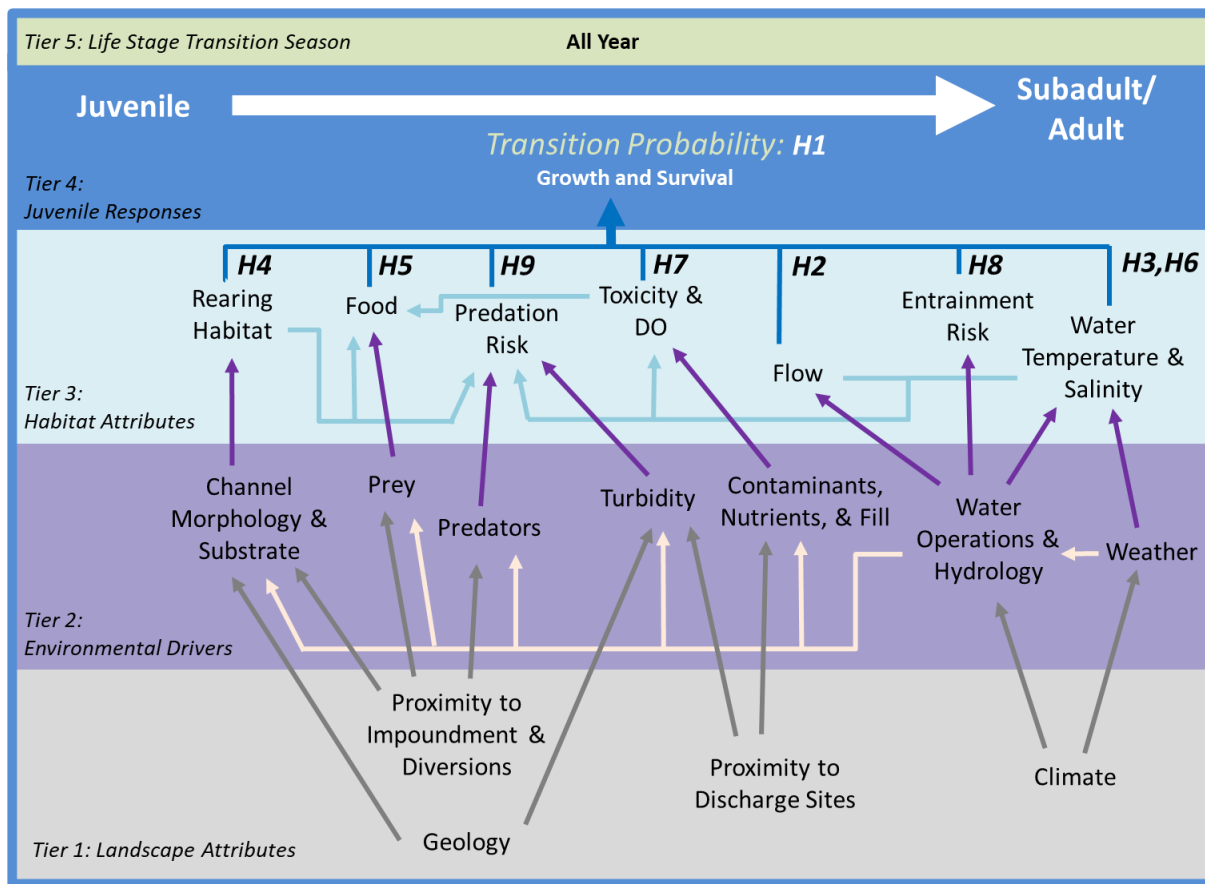


Figure 4. Conceptual Model of Green Sturgeon Juvenile to Subadult Transition in the Delta.

### 3.3 Models

#### 3.3.1 Hydrodynamic Models

DSM2 is a one-dimensional hydrodynamic and water quality simulation model for the Sacramento / San Joaquin Delta, developed by DWR. The state and federal agencies, through the Salmon Monitoring Team (SaMT), model impacts of OMR scenarios associated with changes in operations of the Delta projects on behavior of sheltering, migrating, foraging, and rearing salmonids. DSM2 can simulate flows, velocities, and stage, and these data can be used to compare differences in flow conditions reflecting distinct inputs (i.e., no exports, specific inflows), which allows for visualizing the zone of influence of different releases and diversions in Delta regions. Reclamation conducted a DSM2 scenario sensitivity exercise. This was a collaboration between Reclamation and DWR's operations modeling teams to determine what difference in OMR flows resulted in differences in distribution of velocities and flow. Kolmogorov-Smirnov test (KS) statistic results demonstrated that if the difference in modeled OMR scenarios is less than 500 cfs (possibly even less than 1,000 cfs), then a comparison of DSM2 model runs outputs are not different. This finding is likely due to the dominant control of velocity, flow, and stage due to tides.

### **3.3.1.1 Zone of Influence**

See Attachment 1

### **3.3.1.2 Particle Tracking**

The Particle Tracking Model (PTM) is a component of the DSM2 to simulate the particle movement throughout the Bay-Delta network. The PTM model uses the hydrodynamics calculated from DSM2-HYDRO model and extrapolates the 1D average velocity in a channel to a pseudo 3D velocity with assumed certain cross-sectional velocity profiles. The velocity profiles assume faster velocity at channel center and slower velocity near the channel bank and bottom. Field data are used to guide the selection of the velocity profiles and to calibrate the PTM.

Currently, two applications are commonly used with PTM. One is to estimate the particle residence time. When a certain number of particles (e.g., 1000) are inserted at a certain location, the time for 25%, 50%, and 75% of the particles to exit the system is estimated. The other is to estimate particle traces. When certain number of particles are inserted at a certain location, how many are exported at certain locations after a period. For example, the percentage of particles released at Vernalis of the San Joaquin River and diverted into the SWP and CVP after 90 days can be used to represent the likelihood of fish entrainment.

Applications are available at: <https://water.ca.gov/Library/Modeling-and-Analysis/Bay-Delta-Region-models-and-tools/Delta-Simulation-Model-II>.

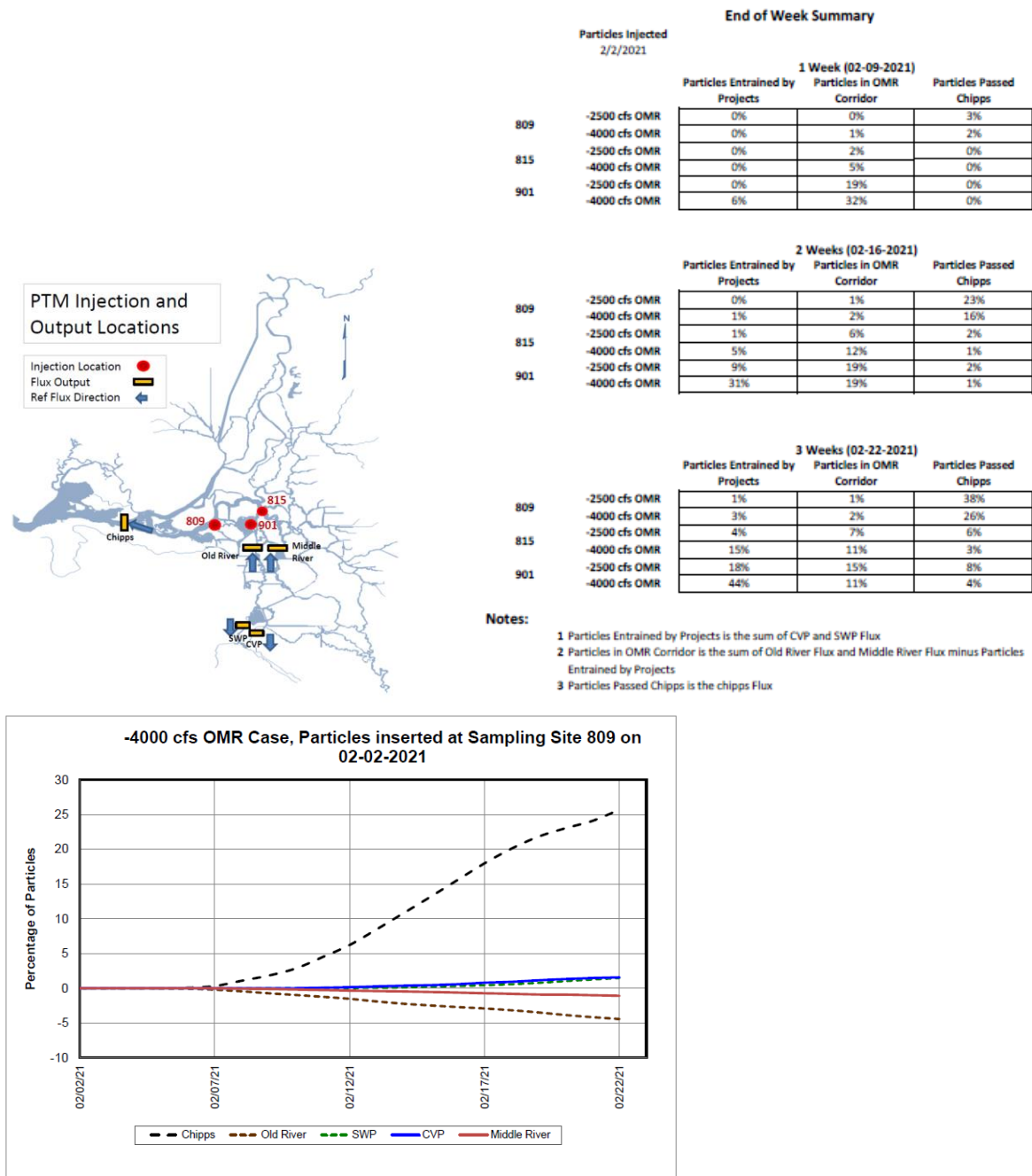


Figure 5. Example Images of PTM output.

### 3.3.2 Fish Behavioral Models

#### 3.3.2.1 Salmonids

##### STARS Model

The STARS model (Survival, Travel time, and Routing Simulation) is an individual-based simulation that predicts fish parameters (survival, travel time, entrainment) of juvenile salmonids



migrating through the Delta. The fish parameters are related to movement of individual acoustically tagged late-fall and winter-run Chinook salmon connected to daily data (DCC gate status and Sacramento River flow at Freeport). Results are for individuals in cohorts, or fish who enter the model's "system" daily at Freeport. The use of the STARS model can inform the migrating behavior of juvenile salmonids and route and total survival in the Delta. It is constructed to understand the space outside the interior Delta, but interpolation could be used to identify possible behavior of fish once they take a specific route away from the Sacramento River (i.e., Delta Cross Channel or Georgiana Slough). STARS provides overall survival and travel time, route-specific survival and travel time, and proportion of fish on a daily timestep that would use individual migration pathways or routes. An application of the STAR models run in real time: <https://oceanview.pfeg.noaa.gov/shiny/FED/CalFishTrack/>. The code and supporting document are available from USGS (Russ Perry, USGS, Personal Communication).

The STARS model can be applied to assess the performance metric of routing probability for winter-run Chinook salmon and possibly also spring-run Chinook salmon.

### **Delta Passage Model**

The Delta Passage Model (DPM) is a simulation model of Chinook salmon survival, routing, and travel time in the Sacramento–San Joaquin Delta, developed by Cramer Fish Sciences. The DPM simulates migration of Chinook salmon smolts entering the Delta from the Sacramento River at Fremont Weir and estimates survival to Chipps Island. The DPM uses available time-series data and values taken from empirical studies or other sources to parameterize model relationships and inform uncertainty.

The DPM model can be used to assess the Survival to Chipps Island performance metrics for winter-run or spring-run Chinook salmon.

### **Winter-Run Chinook Salmon Life Cycle Model (WRLCM)**

The Winter-Run Chinook Salmon Life Cycle Model (WRLCM) is a spatially and temporally explicit stage-structured simulation model that estimates the number of winter-run Chinook salmon at each geographic area and timestep for all stages of their lifecycle. The first version of the WRLCM was developed in 2014. In 2015, the WRLCM underwent a model review by the Center for Independent Experts, which contributed to improvements in more recent versions of the model. See: <https://oceanview.pfeg.noaa.gov/wrlcm/intro>.

The WRLCM has been used by NMFS to evaluate the Survival Probability to Chipps Island and cohort replacement performance metrics for winter-run Chinook salmon. However, the WRLCM model is not available for Reclamation's use; therefore, the WRLCM cannot inform the initial alternative analyses.

### **Oncorhynchus Bayesian Analysis (OBAN)**

The winter-run Chinook salmon Oncorhynchus Bayesian Analysis (OBAN) model has been developed from the conceptual life cycle model of winter-run Chinook salmon and coded into Windows-based software with graphic output capability. The Bayesian estimation of model coefficients was coded into WinBUGS. The software finds a statistical "best fit" to empirical trends by matching model predictions to empirically observed juvenile and adult abundances. The model is capable of fitting any number of abundance data sources and estimating any



number of coefficient values to find the best statistical prediction. This model code is not available for Reclamation's use, so it does not inform the initial alternative analyses.

### **ECO-PTM**

The ecological particle tracking model (ECO-PTM) was developed by DWR. Currently built upon data from acoustically tagged late fall-run Chinook salmon (2006 – 2014), the ECO-PTM estimates routing through Georgiana Slough, Delta Cross Channel route, the Sutter / Steamboat slough complex, or remaining in the Sacramento River. Development of the model is still ongoing and currently focused on the south Delta. This model was recently used in evaluating the biological effects of the spring 2022 Temporary Urgency Change Petition (TUCP), and code is available from DWR at DSM2 v8.2.1 - DSM2 v8.2.1 - California Natural Resources Agency Open Data.

ECO-PTM can be used to evaluate the seasonal loss and zone of entrainment performance metrics for winter-run and spring-run Chinook salmon. This model can incorporate CalSim or DSM2 data as model input. Development of this model is in progress.

### **ePTM**

The enhanced particle tracking model (ePTM) was developed as joint collaboration between the University of California, Santa Cruz and National Marine Fisheries Service's Southwest Fisheries Science Center. It is a data-driven model of juvenile salmonid migration through the Delta built off of behavioral fish decisions based on local environmental variables. The model uses acoustically tagged late fall-run Chinook salmon data with plans to use fall-run Chinook salmon in the future. It is currently still in development but has a downloadable, working version at GitHub: The Enhanced Particle Tracking Model Version 2.0 ([https://github.com/cvclcm/ePTM\\_v2](https://github.com/cvclcm/ePTM_v2)). Attempts to use the model were limited by insufficient calibration/validation documentation and DSM2 versioning, thus it does not inform the initial alternative analyses.

### **Winter-run Chinook Salmon Salvage Machine-Learning Tool**

A new model to predict winter-run Chinook salmon occurrence at the salvage facilities is currently being developed by Jeremy Gaeta (IEP CDFW), Trinh Nguyen (IEP CDFW), and Brian Mahardja (Reclamation). This model (hereinafter, Gaeta et al.'s model) takes a machine learning approach (extreme gradient boosting dropout multiple additive regression trees) to predict winter-run Chinook salmon salvage as a function of various potential environmental drivers. Whereas previously developed machine learning salvage prediction tool (Tillotson et al. 2022) can estimate the number of winter-run Chinook salmon with high accuracy after salvage has occurred, Gaeta et al.'s model is designed to predict winter-run Chinook salmon occurrence prior to any salvage (one-week and three-week ahead models are currently being refined) and, thus, may be useful for on-ramping of OMR management season (Section 4.2).

Gaeta et al.'s model can be used to evaluate the seasonal loss and first entrainment date performance metrics for winter-run Chinook salmon. This model can incorporate daily flow data from the Sacramento and San Joaquin Rivers as well as export level values from the pumping facilities (combined).

## Negative Binomial Salvage Model

To evaluate potential changes to the number of LAD winter-run and spring-run Chinook salmon salvaged at the CVP and SWP pumping facilities based on the alternatives, Reclamation analyzed historical salvage data via negative binomial regression. Negative binomial regression requires estimation of a dispersion parameter rather than assuming the variance is equal to the mean. In doing so, negative binomial regression can account for overdispersion, which is common in ecological data (e.g., the salvage dataset), as well as reduce the likelihood of biased coefficient estimation.

### *Methods:*

Winter-run and spring-run LAD Chinook salmon salvage records from January 1, 1993, to December 31, 2020, were gathered from the CDFW salvage database posted at the SacPAS website ([http://www.cbr.washington.edu/sacramento/data/query\\_loss\\_detail.html](http://www.cbr.washington.edu/sacramento/data/query_loss_detail.html)). To incorporate hydrodynamic effects on salvage count into the models, Delta export (QEXPORT), Sacramento River flow (QSAC), and San Joaquin River (QSJR) were extracted from the California Department of Water Resources Dayflow data (<https://data.cnra.ca.gov/dataset/dayflow>). Additionally, combined Old and Middle River flow (OMR) data were pulled from the U.S. Geological Survey National Water Information System website (<https://nwis.waterdata.usgs.gov/nwis>; stations 11313405 and 11312676). Because data gaps exist in the OMR flow data, ordinary least squares regressions were conducted so that each dataset could be used to predict, and therefore fill, missing data in the other (adjusted  $R^2$ : 0.97). Lastly, to account for the variable numbers of juvenile Chinook salmon entering the Delta by year and month, Sacramento Trawl data were acquired from the Delta Juvenile Fish Monitoring Program through the “deltafish” package available on GitHub (<https://github.com/jeanetteclark/deltaFish>). Sacramento Trawl catch per unit trawl for each day was calculated for both winter-run-sized and spring-run-sized Chinook salmon.

For each variable, data were averaged by month and year with missing data removed. Because monthly salvage values tend to be low or mostly zeroes for most months out of the year, only December to April period was used for winter-run Chinook salmon analysis, and only March to June period was used for spring-run Chinook salmon analysis. Overdispersion was apparent during initial inspection of the response variable data (mean  $\neq$  variance) supporting the use of negative binomial regression in this analysis.

To avoid collinearity, variance inflation factor (VIF) analyses were conducted for all predictor variables mentioned above. A full negative binomial regression model with all predictor variables was constructed for each Chinook salmon race (winter-run and spring-run), followed by an assessment of VIF values. Per Zuur et al. (2010), the variable with the highest VIF value was removed and models were re-run until all VIF values were below 3. For both winter-run and spring-run Chinook salmon models, OMR had the highest VIF value ( $>25$ ) and had to be removed from further analysis along with Sacramento River flow. For the final model selection, the covariates included were San Joaquin River flow, Delta export flow value, Sacramento Trawl catch per unit effort (specific to each race), and monthly categorical variable. Each continuous covariate was standardized to z-score prior to the model selection process.

For both Chinook salmon races, the model selection process included all possible additive combination of covariates, as well as addition combination that involves at least one interaction between a continuous variable and the monthly categorical variable. This resulted in 26 possible models (including null) for each Chinook salmon race, and the top performing model was determined by Akaike Information Criterion for small sample size (AICc). The top model identified through this model selection process was then further evaluated by using leave-one-out cross validation (LOOCV). This was done to provide a measure for model predictive performance. LOOCV involves removal of a single record from the dataset, refitting the top model to the remaining data, estimating the expected salvage count for the ‘out-of-sample’ data, and comparing the predicted versus observed salvage count. This process is repeated for all records in the dataset. Ordinary least squares linear regression is used to compare the relationship between observed and predicted salvage counts, and the resulting  $R^2$  from this regression is a measure agreement between observed and predicted observations.

#### *Results:*

The top supported model for winter-run Chinook salmon salvage included an interaction between the month categorical variable and Sacramento Trawl catch per trawl, as well as export level and San Joaquin River flow (Table 1). The top-ranked winter-run Chinook salmon model was substantially more supported than the null model ( $\Delta\text{AICc} = 111.01$ ) and has the majority of the Akaike weight (0.74). For the winter-run Chinook salmon model, the correlation between observed and predicted data (log10 transformed) based on the LOOCV was positive but relatively weak (Adjusted  $R^2 = 0.49$ ). See Table 2 for model coefficients with z-scored covariates.

Table 1. Summary of the Top-Ranked Negative Binomial Regression Models for Winter-Run Chinook Salmon Salvage That Make Up ~0.99 of the Akaike Weight

Model	AICc	$\Delta\text{AICc}$	Akaike weight	Cumulative weight	Log-likelihood
Month*Sacramento Trawl Catch + Export + San Joaquin River Flow	710.08	0.00	0.74	0.74	-340.60
Month + San Joaquin River Flow + Sacramento Trawl Catch + Export	713.20	3.12	0.15	0.89	-346.91
Month*Sacramento Trawl Catch + Export	714.07	3.98	0.10	0.99	-343.81

AICc = Akaike Information Criterion;  $\Delta\text{AICc}$  = change in Akaike Information Criterion.

Table 2. Summary of Model Coefficients for Negative Binomial Monthly Winter-Run-Sized Chinook Salmon Salvage Model. Month Of January Was Used as the Reference Categorical Variable (i.e., intercept). Dispersion Parameter Was 1.38

Model variable	Estimated coefficient	Standard error
Intercept	0.27	0.27
Month – February	1.06	0.33
Month – March	2.25	0.34
Month – April	16.54	6.03
Month – December	-0.48	0.36
Sac Trawl CPUE	0.37	0.19
Export	1.03	0.12
San Joaquin Flow	-0.31	0.11
Month – February: Sac Trawl CPUE	0.18	0.28
Month – March: Sac Trawl CPUE	-0.88	0.34
Month – April: Sac Trawl CPUE	19.7	7.97
Month – December: Sac Trawl CPUE	0.01	0.26

The top supported model for spring-run Chinook salmon salvage included export level and an interaction between the month categorical variable and San Joaquin River flow (Table 2). The top-ranked spring-run Chinook salmon model was substantially more supported than the null model ( $\Delta AICc = 122.72$ ) and has the majority of the Akaike weight (0.77). For the spring-run Chinook salmon model, the correlation between observed and predicted data (log10 transformed) based on the LOOCV was higher than that for winter-run Chinook salmon (Adjusted  $R^2 = 0.60$ ). Collectively these results suggest the top-ranked models for both races of Chinook salmon provided reasonably fit to the observed data and have some predictive capability. See Table 4 for model coefficients with z-scored covariates.

Table 3. Summary of the Top-Ranked Negative Binomial Regression Models for Spring-Run Chinook Salmon Salvage That Make Up ~0.99 of the Akaike Weight

Model	AICc	$\Delta AICc$	Akaike weight	Cumulative weight	Log-likelihood
Month*San Joaquin River Flow + Export	1018.17	0.00	0.77	0.77	-498.00
Month*San Joaquin River Flow + Sacramento Trawl Catch + Export	1020.61	2.44	0.23	1.00	-497.98

Table 4. Summary of Model Coefficients for Negative Binomial Monthly Spring-Run-Sized Chinook Salmon Salvage Model. Month of March Was Used as the Reference Categorical Variable (i.e., intercept). Dispersion Parameter was 0.84.

Model variable	Estimated coefficient	Standard error
Intercept	2.78	0.24
Month – April	2.88	0.34
Month – May	1.99	0.37
Month - June	-2.71	0.39
San Joaquin Flow	1.31	0.21
Export	1.11	0.16
Month – April: San Joaquin Flow	-1.16	0.28
Month – May: San Joaquin Flow	-0.51	0.31
Month – June: San Joaquin Flow	0.66	0.43

### 3.3.2.2 *Delta Smelt*

#### **Delta Smelt IBM (2022 version)**

For Delta smelt, an Individual-Based Model has been developed by Rose et al. (2013a, 2013b) that was updated in 2022. This model simulates reproduction, movement, growth, and mortality of Delta smelt based on a combination of the approaches described by Rose et al. (2013a). It was calibrated to entrainment mortality, abundances, and growth rates estimated from the wild Delta smelt population between 1995 and 2015.

Delta Smelt IBM can be used to evaluate the population growth, entrainment mortality, and survival probability to the next life stage performance metrics for Delta smelt. This model can incorporate DSM2 flow data from the Sacramento and San Joaquin Rivers, as well as export level values from the pumping facilities (combined).

Page Intentionally Left Blank

## 4. Lines of Evidence

Reclamation's management questions for the formulation of an alternative include:

- Should the onset of OMR management be based on real-time conditions or does a fixed schedule based on the historical migration timing protect species with limited impacts on water supply?
- How does the magnitude of different OMR restrictions change the relative risk of species entrainment at the export facilities and into the central and/or south Delta?
- How does the duration of temporary OMR restrictions change the entrainment of species within the influence of export facilities?
- Does an offramp of OMR management based on real-time conditions protect species and improve water supply performance or does a fixed schedule protect species with limited impacts on water supply?
- What is the effect of different levels of near- and far-field entrainment on population viability?

### 4.1 Common Components

Some components of OMR flow management will be common across all alternatives. These common components pertain to Delta smelt and are described below. These components will function alongside alternative options for an integrated analysis across multiple species (Delta smelt and salmonids). Because these components can be subject to recommendations by the Smelt Monitoring Team, they can be highly dynamic in nature and interact in various unexpected ways with OMR flow management options for salmonids. As such, they will not be included in the initial alternative analysis despite their consideration as common components.

#### 4.1.1 First Flush

- Under the 2020 Record of Decision (ROD), Reclamation and DWR would reduce exports for 14 consecutive days so that the 14-day averaged OMR index for the period shall not be more negative than -2,000 cfs, in response to "First Flush" conditions in the Delta. First Flush conditions may be triggered between December 1 and January 31 and are defined by:
  - Running 3-day average of the daily flows at Freeport is greater than 25,000 cfs; and
  - Running 3-day average of the daily turbidity at Freeport is 50 Nephelometric turbidity units (NTU) or greater; or

- Real-time monitoring indicates a high risk of migration and dispersal into areas at high risk of future entrainment.
- Between water year 2010 to water year 2022, First Flush conditions were met in water years 2012, 2014, 2017, 2019, and 2022.

#### **4.1.2 Turbidity Bridge**

- Under the 2020 ROD, after a First Flush event described above or February 1 (whichever comes first), Reclamation and DWR would manage exports in such a way to maintain daily average turbidity in Old River at Bacon Island at a level of less than 12 NTU. The purpose of this action is to minimize the risk to adult Delta smelt in the Old and Middle River Corridor, where they are subject to higher entrainment risks. This action seeks to avoid the formation of a turbidity bridge from the San Joaquin River shipping channel to the south Delta fish facilities, which historically has been associated with elevated salvage of pre-spawning adult Delta smelt.

## **4.2 Historical, Presence-Based, and Model-Based OMR On-Ramp Analysis**

One variable component to consider regarding OMR flow management is when to initiate the OMR management season (when OMR flow is managed to be more positive than what would normally be operated for if fish species of concern were not an issue). The start dates evaluated here are mainly relevant for salmonids for reasons explained in sections above (Delta smelt components are common across all alternatives).

### **4.2.1 Calendar-Based**

Under the current ROD, OMR management at no more negative than -5,000 cfs is initiated if after January 1 more than 5% of any salmonid species are determined to be present in the Delta by the Salmon Monitoring Team. Unless preceded by a First Flush Action for Delta smelt, January 1 has typically been the start date for OMR management season. As such, the 2020 ROD has a combination of calendar-based and presence-based starting criteria for OMR management season. However, in practice, it has been primarily a fixed calendar-based start date of January 1. An option for evaluating initial alternatives is to use a fixed calendar (date-based) start for OMR management similar to the current ROD (i.e., January 1 as the start of OMR management at -5,000 cfs), an earlier date (e.g., December 1), or in combination with other on-ramping criteria as described below.

### **4.2.2 Presence-based**

Under the current ROD, OMR management at no more negative than -5,000 cfs is initiated after January 1 only if the SaMT has determined that more than five percent of any salmonid species are present in the Delta. Although the percentage of salmonid distribution as determined by the SaMT can be somewhat subjective, they often rely on real-time monitoring data. In lieu of forming a team of salmonid experts to determine start dates for OMR flow management season, historical data from commonly used salmonid surveys were used to identify dates when five% of



each species/race of interest are believed to have entered the Delta (Table 5). This was done by calculating the date at which five % of winter-run Chinook salmon total catch has been reached for the water year (as winter-run Chinook salmon is typically the taxon that initiates OMR management season for salmonids). Note that LAD criteria were used to define winter-run Chinook salmon (Fisher 1992). Water year type based on the Sacramento Valley and in water years when it occurred the date at which the turbidity and flow conditions were met to trigger Integrated Early Winter Pulse Protection are included.

Table 5. Historic Record for Surveys or Rotary Screw Traps Reaching 5% of the Annual Catch Index by Water Year

<b>Water Year</b>	<b>Sac. Valley Water Year Type</b>	<b>Knights Landing Rotary Screw Trap Catch Index</b>	<b>Sacramento River Beach Seine Catch Index</b>	<b>Sacramento River Trawl Catch Index</b>	<b>Total Salvage</b>	<b>Integrated Early Winter Pulse Protection</b>
2016	BN	9/16/2016	10/24/2016	3/14/2017	12/28/2015	NA
2017	W	9/28/2017	11/21/2017	1/13/2018	12/20/2016	1/10/2017
2020	D	9/30/2020	11/9/2020	2/8/2021	1/22/2020	NA
2019	W	10/1/2019	11/1/2019	12/12/2019	1/2/2019	1/11/2019
2021	C	10/28/2021	10/8/2021	10/27/2021	3/8/2021	12/17/2021
2011	W	11/30/2011	10/11/2011	1/27/2012	12/7/2010	NA
2007	D	1/6/2008	10/15/2007	1/7/2008	1/22/2007	NA
2009	D	10/21/2009	10/23/2009	10/23/2009	1/9/2009	NA
2010	BN	10/29/2010	11/18/2010	10/29/2010	1/30/2010	NA
2014	C	10/31/2014	11/20/2014	11/5/2014	3/5/2014	12/7/2014
2015	C	12/15/2015	12/16/2015	11/6/2015	12/24/2014	NA
2004	BN	12/1/2004	11/10/2004	11/10/2004	1/6/2004	NA
2005	AN	11/14/2005	11/14/2005	11/14/2005	1/6/2005	NA
2001	D	NA	11/23/2001	11/19/2001	2/2/2001	NA
2012	BN	11/24/2012	11/26/2012	11/23/2012	2/16/2012	1/25/2012
1998	W	NA	11/25/1998	11/23/1998	12/6/1997	NA
1997	W	NA	11/26/1997	11/25/1997	3/18/1997	NA
2018	BN	12/3/2018	12/4/2018	12/5/2018	3/1/2018	NA
2006	W	12/3/2006	12/11/2006	12/11/2006	12/23/2005	NA
2003	AN	12/8/2003	12/10/2003	12/10/2003	12/24/2002	NA
2002	D	NA	12/18/2002	12/16/2002	12/13/2001	NA
2013	D	2/12/2014	2/12/2014	2/12/2014	12/15/2012	12/2/2012
1999	W	NA	12/22/1999	1/18/2000	2/23/1999	NA
2008	C	12/31/2008	2/24/2009	12/22/2008	1/18/2008	NA
2000	AN	NA	1/13/2001	1/26/2001	1/26/2000	NA

### 4.2.3 Model-Based

Models with the ability to forecast salvage events of winter-run Chinook salmon have been produced (Tillotson et al. 2022), and more are being developed (see Gaeta et al.'s model). Because winter-run Chinook salmon is typically the species that initiates the OMR management season, these predictive models can be used to on-ramp the OMR management season. Complex machine learning models may be able to incorporate complex information and various interacting factors that determine the timing and number of winter-run Chinook salmon entering the Delta. For example, date of first model-predicted entrainment event or certain probability of salvage can be used to initiate the start of OMR management at -5,000 cfs OMR flow (or other thresholds).

Table 6. First Expected Detection for Water Years 2005-2020 Based on Gaeta et al.'s Model (first prediction of winter-run sized Chinook salmon presence at salvage for any model in the 30-model ensemble) and the Date at Which Prediction Was Made (one week earlier)

Water Year	First Actual Observation of Winter-Run-Sized Salmon at Salvage	First Predicted Presence for Any Model in the Ensemble (out of 30)	Date at which prediction was made (potential on-ramp date for OMR management based on historical data)
2005	1/2/2005	12/31/2004	12/24/2004
2006	12/12/2005	12/13/2005	12/6/2005
2007	12/18/2006	12/18/2006	12/11/2006
2008	1/11/2008	1/13/2008	1/6/2008
2009	12/30/2008	1/13/2009	1/6/2009
2010	12/8/2009	1/23/2010	1/16/2010
2011	12/3/2010	12/28/2010	12/21/2010
2012	1/25/2012	1/22/2012	1/15/2012
2013	12/4/2012	12/14/2012	12/7/2012
2014	3/3/2014	3/6/2014	2/27/2014
2015	12/24/2014	12/24/2014	12/17/2014
2016	12/28/2015	12/29/2015	12/22/2015
2017	12/20/2016	12/21/2016	12/14/2016
2018	2/5/2018	2/5/2018	1/29/2018
2019	12/29/2018	12/29/2018	12/22/2018
2020	1/20/2020	1/19/2020	1/12/2020

## 4.3 Hydrological Footprint, Zone of Influence, Fate Mapping Analyses

Another component of the OMR flow management season that can be evaluated is the magnitude of OMR flows that Reclamation and DWR operations would target. Under the 2020 ROD, from the onset of OMR management to the end, Reclamation and DWR would operate to an OMR index no more negative than a 14-day moving average of -5,000 cfs, unless a storm event occurs. However, OMR could be more positive than -5,000 cfs if additional real-time OMR restrictions are triggered or constraints other than OMR control exports exist.

The threshold of -5,000 cfs may not be sufficiently protective of salmonid species or may be unnecessary depending on the date and various environmental conditions. Based on previous hydraulic footprint modeling analysis conducted by Reclamation, a few options can be considered for OMR flow to target during the OMR management season:

- No more negative than -3,500 cfs.
  - Expected: Hydraulic footprint is expected to be behind Head of Old River and Franks Tract, depending on conditions (e.g., wet vs. above normal year).
- No more negative than -5,000 cfs.
  - Expected: Hydraulic footprint is expected to be behind Head of Old River in wetter years, and perhaps into Franks Tract in drier years.
- No more negative than -6,250 cfs.
  - Expected: Hydraulic footprint reaches across the San Joaquin River but might be more limited in wetter years during storms.
- Variable OMR target flows depending on month.
  - For example, no more negative than -3,500 cfs OMR flow during peak salmonid entrainment season (e.g., March – May), and no more negative than -5,000 cfs for other months.

## 4.4 Expanded Loss Autocorrelation Analysis

In addition to managing OMR flow to a certain value, OMR flow may be further adjusted in response to triggers based on biological performance measures (e.g., exceedance of estimated daily loss, % of annual loss, etc.).

Under the 2020 ITP, for the months of November and December, discrete daily loss thresholds have been established at the Salvage Facilities (COA 8.6.2). When winter-run-sized Chinook salmon daily loss is greater than or equal to 6 fish per day in November or greater than or equal to 26 fish per day in December, the SWP is required to manage OMR flow to be no more negative than -5,000 cfs for five consecutive days. Density-dependent trigger or daily loss

thresholds are also set from January to May, where if daily loss equals or exceeds the thresholds, OMR flow is to be managed at no more negative than -3,500 cfs for at least 14 days (COA 8.6.3). These January to May thresholds are percentages of the water year's winter-run Chinook salmon juvenile production estimate (JPE) that vary by month:

- January 1 – January 31: 0.00635% of the winter-run Chinook salmon JPE.
- February 1 – February 28: 0.00991% of the winter-run Chinook salmon JPE.
- March 1 – March 31: 0.0146% of the winter-run Chinook salmon JPE.
- April 1 – April 30: 0.00507% of the winter-run Chinook salmon JPE.
- May 1 – May 31: 0.0077% of the winter-run Chinook salmon JPE.

Under the 2020 ROD, annual loss thresholds are set for each salmonid species/race:

- Natural winter-run Chinook salmon (loss= 1.17% of JPE).
- Hatchery winter-run Chinook salmon (loss= 0.12% of JPE).
- Natural Central Valley steelhead from December through March (loss =1,414).
- Natural Central Valley steelhead from April through June 15 (loss = 1,552).

When 50% of any annual thresholds are reached, Reclamation and DWR are to restrict OMR to a 14-day moving average OMR index of no more negative than -3,500 cfs until the end of the OMR management season. Additionally, if 75% of any annual loss threshold is exceeded, Reclamation and DWR are to restrict OMR to a 14-day moving average OMR index of no more negative than -2,500 cfs until the end of the OMR management season.

To better understand how salvage observation in one day affects salvage observation in subsequent days, autocorrelation analysis was done using winter-run LAD Chinook salmon data at the salvage facilities from the December to May period from 2009 to 2019. Autocorrelation function analysis of the winter-run LAD Chinook salmon salvage data showed high autocorrelation in the time series (Figure 6). However, when partial autocorrelation function analysis was done (where shorter, more immediate time lags are controlled for), it indicated that autocorrelation is mostly prominent for about a week (~7 days) (Figure 7). Because this analysis did not specifically evaluate autocorrelation during times when actions were taken (e.g., OMR shift towards a more positive or negative value), it does not provide a definitive answer on the question of response time for fish such as winter-run Chinook salmon. Nevertheless, these results do suggest that a lagged response to water operation changes is likely and that there may be a carryover effect for roughly a week.

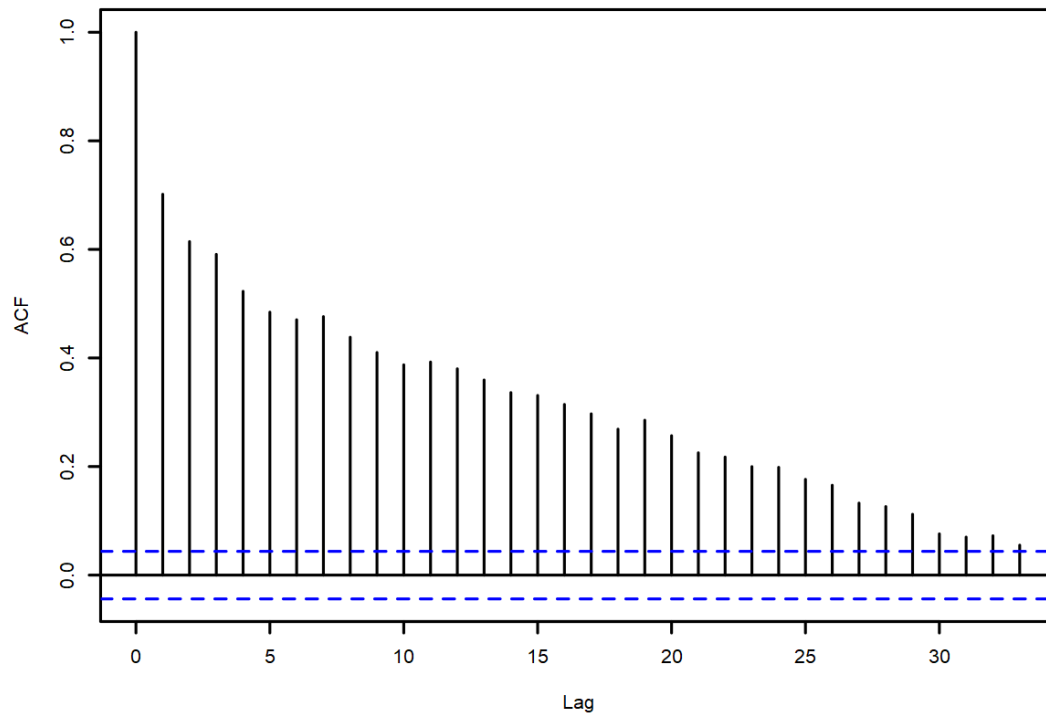


Figure 6. Auto-Correlation Function Plot for Expanded Salvage Numbers of Winter-Run LAD Chinook Salmon (without adipose clip) For December to May Period From 2009 to 2019 (Blue dotted line represents general  $p < 0.05$  threshold, where it is deemed to be "significant" correlation above the line)

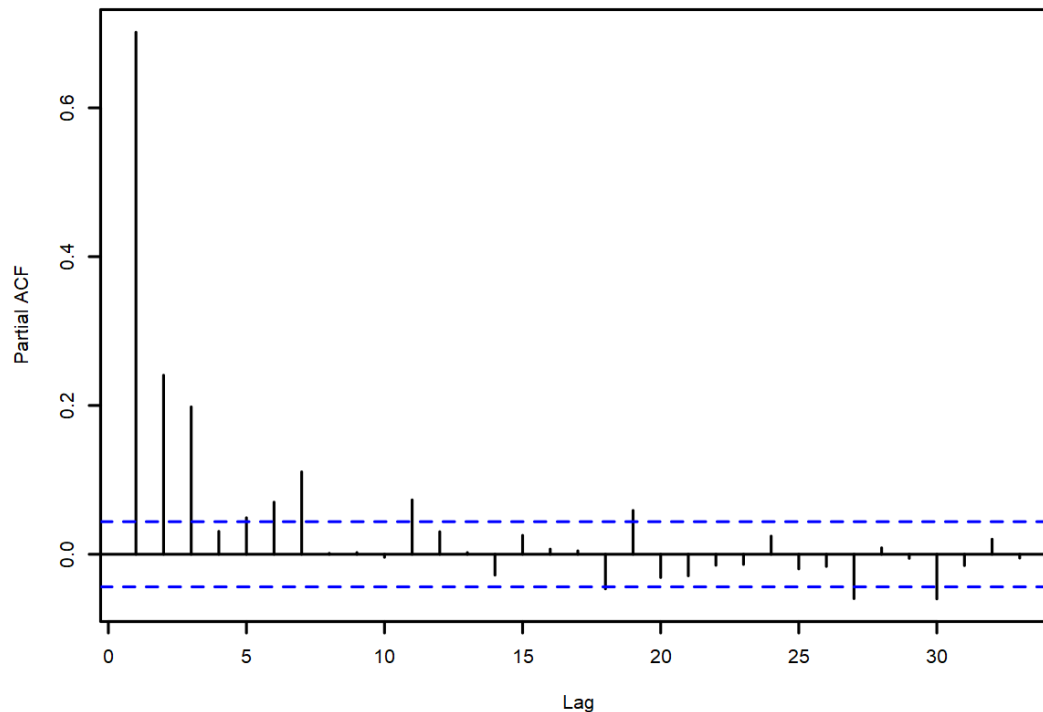


Figure 7. Partial Auto-Correlation Function (PACF) Plot for Expanded Salvage Numbers of Winter-Run LAD Chinook Salmon (without adipose clip) for December to May Period from 2009 to 2019 (Unlike auto-correlation function, PACF finds correlation of the residuals which remains after removing the effects which are already explained by the earlier lag[s])

## 4.5 Historical, Environmental Surrogate, and Calendar-Based OMR Offramp Analysis

The final variable component to consider is the offramp criteria for OMR flow management season. Warm conditions during late-summer and fall would presumably preclude Delta smelt and salmonids from the south Delta and the vicinities of the CVP and SWP pumping facilities. As such, the 2020 ROD and ITP have a combination of criteria that would signify the end of OMR management. These criteria include those based on real-time monitoring data (temperature threshold and SaMT distribution estimates) and a date cut-off (e.g., June 30 hard cut-off).

It is hypothesized that the greater the proportion of fish in the Delta on June 1 subject to OMR flow more negative than -5000 cfs the greater the seasonal loss. It is hypothesized that less than 95% of fish leaving the Delta prior to OMR flow more negative than -5000 cfs results in greater seasonal loss.

#### 4.5.1 Real-Time

Historical data from water year 2010 to water year 2021 was used to identify the date when 95% of each species on interest exited the Delta (presented from Salvage and Chipps Trawl). This date was compared to June 30 and the temperature exceedance date to determine when OMR management to reduce entrainment would end.

#### 4.5.2 Temperatures

Historical data from water year 2010 to 2021 was used to estimate the date of PA temperature exceedances, and then the proportion of each species of interest remaining in the Delta (presented from Salvage and Chipps Trawl) as of that date was compared to other potential variable end of OMR management approaches.

Table 7. List of Dates for Each Water Year That the Following Temperature-Based Off-Ramp Criteria Were Met: Daily Average Water Temperatures at Mossdale (station MSD) Exceed 71.6°F for 7 Days Starting in June (the 7 days do not have to be consecutive)

Water Year	Date Which Criteria Were Met	Date Which 100% WCS past Chipps Island	Date Which 100% STH past Chipps Island
2011	Never met	4/22/2011	5/13/2011
2012	6/14/2012	4/27/2012	4/13/2012
2013	6/7/2013	4/12/2013	5/10/2013
2014	6/7/2014	4/11/2014	5/22/2014
2015	6/7/2015	4/17/2015	2/18/2015
2016	6/7/2016	4/27/2016	3/30/2016
2017	Never met	5/5/2017	5/27/2017
2018	6/23/2018	4/21/2018	5/14/2018
2019	7/15/2019	5/20/2019	5/14/2019
2020	6/27/2020	4/10/2020	5/22/2020
2021	6/7/2021	4/25/2021	5/10/2021

Table 8. List of Dates for Each Water Year That the Following Temperature-Based Off-Ramp Criteria Were Met: Daily Average Water Temperatures at Mossdale (station MSD) Exceed 22.2°C for 7 Days Starting in June (the 7 days do not have to be consecutive)

Water Year	Date Which Criteria Were Met
2012	6/16/2012
2013	6/7/2013
2014	6/7/2014
2015	6/7/2015
2016	6/7/2016

Water Year	Date Which Criteria Were Met
2017	Never met
2018	6/24/2018
2019	7/17/2019
2020	6/28/2020
2021	6/7/2021

Table 9. List Of Dates for Each Water Year That the Following Temperature-Based Off-Ramp Criteria Were Met: Daily Average Water Temperatures at Prisoner's Point (station PPT) Exceed 22.2°C for 7 Days Starting in June (the 7 days do not have to be consecutive)

Water Year	Date Which Criteria Were Met
2020	6/7/2020
2021	6/7/2021
2022	6/22/2022

#### 4.5.3 Calendar

Historical data from water year 2010 to water year 2021 was used to estimate when 100% of each species of interest exited the Delta (Chippis Island) and considered this against a calendar end date of June 30.



## 5. Conclusions

**Should the onset of OMR management be based on real-time conditions, or does a fixed schedule based on the historical migration timing protect species with limited impacts on water supply?**

Onset of OMR management based on real-time fisheries monitoring indicating >5% of winter-run Chinook salmon have passed real-time Delta entry and exit location or salvage much more frequently than a calendar-based schedule starting January 1. At Knights Landing, 5% of fish observed occurred as early as September 16, with 17 of 19 (89%) years showing >5% of passage before January 1. In the Sacramento Trawl, >5% of fish observed there occurred as early as October 8, with 22 of 25 (88%) years showing >5% of passage before January 1. At Chipps Island 5% of fish observed in monitoring are detected as early as December 6, with 9 of 25 (36%) years showing >5% passage before January 1. The triggers for an integrated early winter pulse protections were observed as early as December 7 in the past 25 years, with 3 of 6 (50%) years when these triggers were exceeded occurring before January 1. Onset of OMR management based on >5% salvage occurred as early as December 6 (prior to the 2009 NMFS Biological Opinion), with 9 of 25 (36%) years showing >5% passage before January 1. Using a fixed schedule based on the historical migration timing for Delta entry at Knights Landing or Sacramento Trawl rather than a January 1 onset may reduce OMR management flexibility prior to January 1. A schedule based on Chipps Island or salvage rather than a January 1 onset may increase OMR management impacts on winter-run Chinook salmon entrainment.

**How does the magnitude of different OMR restrictions change the relative risk of species entrainment at the export facilities and into the central and/or south Delta?**

See OMR Fate Mapping and Zone of Influence Analyses.

**How does the magnitude of different OMR restrictions change the relative risk of species entrainment at the export facilities and into the central and/or south Delta?**

See OMR Fate Mapping and Zone of Influence Analyses.

**Does the duration of temporary OMR restrictions change the entrainment of species within the influence of export facilities?**

See OMR Fate Mapping and Zone of Influence Analyses.

It is not entirely clear how long temporary OMR restrictions based on species loss triggers need to be for it to be effective in re-routing fish out of the central and south Delta. However, based on the expanded salvage autocorrelation analysis and other studies (Tillotson et al. 2022), it seems likely that fish response to changes in OMR would not be instantaneous and may take several days or a week. With regards to OMR management to reduce entrainment of fish species into the interior Delta, it is also preferable to have a more proactive approach rather than a reactive one.

**Does an offramp of OMR management based on real-time conditions protect species and improve water supply performance, or does a fixed schedule protect species with limited impacts on water supply?**

An offramp for OMR management based on real-time fisheries monitoring indicating 100% of winter-run Chinook salmon and steelhead have exited the Delta earlier than June 30 (calendar-based offramp) and temperature-based offramp criteria at Mossdale and Prisoner Point. Using a fixed schedule based on the historical migration timing for Delta exit at Chipps Island rather than a June 30 offramp may increase OMR management flexibility with similar fish protection. A schedule-based temperature criteria rather than a real-time fishery monitoring offramp may increase water supply impacts without benefiting steelhead entrainment protection.

**What is the effect of different levels of near- and far-field entrainment on population viability?**

There is not a tool to evaluate this.

## 6. References

- Baxter, R., L. R. Brown, G. Castillo, L. Conrad, S. Culberson, M. Dekar, F. Feyrer, T. Hunt, K. Jones, and J. Kirsch. 2015. *An Updated Conceptual Model of Delta Smelt Biology: Our Evolving Understanding of an Estuarine Fish*. Interagency Ecological Program for the San Francisco Bay/Delta Estuary. IEP MAST. Technical Report 90. Sacramento, CA. California Department of Water Resources. Available: [https://www.waterboards.ca.gov/waterrights/water\\_issues/programs/bay\\_delta/california\\_waterfix/exhibits/docs/petitioners\\_exhibit/dwr/part2/DWR-1089%20IEP\\_MAST\\_Team\\_2015\\_Delta\\_Smelt\\_MAST\\_Synthesis\\_Report\\_January%202015.pdf](https://www.waterboards.ca.gov/waterrights/water_issues/programs/bay_delta/california_waterfix/exhibits/docs/petitioners_exhibit/dwr/part2/DWR-1089%20IEP_MAST_Team_2015_Delta_Smelt_MAST_Synthesis_Report_January%202015.pdf). Accessed: DATE.
- Beakes, M., R. Bilski, A. Collins, E. Ferguson, J. Ferguson, P. Goertler, E. Greene, B. Mahardja, B. Matthias, and P. Vick. 2022. *Southern Sierra Nevada Diversity Group Steelhead Science Plan (draft)*.
- Buchanan, R.A., E. Buttermore, and J. Israel. 2021. Outmigration Survival of A Threatened Steelhead Population through a Tidal Estuary. *Canadian Journal of Fisheries and Aquatic Sciences* 78:1869–1886.
- California Department of Water Resources (DWR). 2017. Yolo Bypass Salmonid Habitat Restoration and Fish Passage. Draft Environmental Impact Statement/Environmental Impact Report. December.
- Fisher, F. W. 1992. *Chinook Salmon, Oncorhynchus tshawytscha, Growth and Occurrence in the Sacramento-San Joaquin River System*. California Department of Fish and Game, Inland Fisheries Division. Draft Office Report. Redding, CA.
- Moyle, P. B. 2002. *Inland Fishes of California, Revised and Expanded*. Berkeley: University of California Press.
- Tillotson M., J. Hassrick, A. Collins, and C. Phillis. 2022. Machine Learning Forecasts to Reduce Risk of Entrainment Loss of Endangered Salmonids at Large-Scale Water Diversions in the Sacramento-San Joaquin Delta, California. *San Fr Estuary Watershed Sci.* 20(2):0–21. doi:10.15447/sfew.s.2022v20iss2art3.
- Windell S, P. L. Brandes, J. L. Conrad, J. W. Ferguson, P. A. L. Goertler, B. N. Harvey, J. Heublein, J. I. Israel, D. W. Kratville, and J. E. Kirsch. 2017. *Scientific Framework for Assessing Factors Influencing Endangered Sacramento River Winter-Run Chinook Salmon (Oncorhynchus tshawytscha) across the Life Cycle*. U.S. Department of Commerce. NOAA Technical Memorandum NMFS- SWFSC-586. <http://doi.org/10.7289/V5/TM-SWFSC-586>

Page Intentionally Left Blank

## **I.1. Attachment 1: Delta Particle Tracking Modeling under Varying OMR Conditions**

A sensitivity analysis using CalSim II and DSM2 Hydro and PTM models were conducted to assess relative risk of species at the export facilities and water supply effects under a set of different OMR limits on Delta operations. The CalSim II model simulated operational conditions (flows into the Delta and exports) under an OMR limit of -3000 cfs, -4000 cfs, -5000 cfs, -6000 cfs, and -7000 cfs. Using results of these CalSim II scenarios, DSM2 Hydro was used to determine Delta flow conditions, and respectively, DSM2 PTM module was used to assess entrainment of particles at export facilities under these varying conditions. DSM2 PTM was run in two modes: one assuming neutrally buoyant and one assuming surface-oriented particles. For each year in the 82-year CalSim II simulation period and for each mode, the model was run at 39 particle insertion locations in the Delta. And for each insertion location it was run for two seasons: December through March, starting at the beginning of each month for each period and lasting for 45 days; and March through June, starting at the beginning of each month for each period and lasting for 30 days. The resulting 40,000+ simulations provided a wide variety of flow, particle insertion, and particle behavior conditions from which to draw conclusions.

## **I.1.1 Methods**

### **I.1.1.1 DSM2 - PTM**

DSM2-PTM simulates pseudo-3D transport of neutrally buoyant particles based on the flow field simulated by HYDRO. The PTM module simulates the transport and fate of individual particles traveling throughout the Delta. The model uses geometry files, velocity, flow, and stage output from the HYDRO module to monitor the location of each individual particle using assumed vertical and lateral velocity profiles and specified random movement to simulate mixing. The location of a particle in a channel is determined as the distance from the downstream end of the channel segment (x), the distance from the centerline of the channel (y), and the distance above the channel bottom (z). PTM has multiple applications ranging from visualization of flow patterns to simulation of discrete organisms such as fish eggs and larvae.

The longitudinal distance traveled by a particle is determined from a combination of the lateral and vertical velocity profiles in each channel. The transverse velocity profile simulates the effects of channel shear that occurs along the sides of a channel. The result is varying velocities across the width of the channel. The average cross-sectional velocity is multiplied by a factor based on the particle's transverse location in the channel. The model uses a fourth order polynomial to represent the velocity profile. The vertical velocity profile shows that particles located near the bottom of the channel move more slowly than particles located near the surface. The model uses the Von Karman logarithmic profile to create the velocity profile. Particles also move as a result of random mixing. The mixing rates (i.e., distances) are a function of the water depth and the velocity in the channel. Higher velocities and deeper water result in greater mixing.

At a junction, the path of a particle is determined randomly based on the proportion of flow. The proportion of flow determines the probability of movement into each reach. A random number, based on this determined probability, then governs where the particle will go. A particle that moves into an open water area, such as a reservoir, no longer retains its position information. A DSM2 open water area is considered a fully mixed reactor. The path out of the open water area is

a decision based on the volume in the open water area, the time step, and the flow out of the area. At the beginning of a time step, the volume of the open water area, the volume of water leaving at each opening of the open water area, is determined. From that, the probability of the particle leaving the open water area is calculated. Particles entering exports or agricultural diversions are considered "lost" from the system. Their final destination is recorded. Once particles pass the Martinez boundary, they have no opportunity to return to the Delta (Smith 1998; Wilbur 2001; Miller 2002).

Particle tracking models (PTM) are excellent tools to visualize and summarize the impacts of modified hydrodynamics in the Delta. These tools can simulate the movement of passive particles or particles with behavior representing either larval or adult fish through the Delta. The PTM tools can provide important information relating hydrodynamic results to the analysis needs of biologists that are essential in assessing the impacts to the habitat in the Delta.

#### ***I.1.1.1.1 DSM2 – PTM Metrics***

Fate Mapping – an indicator of entrainment. It is the percent of particles that go past various exit points in the system at the end of a given number of days after insertion.

#### ***I.1.1.1.2 PTM Particle Behavior***

PTM simulations were conducted with passive particles and surface-oriented particles. Passive particles, representing behavior of larval Delta smelt, are distributed throughout the water column. Surface-oriented particles, representing behavior of larval longfin smelt, tend towards the top 10% of the water column. To assess effects of surface-oriented assumptions of larval longfin smelt fate, passive particle simulations were also conducted for larval longfin smelt.

#### ***I.1.1.1.3 PTM Period selection***

PTM simulation periods for the fate computations were in December through June in all of the 82 years of the planning simulation period. December through March periods reflect timing for larval longfin smelt. As such, passive and surface-oriented particle simulations were conducted during this period. March through June periods reflect timing of larval Delta smelt. As such, passive particle simulations were conducted during this period.

#### ***I.1.1.1.4 PTM simulations***

PTM simulations are performed to derive the metrics described above. The particles are inserted at the 39 locations listed in Table I.1-1. The locations were identified based on the 20 mm Delta Smelt Survey Stations. Figure I.1-1 displays 20 mm Delta Smelt Survey Stations and particle insertion locations.

A total of 39 PTM simulations are performed in a batch mode for each insertion period. For each insertion period, 4000 particles are inserted at the identified locations over a 24.75-hour period, starting on the 1st of the selected month. The fate of the inserted particles is tracked continuously over a 60-day simulation period. The particle flux is tracked at the key exit locations – exports, Delta agricultural intakes, past Chipps Island, to Suisun Marsh and past Martinez, and at several internal tracking locations. Generally, the fate of particles at the end of 30 days or 45 days after insertion is computed for the fate mapping analysis.

Table I.1-1: List of Particle Insertion Locations for Residence Time and Fate Computations

<b>Location</b>	<b>DSM2 Node</b>
San Joaquin River at Vernalis	1
San Joaquin River at Mossdale	7
San Joaquin River D/S of Rough and Ready Island	21
San Joaquin River at Buckley Cove	25
San Joaquin River near Medford Island	34
San Joaquin River at Potato Slough	39
San Joaquin River at Twitchell Island	41
Old River near Victoria Canal	75
Old River at Railroad Cut	86
Old River near Quimby Island	99
Middle River at Victoria Canal	113
Middle River u/s of Mildred Island	145
Grant Line Canal	174
Frank's Tract East	232
Threemile Slough	240
Little Potato Slough	249
Mokelumne River d/s of Cosumnes confluence	258
South Fork Mokelumne	261
Mokelumne River d/s of Georgiana confluence	272
North Fork Mokelumne	281
Georgiana Slough	291
Miner Slough	307
Sacramento Deep Water Ship Channel	314
Cache Slough at Shag Slough	321
Cache Slough at Liberty Island	323
Lindsey slough at Barker Slough	322
Sacramento River at Sacramento	330
Sacramento River at Sutter Slough	339
Sacramento River at Ryde	344
Sacramento River near Cache Slough confluence	350
Sacramento River at Rio Vista	351
Sacramento River d/s of Decker Island	353
Sacramento River at Sherman Lake	354
Sacramento River at Port Chicago	359



Location	DSM2 Node
Montezuma Slough at Head	418
Montezuma Slough at Suisun Slough	428
San Joaquin River d/s of Dutch Slough	461
Sacramento River at Pittsburg	465
San Joaquin River near Jersey Point	469

#### ***1.1.1.1.5 Output Parameters***

The particle tracking models can be used to assist in understanding passive fate and transport, or through consideration of behavior or residence time. In, general the following outputs are generated:

- Fate of particles and cut lines or regions.
- Time of travel breakthrough curves.
- Residence time.

For the purposes of this effort, only particle fate outputs were assessed.

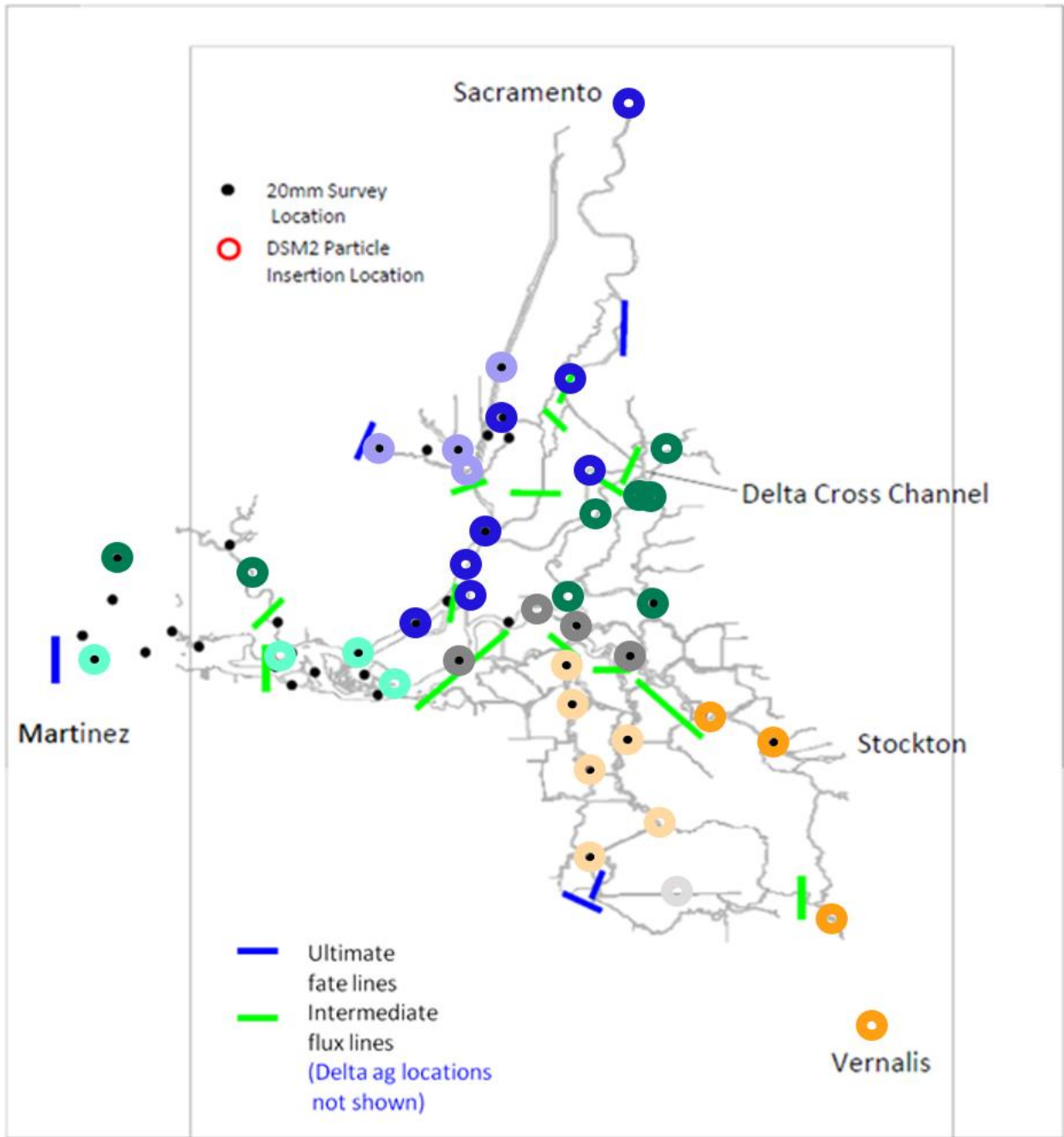


Figure I.1-1. Particle Insertion Locations for Fate Computations, Color-Coded By Yolo (purple), Sacramento River (dark blue), Mokelumne River (green), Central (dark gray), Old and Middle River (OMR) (light orange), San Joaquin River (orange), South Delta (light gray), West Delta (turquoise), and Suisun Marsh Regions (green)

## **I.1.2 Results**

### **I.1.2.1 Larval Longfin Smelt**

Exceedance plots were developed to demonstrate the range of particle fates. Exceedance plots of surface-oriented particle fate (percent of particles that reach a given fate location) are presented by month and fate location. The month presented in each plot refers to the month in which the particles are inserted. For example, Figure I.1-2 presents results from particles that were inserted on December 1. In Figures I.1-2 through I.1-5, percent of particles entrained at exports are shown for the months of December through March. Percent of particles crossing the San Joaquin River (from north to south) and exiting the Delta (west of Chipps Island) are presented in Figures I.1-6 through I.1-9 and Figures I.1-10 through I.1-13, respectively.

Under most circumstances in December (Figure I.1-2), the percentage of particles entrained at the export facilities varies by the OMR flow condition specified by the sensitivity analysis. Consistently, the smallest percent of particles entrained at the export facilities occurs under the simulation with OMR flow set to a minimum of -3,000 cfs (OMR3k). As the OMR flow condition incrementally decreases (e.g., from -3,000 to -4,000 cfs), the percentage of particles entrained at the exports incrementally increases. Conversely, the percent of particles that exit the Delta (west of Chipps) decreases as the OMR flow condition incrementally decreases (Figure I.1-10). However, the response for exiting the Delta is not as linear as the particle entrainment response. As OMR flow conditions decrease, the response of particles exiting the Delta is increasingly muted.

Similar patterns are observed in the months of January through March (Figures I.1-3 to I.1-5, Figures I.1-7 to I.1-9, and Figures I.1-11 to I.1-13). As compared to December, for each OMR flow condition, the portion of particles entrained is reduced in January, February, and March. Delta inflow is generally higher in January through March than February. With higher Delta inflow and less entrainment in the Delta, more particles exit the Delta (west of Chipps) in January through March as compared to December in each OMR flow condition.

As the No Action Alternative (NAA) model considers all OMR flow requirements documented in the 2019 biological opinions, the magnitude of OMR flow changes between the months. NAA particle entrainment at exports are most similar to the OMR flow condition of -5,000 cfs (OMR5k) in December. NAA particle entrainment at the exports is between the -4,000 cfs and -5,000 cfs in January and February, and similar to -3,000 cfs in March.

As evidenced by the range of particles entrained at the exports, the range of pumping varies across the months of December through March.

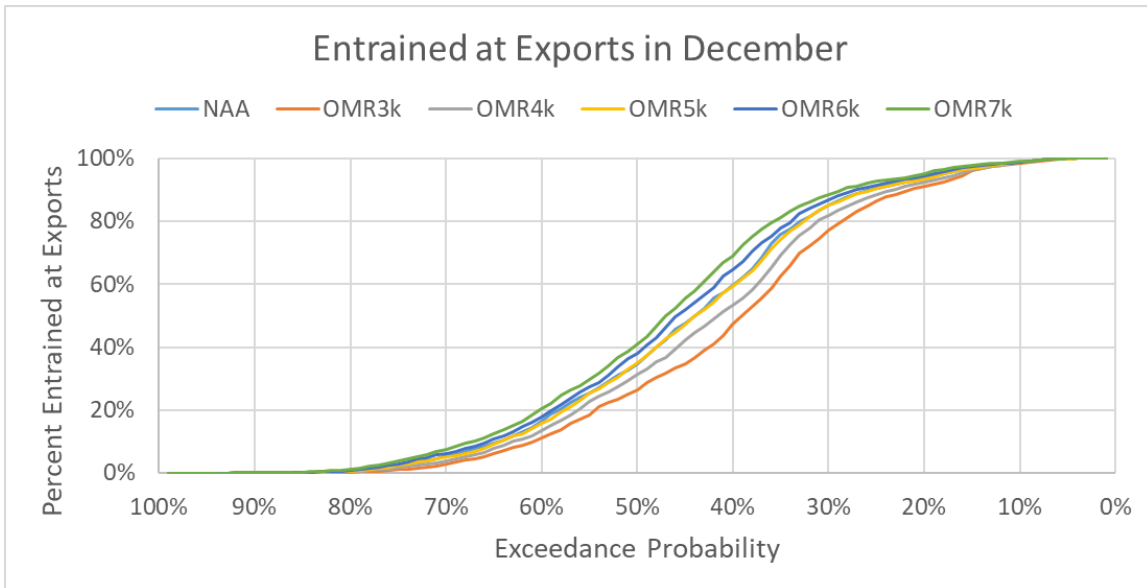


Figure I.1-2. Percent of Surface Oriented Particles Entrained at Exports in December, 45-days after Insertion

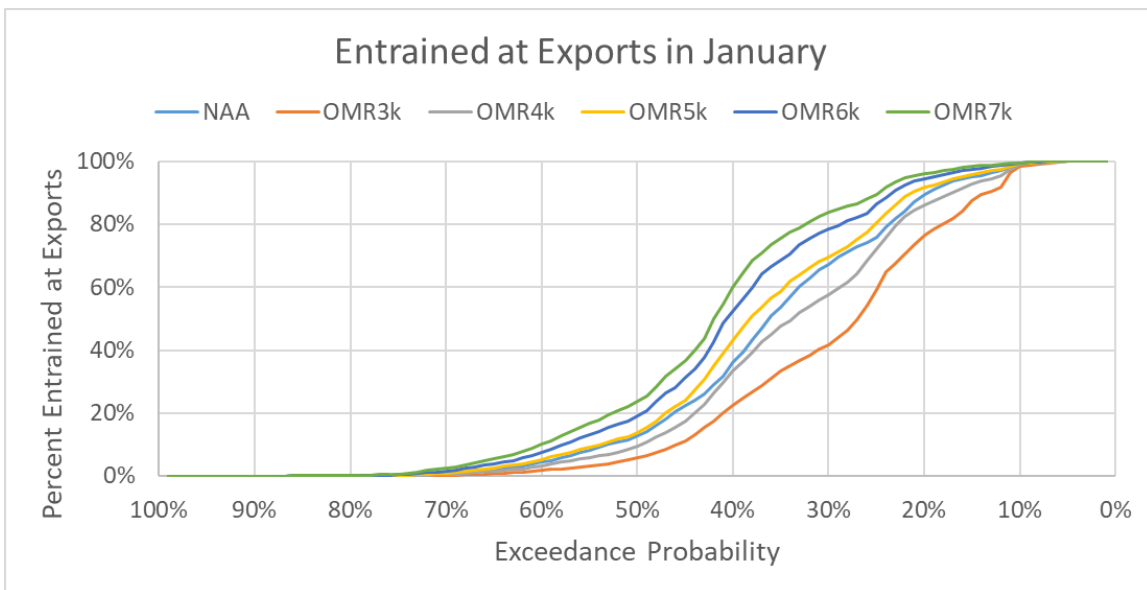


Figure I.1-3. Percent of Surface Oriented Particles Entrained at Exports in January, 45-days after Insertion

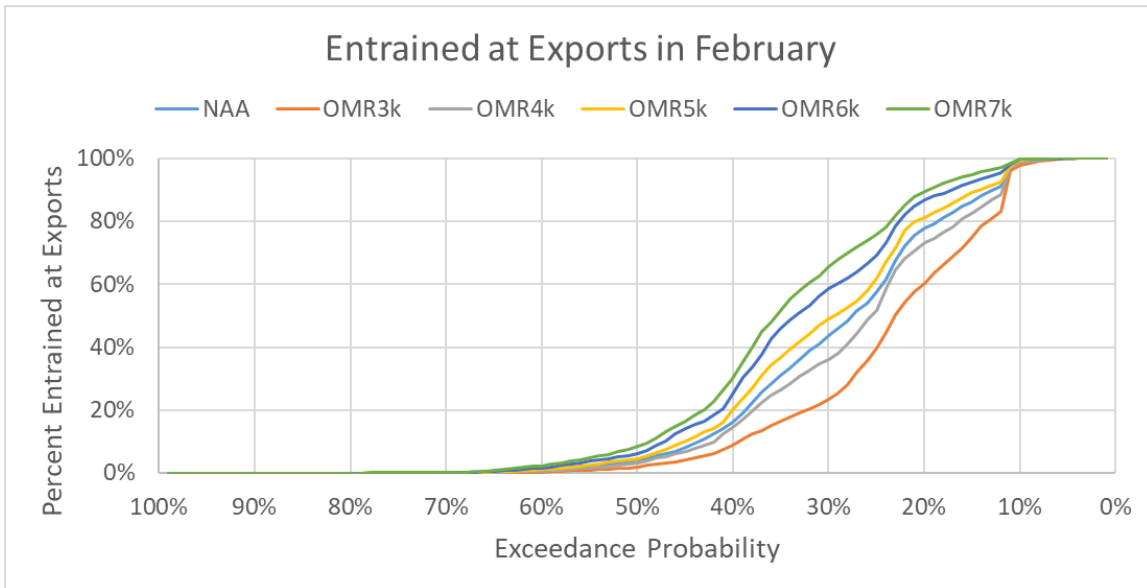


Figure I.1-4. Percent of Surface Oriented Particles Entrained at Exports in February, 45-days after Insertion

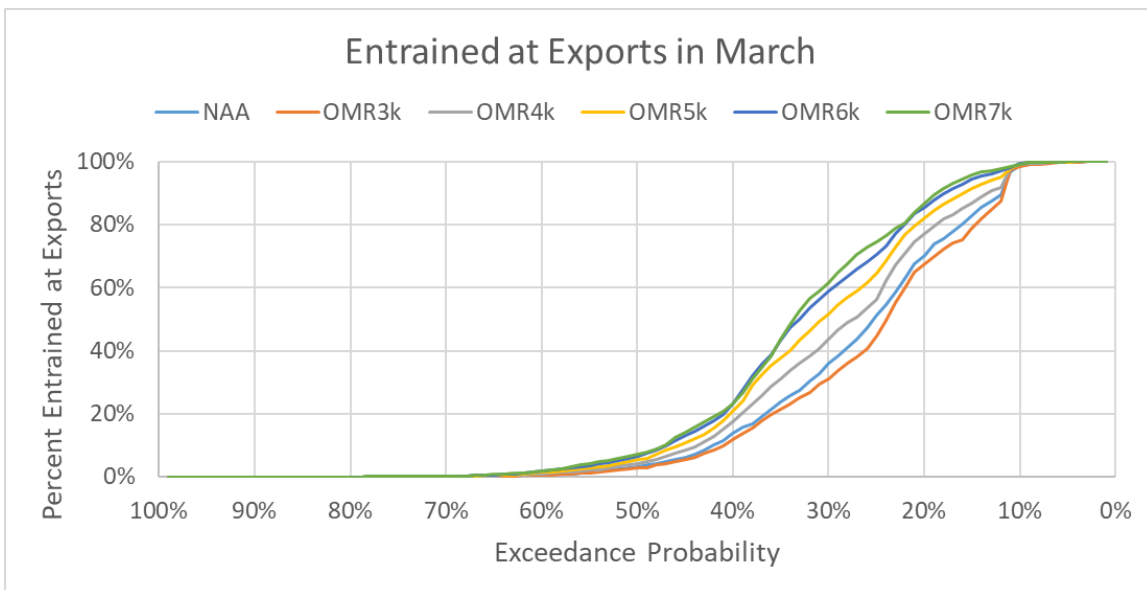


Figure I.1-5. Percent of Surface Oriented Particles Entrained at Exports in March, 45-days after Insertion

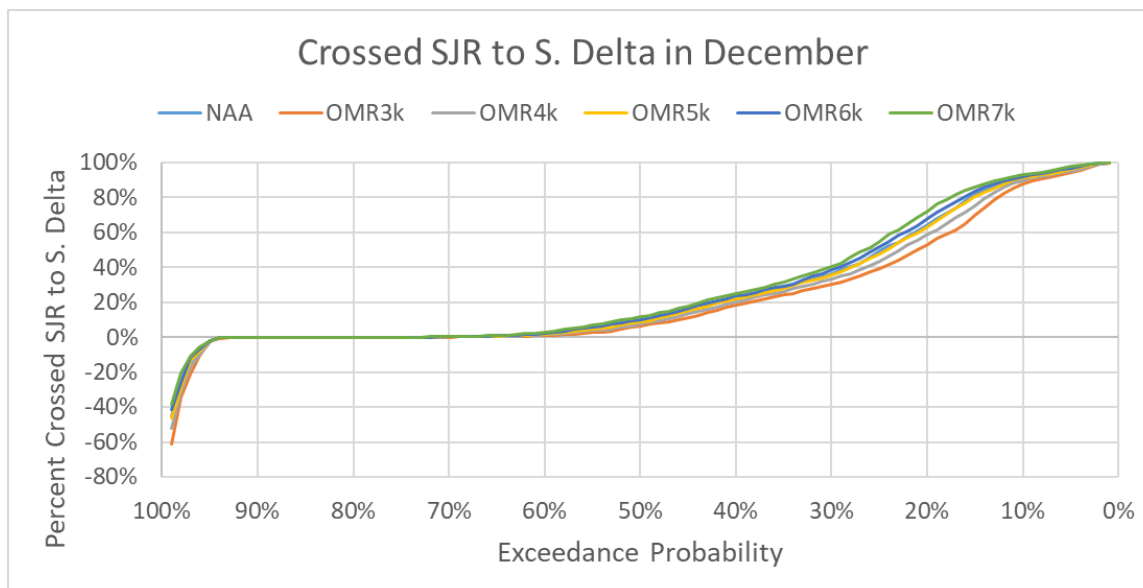


Figure I.1-6. Percent of Surface Oriented Particles Crossing the San Joaquin River in December, 45-days after Insertion

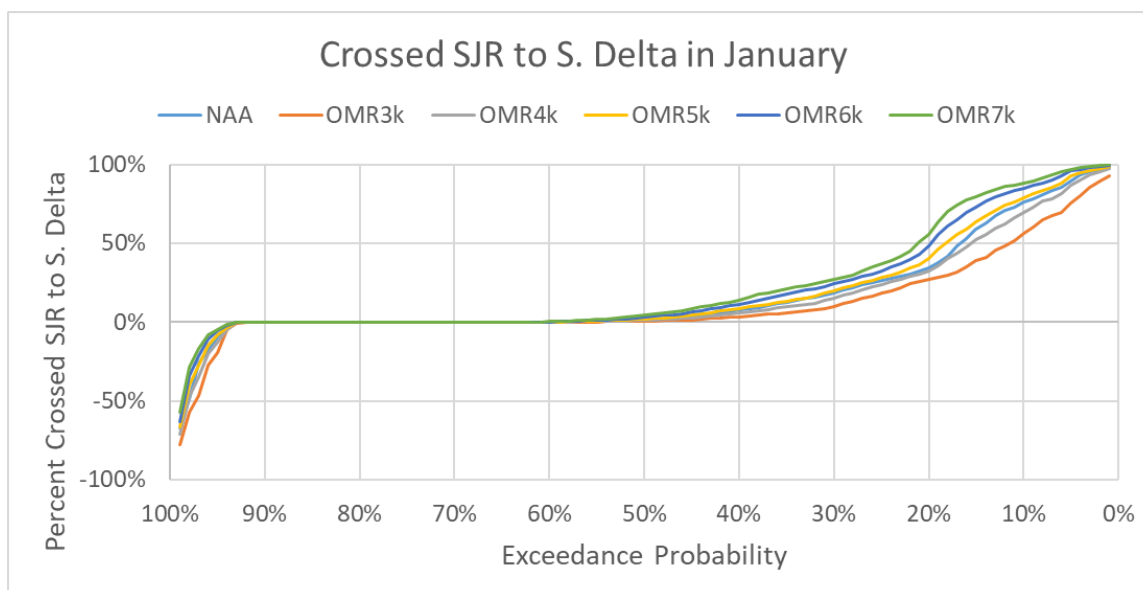


Figure I.1-7. Percent of Surface Oriented Particles Crossing the San Joaquin River in January, 45-days after Insertion

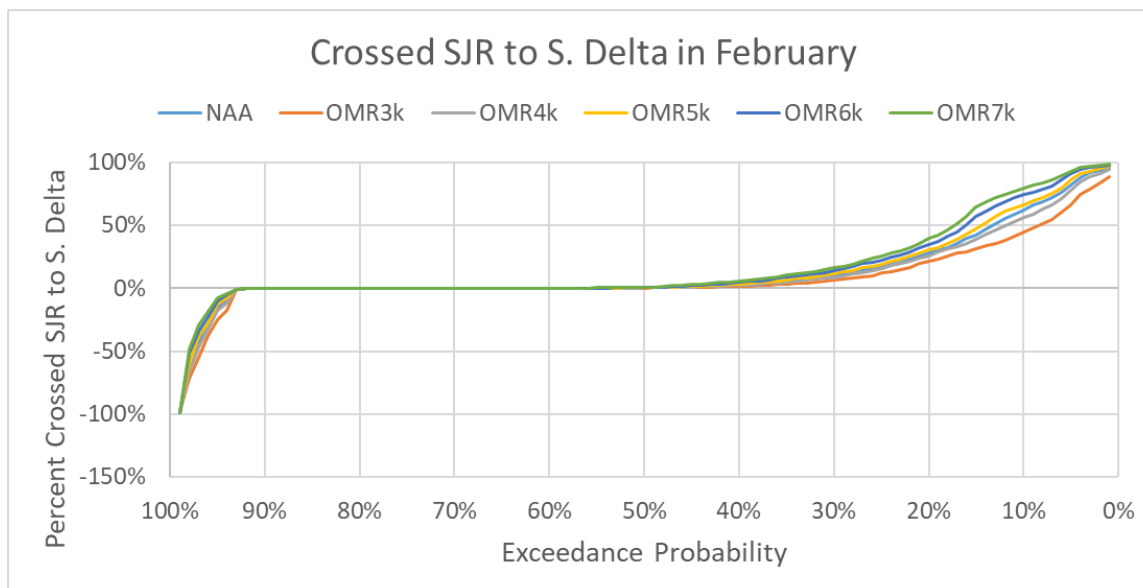


Figure I.1-8. Percent of Surface Oriented Particles Crossing the San Joaquin River in February, 45-days after Insertion

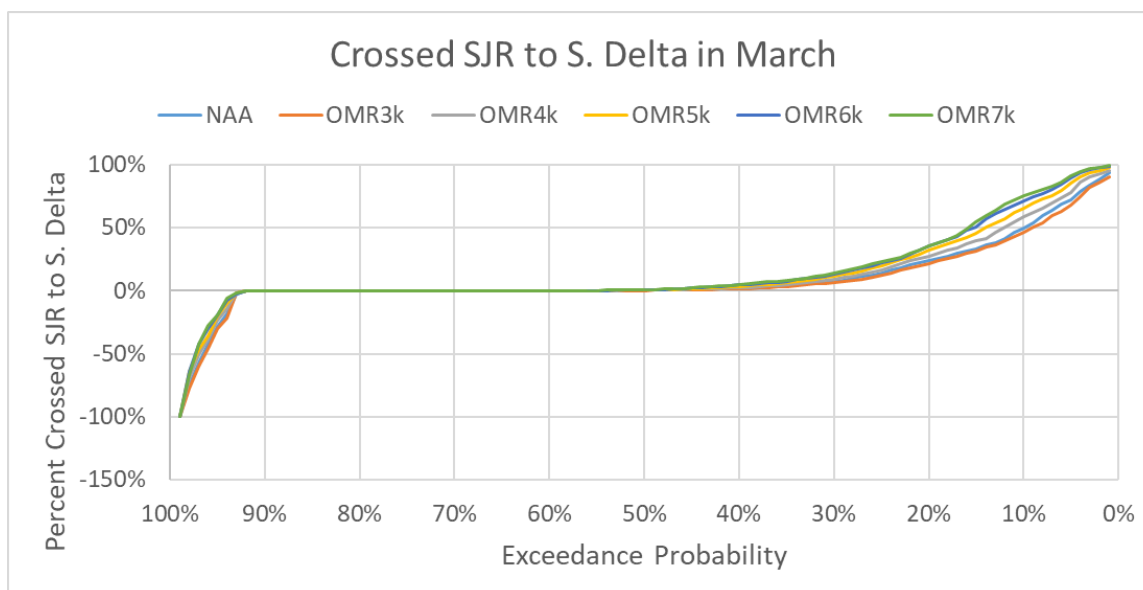


Figure I.1-9. Percent of Surface Oriented Particles Crossing the San Joaquin River in March, 45-days after Insertion

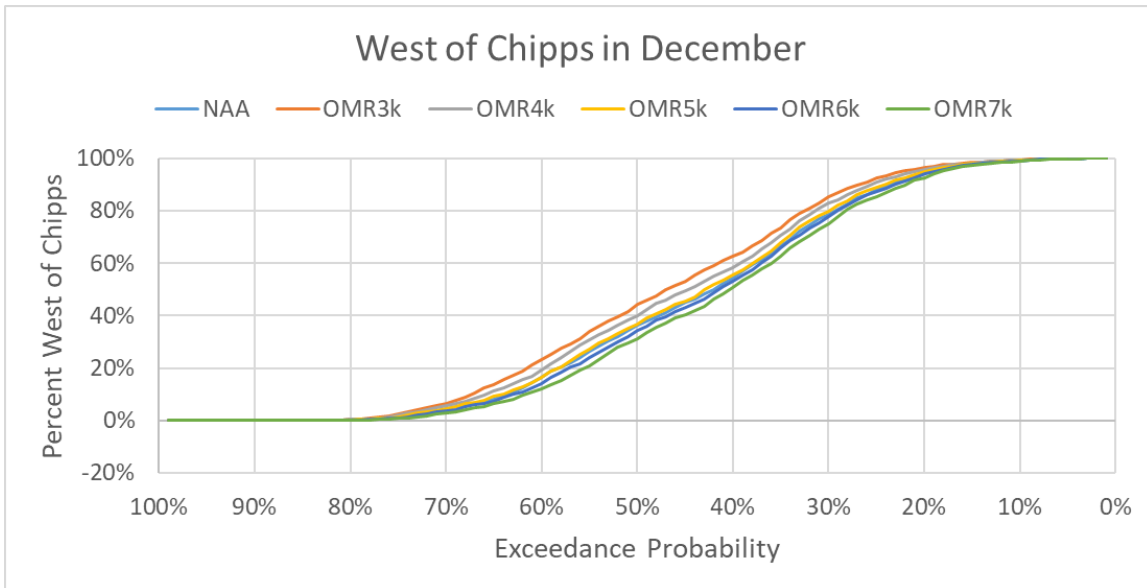


Figure I.1-10. Percent of Surface Oriented Particles West of Chipps in December, 45-days after Insertion

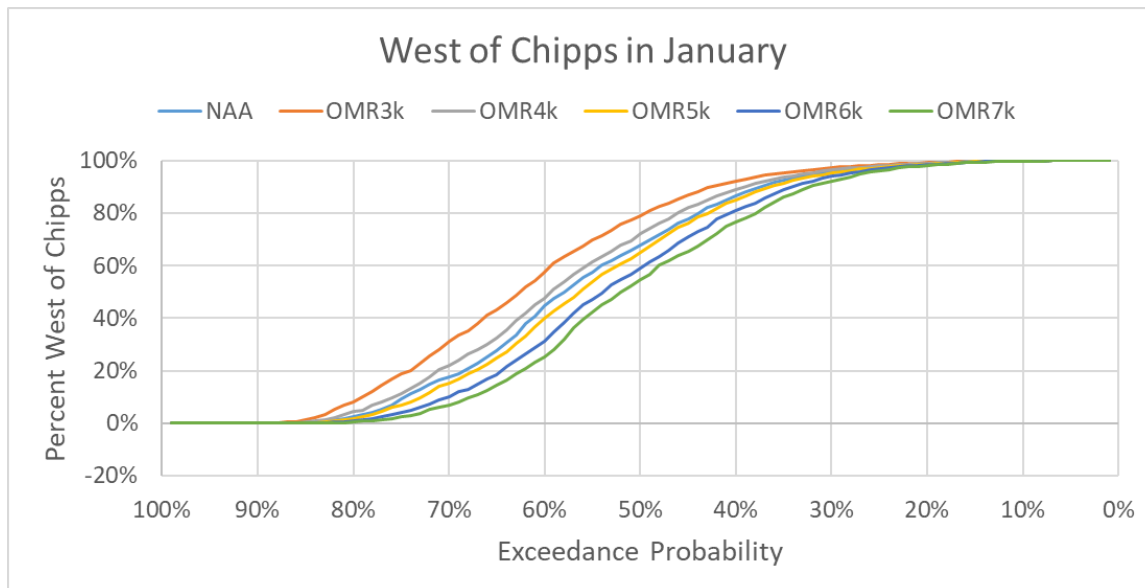


Figure I.1-11. Percent of Surface Oriented Particles West of Chipps in January, 45-days after Insertion



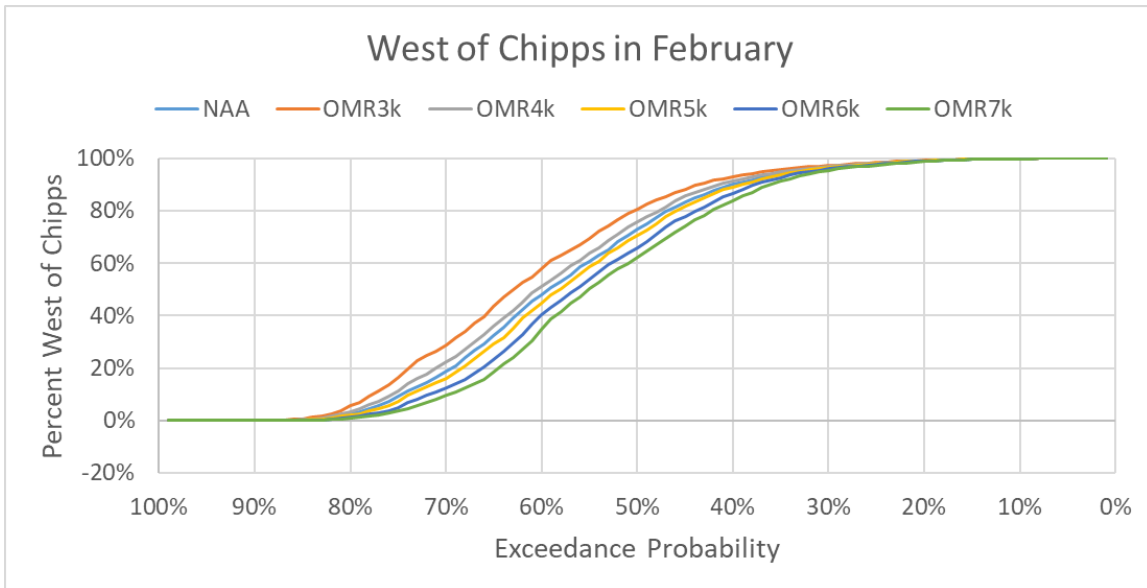


Figure I.1-12. Percent of Surface Oriented Particles West of Chipps in February, 45-days after Insertion

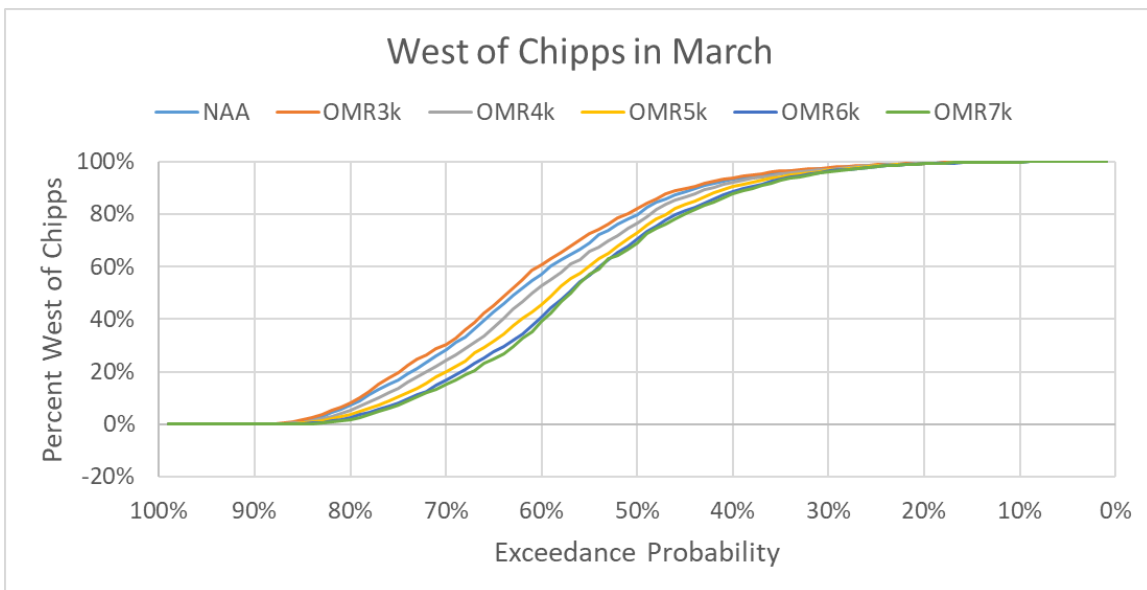


Figure I.1-13. Percent of Surface Oriented Particles West of Chipps in March, 45-days after Insertion

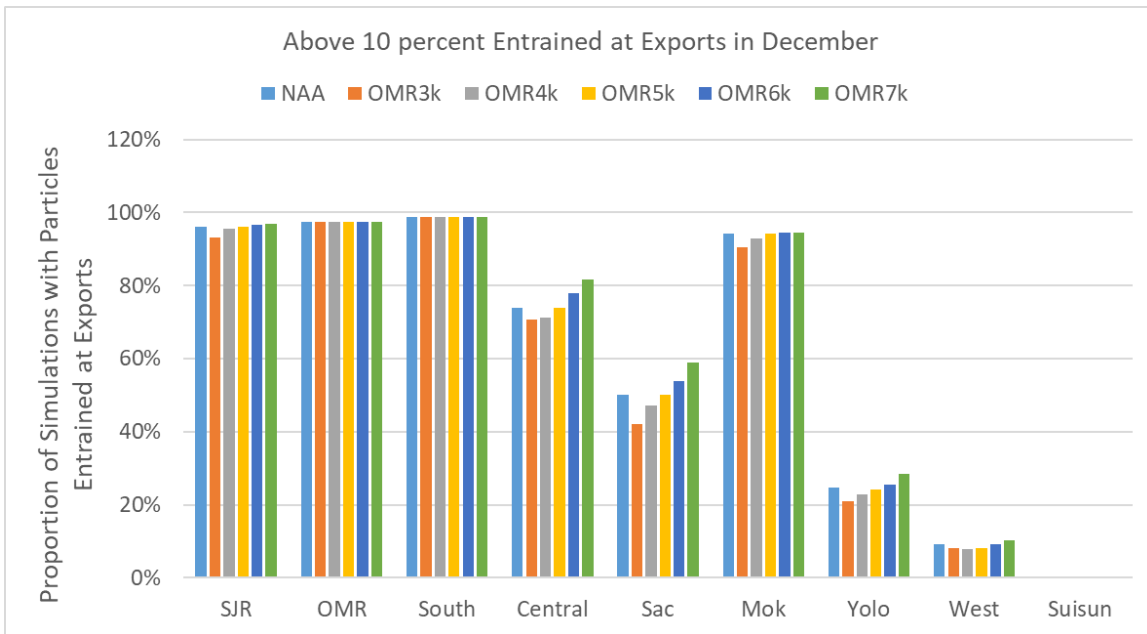
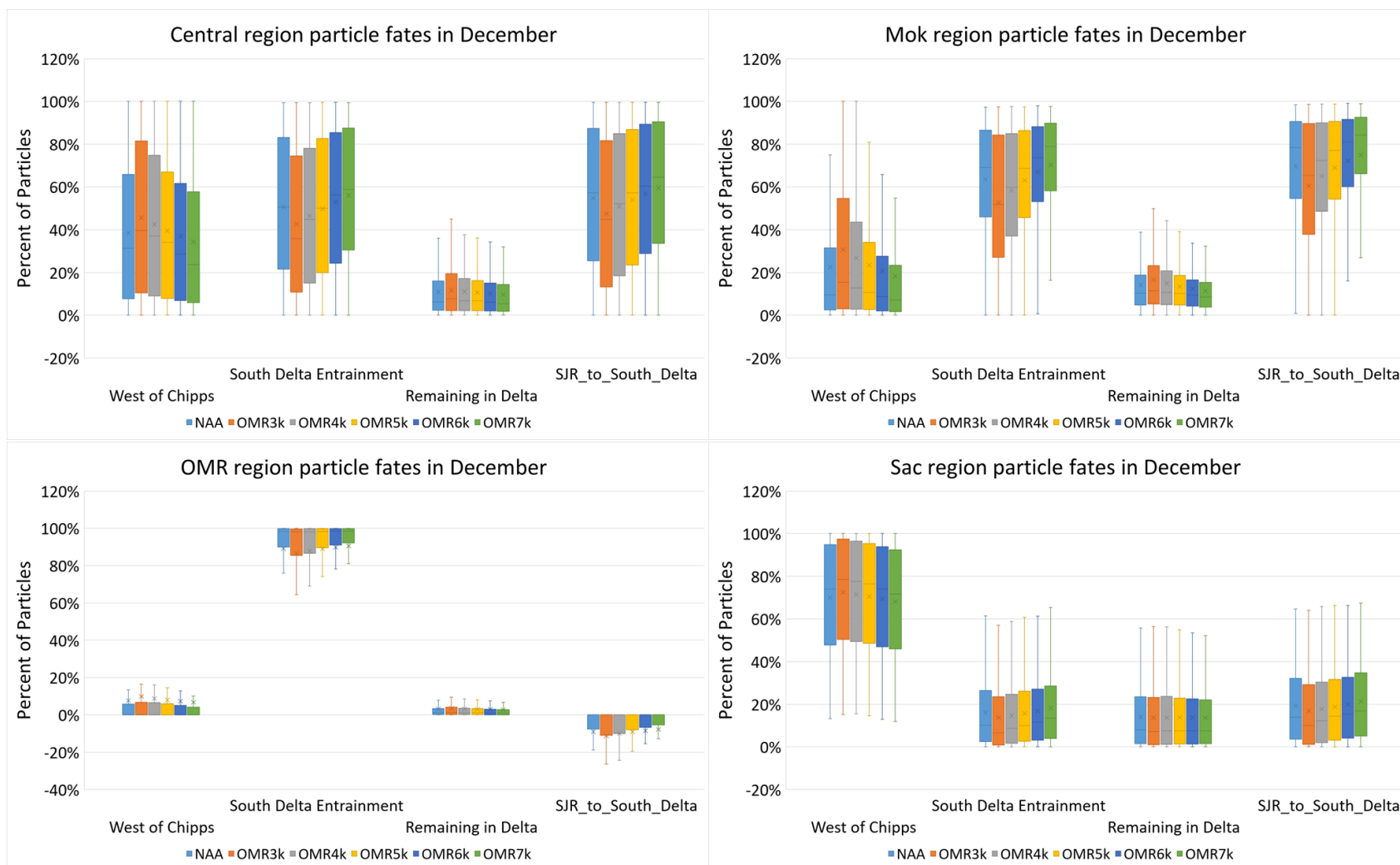
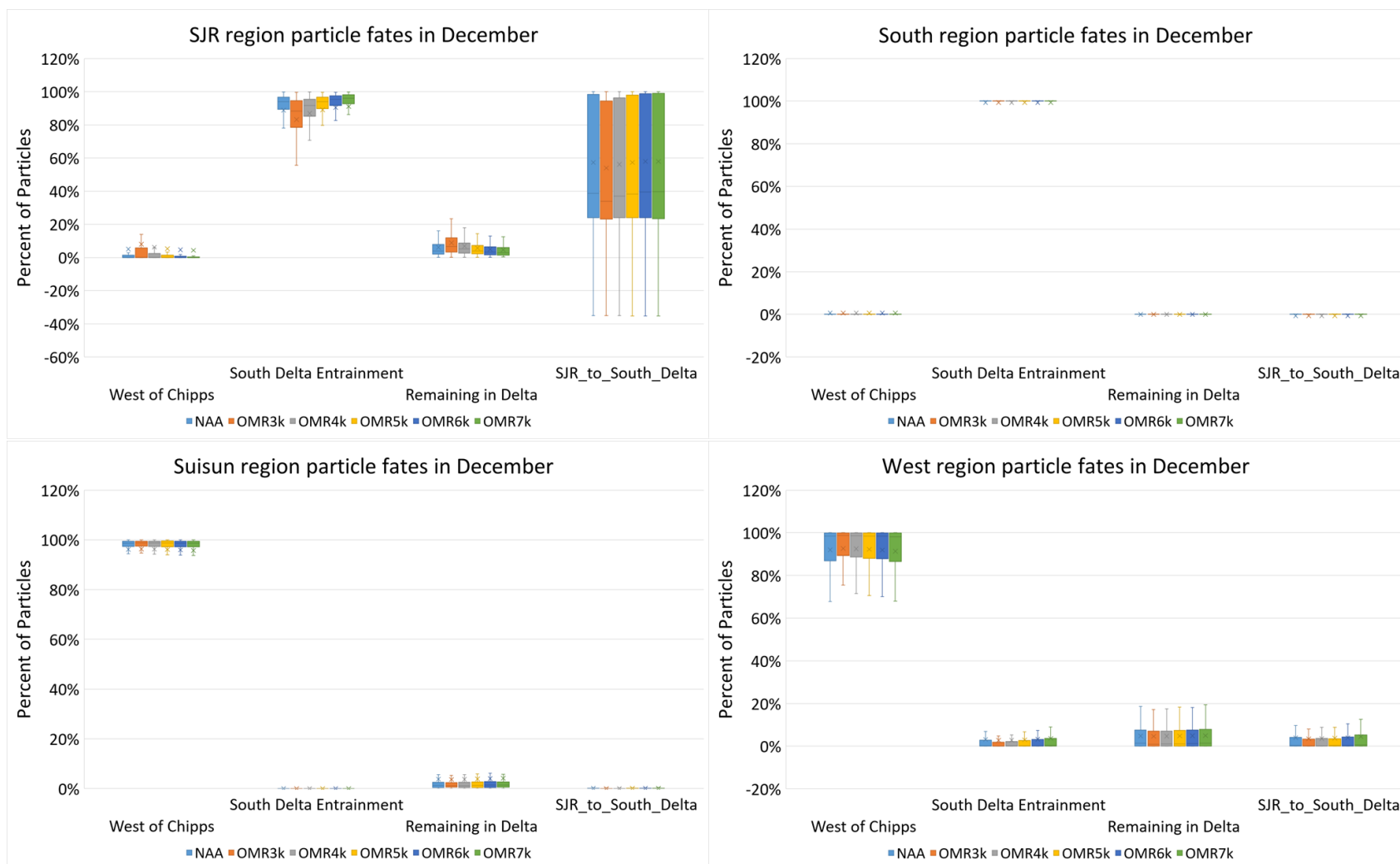
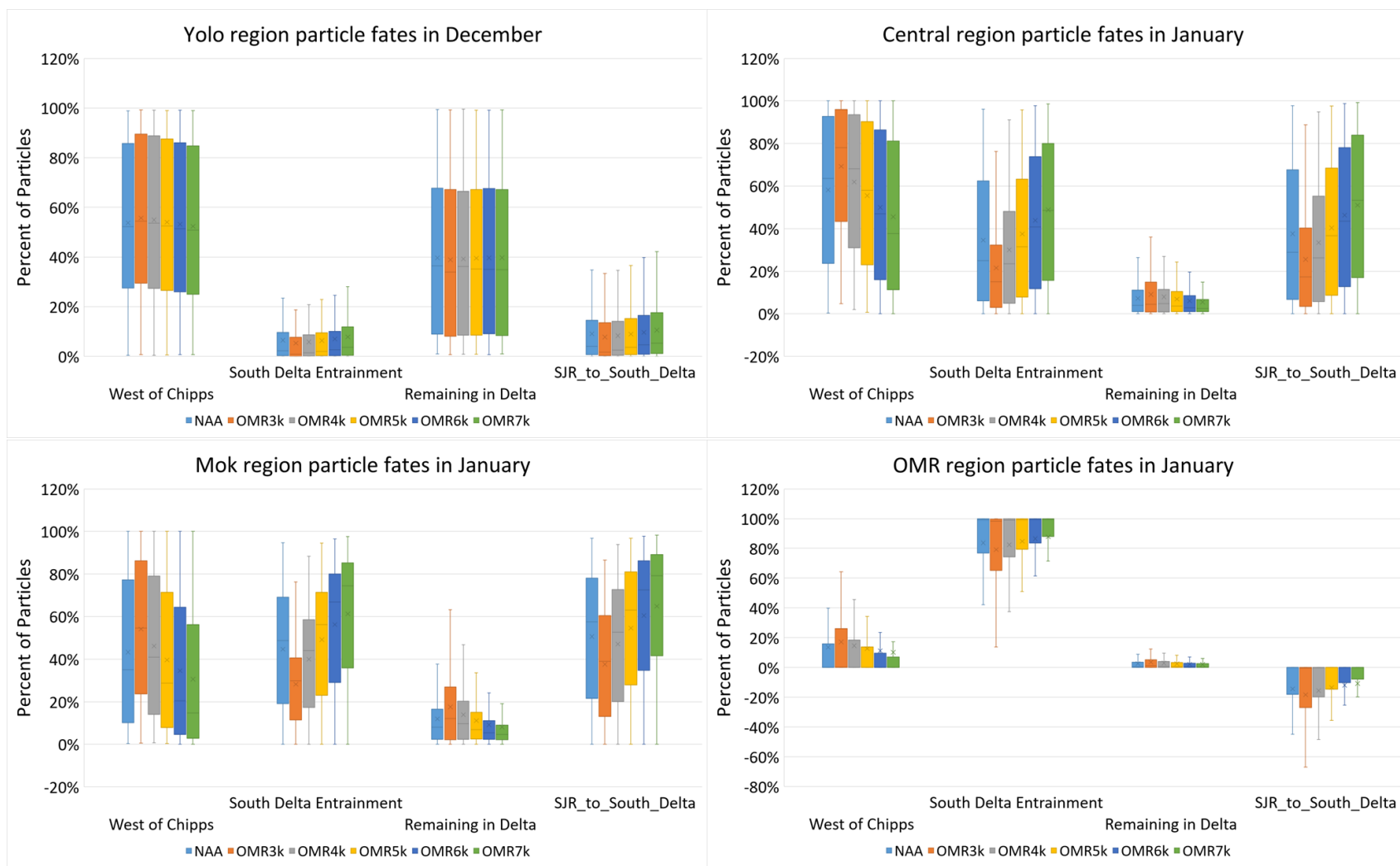
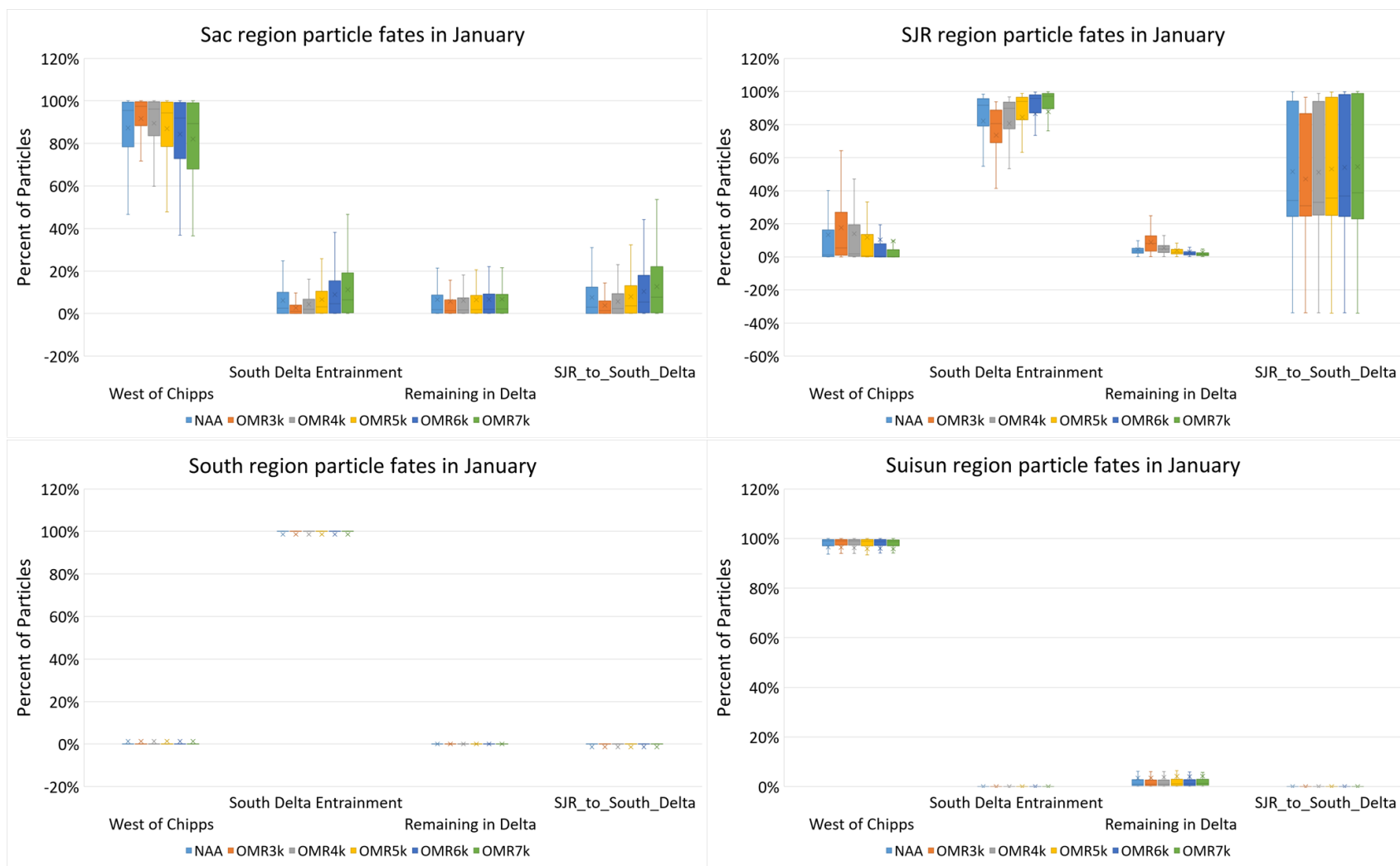


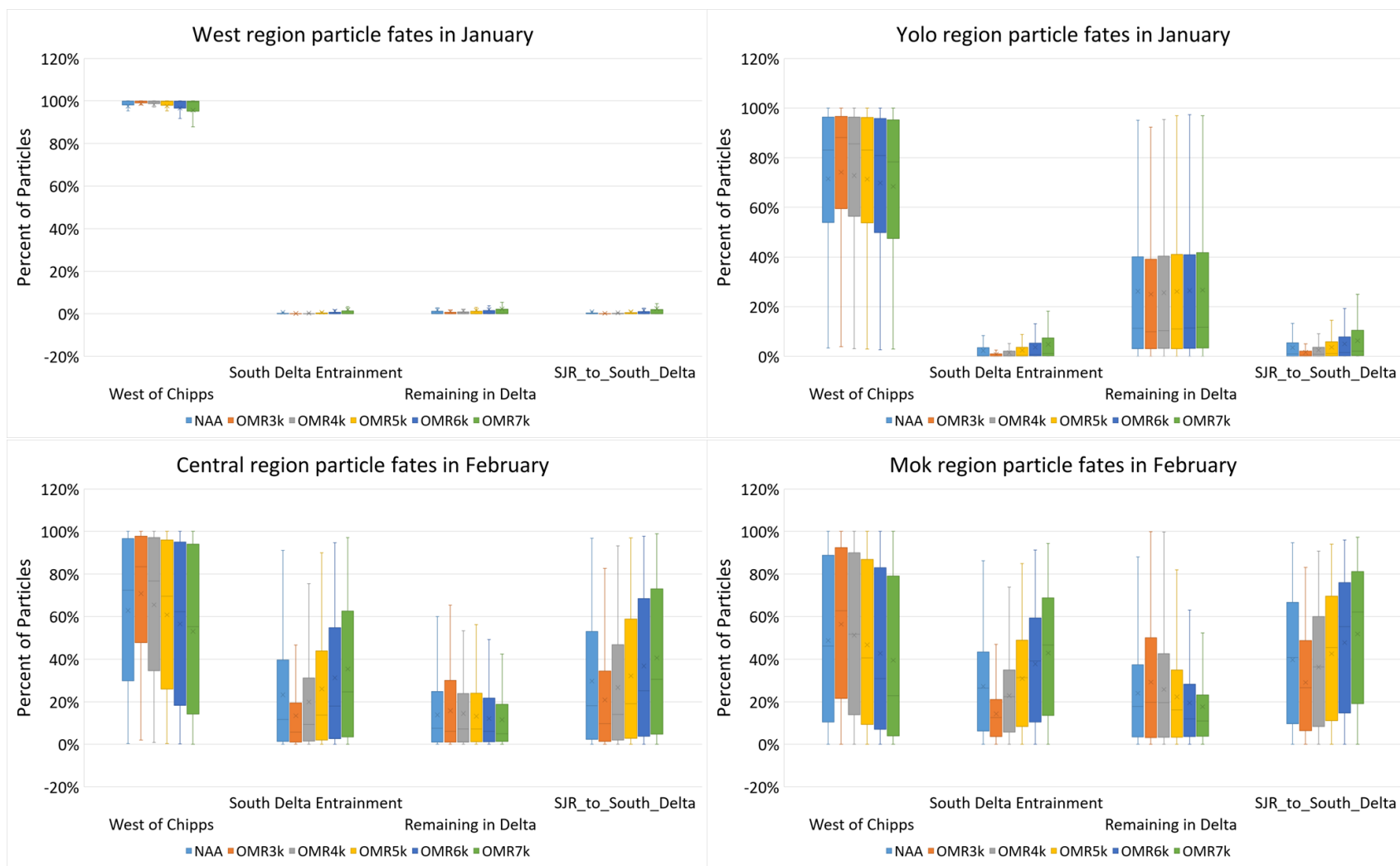
Figure I.1-14. Proportion of Simulations with 10 Percent of Particles Entrained at Export Facilities in December, 45-days after Insertion

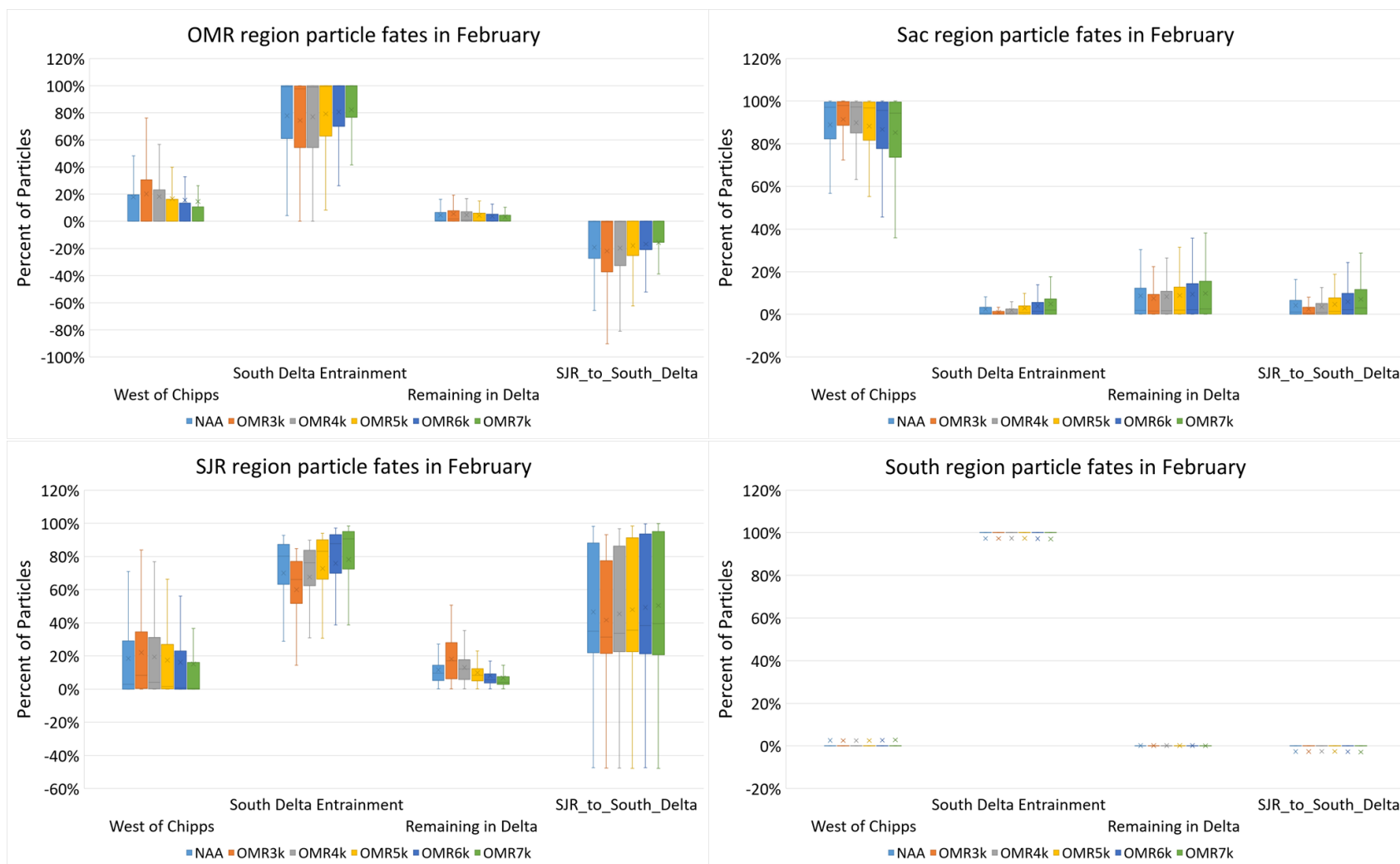




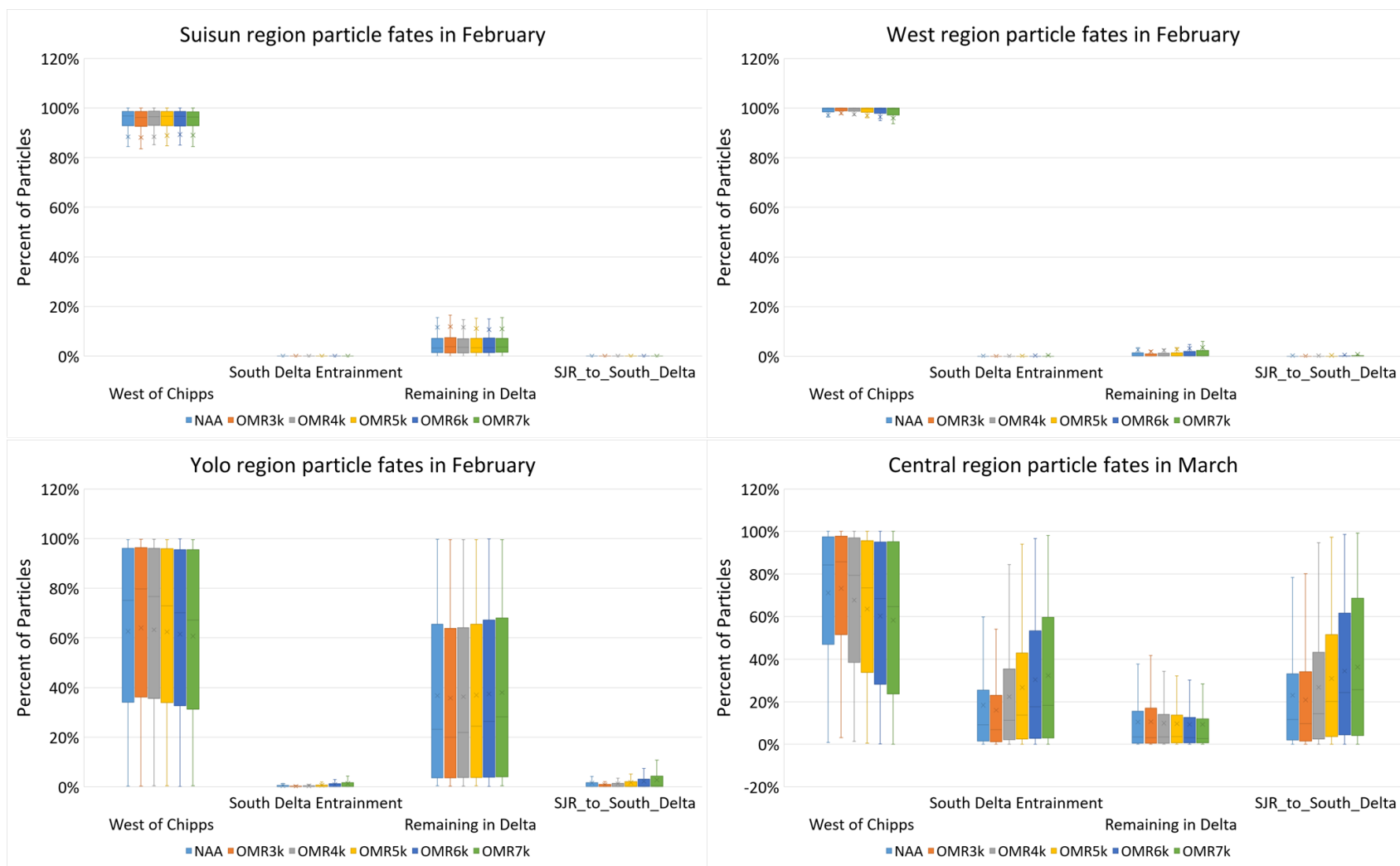


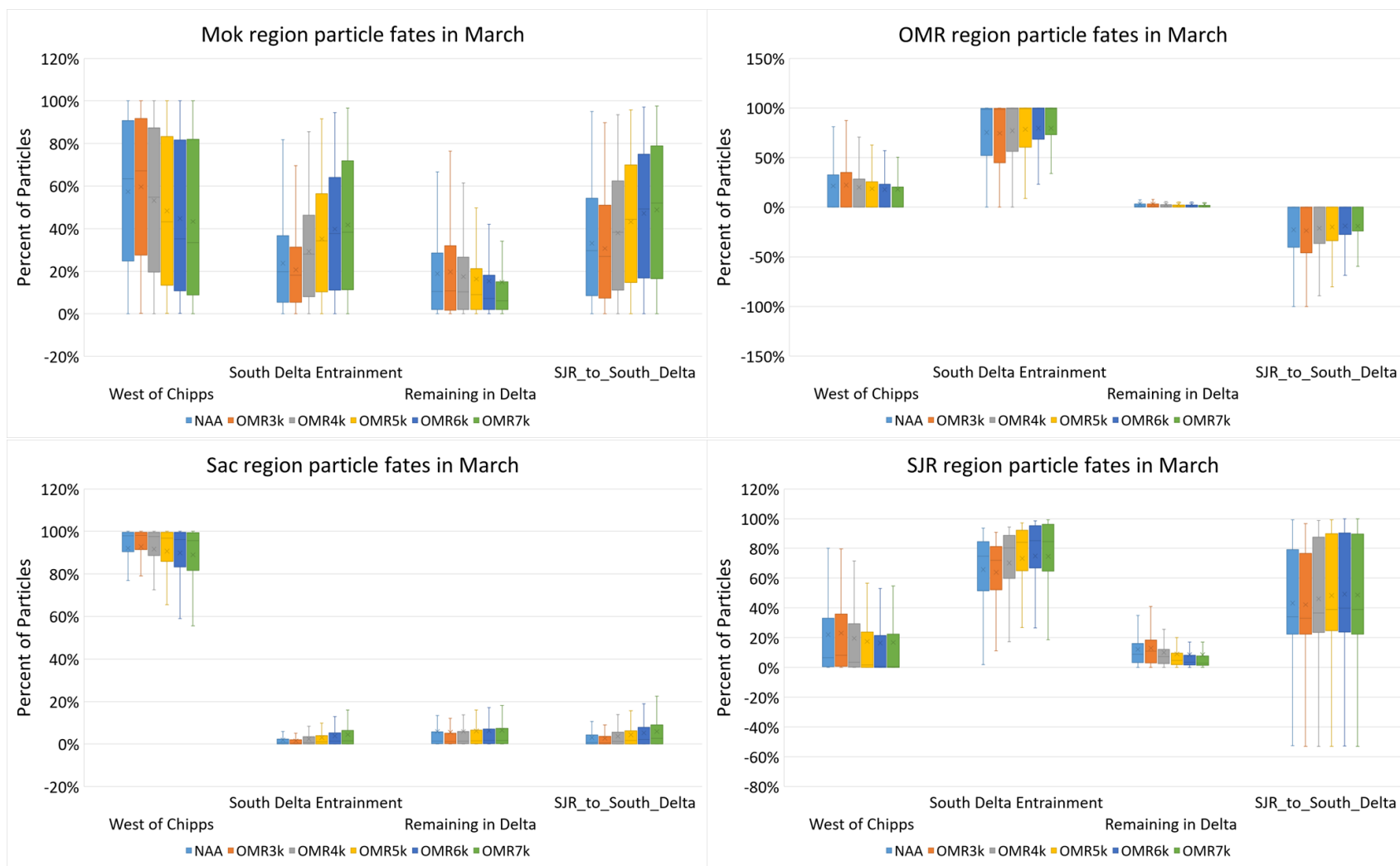


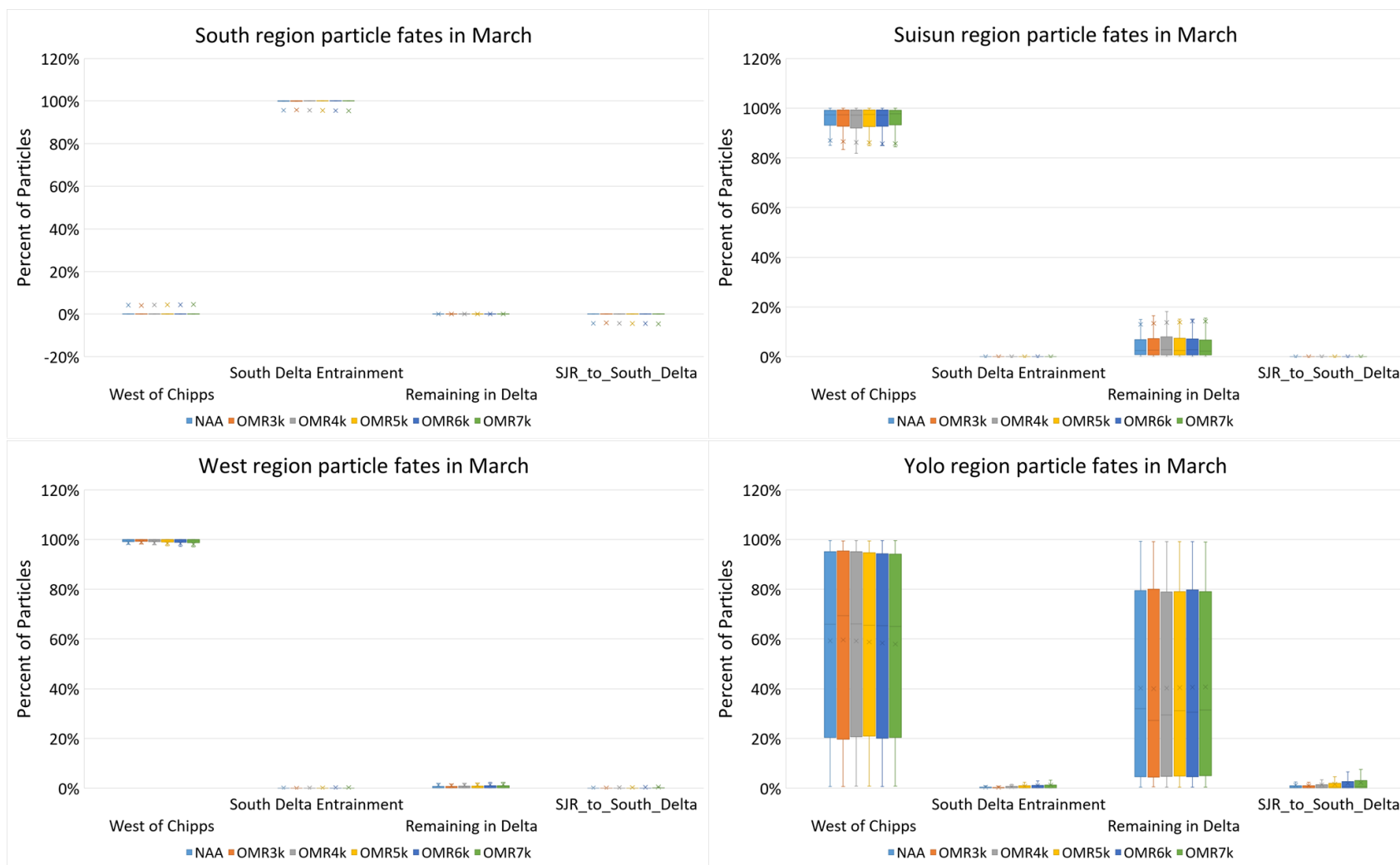












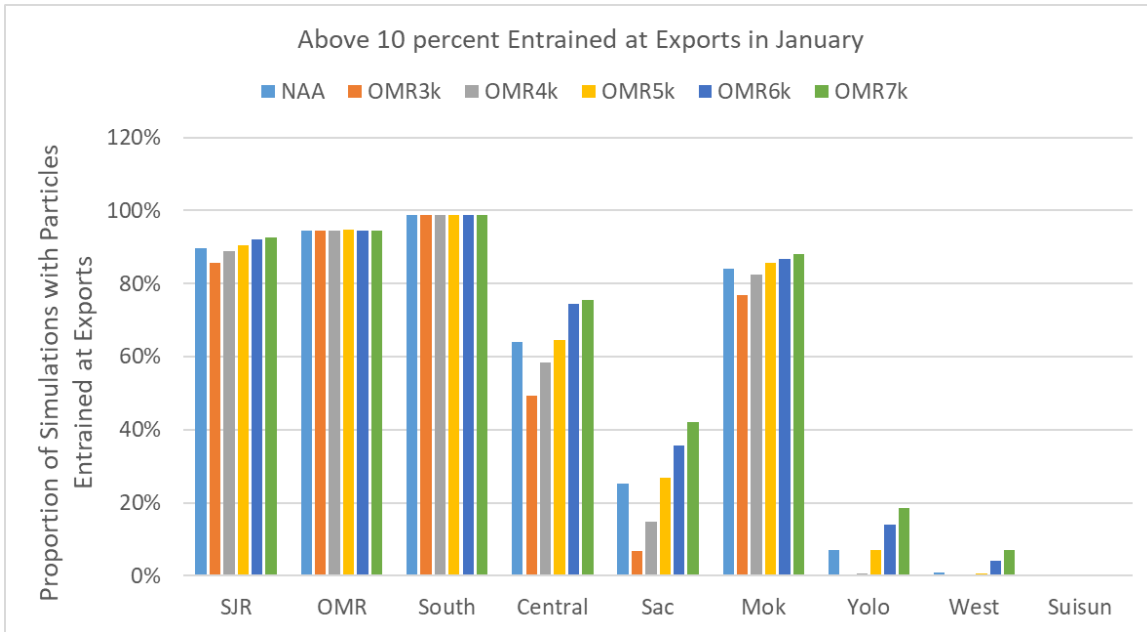


Figure I.1-15. Proportion of Simulations with Particles Entrained at Export Facilities in January, 45-days after Insertion

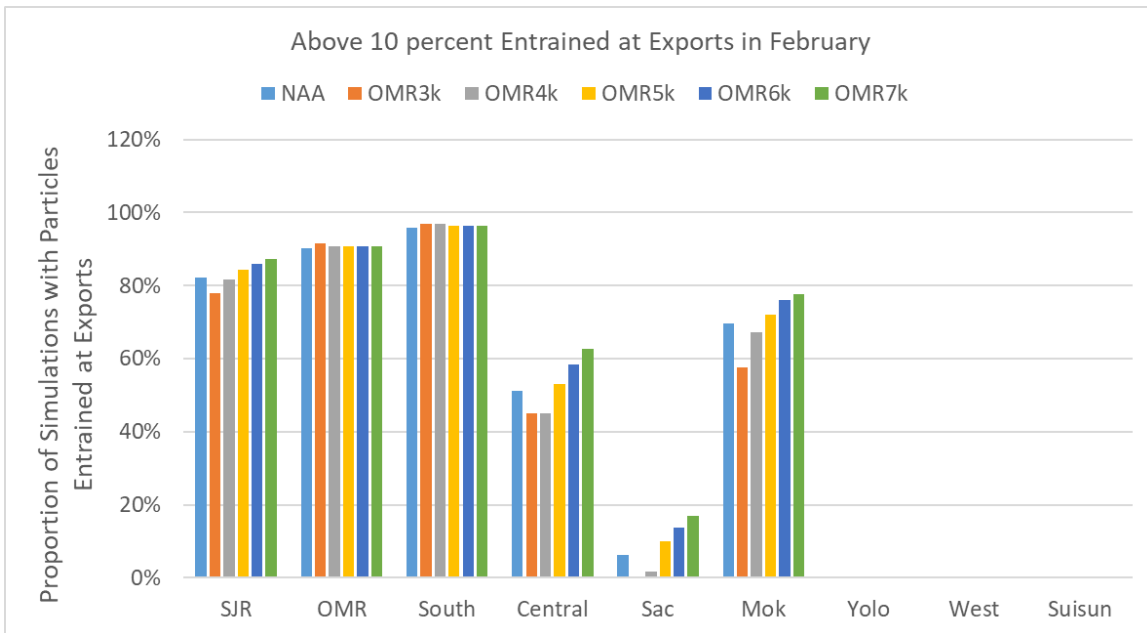


Figure I.1-16. Proportion of Simulations with Particles Entrained at Export Facilities in February, 45-days after Insertion

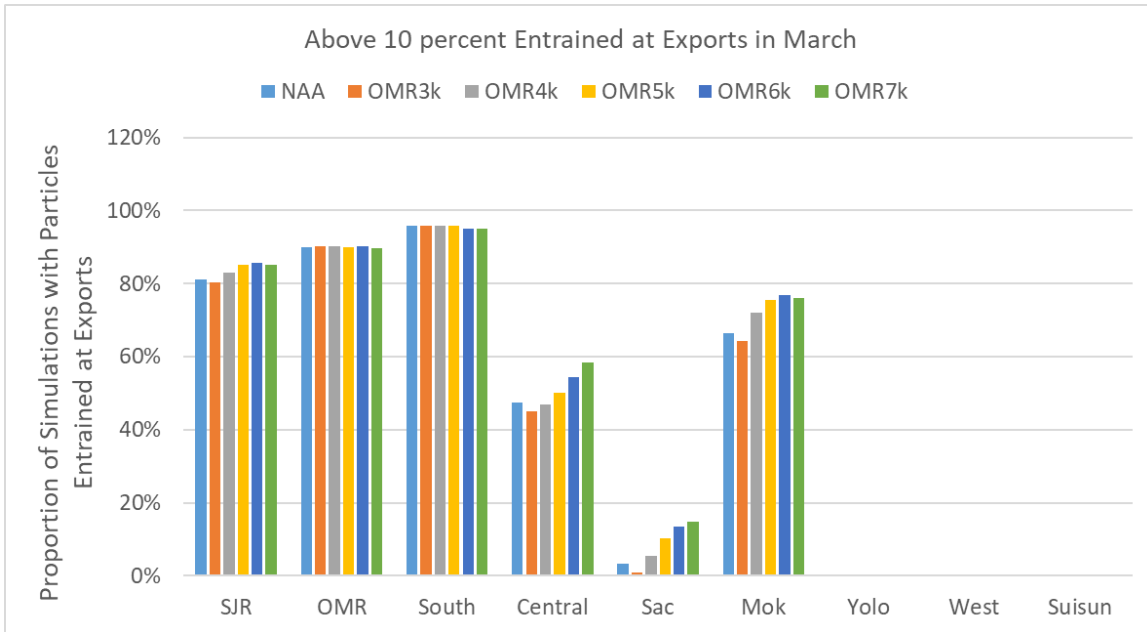


Figure I.1-17. Proportion of Simulations with Particles Entrained at Export Facilities in March, 45-days after Insertion

Identical simulations (same insertion dates and output times) were conducted with neutrally buoyant particles, as a sensitivity analysis. Exceedance plots of particle entrainment at export facilities for neutrally buoyant particles are presented in Figures I.1-14 through I.1-17. Although there are slight variations in results, the conclusions based on the neutrally buoyant particles are consistent with the surface-oriented particles.

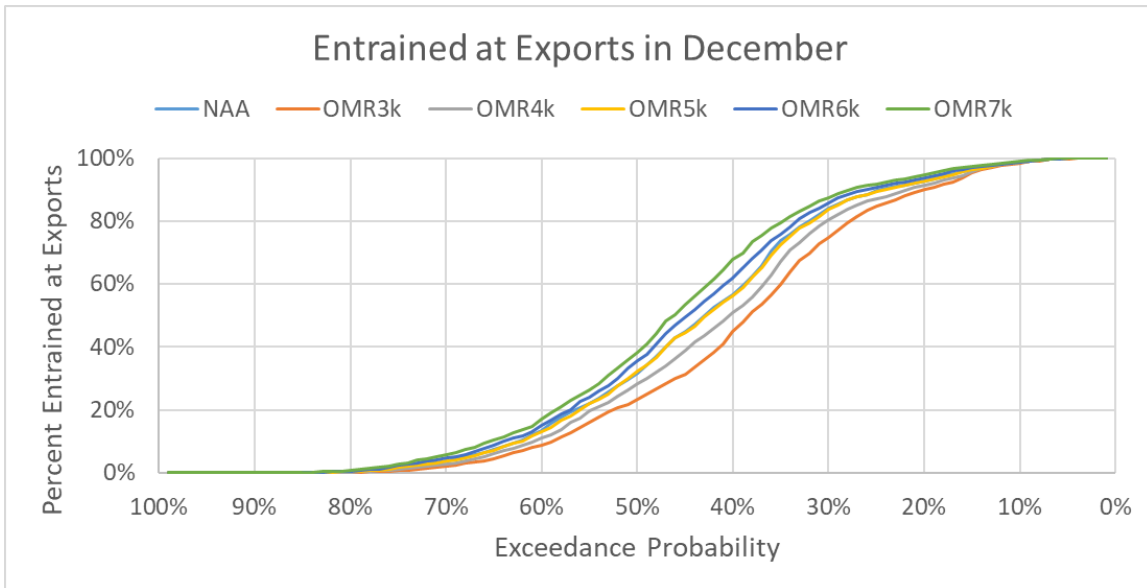


Figure I.1-18. Percent of Neutrally Buoyant Particles Entrained at Exports in December, 45-days after Insertion

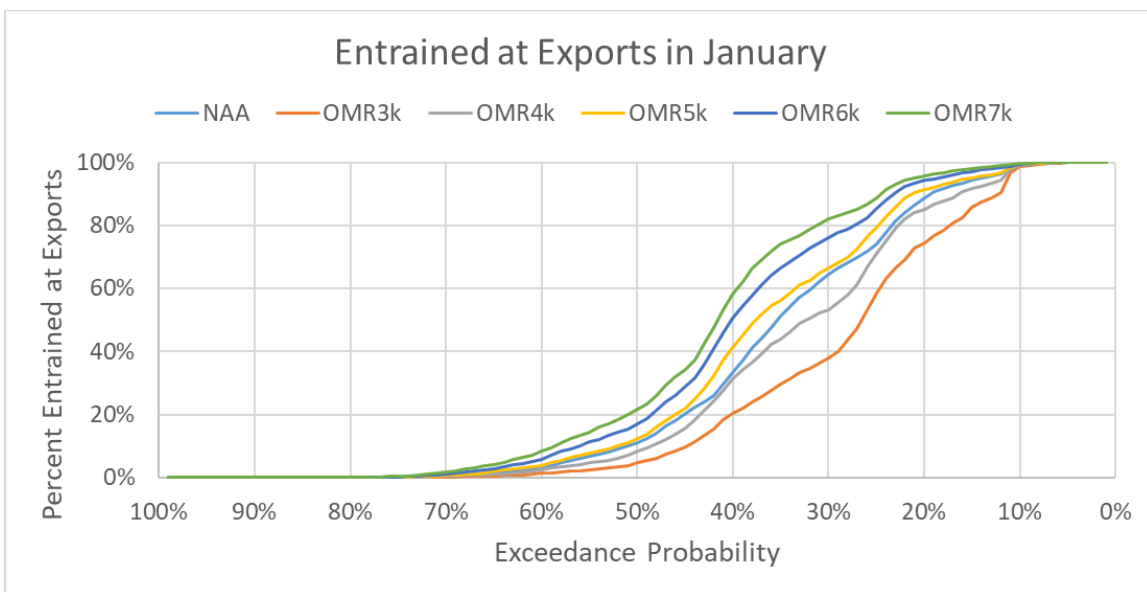


Figure I.1-19. Percent of Neutrally Buoyant Particles Entrained at Exports in January, 45-days after Insertion

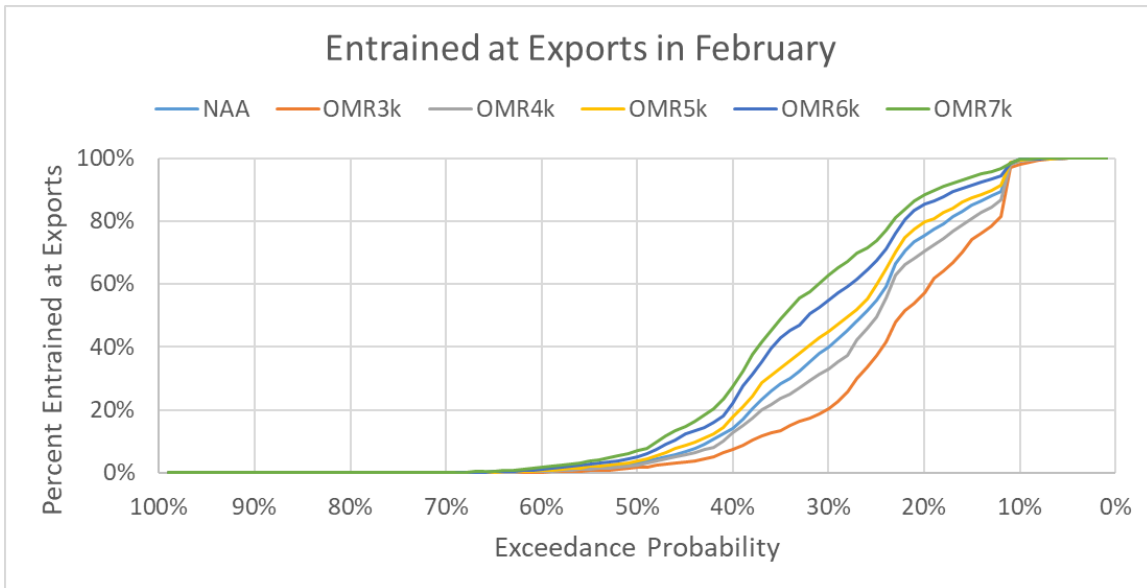


Figure I.1-20. Percent of Neutrally Buoyant Particles Entrained at Exports in February, 45-days after Insertion

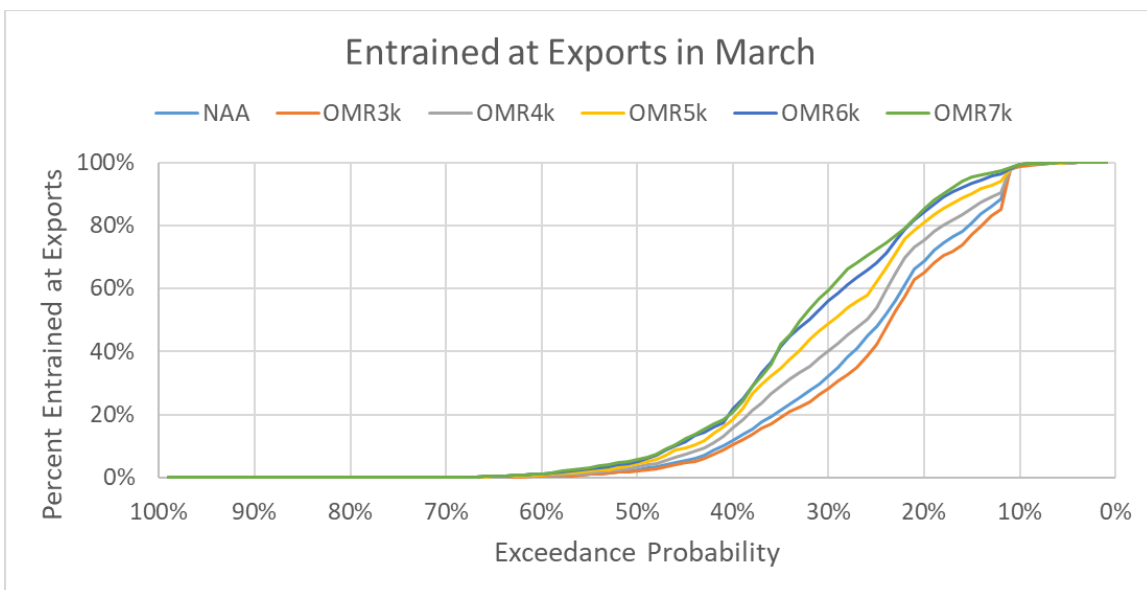


Figure I.1-21. Percent of Neutrally Buoyant Particles Entrained at Exports in March, 45-days after Insertion

### I.1.2.2 Larval Delta Smelt

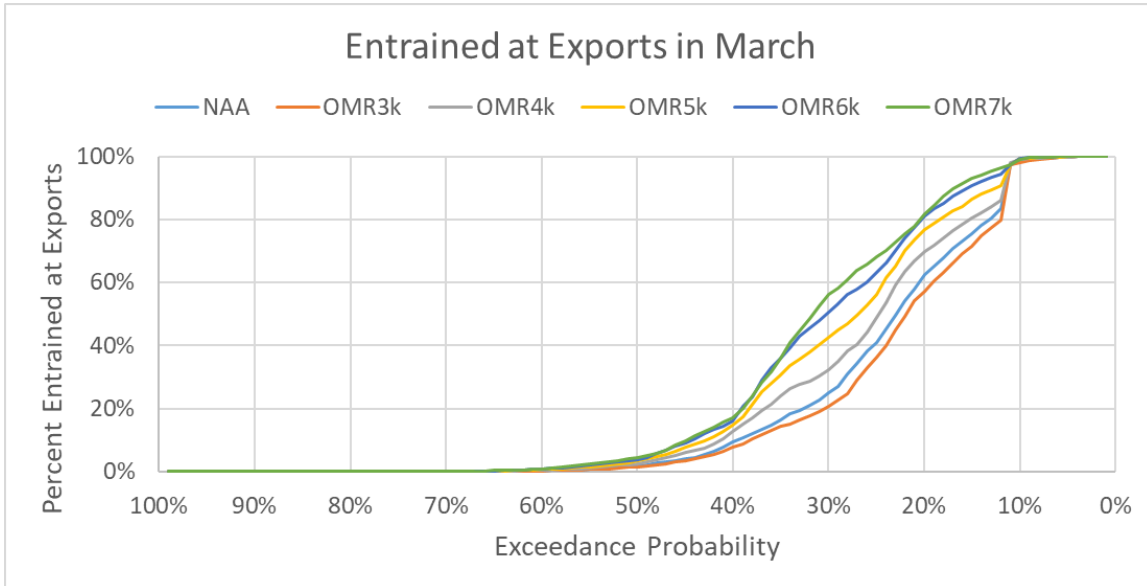


Figure I.1-22. Percent of Neutrally Buoyant Particles Entrained at Exports in March, 30 days after Insertion

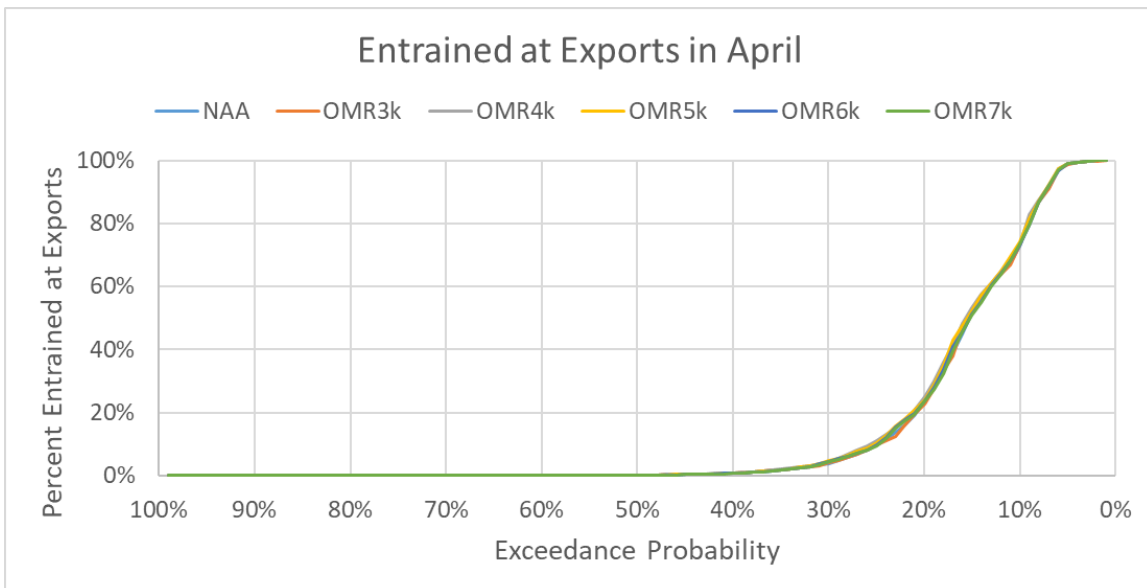


Figure I.1-23. Percent of Neutrally Buoyant Particles Entrained at Exports in April, 30 days after Insertion



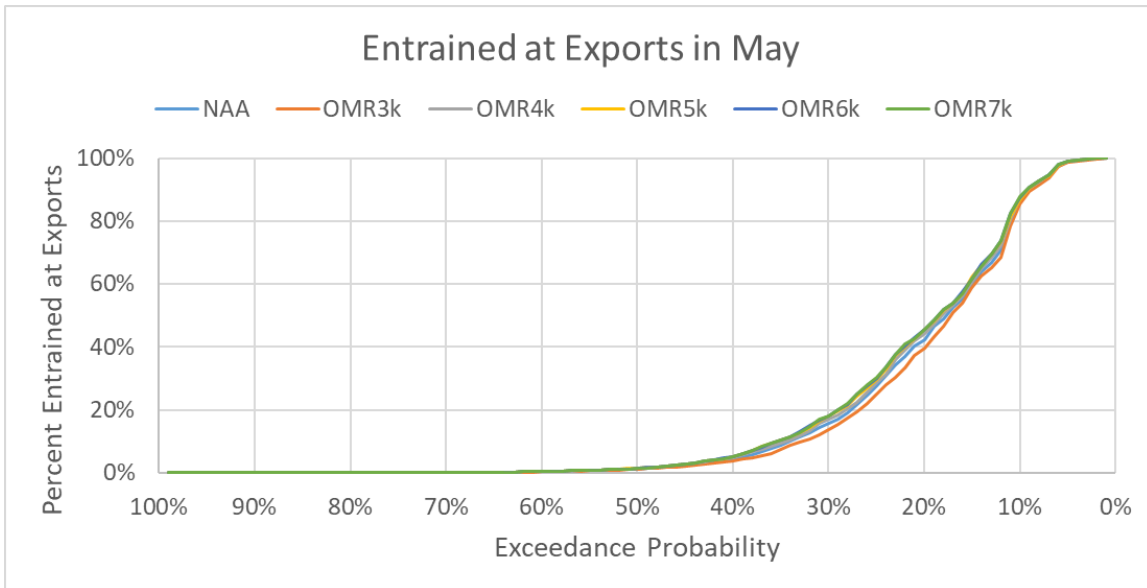


Figure I.1-24. Percent of Neutrally Buoyant Particles Entrained at Exports in May, 30 days after Insertion

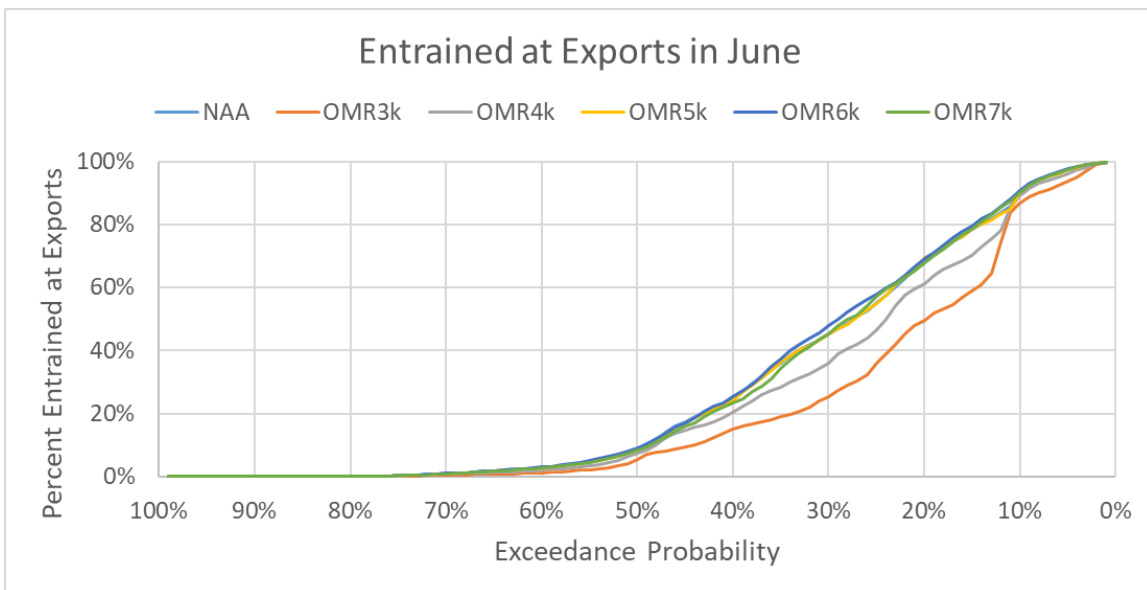


Figure I.1-25. Percent of Neutrally Buoyant Particles Entrained at Exports in June, 30 days after Insertion

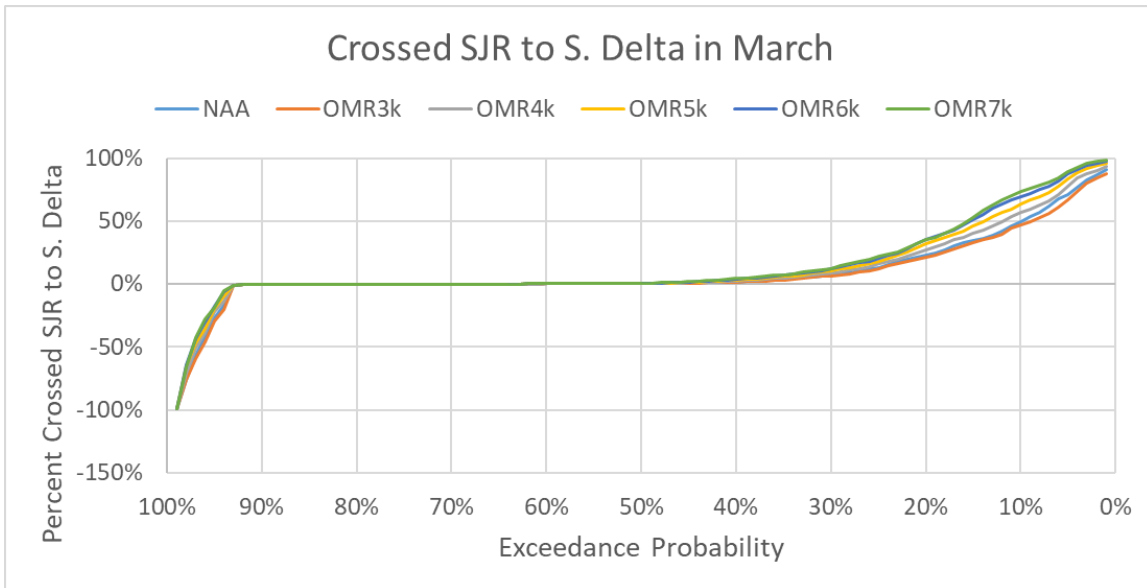


Figure I.1-26. Percent of Neutrally Buoyant Particles Crossing the San Joaquin River in March, 30 days after Insertion

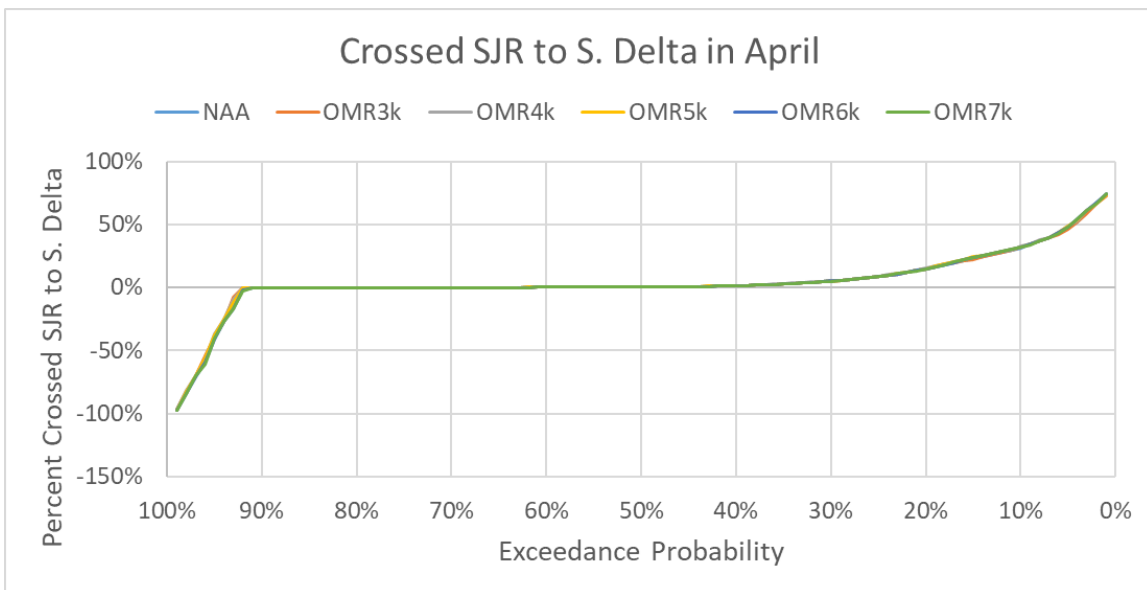


Figure I.1-27. Percent of Neutrally Buoyant Particles Crossing the San Joaquin River in April, 30 days after Insertion

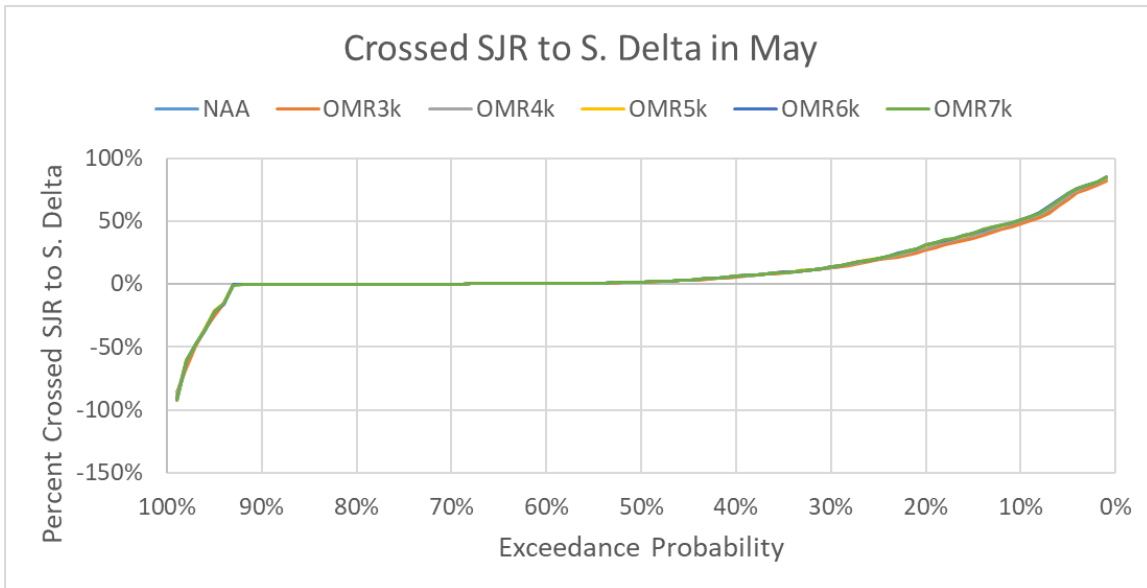


Figure I.1-28. Percent of Neutrally Buoyant Particles Crossing the San Joaquin River in May, 30 days after Insertion

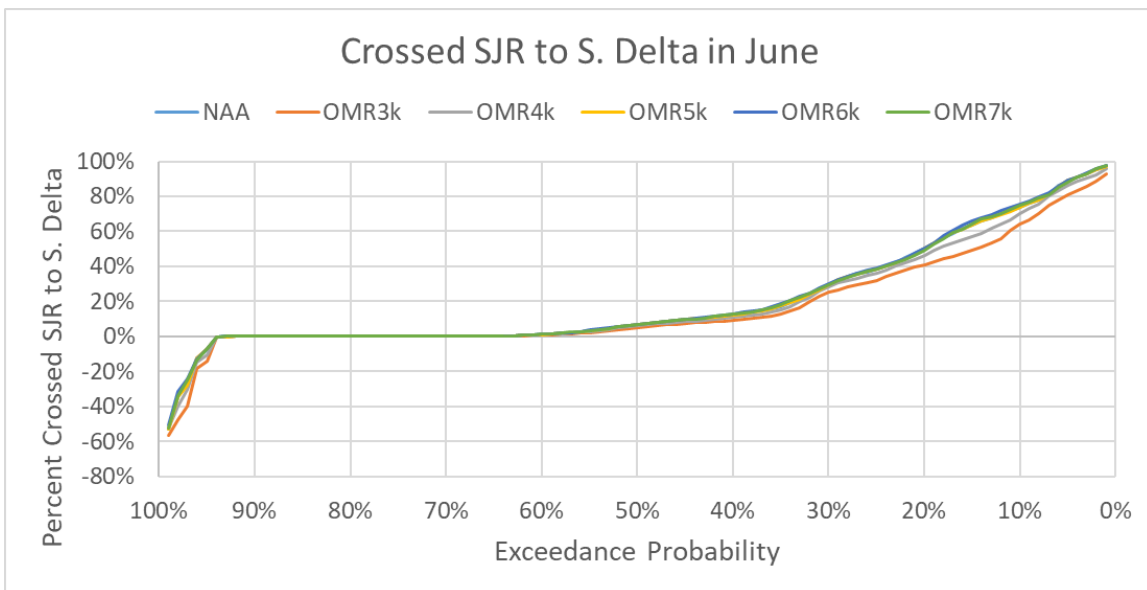


Figure I.1-29. Percent of Neutrally Buoyant Particles Crossing the San Joaquin River in June, 30 days after Insertion

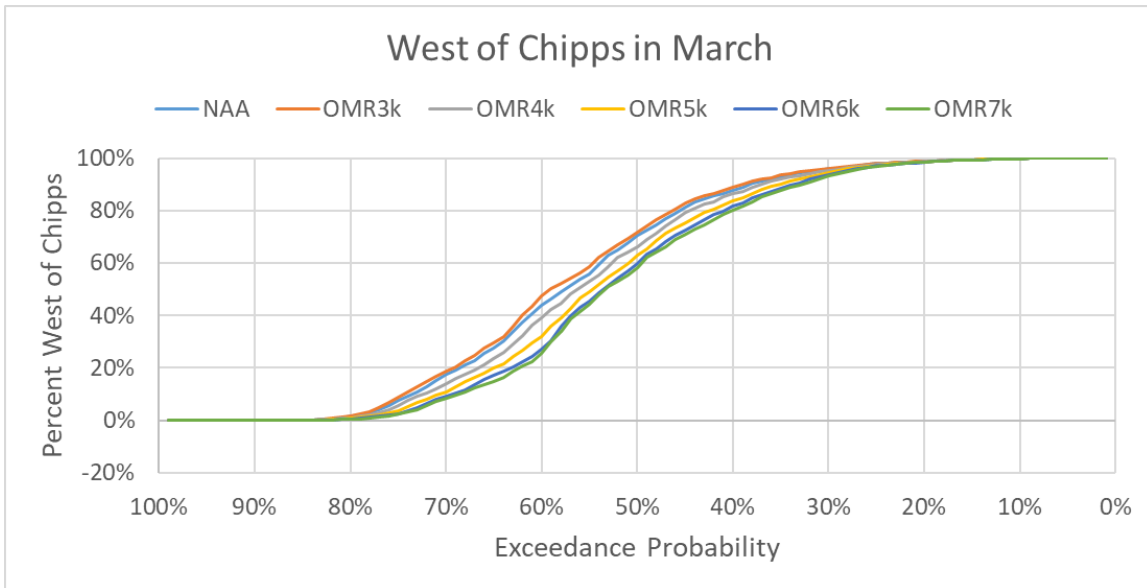


Figure I.1-30. Percent of Neutrally Buoyant Particles West of Chipps in March, 30 days after Insertion

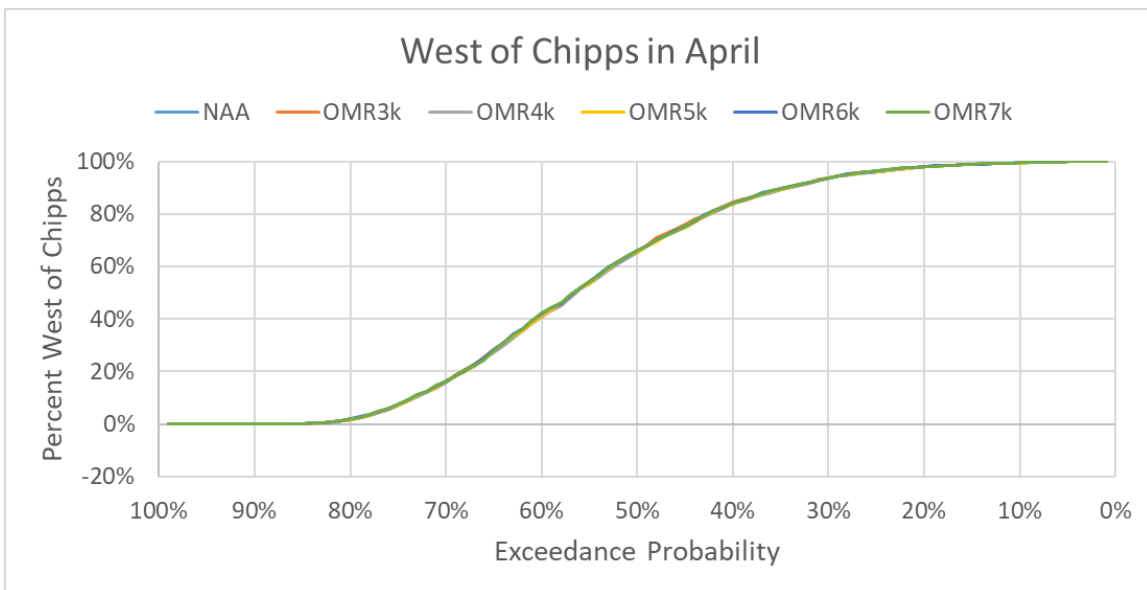


Figure I.1-31. Percent of Neutrally Buoyant Particles West of Chipps in April, 30 days after Insertion

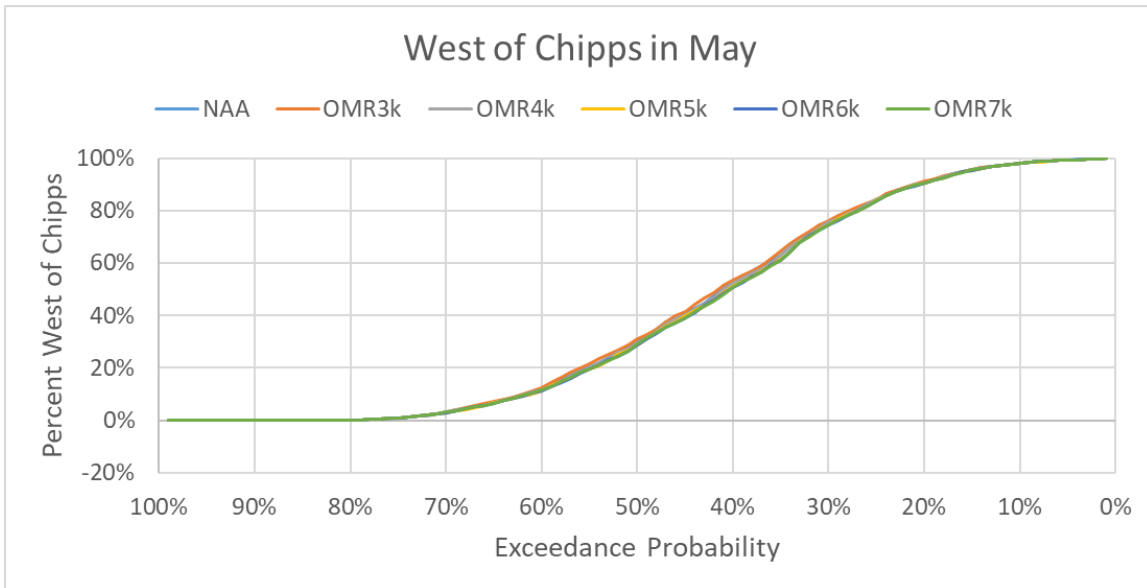


Figure I.1-32. Percent of Neutrally Buoyant Particles West of Chipps in May, 30 days after Insertion

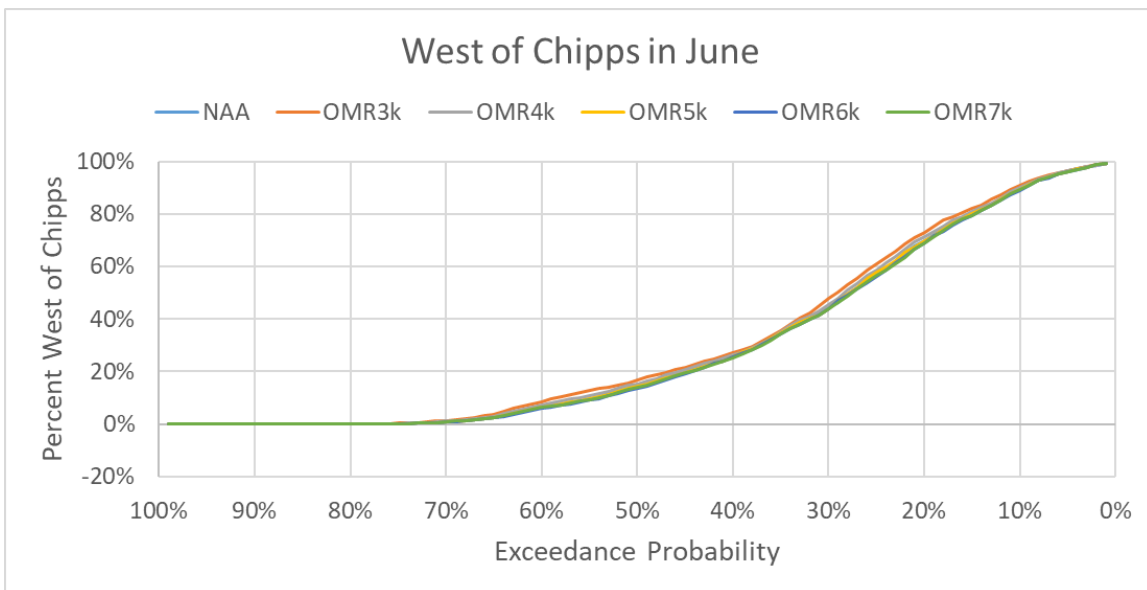


Figure I.1-33. Percent of Neutrally Buoyant Particles West of Chipps in June, 30 days after Insertion

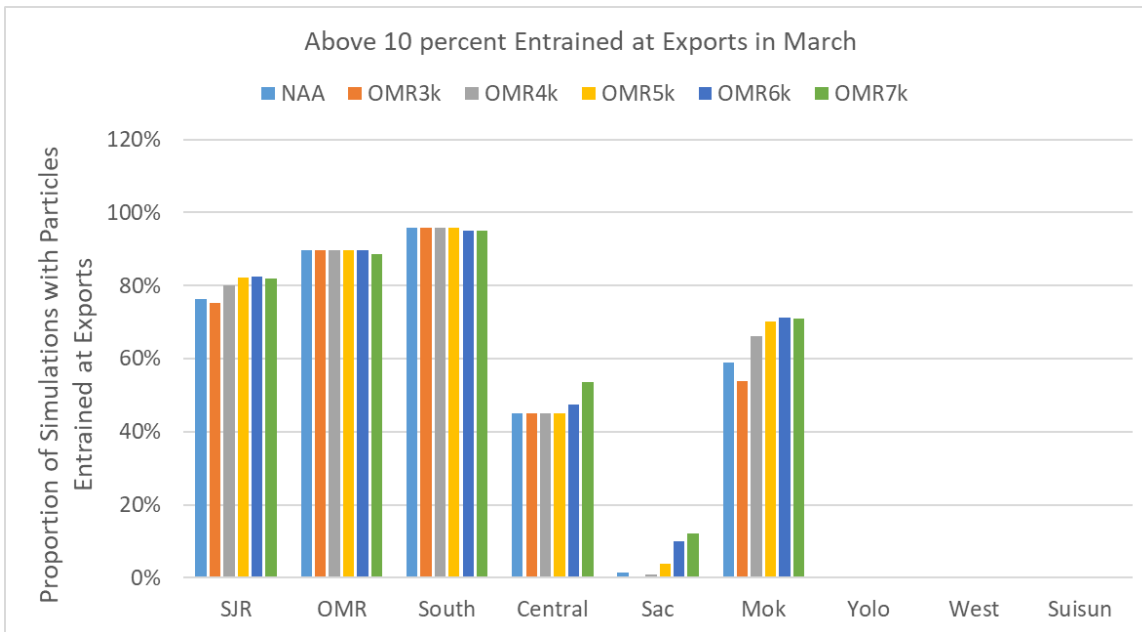


Figure I.1-34. Proportion of Simulations with Particles Entrained at Export Facilities in March, 30 days after Insertion

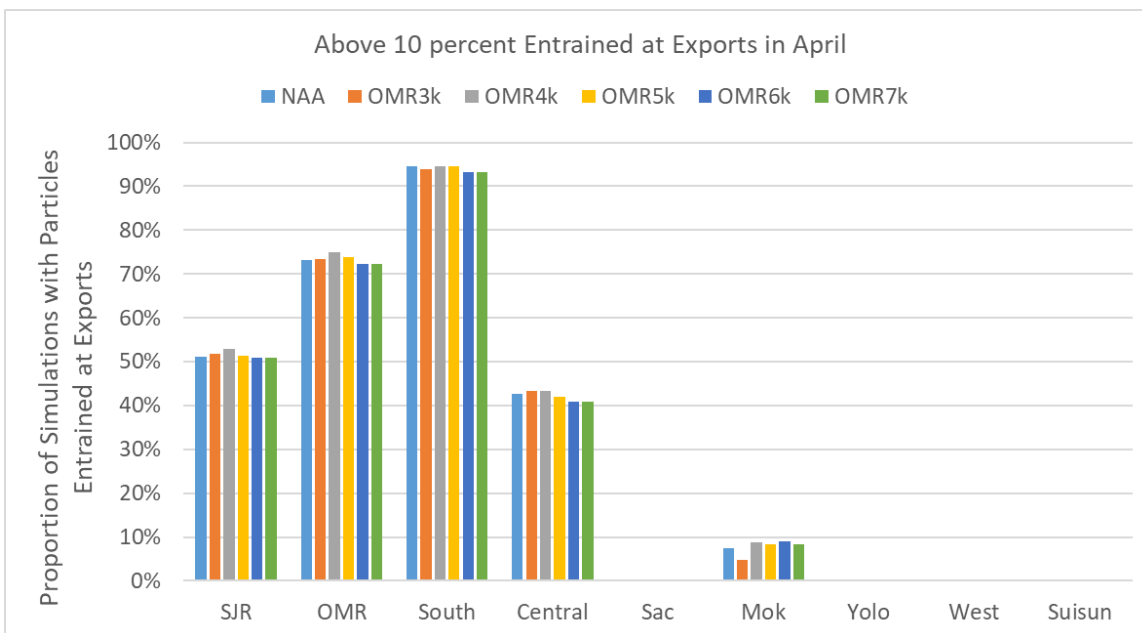


Figure I.1-35. Proportion of Simulations with Particles Entrained at Export Facilities in April, 30 days after Insertion

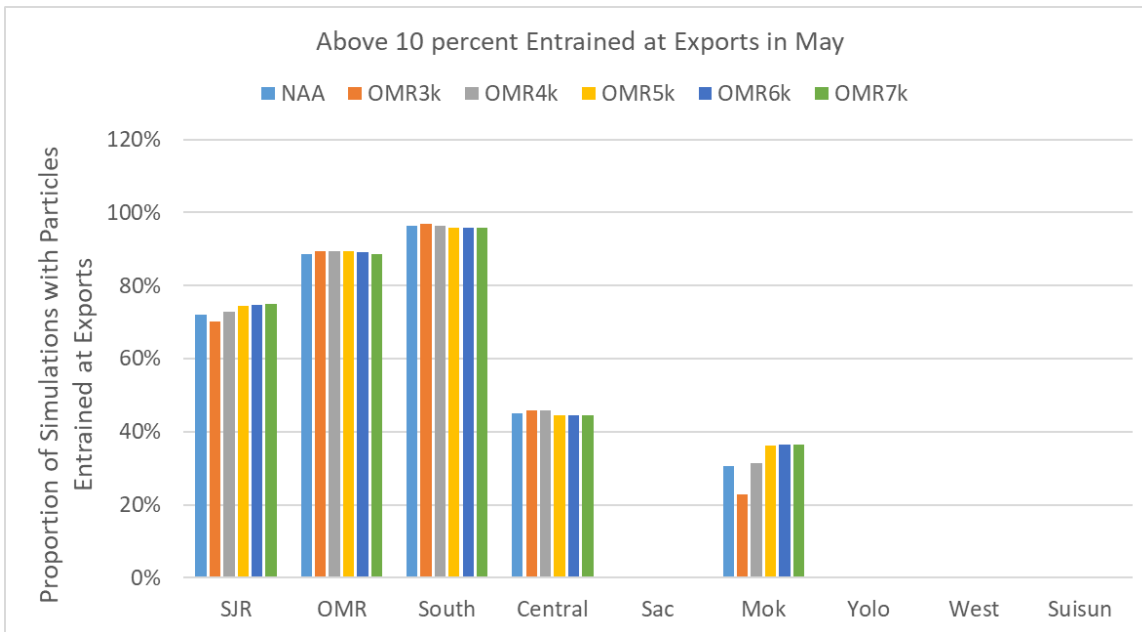


Figure I.1-36. Proportion of Simulations with Particles Entrained at Export Facilities in May, 30 days after Insertion

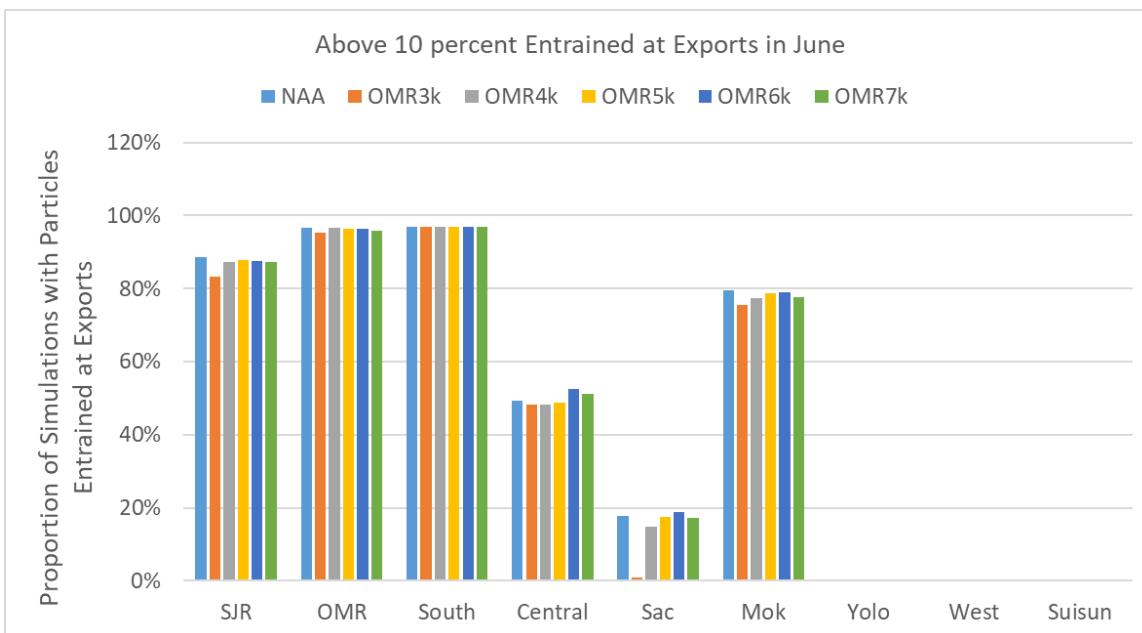
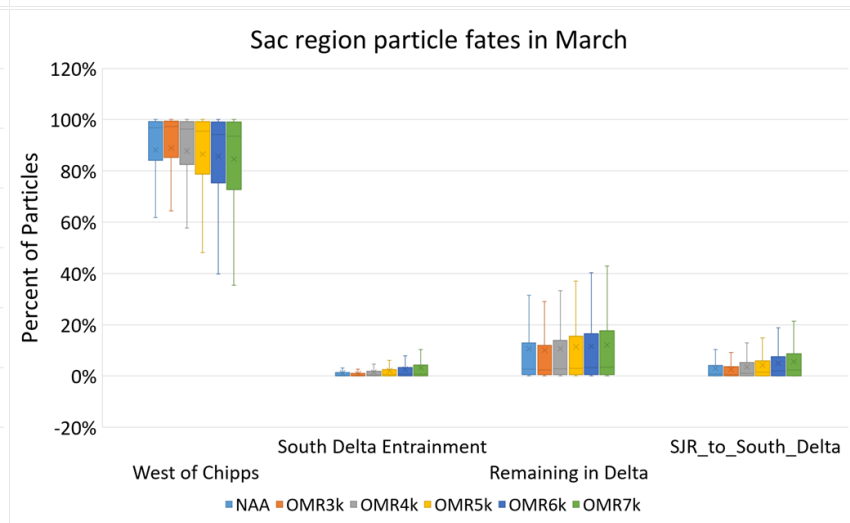
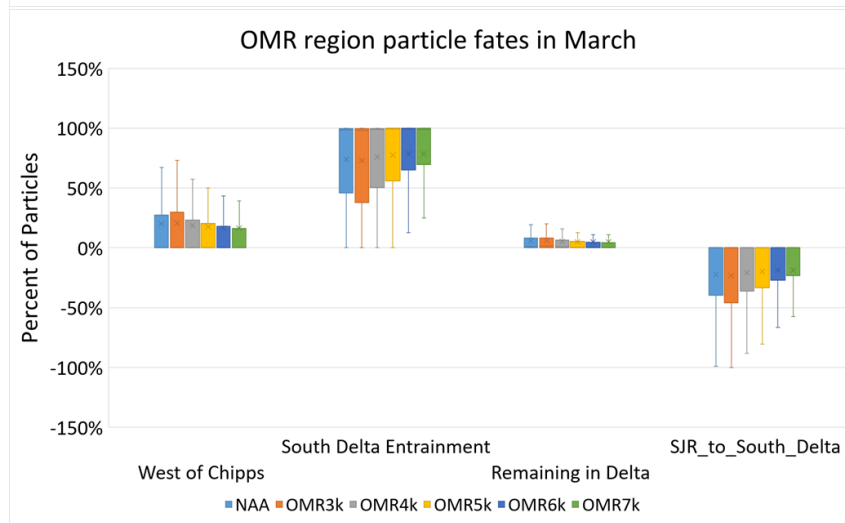
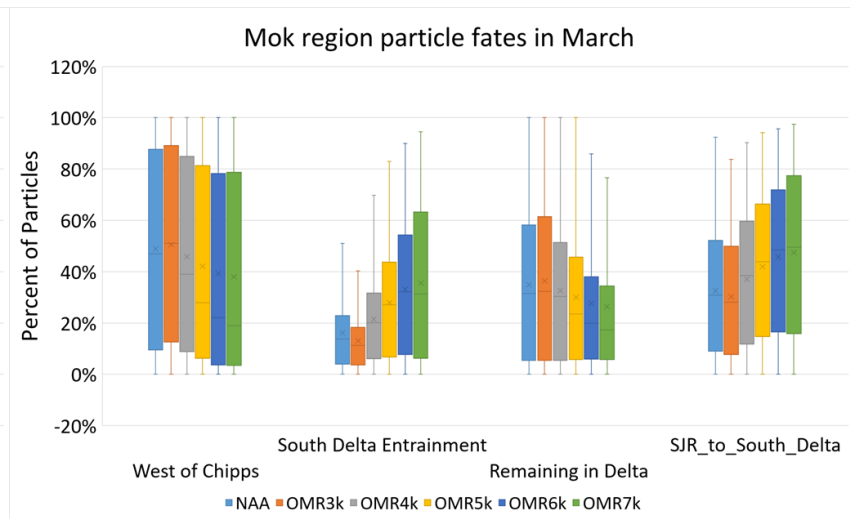
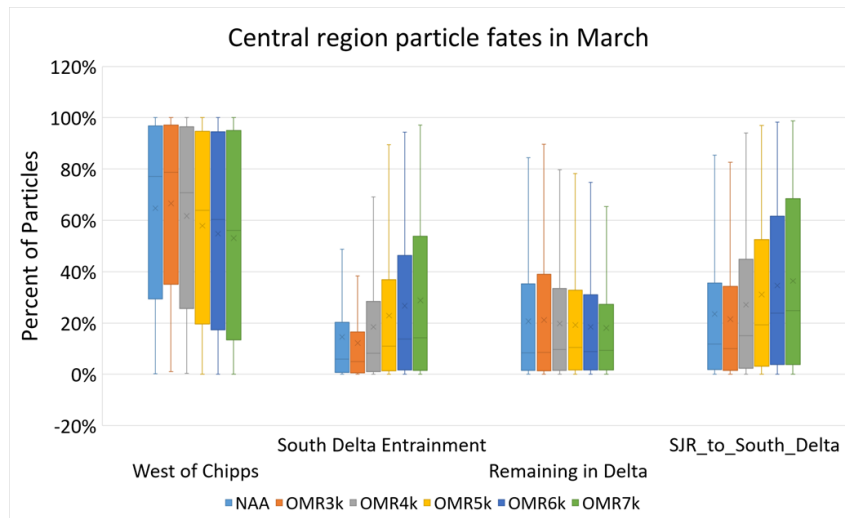
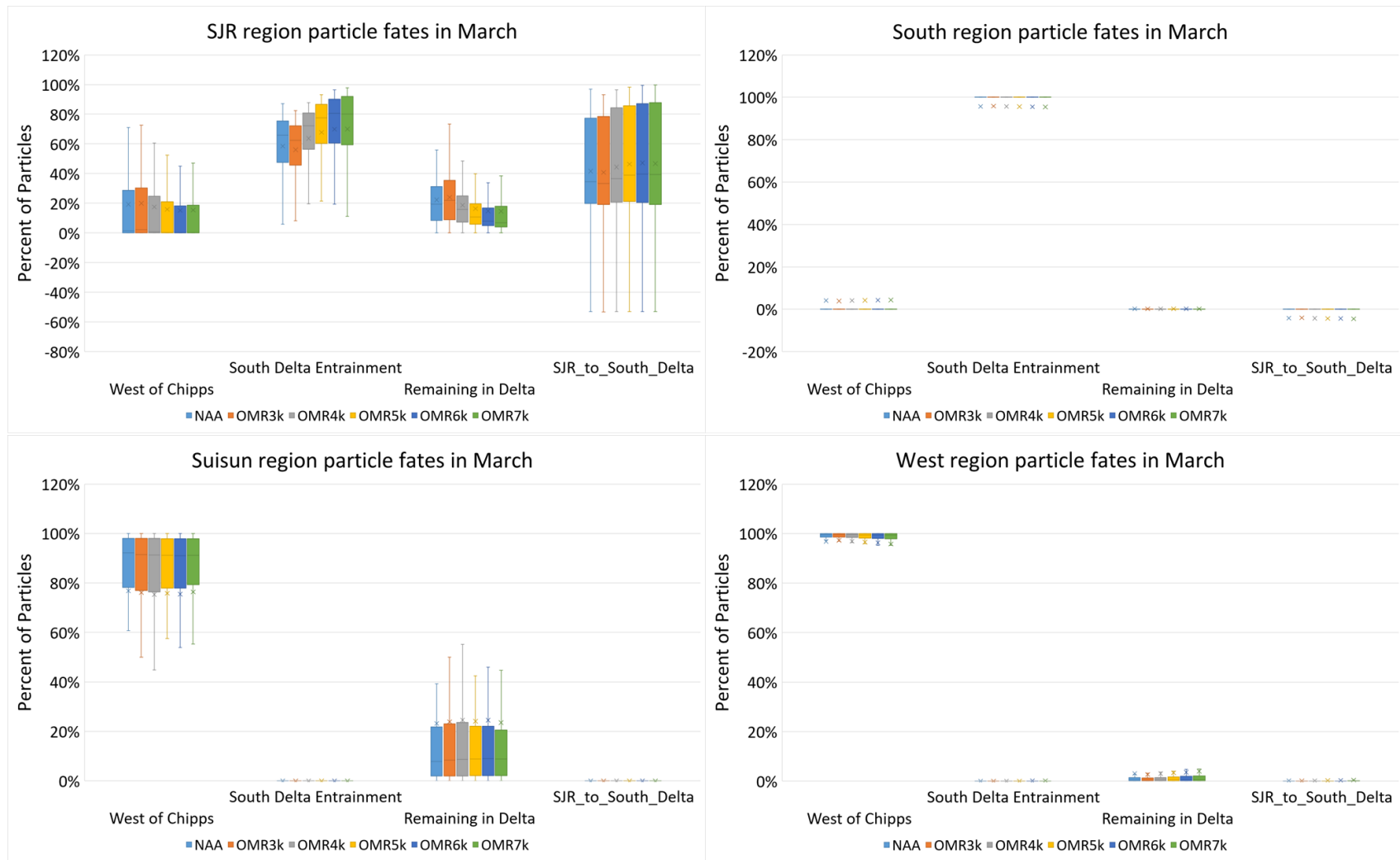
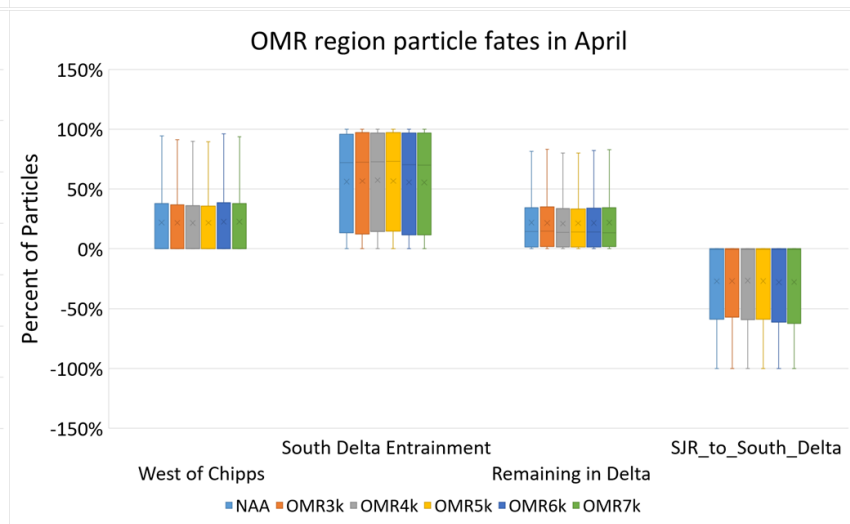
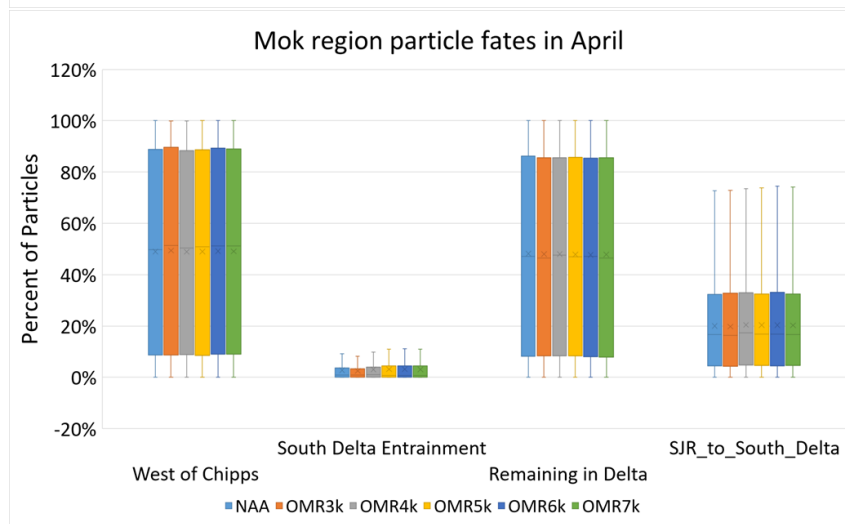
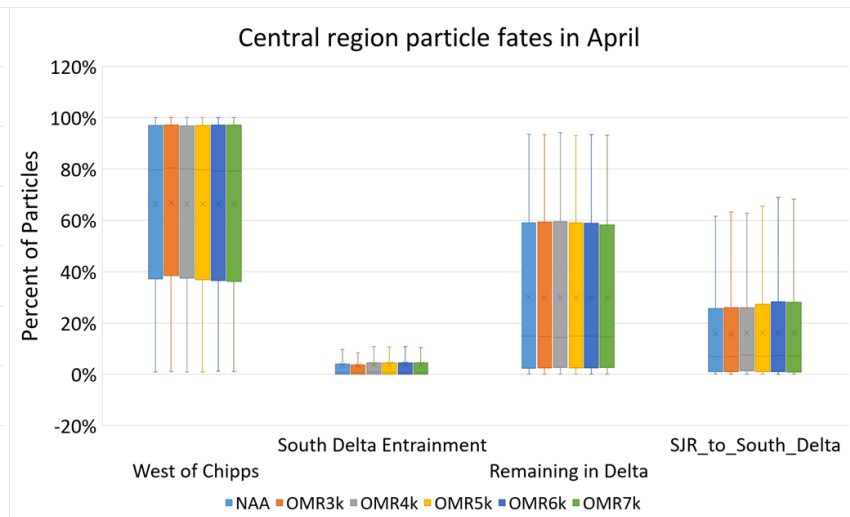
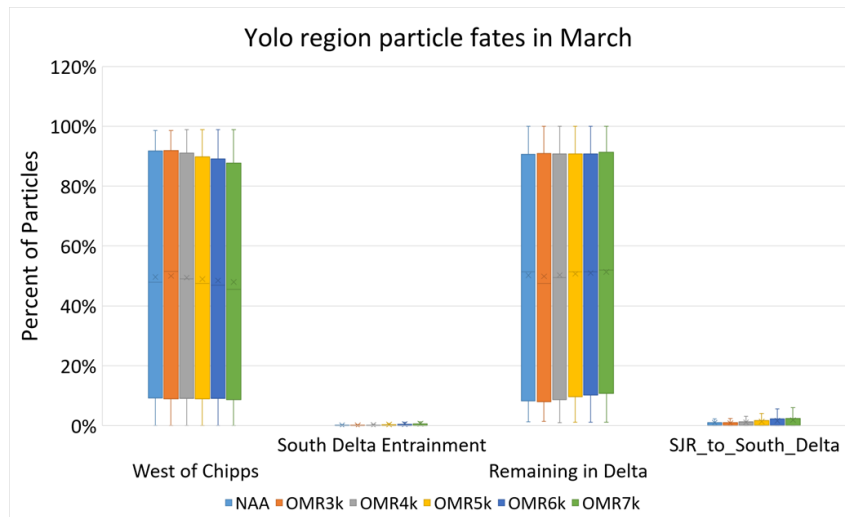


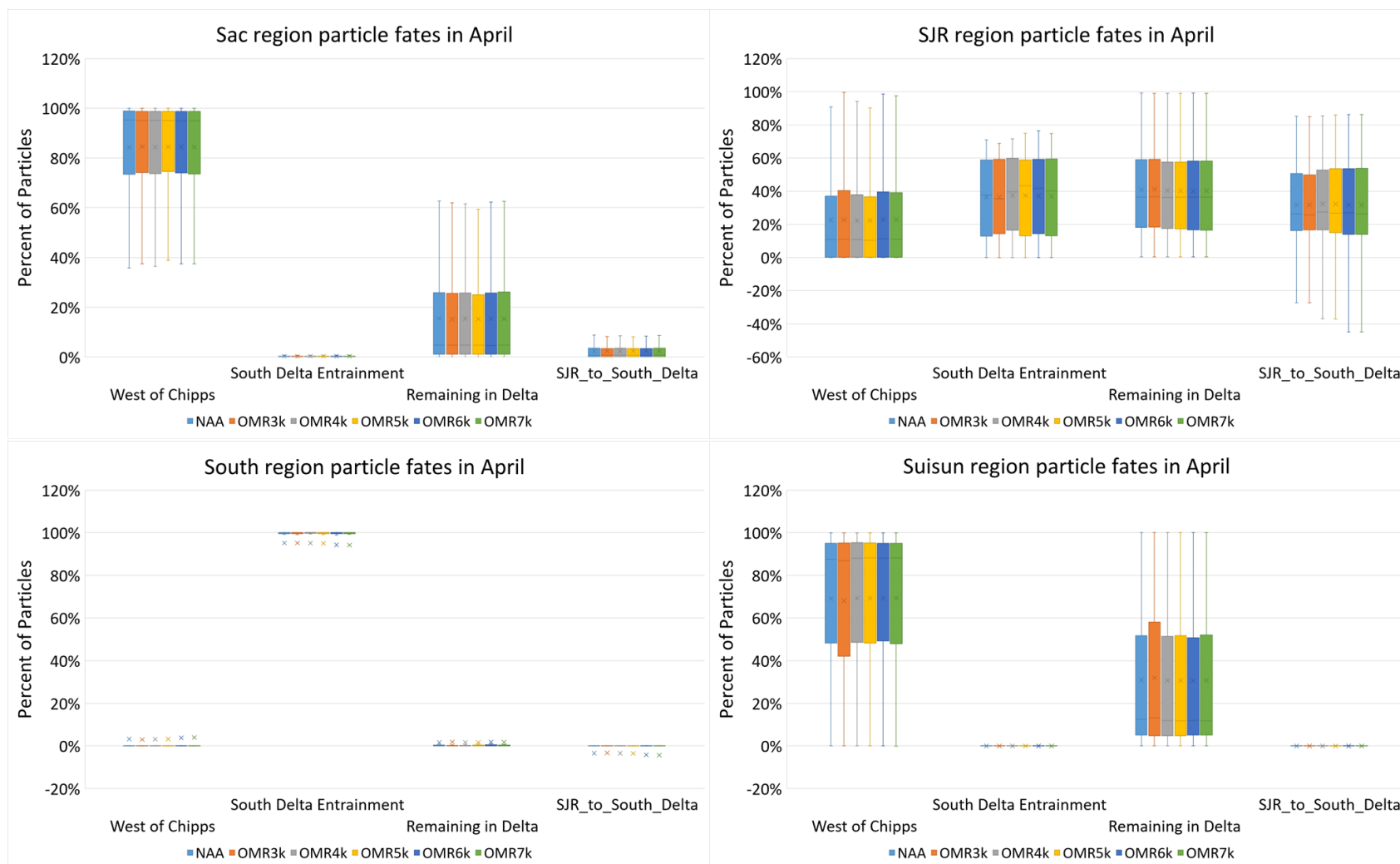
Figure I.1-37. Proportion of Simulations with Particles Entrained at Export Facilities in June, 30 days after Insertion

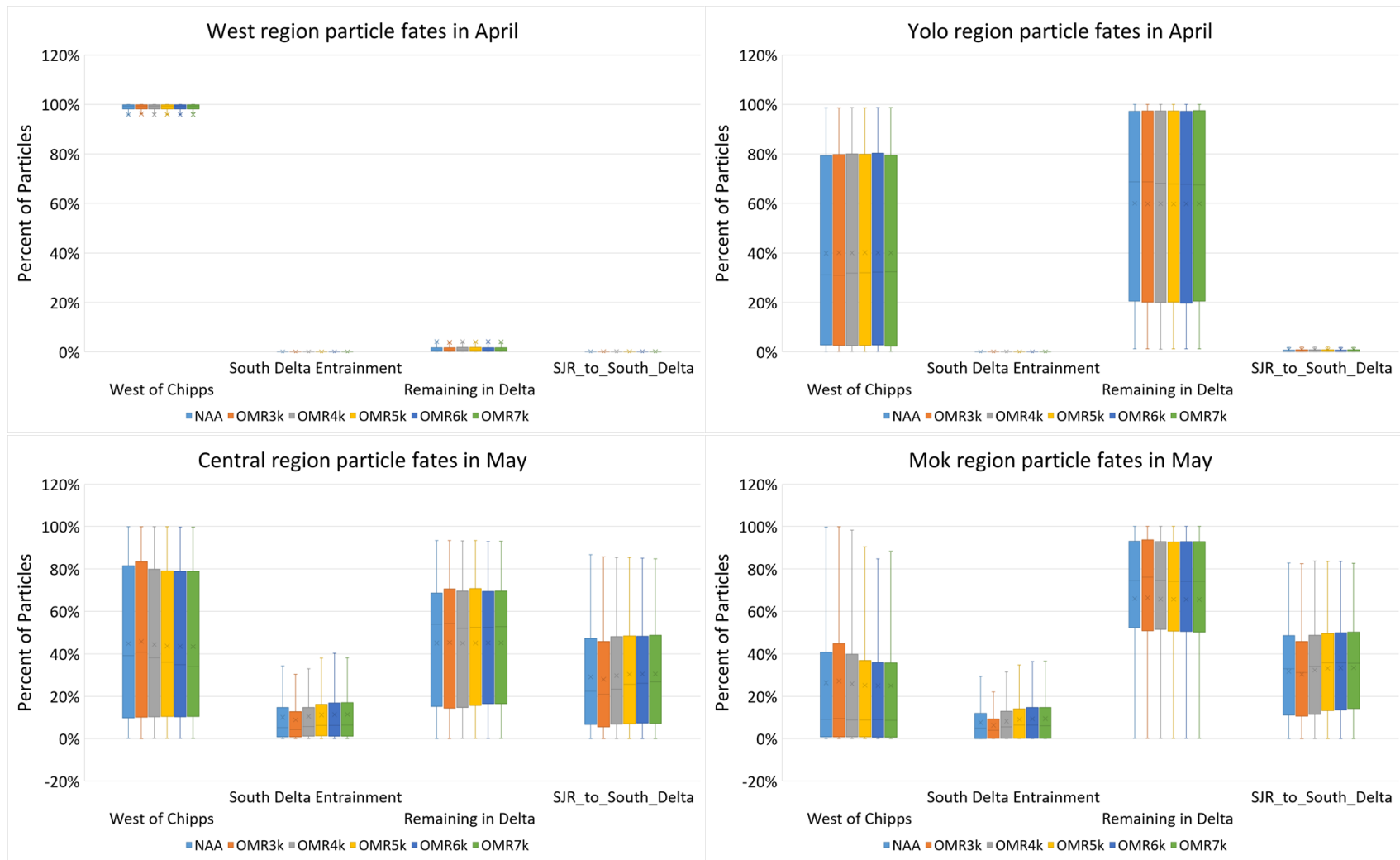


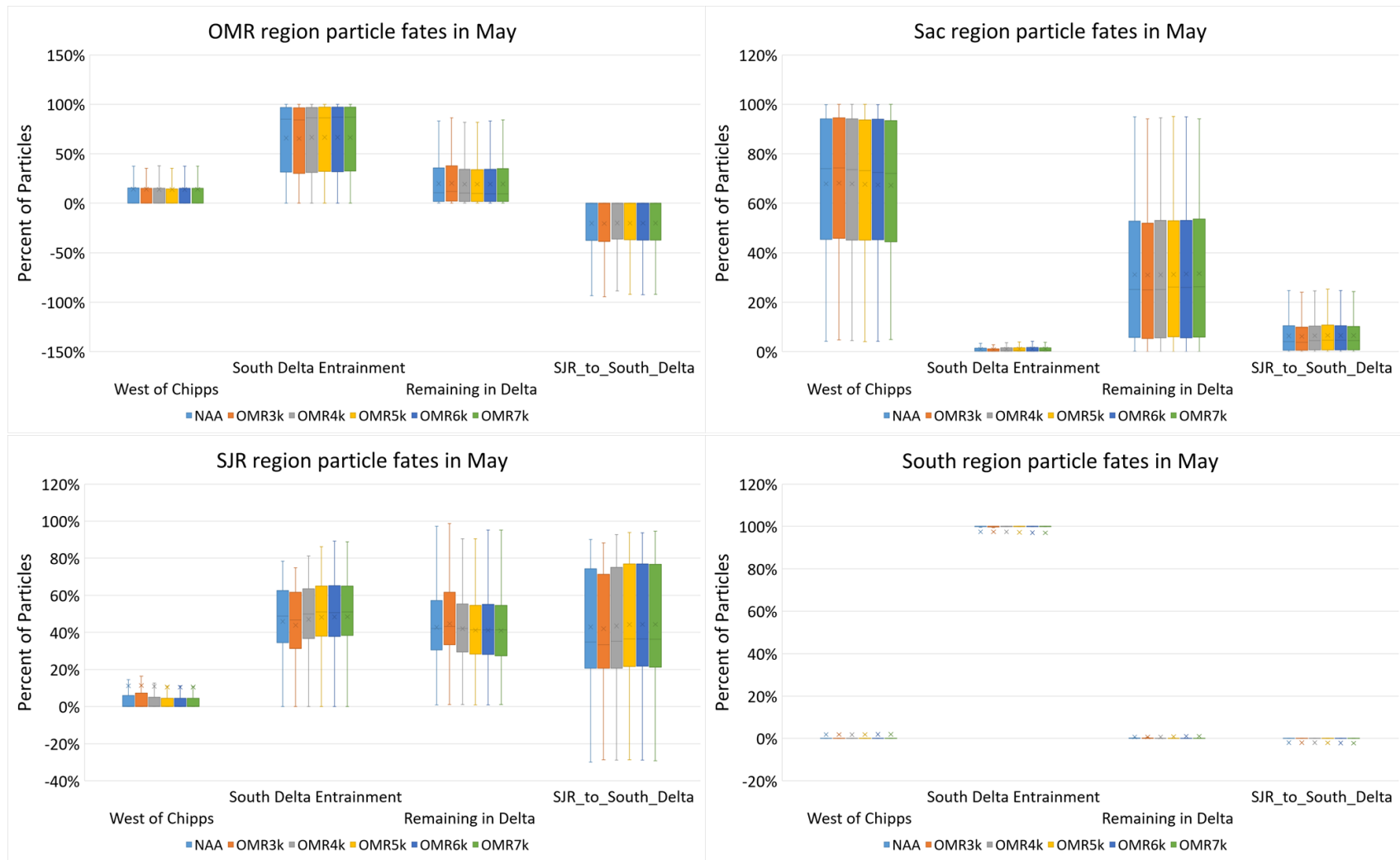


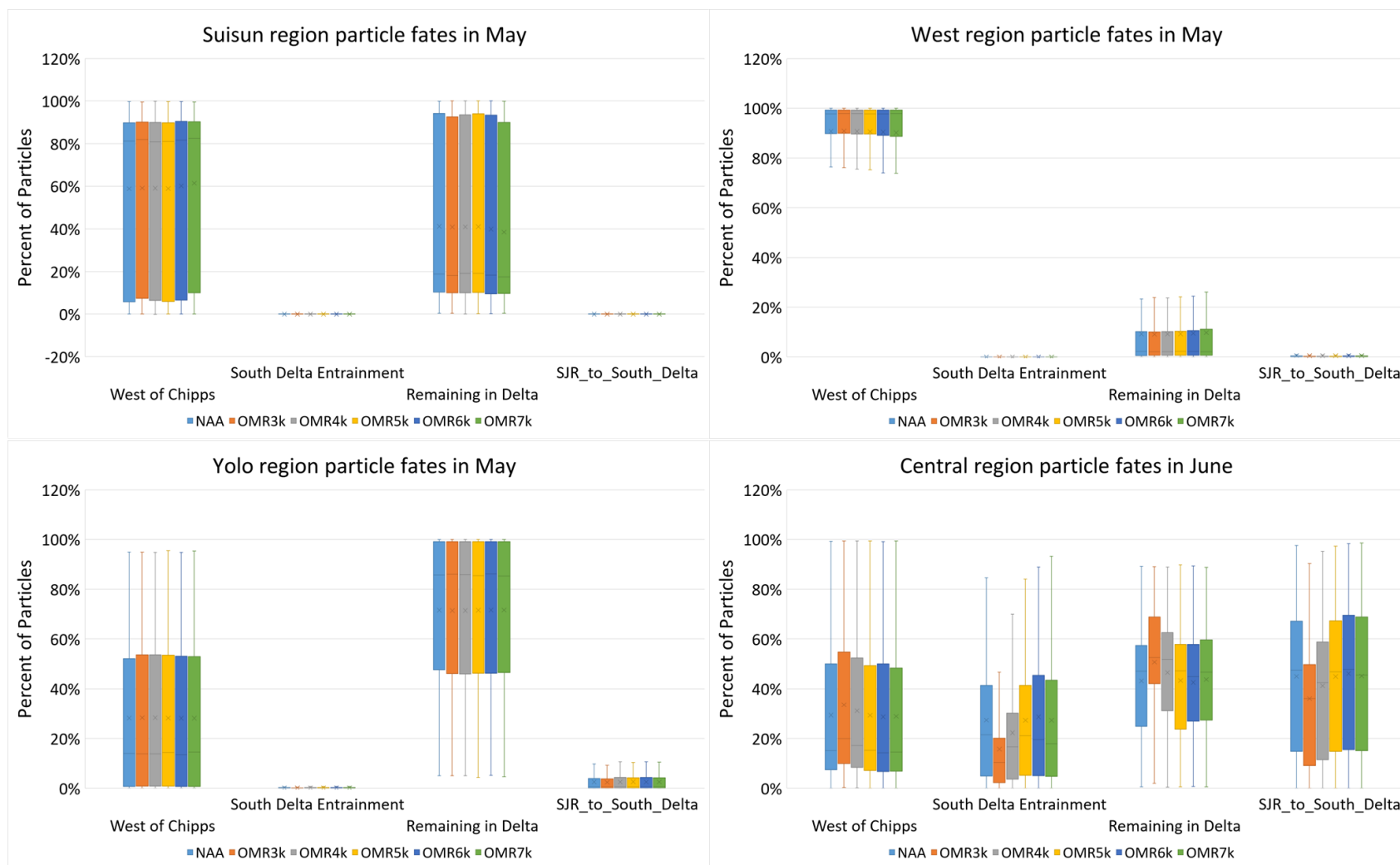


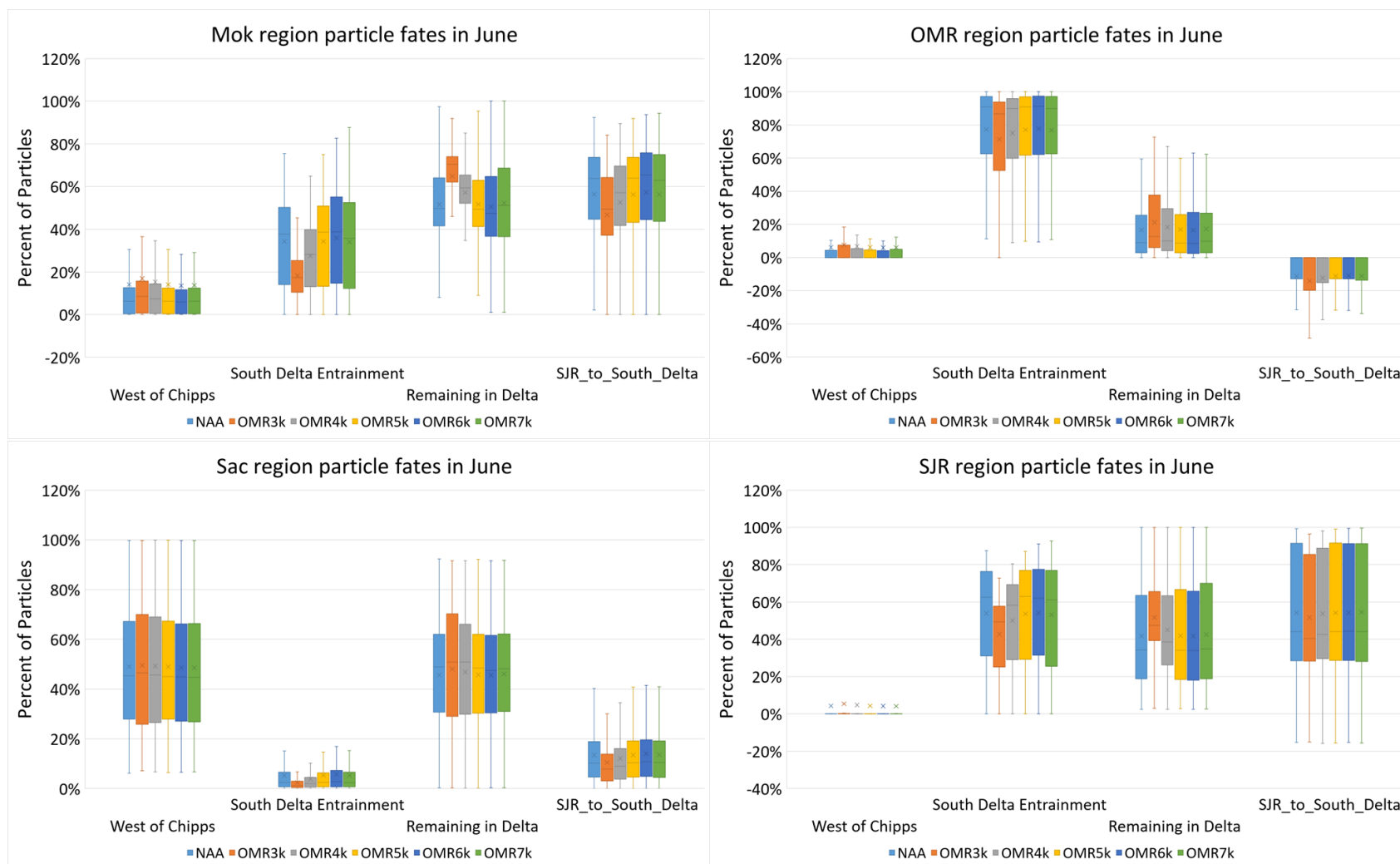


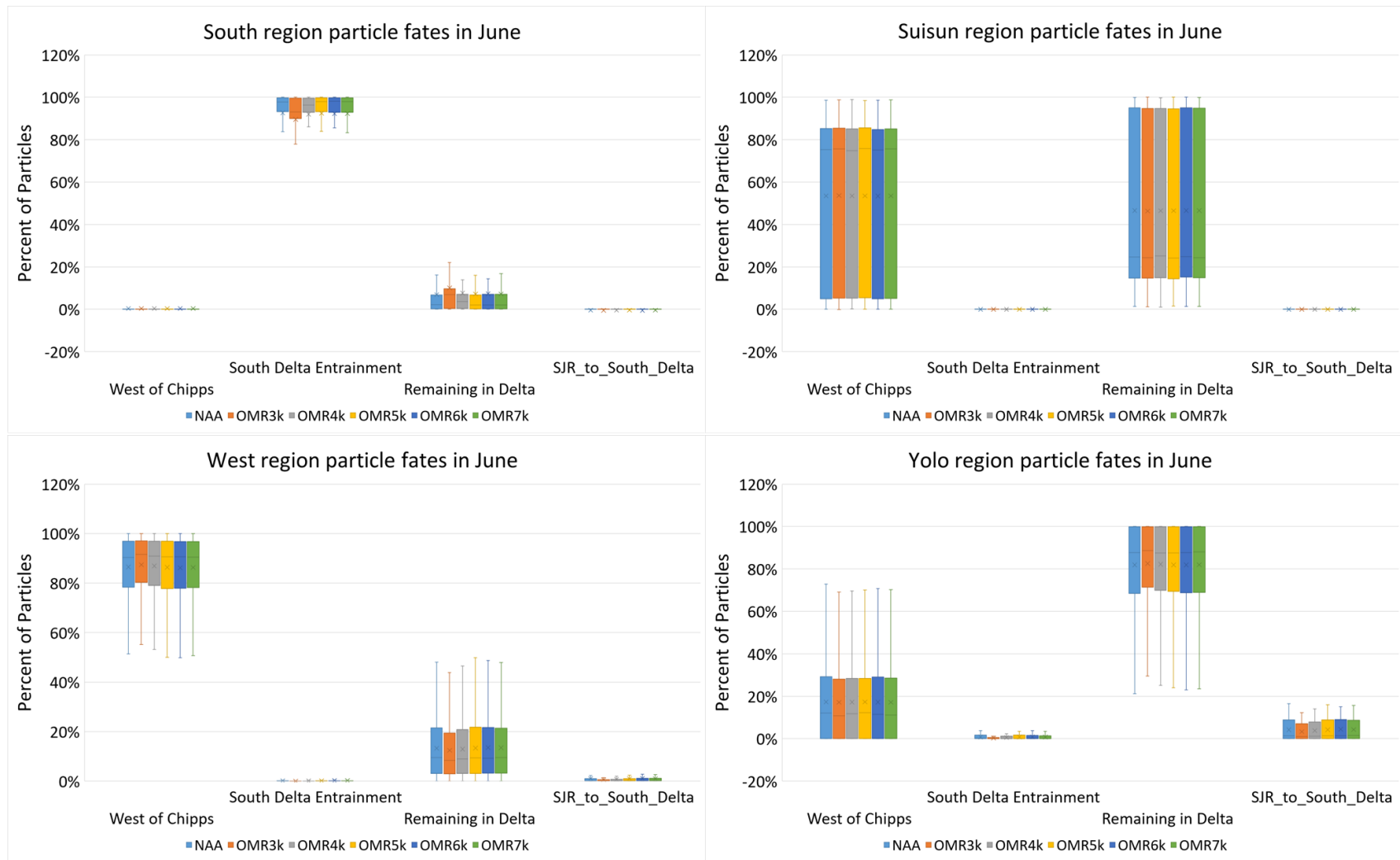














### I.1.3 References

- Miller, A. 2002. *Methodology for Flow and Salinity Estimates in the Sacramento–San Joaquin Delta and Suisun Marsh*. Twenty-Second Annual Progress Report to the State Water Resources Control Board. Chapter 2: Particle Tracking Model Verification and Calibration. Sacramento, CA.
- Smith, T. 1998. *Methodology for Flow and Salinity Estimates in the Sacramento–San Joaquin Delta and Suisun Marsh*. Twenty-Second Annual Progress Report to the State Water Resources Control Board. Chapter 4: DSM2-PTM. Sacramento, CA.
- Wilbur, R. 2001. *Methodology for Flow and Salinity Estimates in the Sacramento–San Joaquin Delta and Suisun Marsh*. Twenty-Second Annual Progress Report to the State Water Resources Control Board. Chapter 4: Validation of Dispersion Using the Particle Tracking Model in the Sacramento–San Joaquin Delta. Sacramento, CA.

Page Intentionally Left Blank

## **I.2. Attachment 2: Zone of Influence Analysis**

## **I.2.1 Introduction and Background**

The Sacramento–San Joaquin River Delta (Delta) provides habitat for migrating anadromous fish while also serving as critical infrastructure for California water supply. In the winter and spring months, Old and Middle River (OMR) flows are managed to protect emigrating juvenile winter-run Chinook salmon, yearling spring-run Chinook salmon, and Central Valley steelhead from entrainment into the export facilities in the south Delta. During these months, changes to velocity distributions at channel junctions, due to south Delta exports, may affect the fate of migrating anadromous fish. This document describes a technique to evaluate the spatial extent of hydrologic alteration considering changes to velocity (hereinafter described as “zone of influence”) and changes to the probability distributions of daily average velocity as a result of pumping under varying OMR flow conditions.

## **I.2.2 Methods**

A sensitivity analysis using DSM2 Hydro was conducted to analyze the spatial extent of influence of exports under varying OMR conditions. For this analysis, inflows to Delta were assumed fixed between scenarios, and DSM2 was used to vary export levels (synthetically, without any consideration of system-wide operations) to generate varying export conditions under the same inflow scheme to the Delta. This modeling scheme demonstrates effects of Delta exports on Delta flows. The DSM2 Hydro flow and velocity results were then used to generate zone of influence contour maps in the Delta.

The subsections below describe the DSM2 modeling and post-processing steps to quantify the influence of the export facilities in the south Delta (DSM2 Modeling and Post-Processing). Then, two methods for evaluating zone of influence are presented: (1) probability density curves of daily average velocity at a specific location (described in Gaussian Kernel Density Estimation); and (2) spatial maps that illustrate changes to velocity throughout the Delta (described in Gaussian KDE Proportional Overlap Maps).

## **I.2.3 DSM2 Modeling and Post-Processing**

For each analysis, two DSM2 simulations must be run to isolate hydrologic alteration by exports: (1) scenario of interest and (2) scenario of interest without south Delta exports. The second simulation is required to assess the effect of pumping throughout the Delta in the scenario of interest. For both simulations (water year 1922 through 2003), daily average velocity results are retrieved at several Delta locations to assess the spatial influence of Delta pumping under various OMR flow conditions.

To review effects under various OMR flow conditions, monthly averaged OMR flow results from the scenario of interest are categorized into bins. The number of OMR bins vary with each scenario of interest. Monthly averaged OMR flow within 500 cfs of the bin label are categorized into that bin. For example, the -1,000 cfs OMR bin considers monthly averaged OMR flow

conditions from -500 cfs to -1,500 cfs. More details regarding the application and breakdown of OMR bins are provided in Section 14.6.1.

To assess the effect of pumping for a given OMR flow condition, the simulation results from the scenario of interest are reviewed to identify the months during which OMR flow falls within each OMR bin. Then, velocity results from the scenario of interest and scenario of interest w/out pumps are compared across the same set of months for each OMR flow bin. Based on the OMR flow value in the scenario of interest, a group of months are selected. For a given OMR bin, regardless of OMR flow in the scenario of interest w/out pumps, the same set of months are retrieved for comparison.

### I.2.3.1 Gaussian Kernel Density Estimation

For the months corresponding to each OMR flow bin, the Gaussian Kernel Density Estimate (KDE) compares daily average velocity at a given location for the scenario of interest with and without pumps. An example KDE plot is presented in Figure I.2-1. Each figure presents: (1) location, (2) OMR bin of interest, (3) proportion of the simulation presented, (4) proportional overlap area of the Gaussian KDE curves, (5) differential of the median velocity between the two simulations, and (6) reference directional on the x-axis.

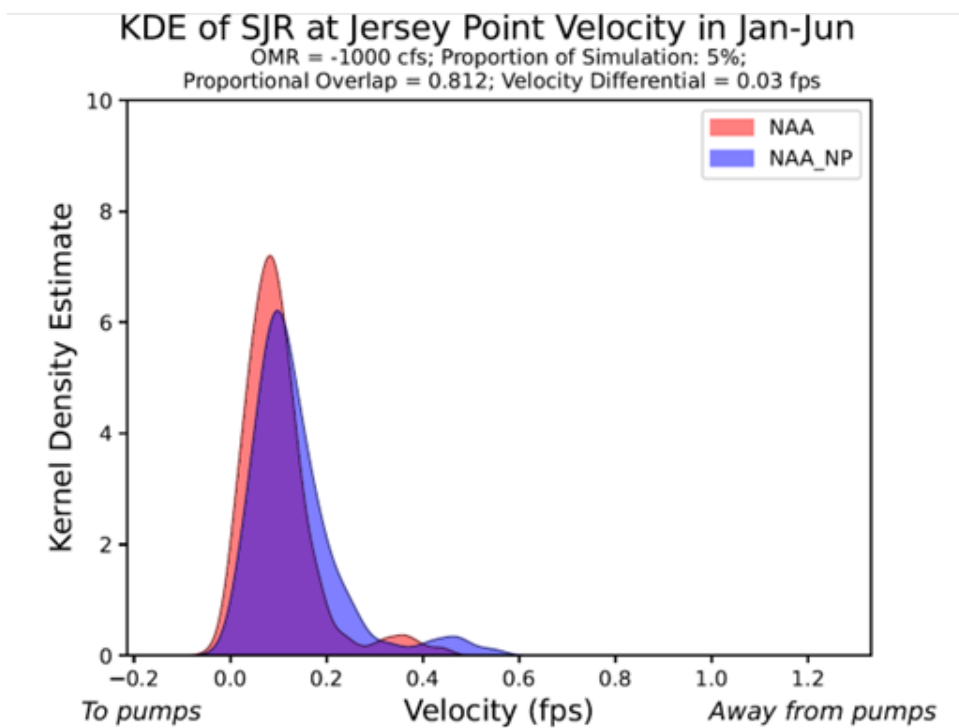


Figure I.2-1. Gaussian KDE of Velocity at San Joaquin River at Jersey Point in January through June with OMR of -1,000 cfs

In Figure I.2-1, a proportional overlap value of 0.812 indicates that the distribution of velocity is similar under the NAA and NAA w/out pumps (NAA\_NP) 81% of the time. A velocity differential value of 0.03 fps indicates that there is only a 0.03 fps change in the median daily

average velocity between the scenario of interest with- and w/out pumps. Details regarding the NAA and NAA\_NP simulations are provided in Section 14.6.1.

The proportional overlap value and velocity differential explain the change in the velocity distribution and the magnitude to which the velocities have changed, respectively. For example, in Figure I.2-2 (below), when OMR flows are -1,000 cfs at Middle River near Holt, the channel experiences a very narrow range of velocities. Given the narrow range of possible velocities, the proportional overlap value is 0.295 and the velocity differential is 0.05 fps. The relatively low value in proportional overlap indicates a significant difference in velocity distribution. However, the velocity differential is 0.05 fps, a very small change in median velocities. Together, these values indicate that the KDE curves may be different, but the actual change to velocity at that location is relatively small.

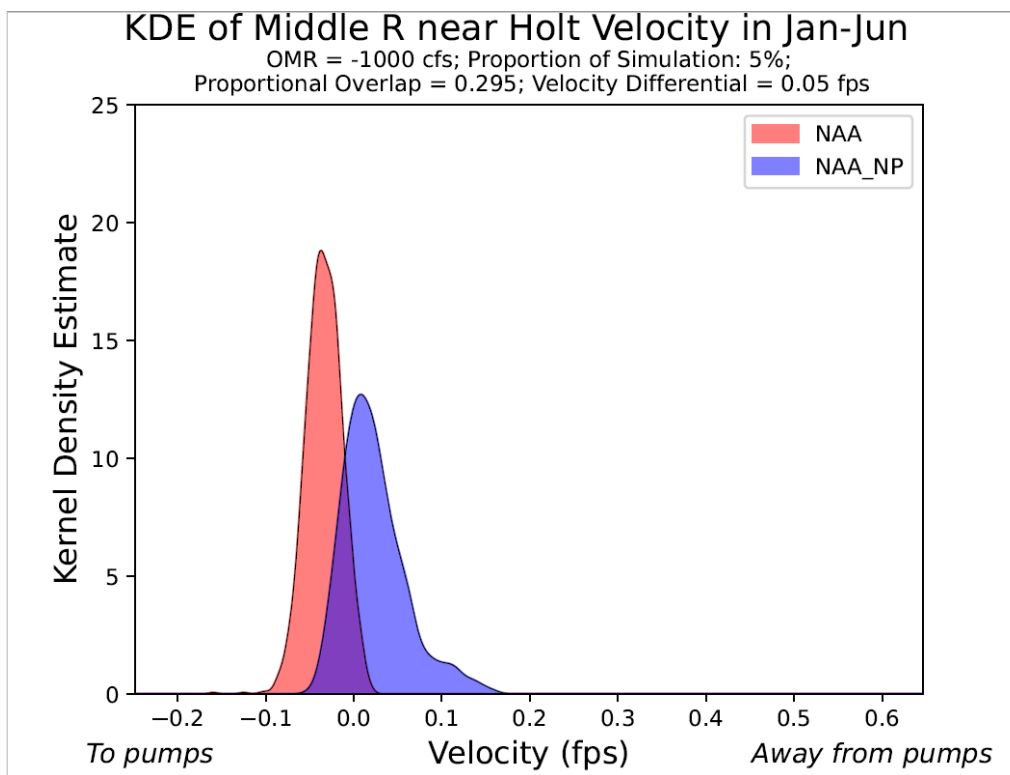


Figure I.2-2. Gaussian KDE of Velocity at Middle River near Holt in January through June with OMR of -1,000 cfs

### I.2.3.2 Gaussian KDE Proportional Overlap Maps

For each month of the OMR management period (January through June), the proportional overlap of the daily average velocity Gaussian KDEs for the scenario of interest with and w/out pumps at each location in the Delta are compared in each OMR bin. These maps depict four categories for proportional overlap of daily velocity: (1) 0.00 to 0.50, (1) 0.50 to 0.90, (2) 0.90 to 0.95, and (3) 0.95 to 1.00. The first (0.00 to 0.50) and last (0.95 to 1.00) categories represent the greatest and least change to flow, respectively. An example zone of influence map is presented in Figure I.2-3. Generally, as OMR flow incrementally decreases (a result of increased exports), the

area categorized in the 0.00 to 0.50 and 0.50 to 0.90 ranges of proportional overlap increases. In essence, the zone of influence increases as the magnitude of pumping increases.

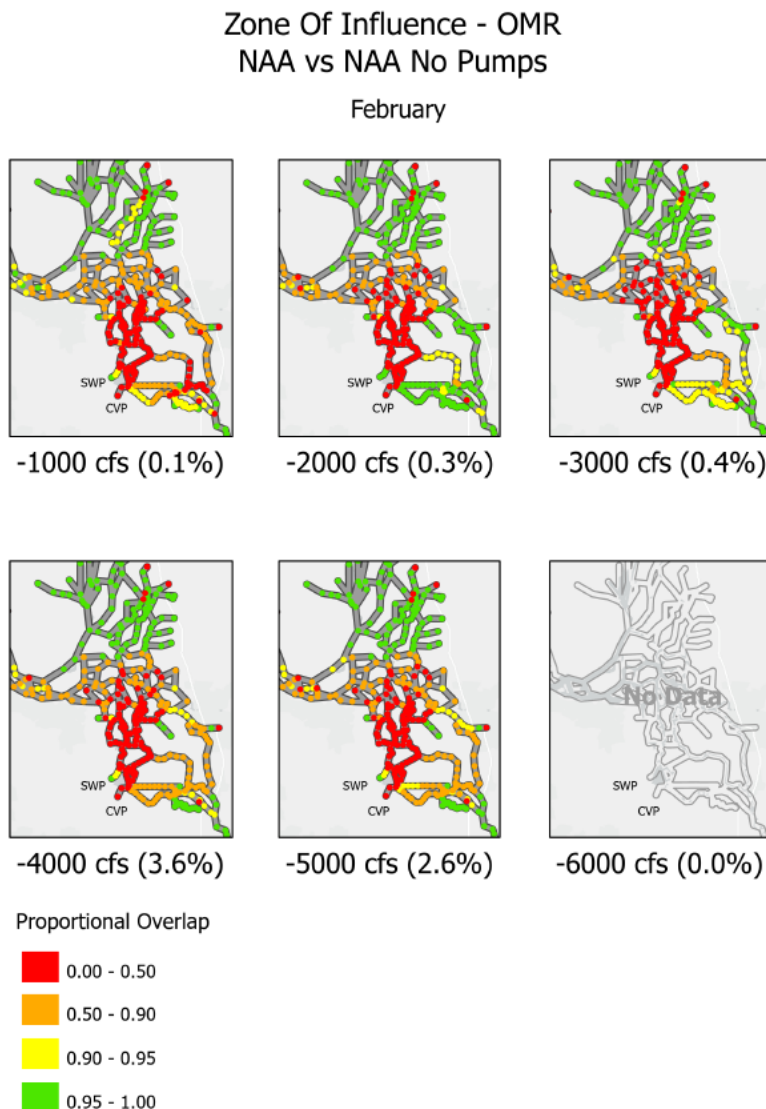


Figure I.2-3. Zone of Influence in February with OMR of -1,000 cfs to -6,000 cfs

This set of plots presents the proportional overlap between the NAA and NAA w/out pumps in February under five OMR conditions: -1,000 cfs, -2,000 cfs, -3,000 cfs, -4,000 cfs, and -5,000 cfs. Next to each sub-plot label, the percent of the total DSM2 simulation period shown in the sub-plot (e.g., number of Februarys when OMR is -1,000 divided by all months in the simulation) are in parentheses. Details regarding the NAA and NAA\_NP simulations are provided in Section 14.6.1.

## I.2.4 Results

With the methodology described above, two sets of results were prepared: (1) plots of January through June velocity KDE (Figures I.2-1 and I.2-2) for various locations and OMR conditions, and (2) maps of proportional overlap by month and OMR condition (Figure I.2-3). Details regarding the scenarios examined, Gaussian KDE curves, and proportional overlap maps are provided in the subsections below.

### I.2.4.1 Scenarios

The Reinitiation of Consultation on the Long-Term Operation of the Central Valley Project and State Water Project (ROC on LTO) model was applied as the base model for this analysis. As of the 2019 BiOps, the ROC on LTO model is the regulatory environment for operations. For the purposes of this document, the 2019 BiOps model with future climate hydrology (2035CT) and 15 cm of sea level rise is described as the No Action Alternative (NAA). Consistent with the ROC on LTO modeling, DSM2 version 8.0.6 with 15 cm of sea level rise was utilized to estimate daily channel-averaged velocity distribution. To evaluate the effect of pumping, a second DSM2 simulation, identical to the ROC on LTO model without any Delta pumping (NAA w/out pumps), was conducted.

To review effects under various OMR flow conditions, monthly average OMR flow results from the NAA simulation were categorized into five bins: -1,000 cfs, -2,000 cfs, -3,000 cfs, -4,000 cfs, and -5,000 cfs. It should be noted that the five OMR flow bins in Table I.2-1 consider 46.2% of the planning simulation period, or the majority of the January through June time periods. OMR flows in the remaining 3.8% of the January through June periods in the simulation fall above -500 cfs.

Table I.2-1. Range of Flows and Proportion of Simulation for each OMR Flow Bin

OMR Bin (cfs)	OMR Bin Range (cfs)	Proportion of Simulation Period
-1,000	-1,500 to -500	4.6%
-2,000	-2,500 to -1,500	9.9%
-3,000	-3,500 to -2,500	9.7%
-4,000	-4,500 to -3,500	10.0%
-5,000	-5,500 to -4,500	11.2%

In addition to an evaluation of the NAA, zone of influence analyses are applied to a DSM2 planning simulation that represents the D1641 regulatory requirements. Although the examples in this document are specific to the NAA model results, D1641 results are also included in the velocity KDE plot results attachment to this document.

### I.2.4.2 Velocity KDE Plots

Plots of velocity KDE in the months from January through June are presented below. The plots demonstrate change to velocities at the locations listed in Table I.2-2. At each location, several

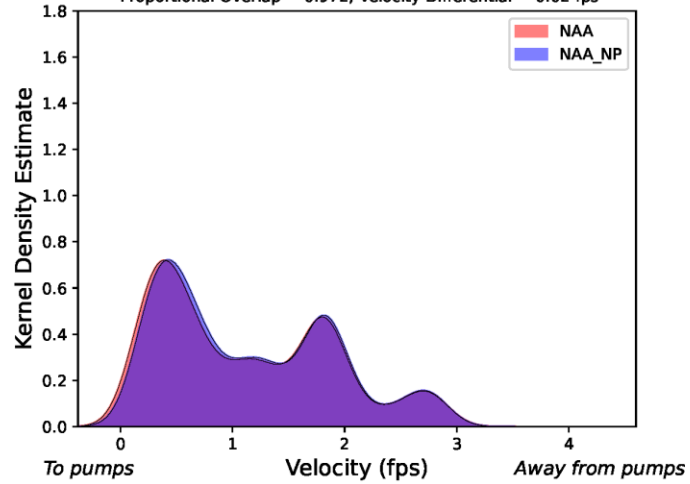


plots (one for each OMR bin) are included. As the regulatory environment changes in the scenarios of interest, the number of OMR bins associated with each analysis changes.

The set of figures below represent the NAA results.

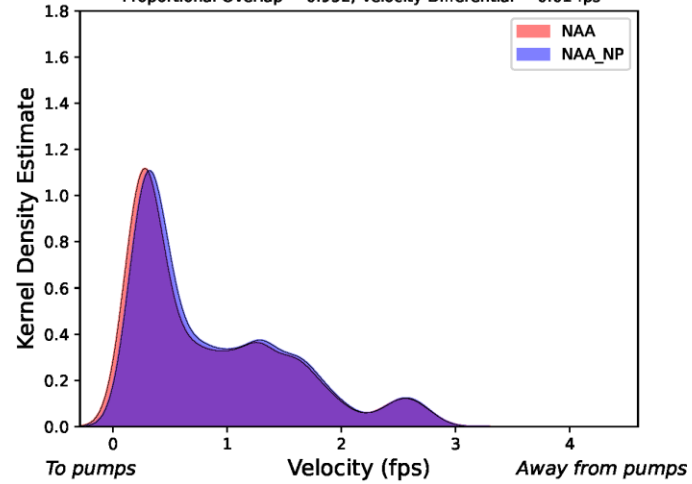
KDE of SJR at Brandt Bridge Velocity in Jan-Jun

OMR = -1000 cfs; Proportion of Simulation: 5%;  
Proportional Overlap = 0.972; Velocity Differential = 0.02 fps



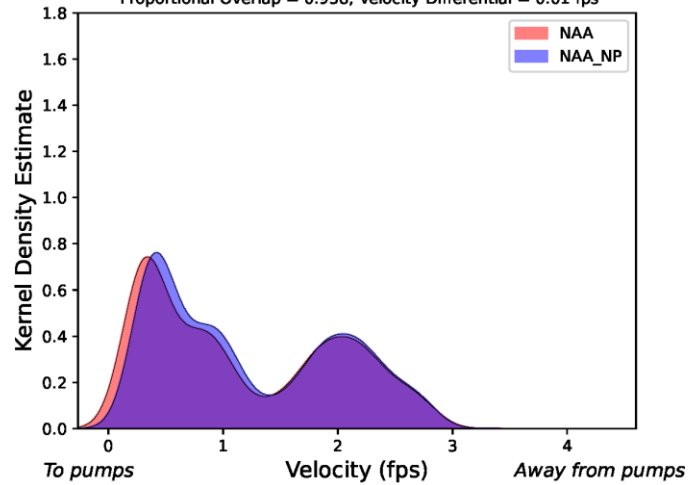
KDE of SJR at Brandt Bridge Velocity in Jan-Jun

OMR = -2000 cfs; Proportion of Simulation: 10%;  
Proportional Overlap = 0.952; Velocity Differential = 0.01 fps



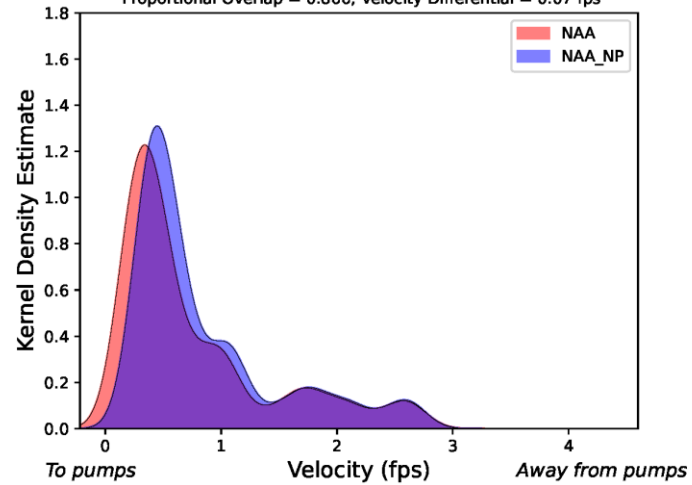
KDE of SJR at Brandt Bridge Velocity in Jan-Jun

OMR = -3000 cfs; Proportion of Simulation: 10%;  
Proportional Overlap = 0.938; Velocity Differential = 0.01 fps



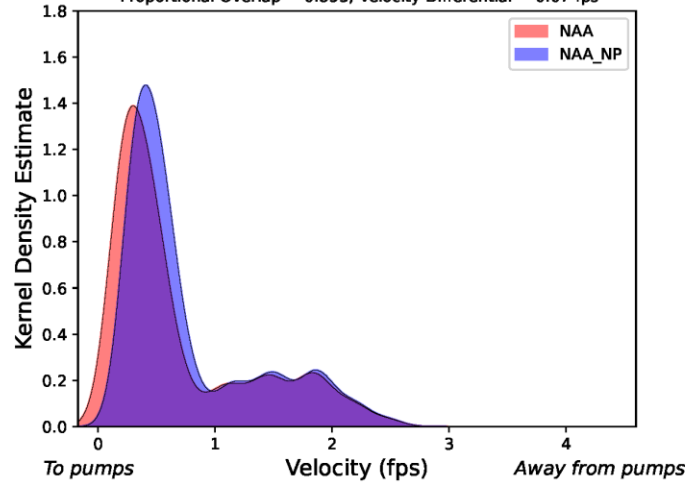
KDE of SJR at Brandt Bridge Velocity in Jan-Jun

OMR = -4000 cfs; Proportion of Simulation: 10%;  
Proportional Overlap = 0.866; Velocity Differential = 0.07 fps



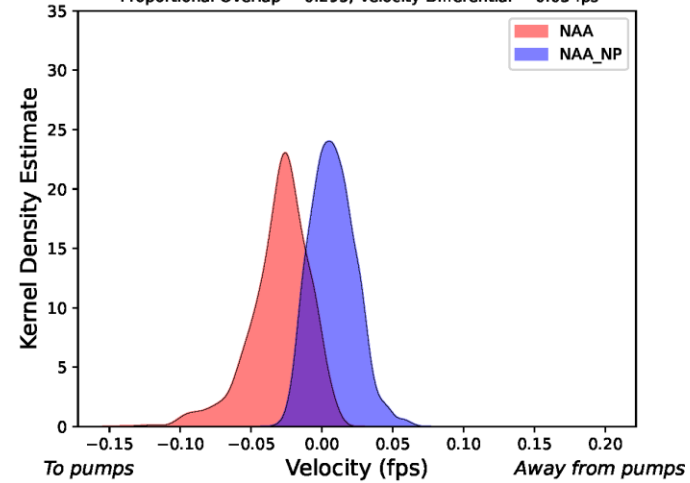
KDE of SJR at Brandt Bridge Velocity in Jan-Jun

OMR = -5000 cfs; Proportion of Simulation: 11%;  
Proportional Overlap = 0.853; Velocity Differential = 0.07 fps



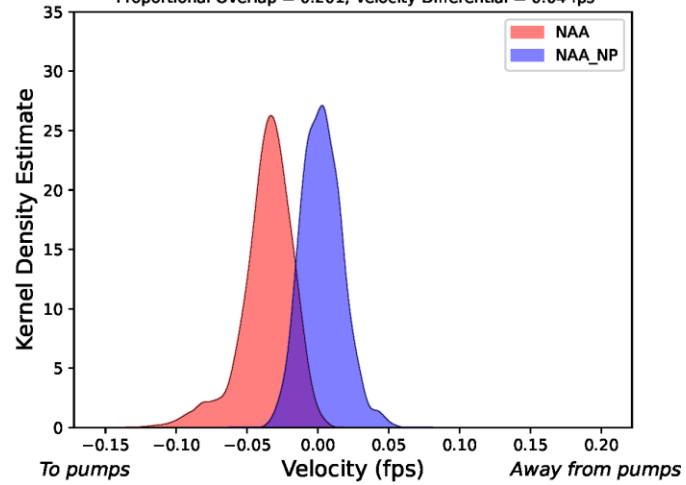
KDE of Turner Cut Velocity in Jan-Jun

OMR = -1000 cfs; Proportion of Simulation: 5%;  
Proportional Overlap = 0.295; Velocity Differential = 0.03 fps



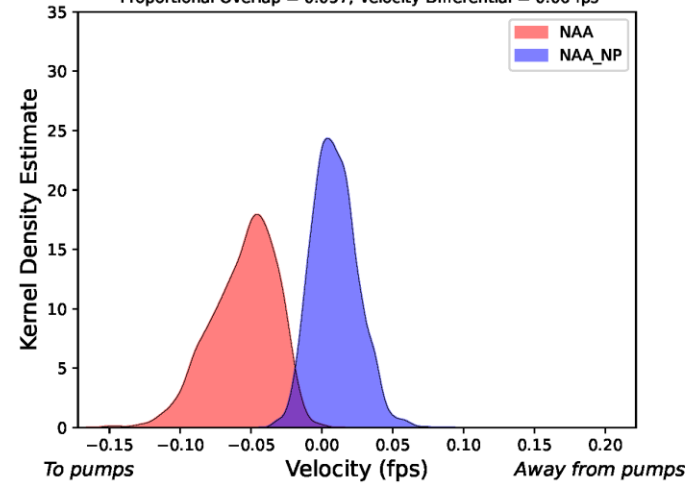
KDE of Turner Cut Velocity in Jan-Jun

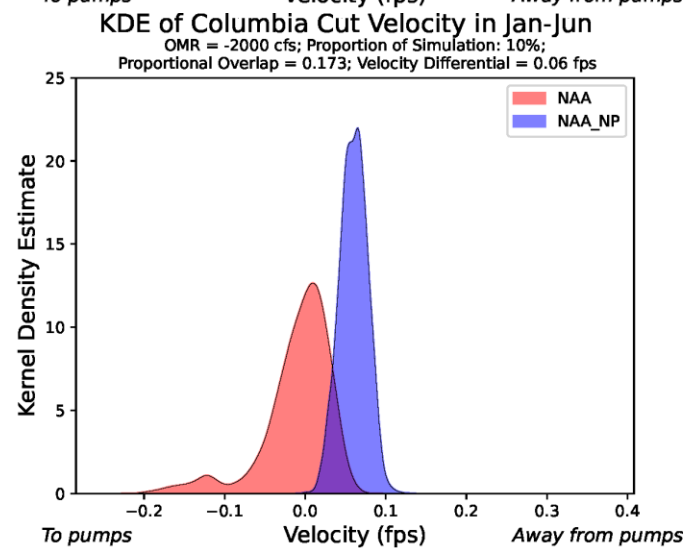
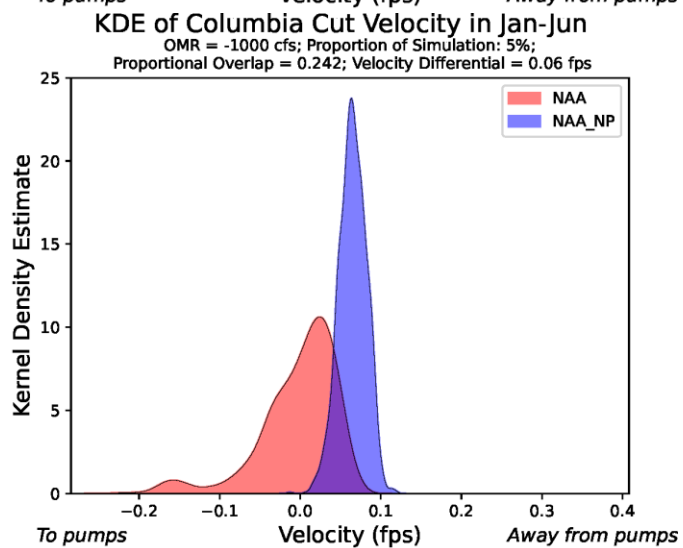
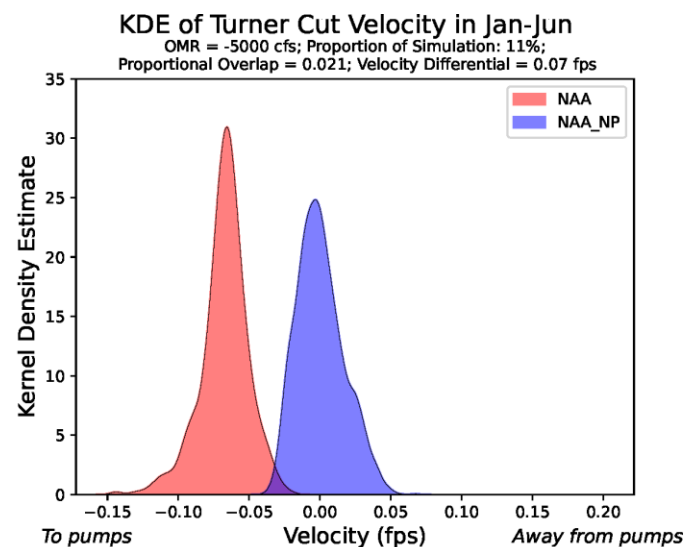
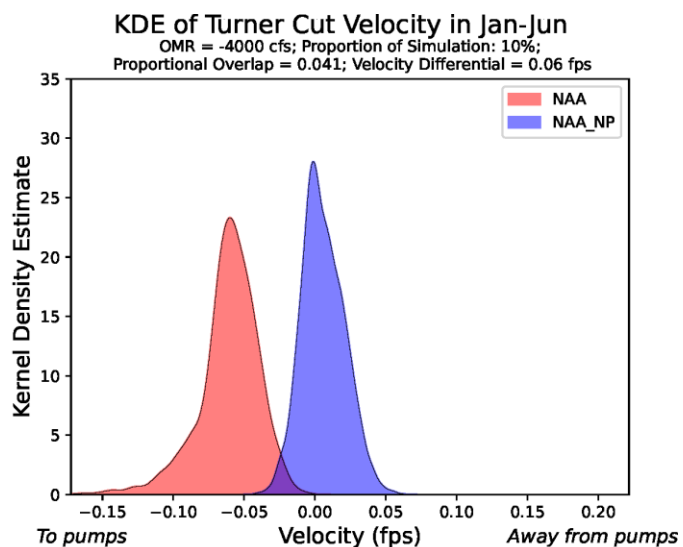
OMR = -2000 cfs; Proportion of Simulation: 10%;  
Proportional Overlap = 0.201; Velocity Differential = 0.04 fps

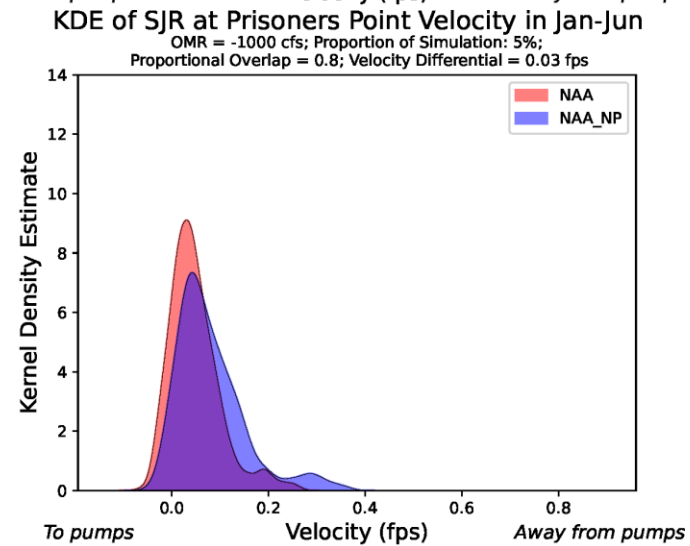
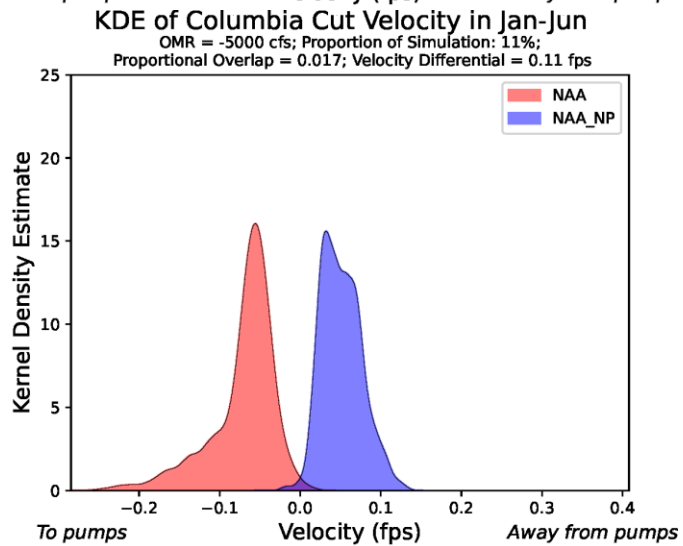
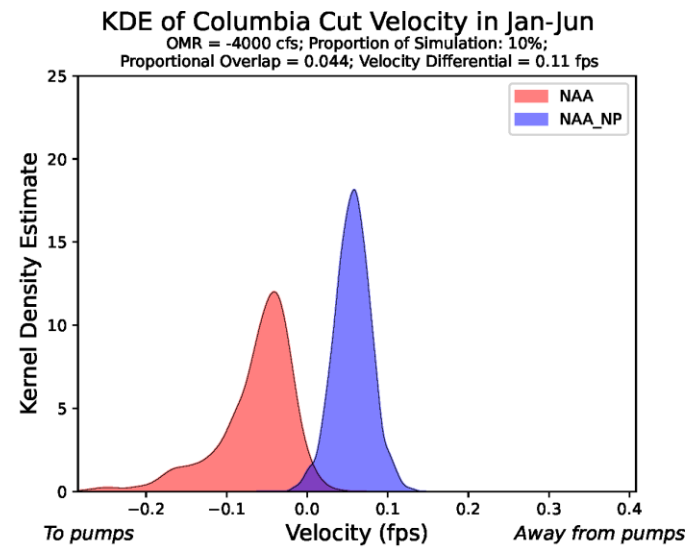
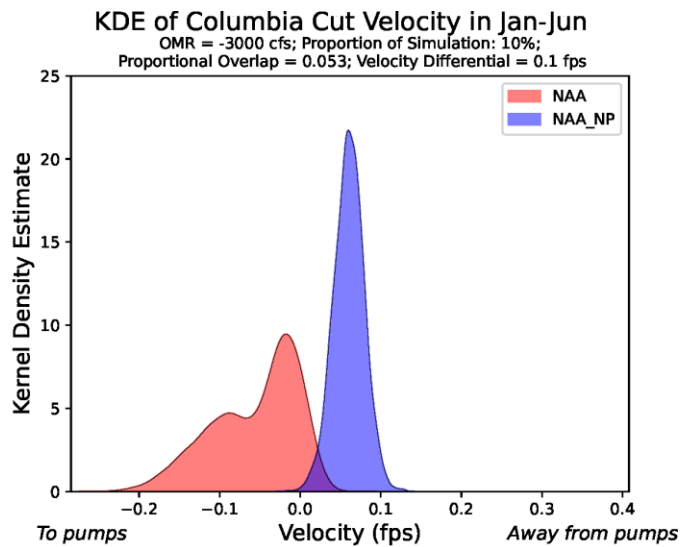


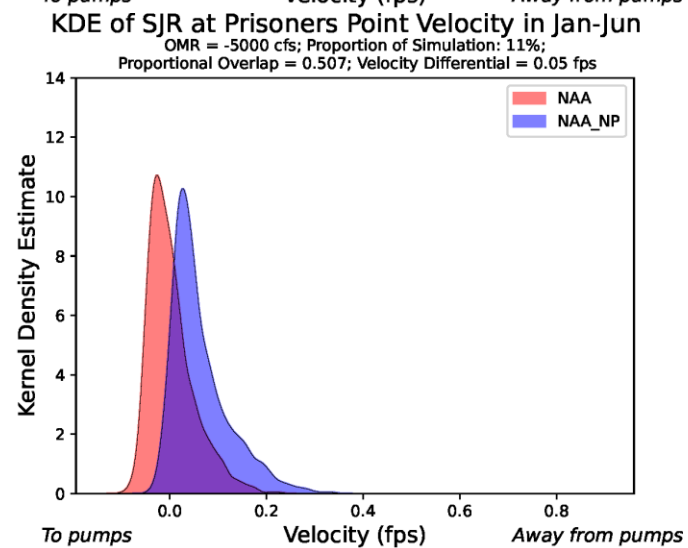
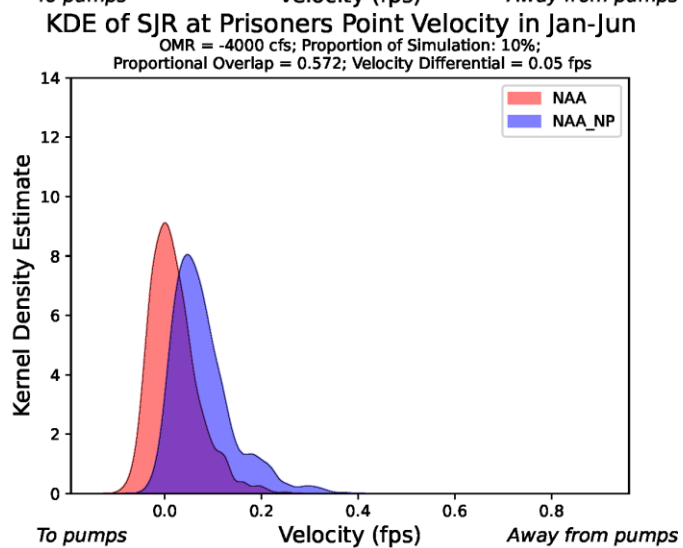
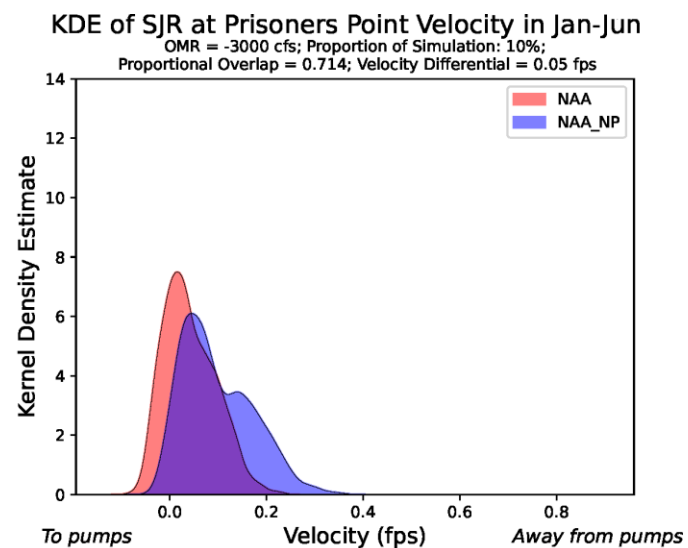
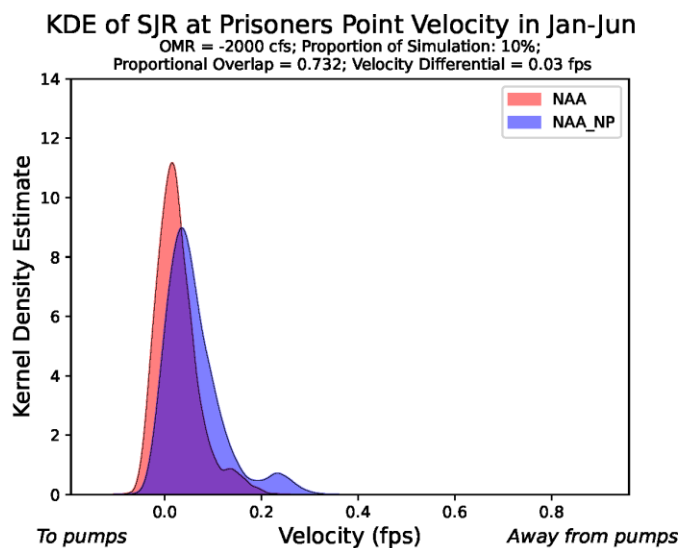
KDE of Turner Cut Velocity in Jan-Jun

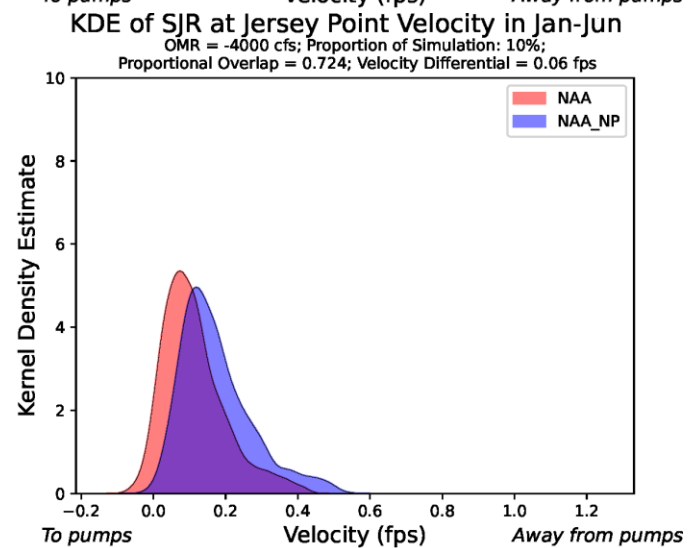
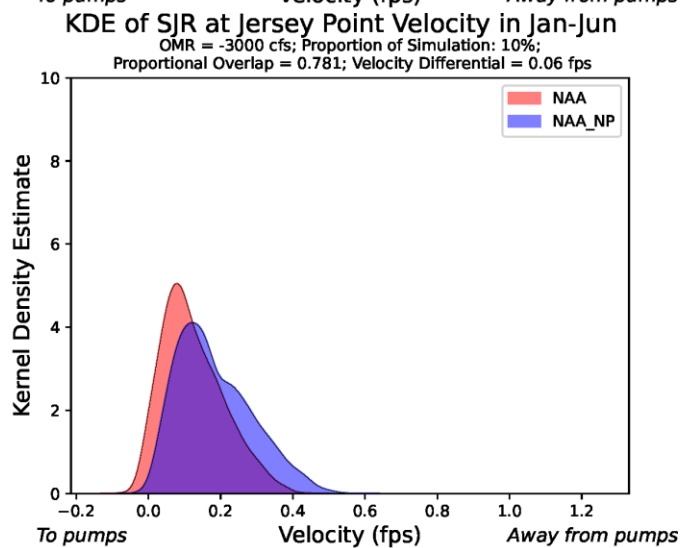
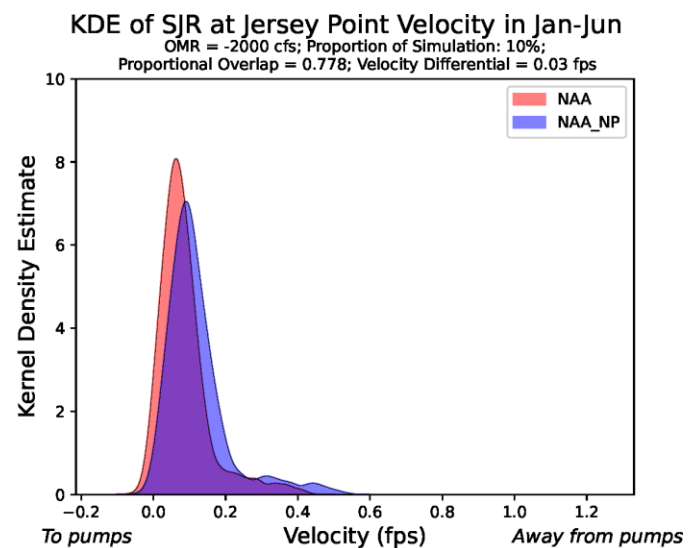
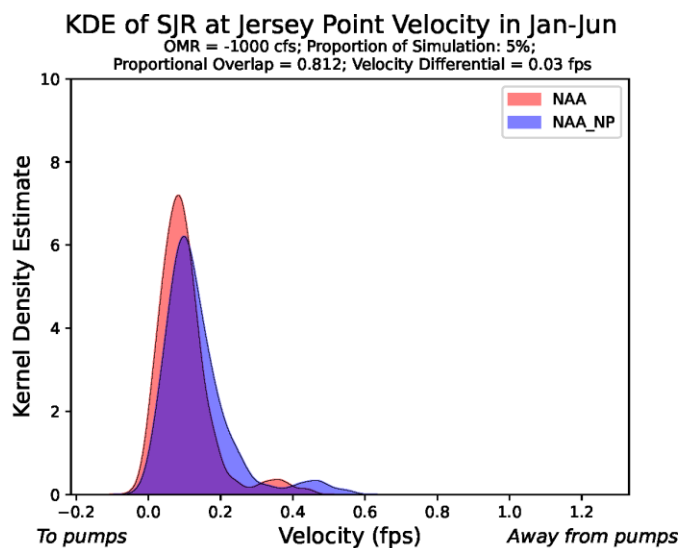
OMR = -3000 cfs; Proportion of Simulation: 10%;  
Proportional Overlap = 0.057; Velocity Differential = 0.06 fps





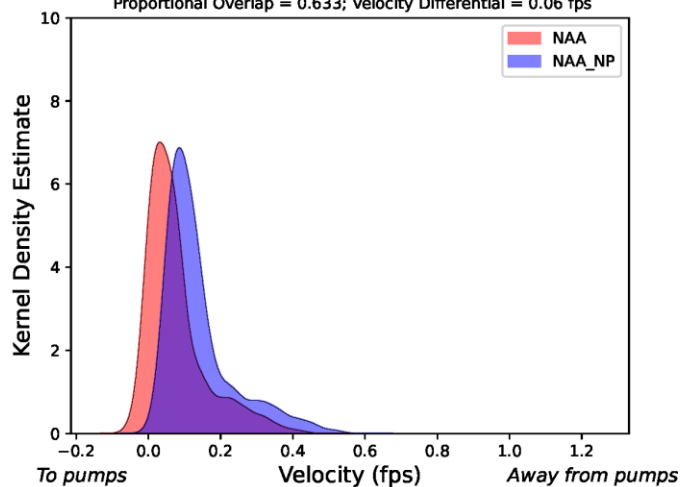






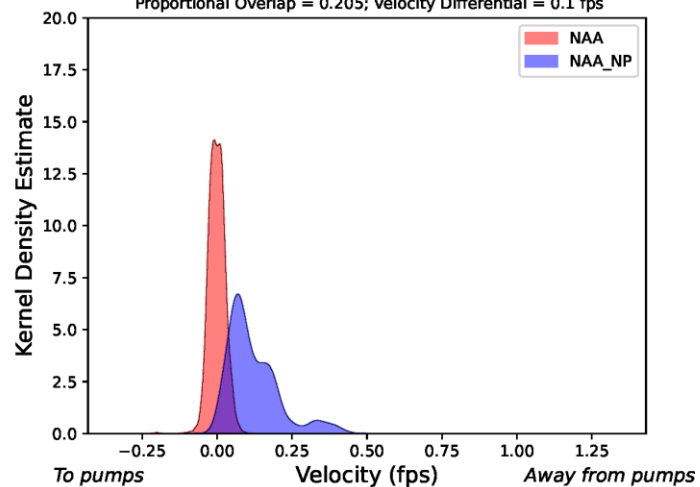
KDE of SJR at Jersey Point Velocity in Jan-Jun

OMR = -5000 cfs; Proportion of Simulation: 11%;  
Proportional Overlap = 0.633; Velocity Differential = 0.06 fps



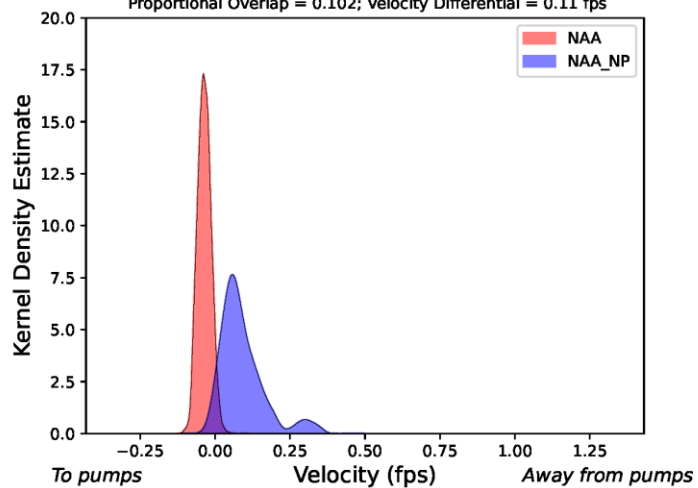
KDE of Old R at Bacon Island Velocity in Jan-Jun

OMR = -1000 cfs; Proportion of Simulation: 5%;  
Proportional Overlap = 0.205; Velocity Differential = 0.1 fps



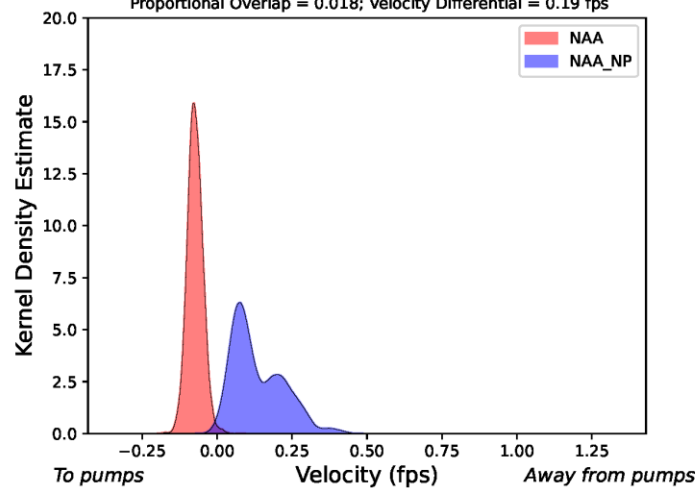
KDE of Old R at Bacon Island Velocity in Jan-Jun

OMR = -2000 cfs; Proportion of Simulation: 10%;  
Proportional Overlap = 0.102; Velocity Differential = 0.11 fps



KDE of Old R at Bacon Island Velocity in Jan-Jun

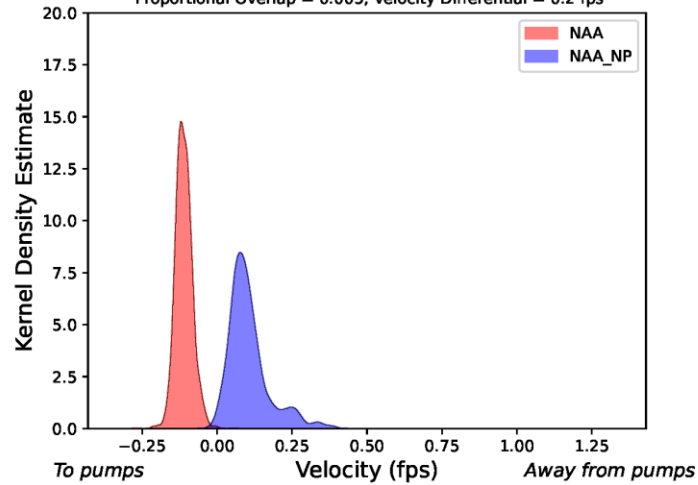
OMR = -3000 cfs; Proportion of Simulation: 10%;  
Proportional Overlap = 0.018; Velocity Differential = 0.19 fps





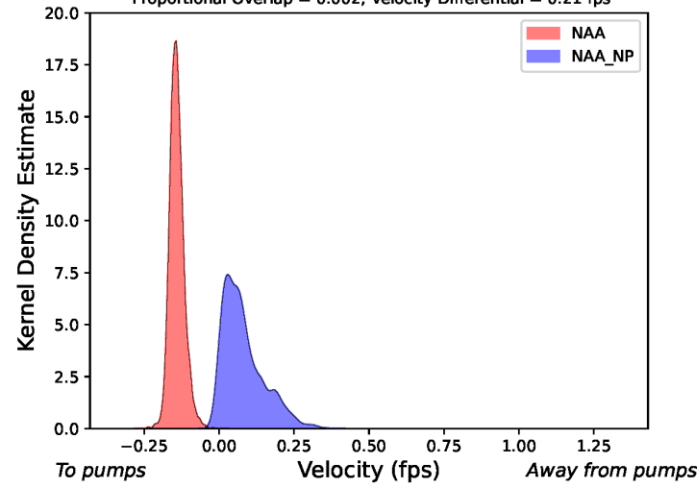
KDE of Old R at Bacon Island Velocity in Jan-Jun

OMR = -4000 cfs; Proportion of Simulation: 10%;  
Proportional Overlap = 0.005; Velocity Differential = 0.2 fps



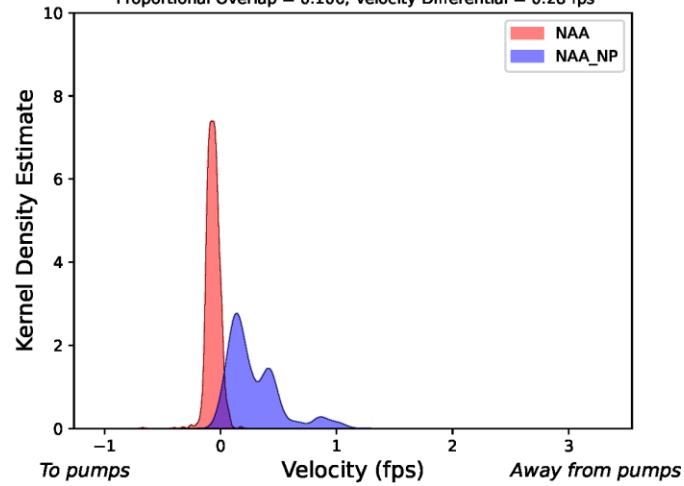
KDE of Old R at Bacon Island Velocity in Jan-Jun

OMR = -5000 cfs; Proportion of Simulation: 11%;  
Proportional Overlap = 0.002; Velocity Differential = 0.21 fps



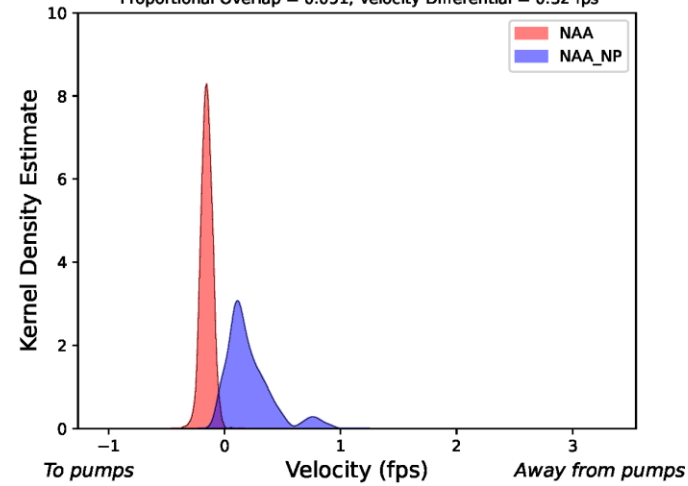
KDE of Old R at HWY4 Velocity in Jan-Jun

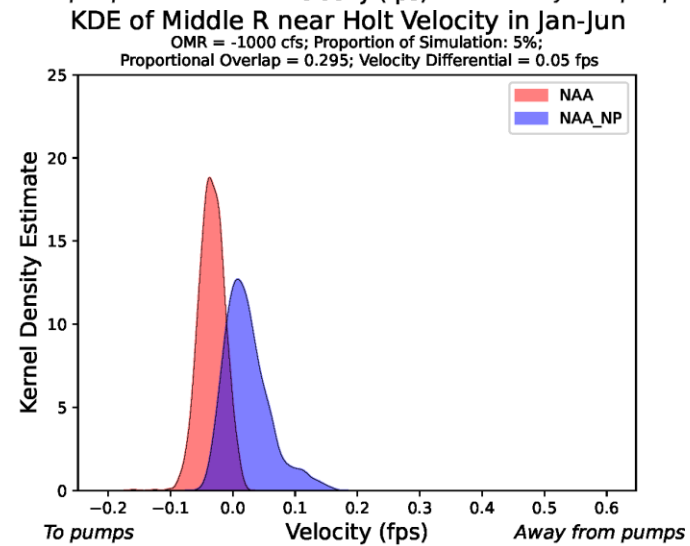
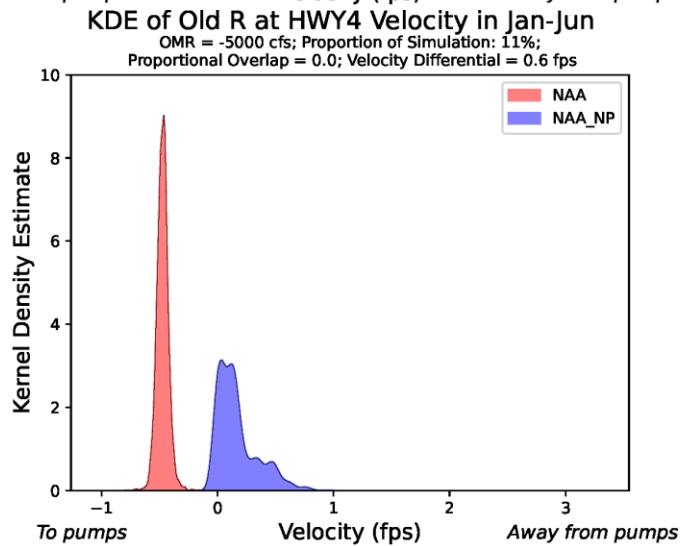
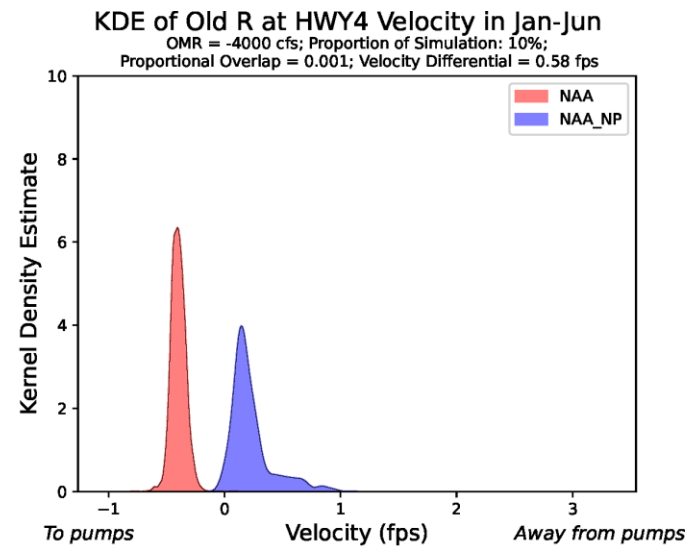
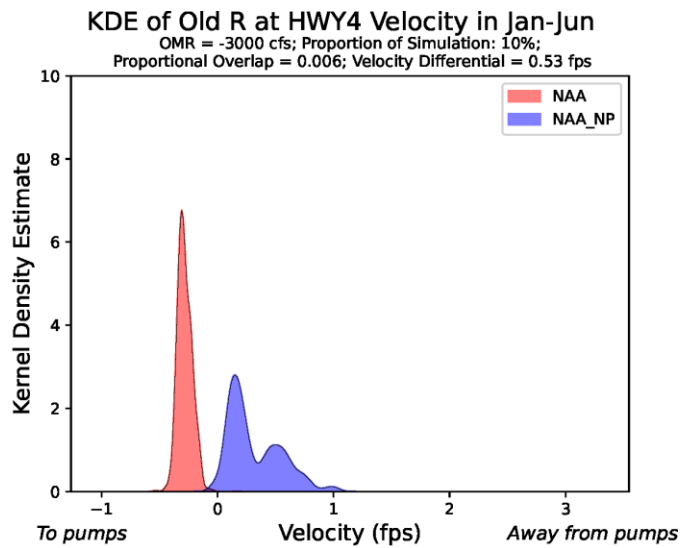
OMR = -1000 cfs; Proportion of Simulation: 5%;  
Proportional Overlap = 0.106; Velocity Differential = 0.28 fps

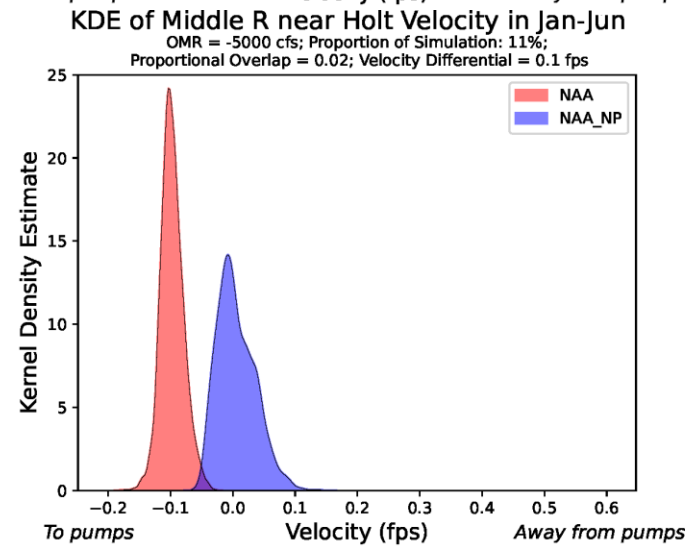
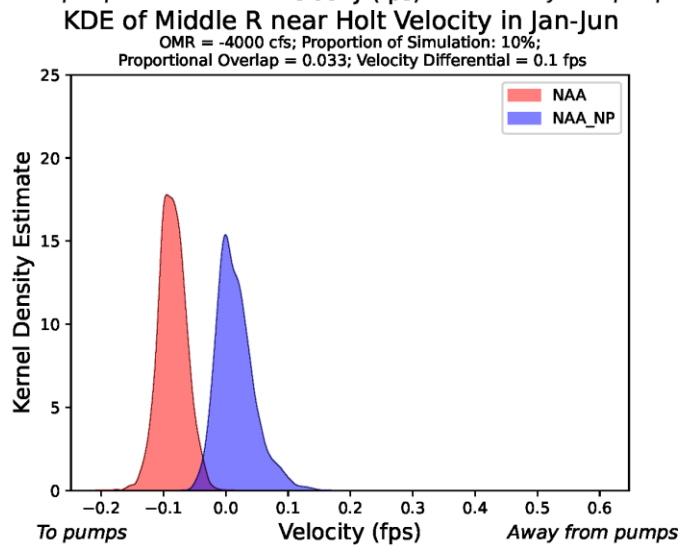
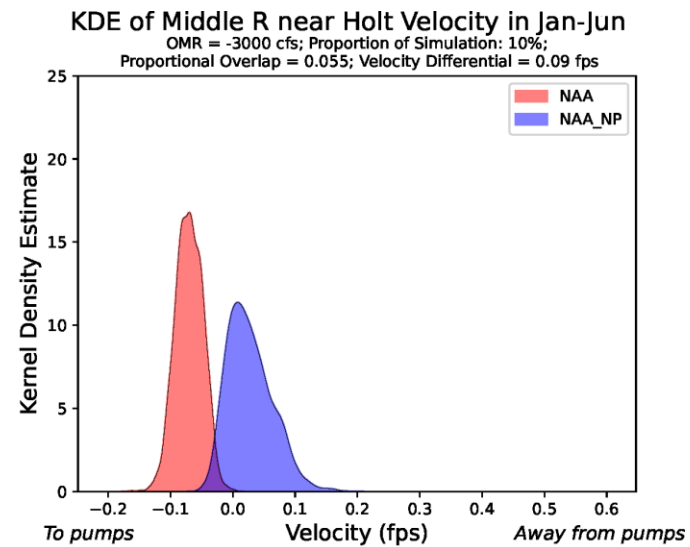
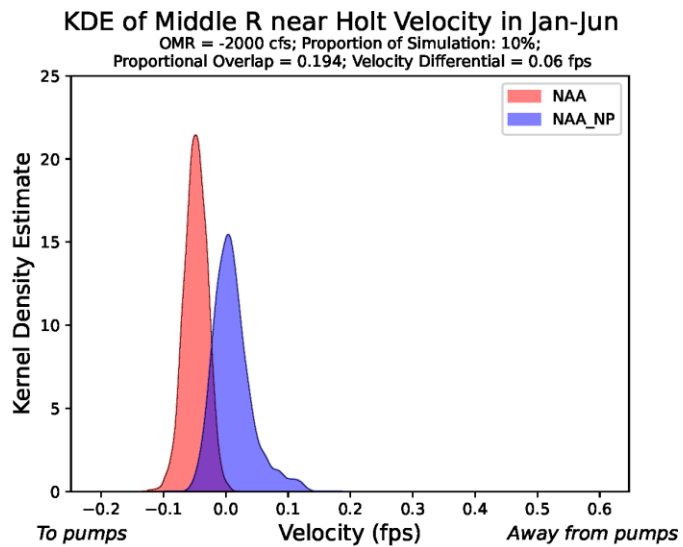


KDE of Old R at HWY4 Velocity in Jan-Jun

OMR = -2000 cfs; Proportion of Simulation: 10%;  
Proportional Overlap = 0.051; Velocity Differential = 0.32 fps

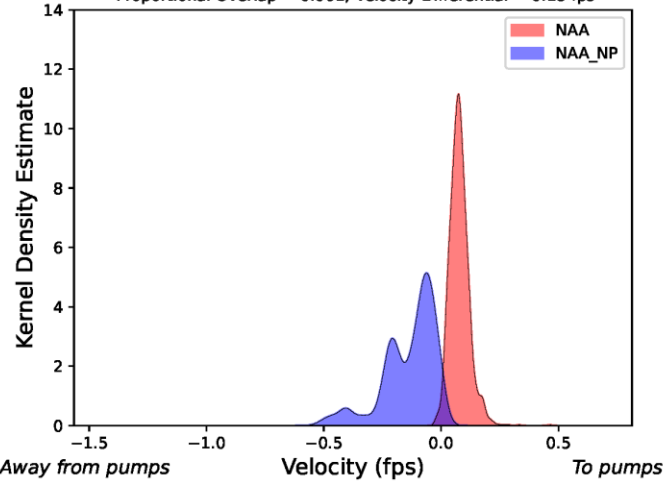






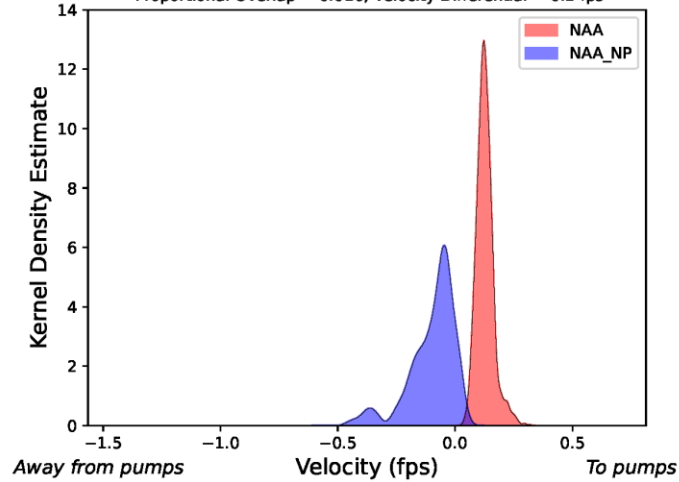
KDE of Victoria Canal near Byron Velocity in Jan-Jun

OMR = -1000 cfs; Proportion of Simulation: 5%;  
Proportional Overlap = 0.061; Velocity Differential = 0.18 fps



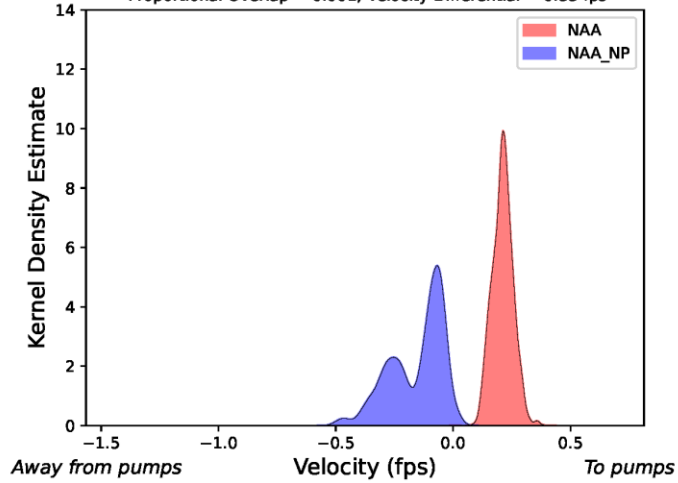
KDE of Victoria Canal near Byron Velocity in Jan-Jun

OMR = -2000 cfs; Proportion of Simulation: 10%;  
Proportional Overlap = 0.016; Velocity Differential = 0.2 fps



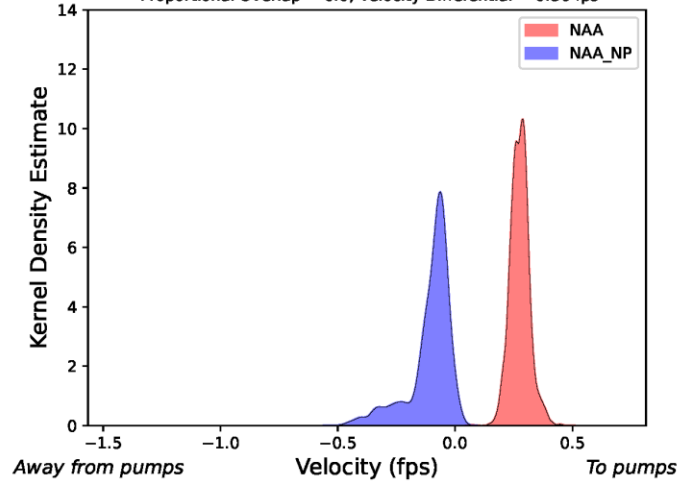
KDE of Victoria Canal near Byron Velocity in Jan-Jun

OMR = -3000 cfs; Proportion of Simulation: 10%;  
Proportional Overlap = 0.001; Velocity Differential = 0.33 fps



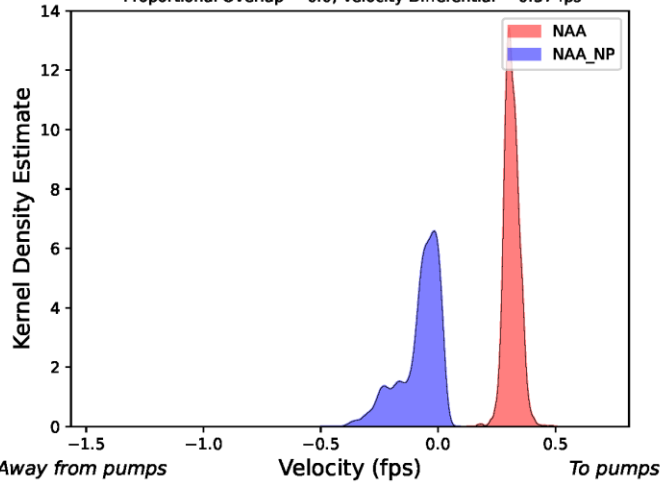
KDE of Victoria Canal near Byron Velocity in Jan-Jun

OMR = -4000 cfs; Proportion of Simulation: 10%;  
Proportional Overlap = 0.0; Velocity Differential = 0.36 fps



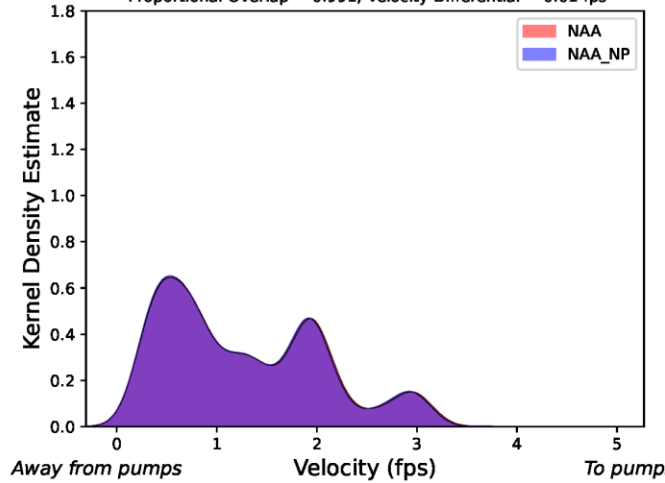
KDE of Victoria Canal near Byron Velocity in Jan-Jun

OMR = -5000 cfs; Proportion of Simulation: 11%;  
Proportional Overlap = 0.0; Velocity Differential = 0.37 fps



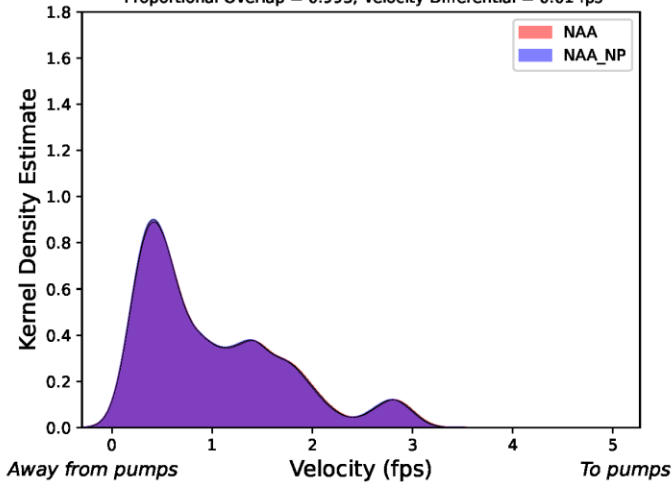
KDE of SJR US of Head of Old River Velocity in Jan-Jun

OMR = -1000 cfs; Proportion of Simulation: 5%;  
Proportional Overlap = 0.991; Velocity Differential = 0.01 fps



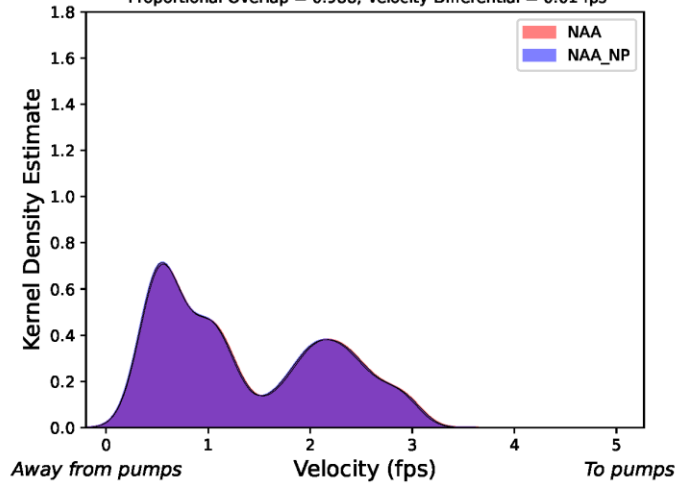
KDE of SJR US of Head of Old River Velocity in Jan-Jun

OMR = -2000 cfs; Proportion of Simulation: 10%;  
Proportional Overlap = 0.993; Velocity Differential = 0.01 fps



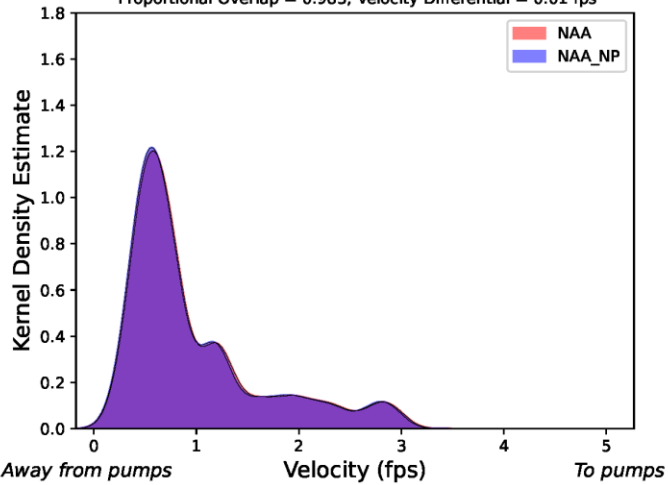
KDE of SJR US of Head of Old River Velocity in Jan-Jun

OMR = -3000 cfs; Proportion of Simulation: 10%;  
Proportional Overlap = 0.988; Velocity Differential = 0.01 fps



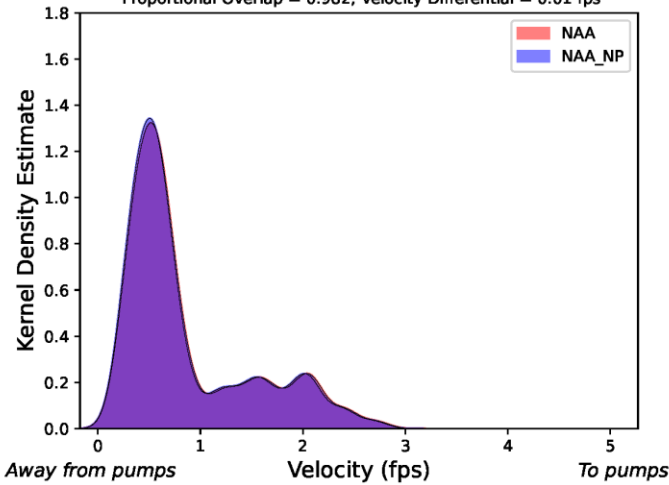
KDE of SJR US of Head of Old River Velocity in Jan-Jun

OMR = -4000 cfs; Proportion of Simulation: 10%;  
Proportional Overlap = 0.983; Velocity Differential = 0.01 fps



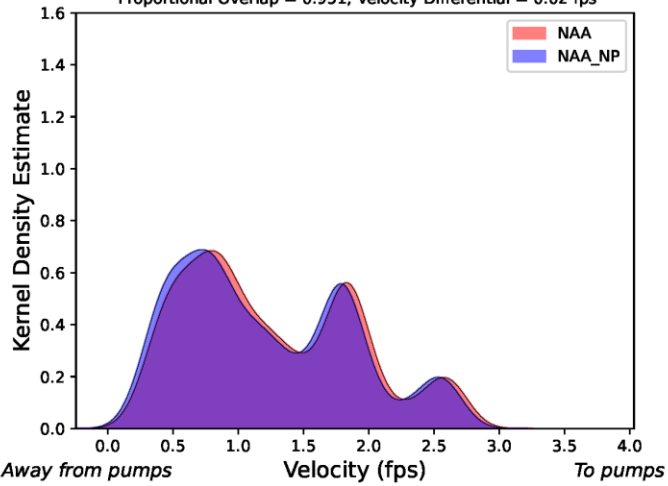
KDE of SJR US of Head of Old River Velocity in Jan-Jun

OMR = -5000 cfs; Proportion of Simulation: 11%;  
Proportional Overlap = 0.982; Velocity Differential = 0.01 fps



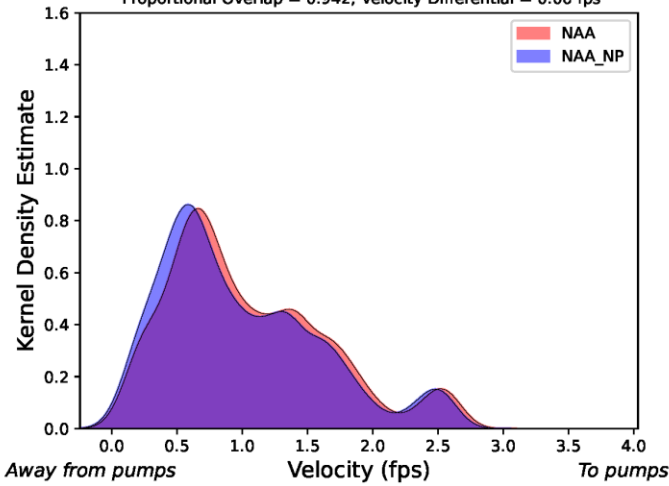
KDE of Old R at Head of Old River Velocity in Jan-Jun

OMR = -1000 cfs; Proportion of Simulation: 5%;  
Proportional Overlap = 0.951; Velocity Differential = 0.02 fps



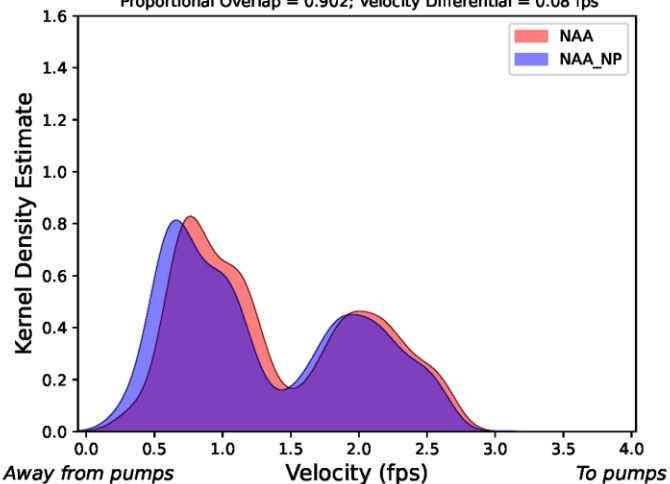
KDE of Old R at Head of Old River Velocity in Jan-Jun

OMR = -2000 cfs; Proportion of Simulation: 10%;  
Proportional Overlap = 0.942; Velocity Differential = 0.06 fps



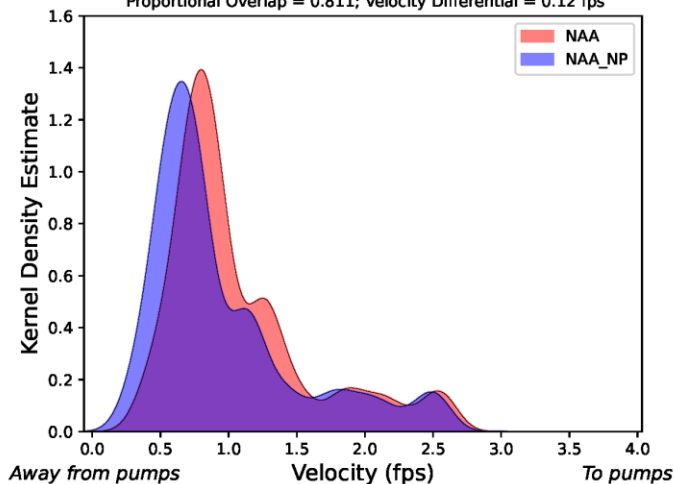
KDE of Old R at Head of Old River Velocity in Jan-Jun

OMR = -3000 cfs; Proportion of Simulation: 10%;  
Proportional Overlap = 0.902; Velocity Differential = 0.08 fps



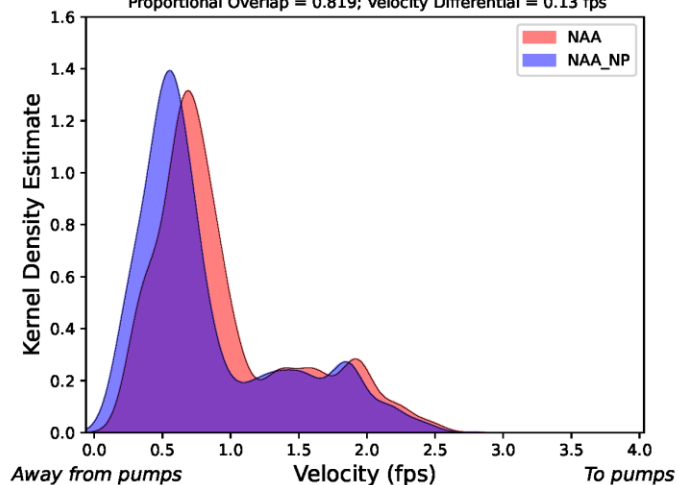
KDE of Old R at Head of Old River Velocity in Jan-Jun

OMR = -4000 cfs; Proportion of Simulation: 10%;  
Proportional Overlap = 0.811; Velocity Differential = 0.12 fps



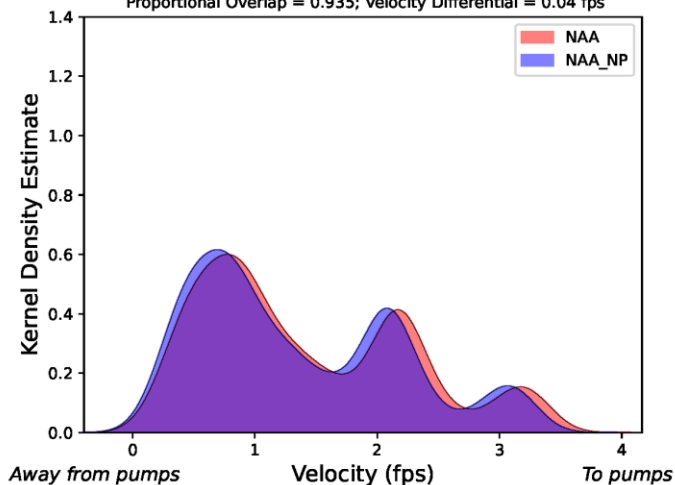
KDE of Old R at Head of Old River Velocity in Jan-Jun

OMR = -5000 cfs; Proportion of Simulation: 11%;  
Proportional Overlap = 0.819; Velocity Differential = 0.13 fps



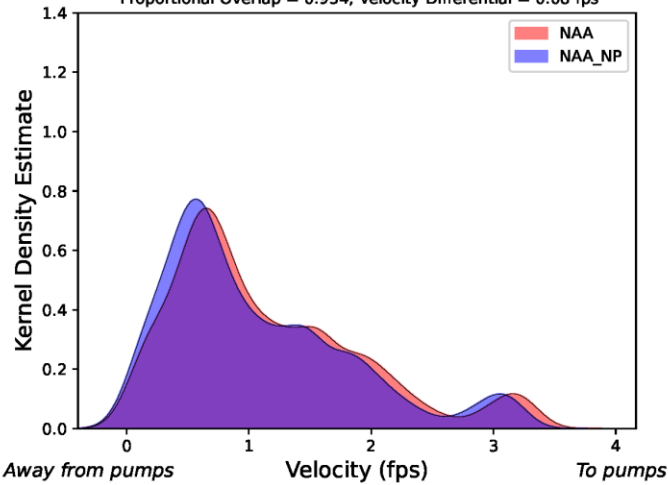
KDE of Old R at Middle River Velocity in Jan-Jun

OMR = -1000 cfs; Proportion of Simulation: 5%;  
Proportional Overlap = 0.935; Velocity Differential = 0.04 fps



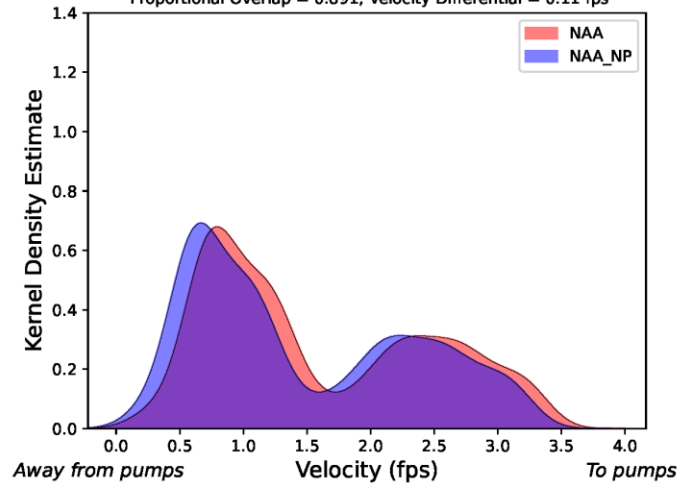
KDE of Old R at Middle River Velocity in Jan-Jun

OMR = -2000 cfs; Proportion of Simulation: 10%;  
Proportional Overlap = 0.934; Velocity Differential = 0.08 fps



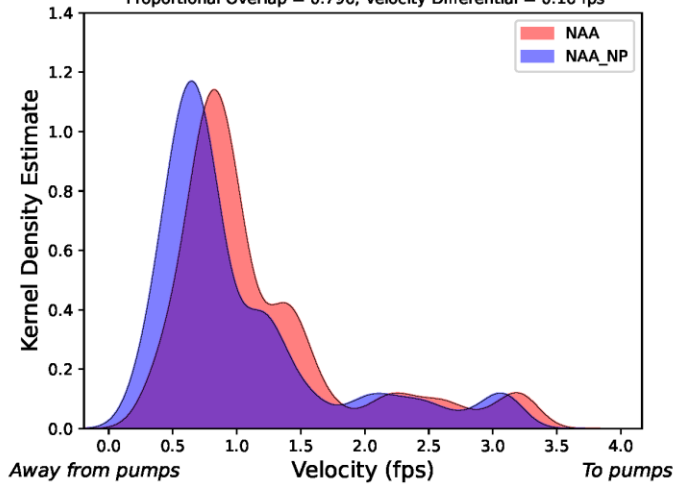
KDE of Old R at Middle River Velocity in Jan-Jun

OMR = -3000 cfs; Proportion of Simulation: 10%;  
Proportional Overlap = 0.891; Velocity Differential = 0.11 fps



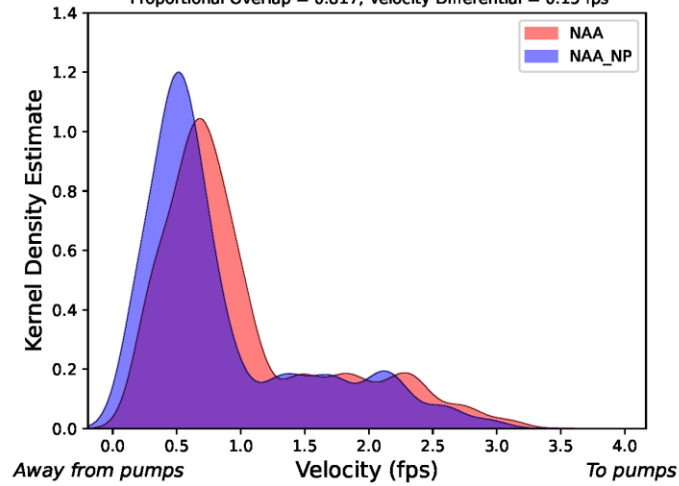
KDE of Old R at Middle River Velocity in Jan-Jun

OMR = -4000 cfs; Proportion of Simulation: 10%;  
Proportional Overlap = 0.796; Velocity Differential = 0.16 fps



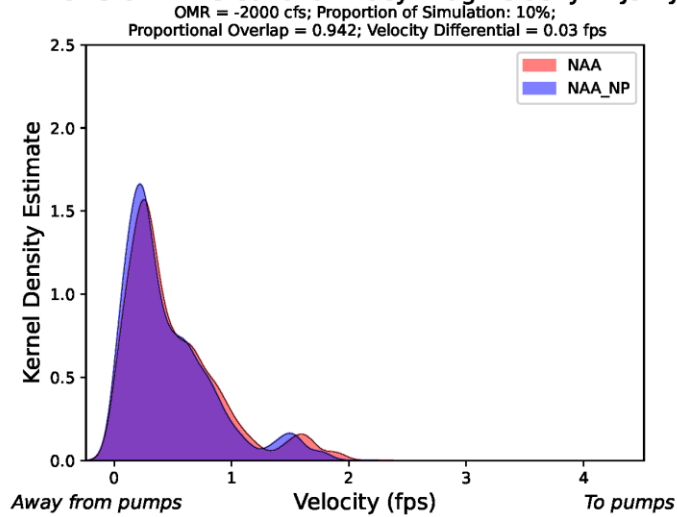
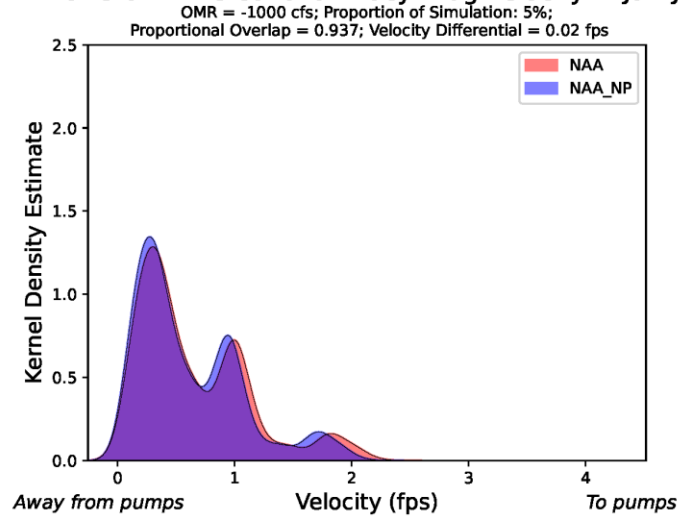
KDE of Old R at Middle River Velocity in Jan-Jun

OMR = -5000 cfs; Proportion of Simulation: 11%;  
Proportional Overlap = 0.817; Velocity Differential = 0.15 fps

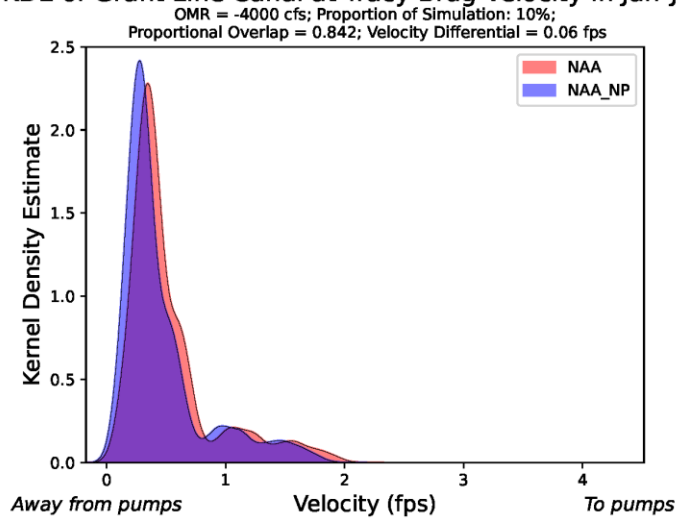
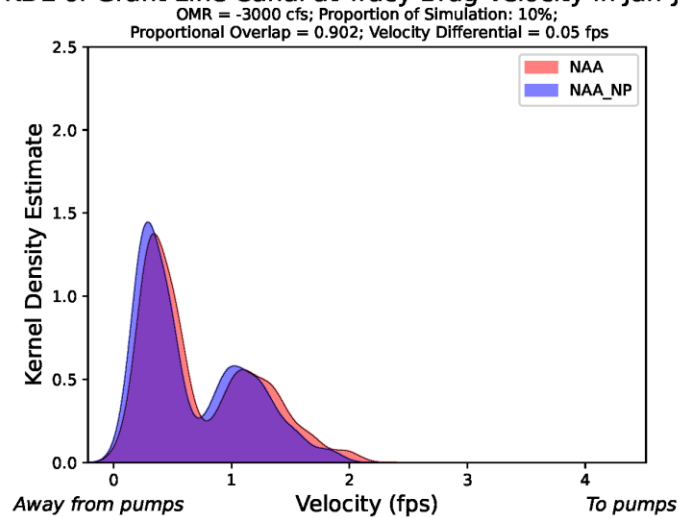




# KDE of Grant Line Canal at Tracy Brdg Velocity in Jan-Jun

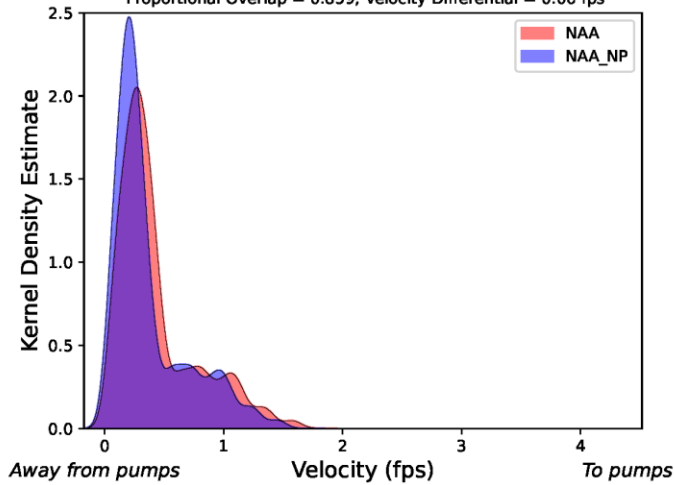


# KDE of Grant Line Canal at Tracy Brdg Velocity in Jan-Jun



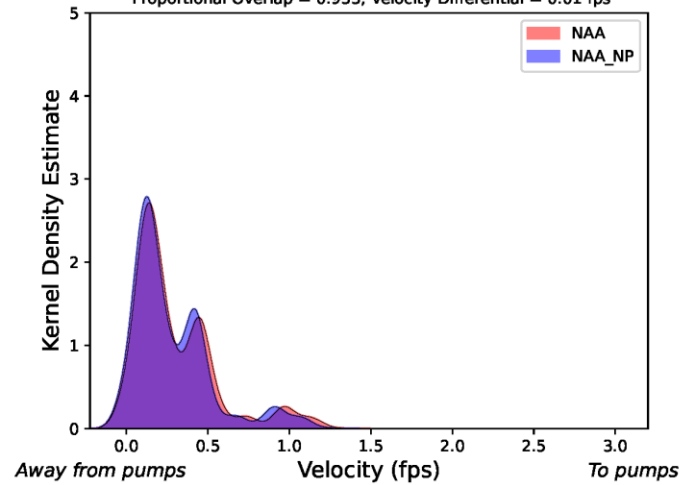
KDE of Grant Line Canal at Tracy Brdg Velocity in Jan-Jun

OMR = -5000 cfs; Proportion of Simulation: 11%;  
Proportional Overlap = 0.859; Velocity Differential = 0.06 fps



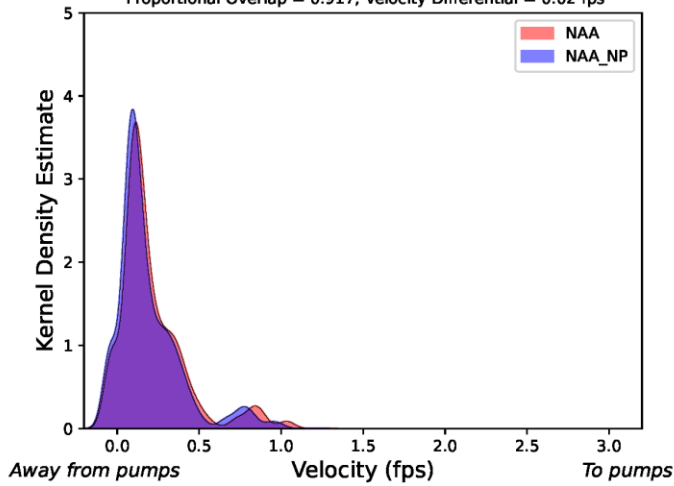
KDE of Old R near Tracy Velocity in Jan-Jun

OMR = -1000 cfs; Proportion of Simulation: 5%;  
Proportional Overlap = 0.933; Velocity Differential = 0.01 fps



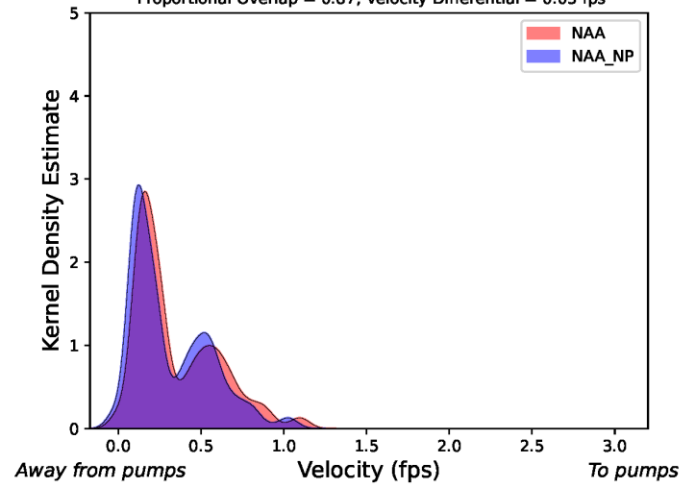
KDE of Old R near Tracy Velocity in Jan-Jun

OMR = -2000 cfs; Proportion of Simulation: 10%;  
Proportional Overlap = 0.917; Velocity Differential = 0.02 fps



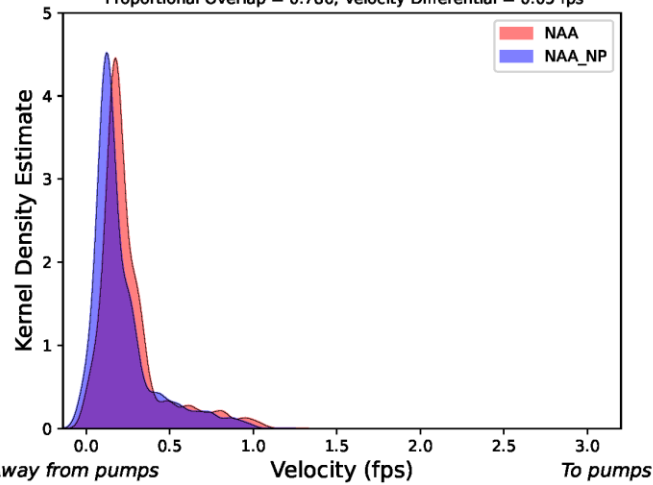
KDE of Old R near Tracy Velocity in Jan-Jun

OMR = -3000 cfs; Proportion of Simulation: 10%;  
Proportional Overlap = 0.87; Velocity Differential = 0.03 fps



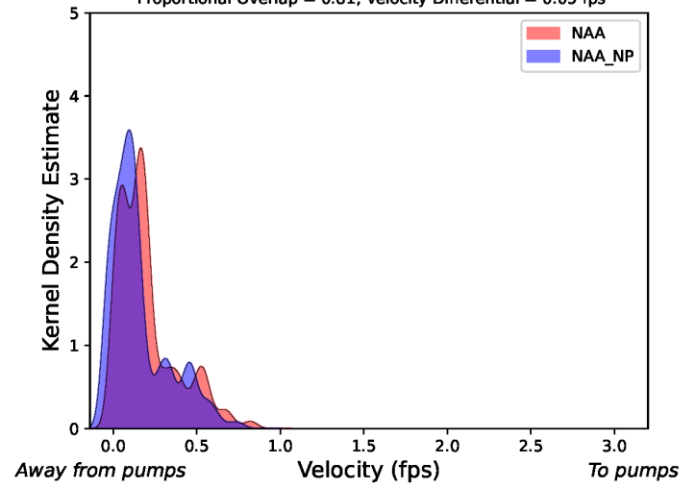
KDE of Old R near Tracy Velocity in Jan-Jun

OMR = -4000 cfs; Proportion of Simulation: 10%;  
Proportional Overlap = 0.786; Velocity Differential = 0.05 fps



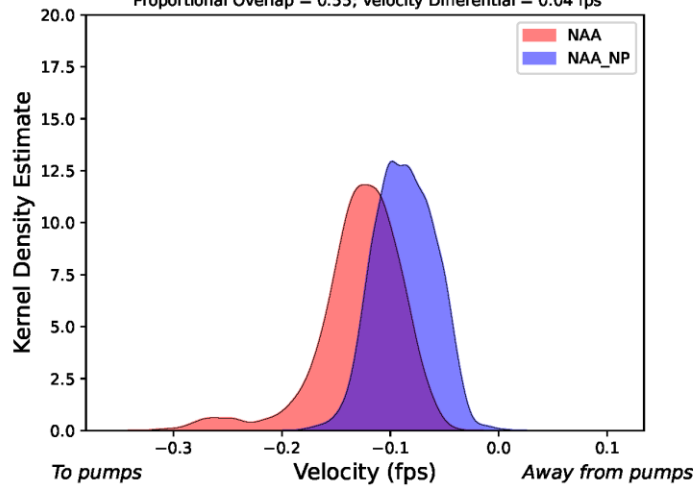
KDE of Old R near Tracy Velocity in Jan-Jun

OMR = -5000 cfs; Proportion of Simulation: 11%;  
Proportional Overlap = 0.81; Velocity Differential = 0.05 fps



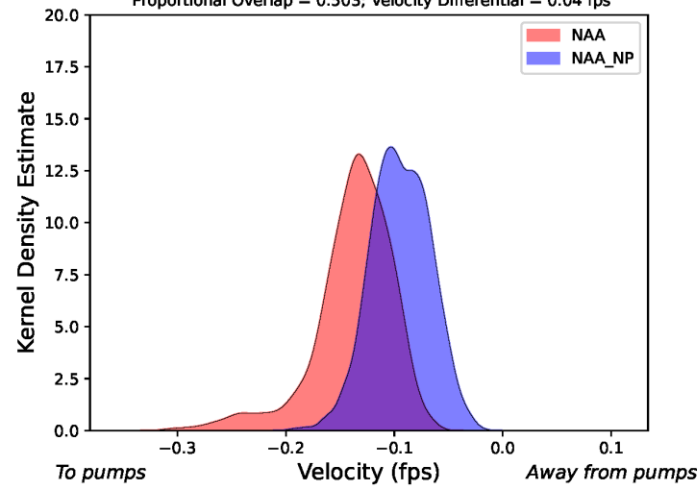
KDE of Old R before Franks Tract Velocity in Jan-Jun

OMR = -1000 cfs; Proportion of Simulation: 5%;  
Proportional Overlap = 0.55; Velocity Differential = 0.04 fps



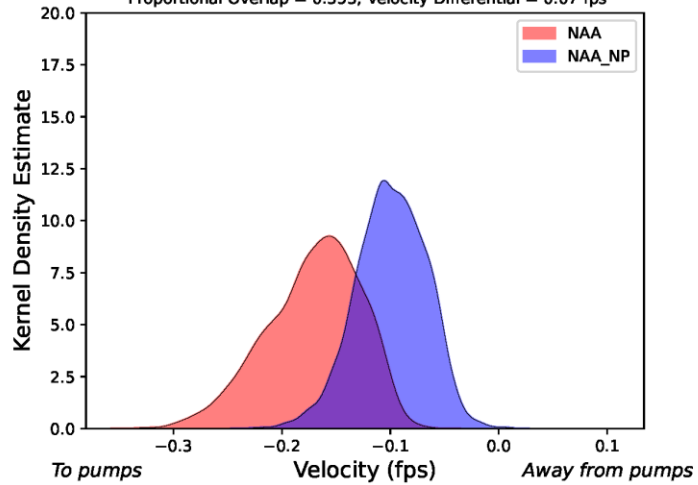
KDE of Old R before Franks Tract Velocity in Jan-Jun

OMR = -2000 cfs; Proportion of Simulation: 10%;  
Proportional Overlap = 0.503; Velocity Differential = 0.04 fps



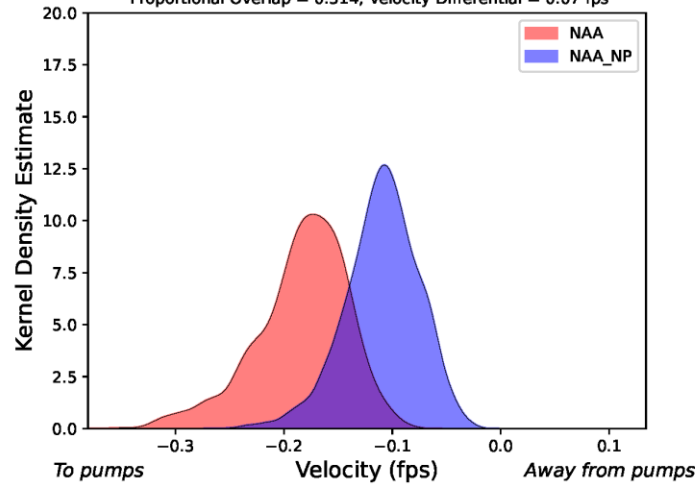
KDE of Old R before Franks Tract Velocity in Jan-Jun

OMR = -3000 cfs; Proportion of Simulation: 10%;  
Proportional Overlap = 0.353; Velocity Differential = 0.07 fps



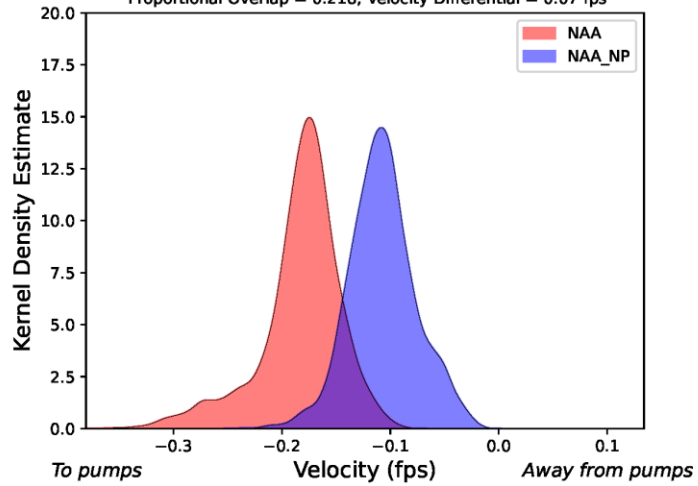
KDE of Old R before Franks Tract Velocity in Jan-Jun

OMR = -4000 cfs; Proportion of Simulation: 10%;  
Proportional Overlap = 0.314; Velocity Differential = 0.07 fps



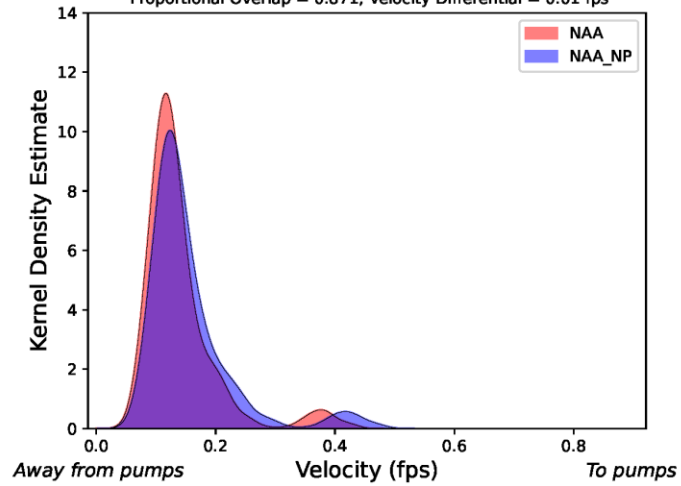
KDE of Old R before Franks Tract Velocity in Jan-Jun

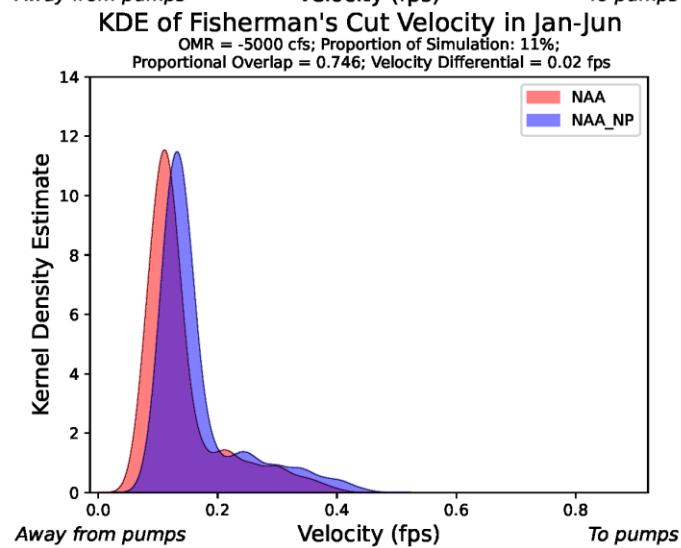
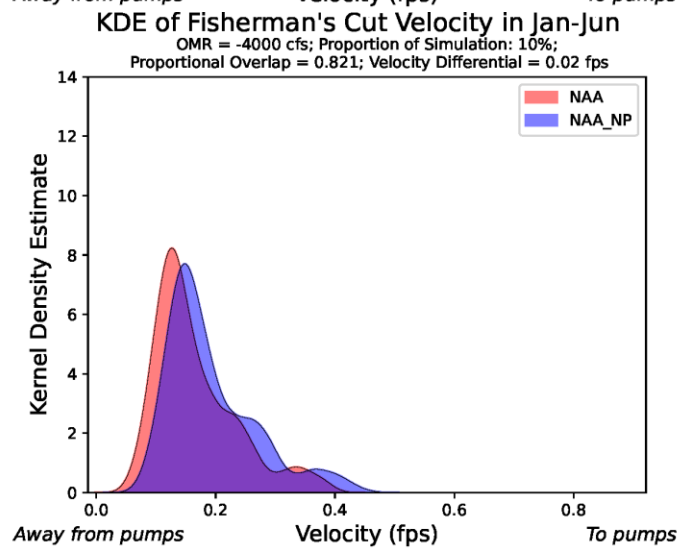
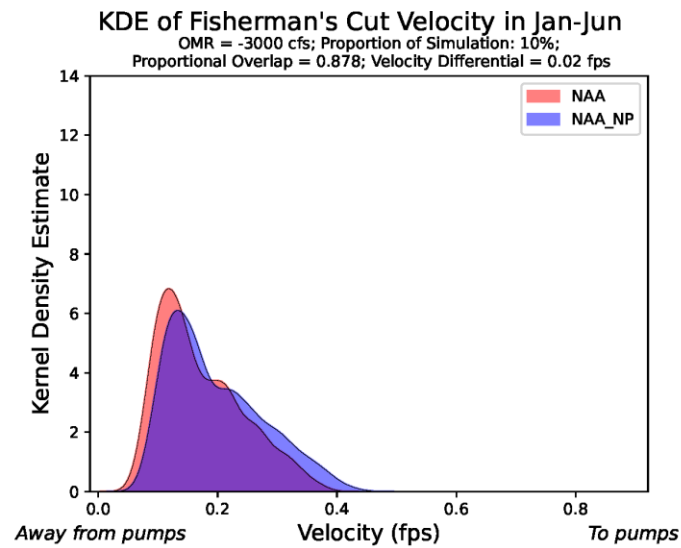
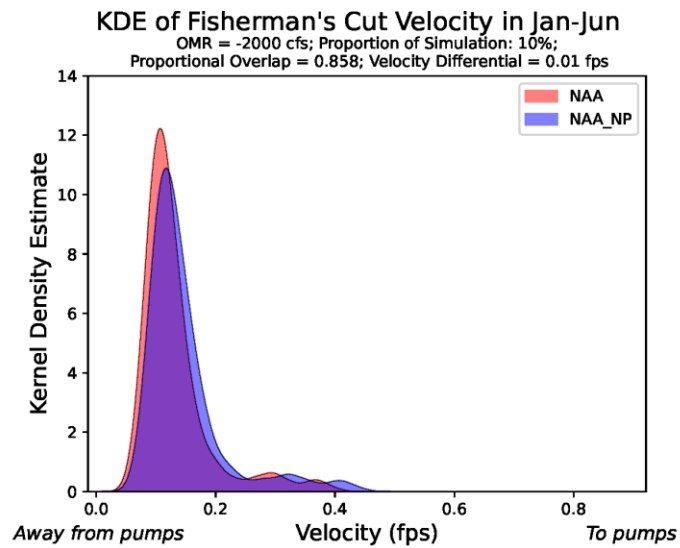
OMR = -5000 cfs; Proportion of Simulation: 11%;  
Proportional Overlap = 0.218; Velocity Differential = 0.07 fps



KDE of Fisherman's Cut Velocity in Jan-Jun

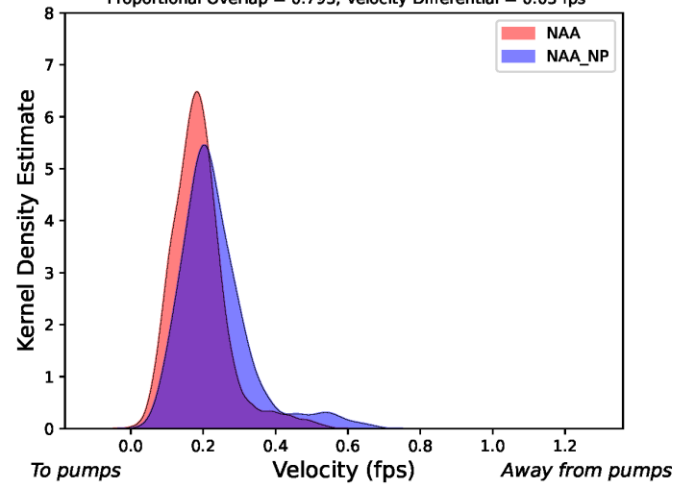
OMR = -1000 cfs; Proportion of Simulation: 5%;  
Proportional Overlap = 0.871; Velocity Differential = 0.01 fps





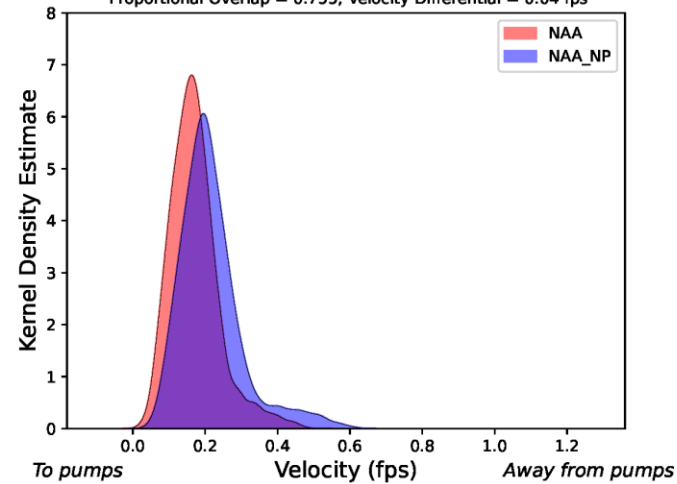
KDE of False R before Franks Tract Velocity in Jan-Jun

OMR = -1000 cfs; Proportion of Simulation: 5%;  
Proportional Overlap = 0.793; Velocity Differential = 0.03 fps



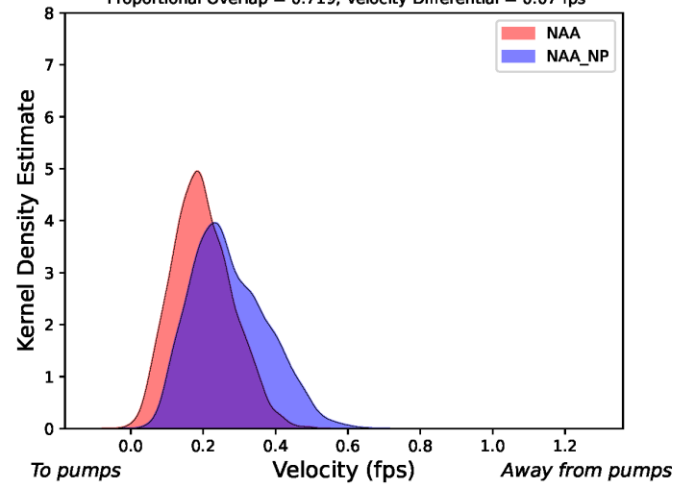
KDE of False R before Franks Tract Velocity in Jan-Jun

OMR = -2000 cfs; Proportion of Simulation: 10%;  
Proportional Overlap = 0.755; Velocity Differential = 0.04 fps



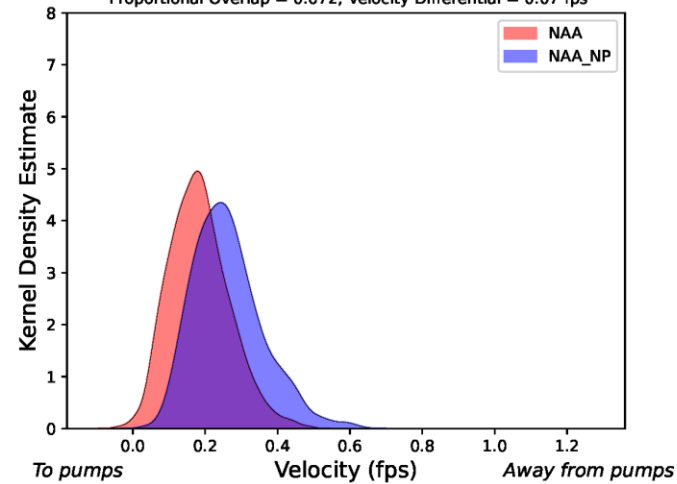
KDE of False R before Franks Tract Velocity in Jan-Jun

OMR = -3000 cfs; Proportion of Simulation: 10%;  
Proportional Overlap = 0.719; Velocity Differential = 0.07 fps



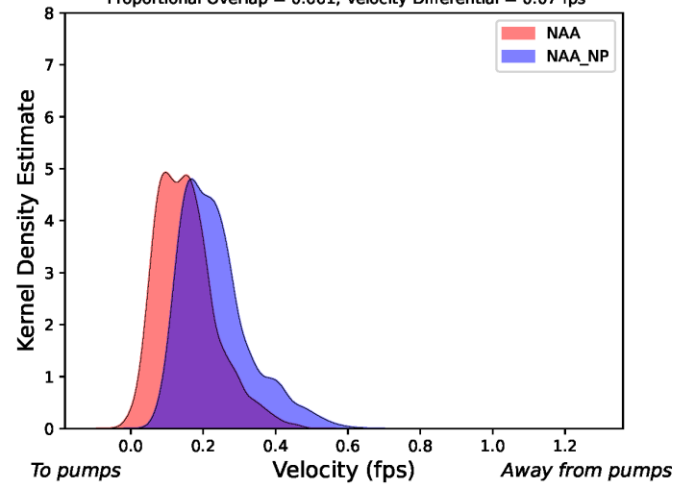
KDE of False R before Franks Tract Velocity in Jan-Jun

OMR = -4000 cfs; Proportion of Simulation: 10%;  
Proportional Overlap = 0.672; Velocity Differential = 0.07 fps



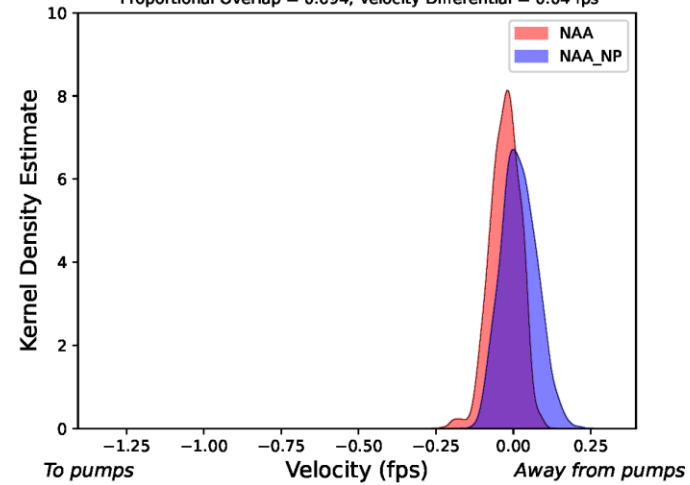
KDE of False R before Franks Tract Velocity in Jan-Jun

OMR = -5000 cfs; Proportion of Simulation: 11%;  
Proportional Overlap = 0.661; Velocity Differential = 0.07 fps



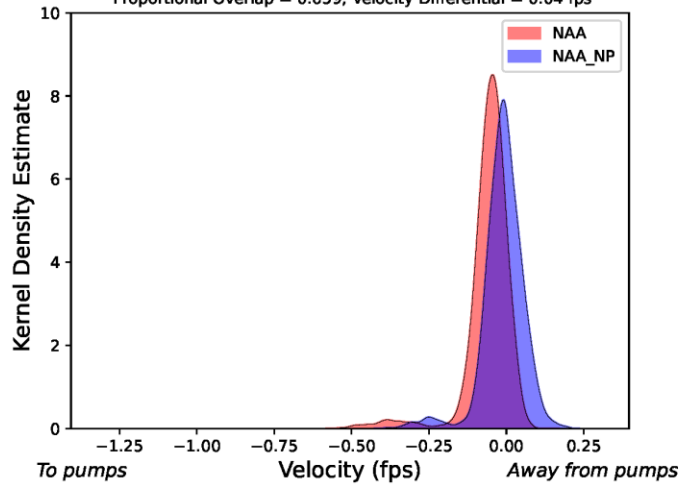
KDE of Threemile Slough Velocity in Jan-Jun

OMR = -1000 cfs; Proportion of Simulation: 5%;  
Proportional Overlap = 0.694; Velocity Differential = 0.04 fps



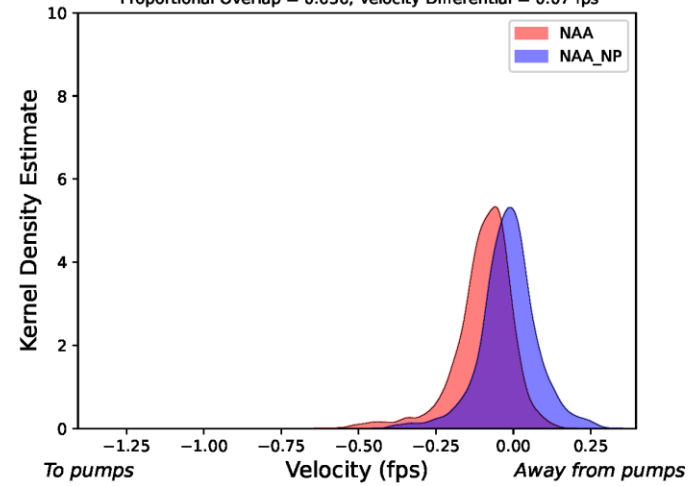
KDE of Threemile Slough Velocity in Jan-Jun

OMR = -2000 cfs; Proportion of Simulation: 10%;  
Proportional Overlap = 0.659; Velocity Differential = 0.04 fps



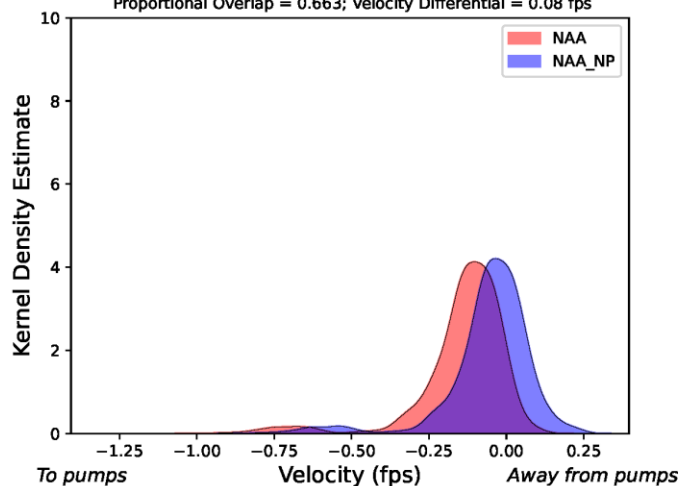
KDE of Threemile Slough Velocity in Jan-Jun

OMR = -3000 cfs; Proportion of Simulation: 10%;  
Proportional Overlap = 0.636; Velocity Differential = 0.07 fps



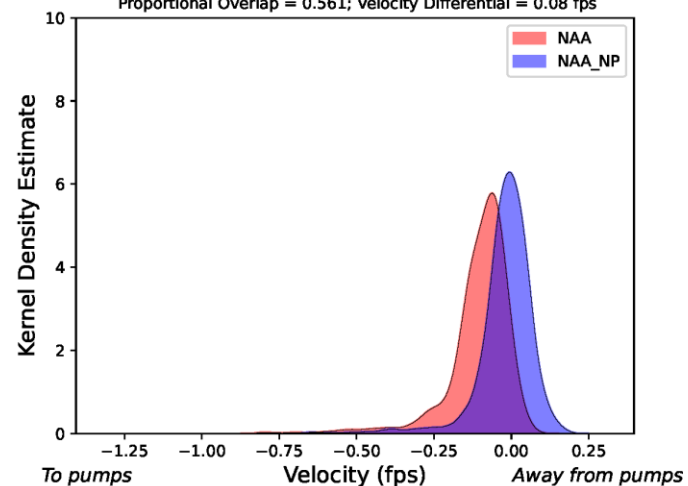
KDE of Threemile Slough Velocity in Jan-Jun

OMR = -4000 cfs; Proportion of Simulation: 10%;  
Proportional Overlap = 0.663; Velocity Differential = 0.08 fps



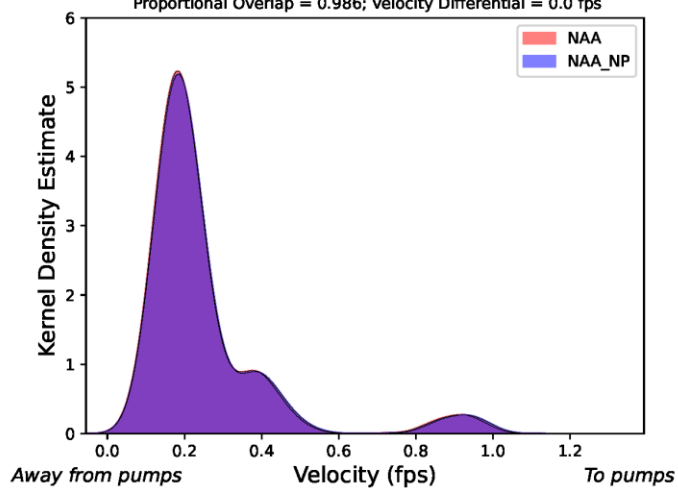
KDE of Threemile Slough Velocity in Jan-Jun

OMR = -5000 cfs; Proportion of Simulation: 11%;  
Proportional Overlap = 0.561; Velocity Differential = 0.08 fps



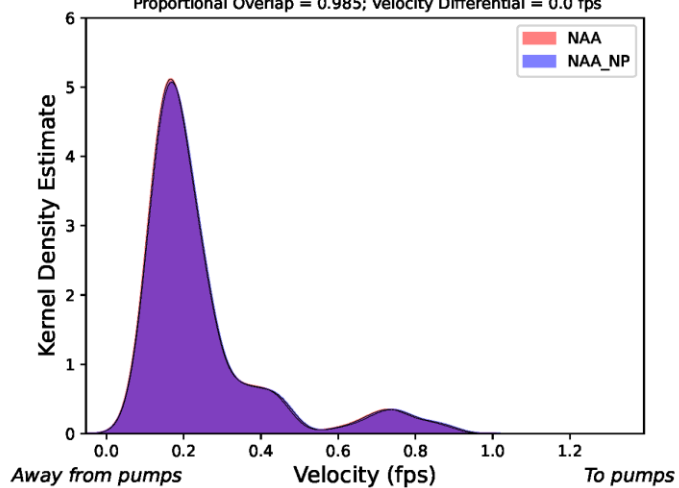
KDE of Mokelumne R Velocity in Jan-Jun

OMR = -1000 cfs; Proportion of Simulation: 5%;  
Proportional Overlap = 0.986; Velocity Differential = 0.0 fps

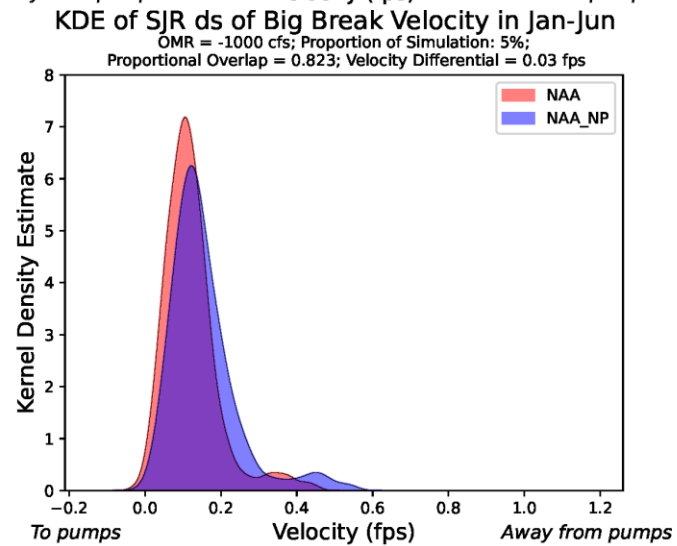
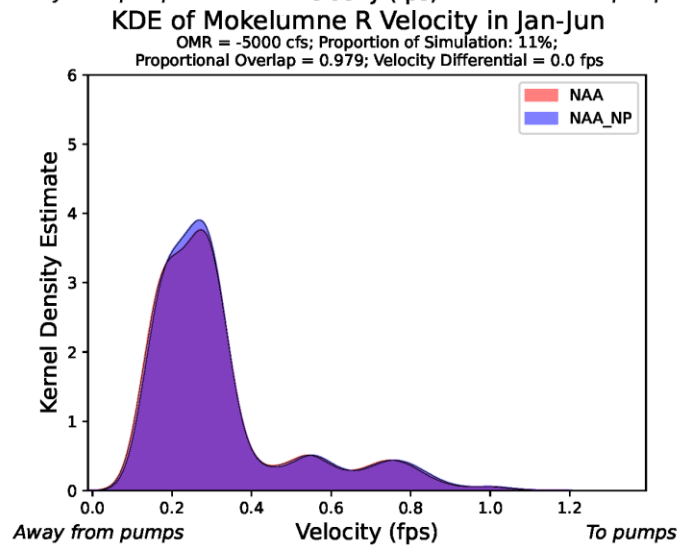
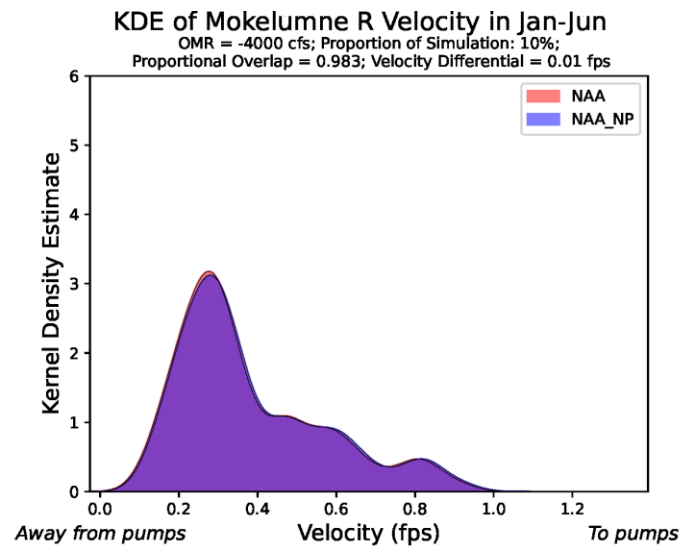
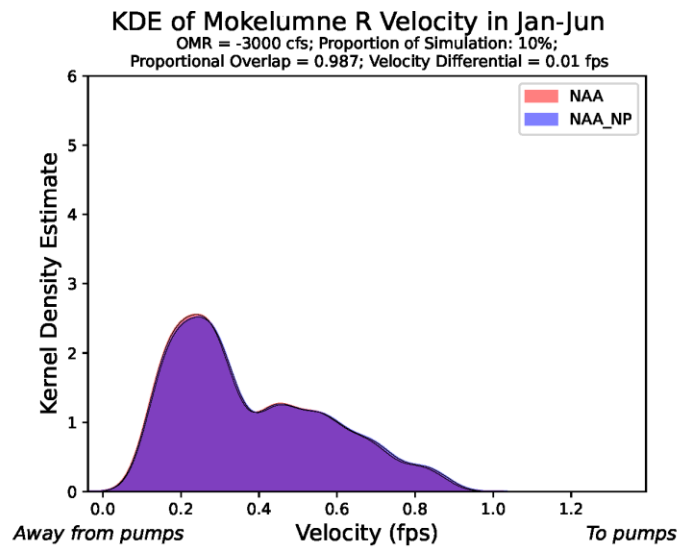


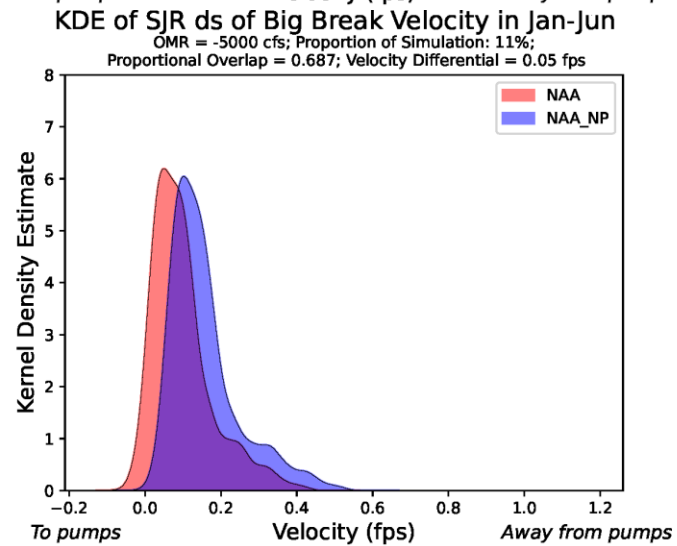
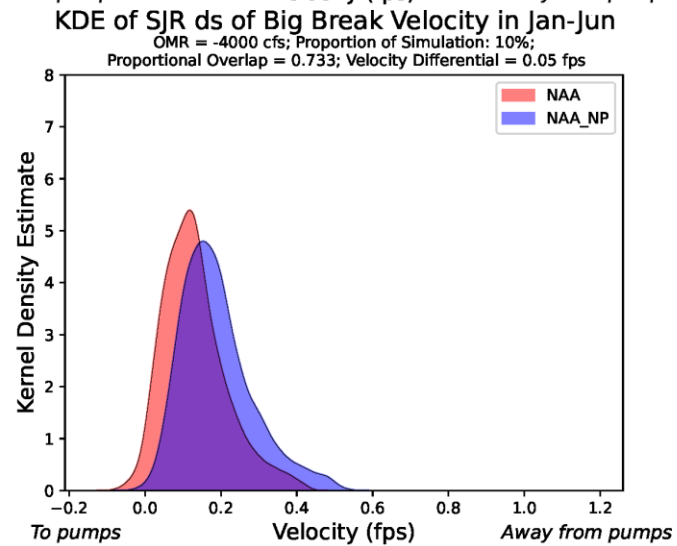
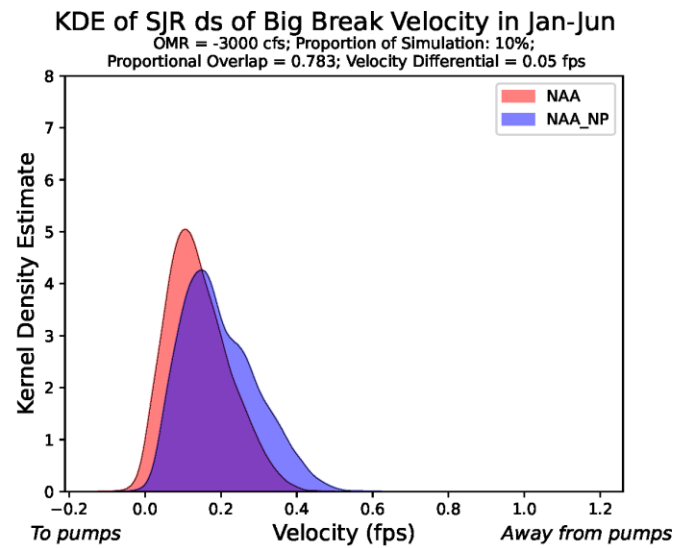
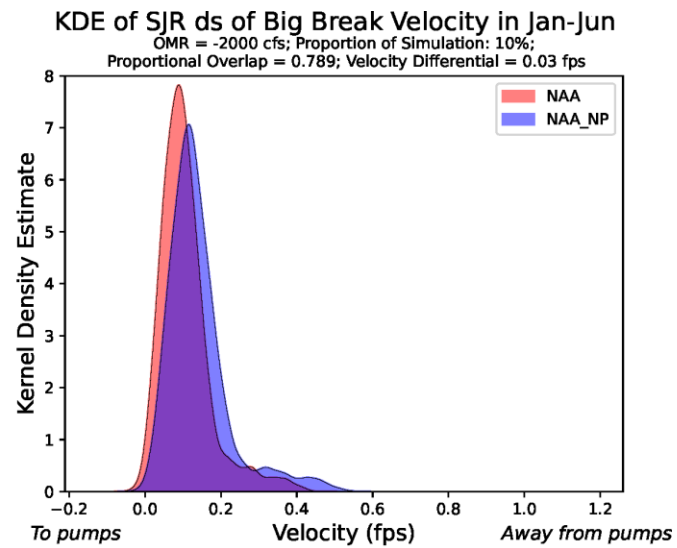
KDE of Mokelumne R Velocity in Jan-Jun

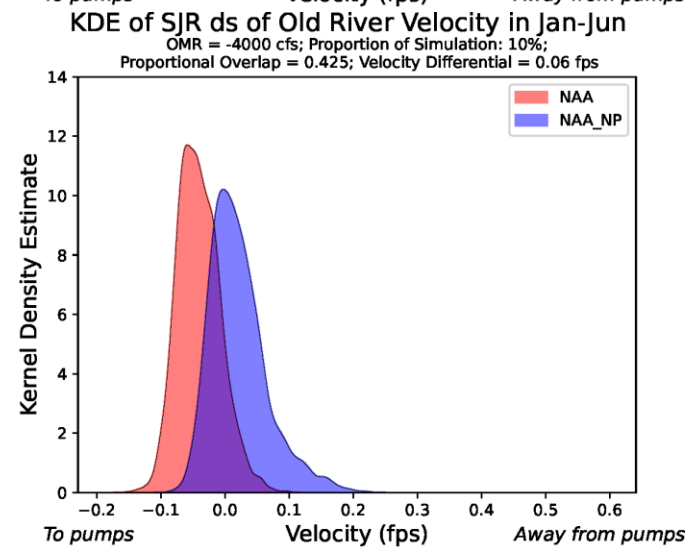
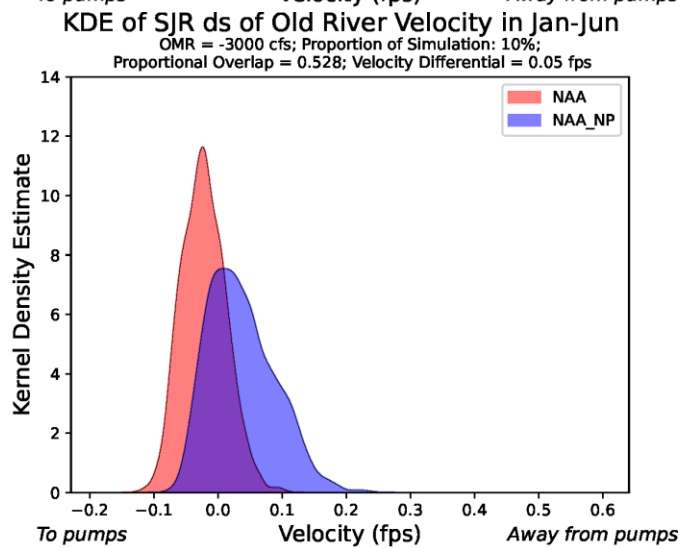
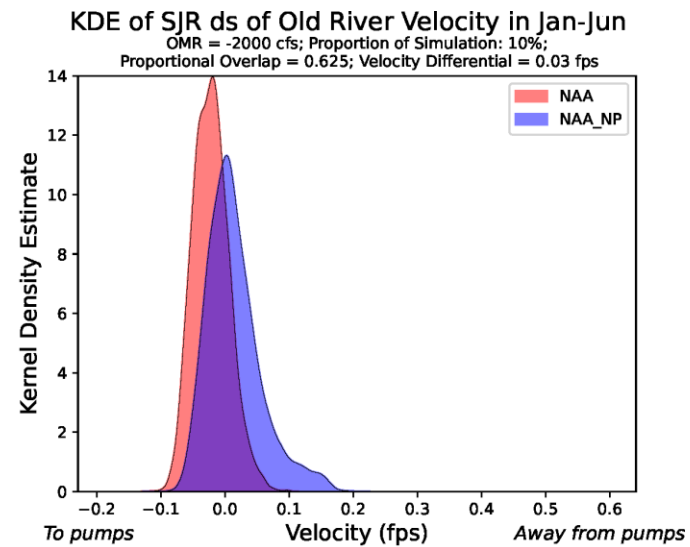
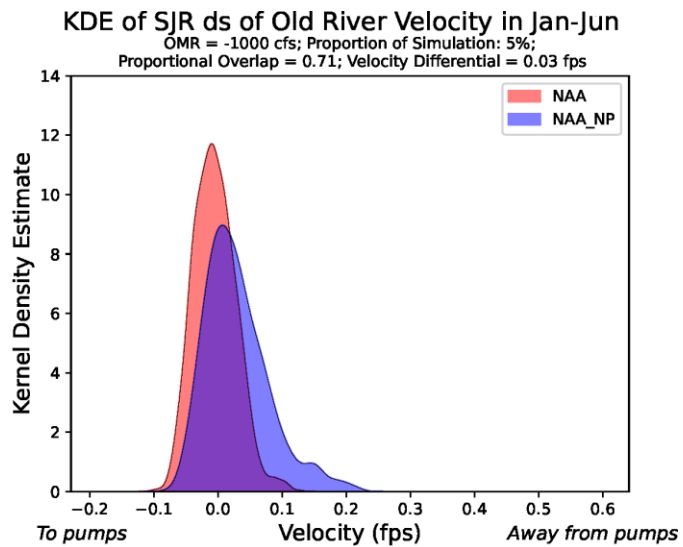
OMR = -2000 cfs; Proportion of Simulation: 10%;  
Proportional Overlap = 0.985; Velocity Differential = 0.0 fps

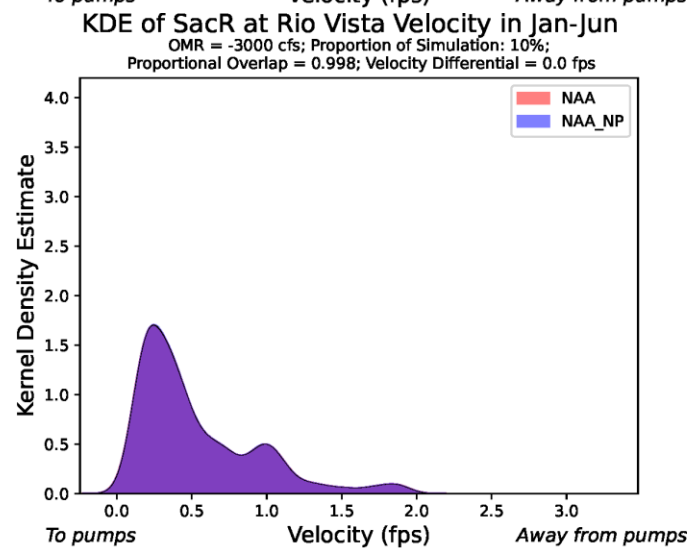
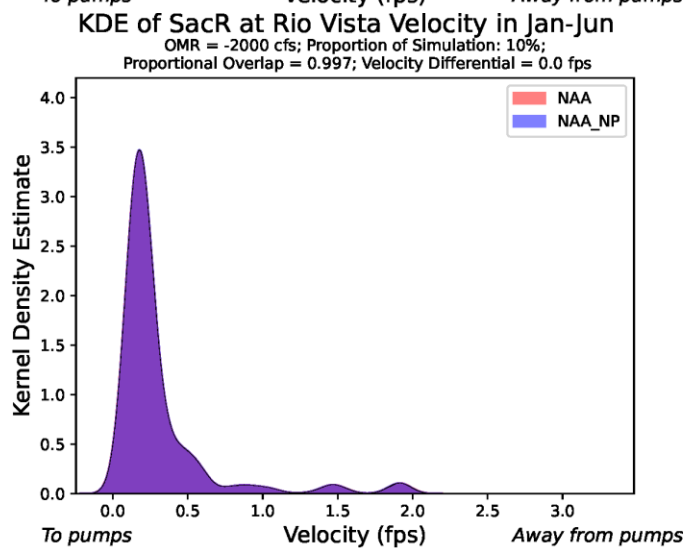
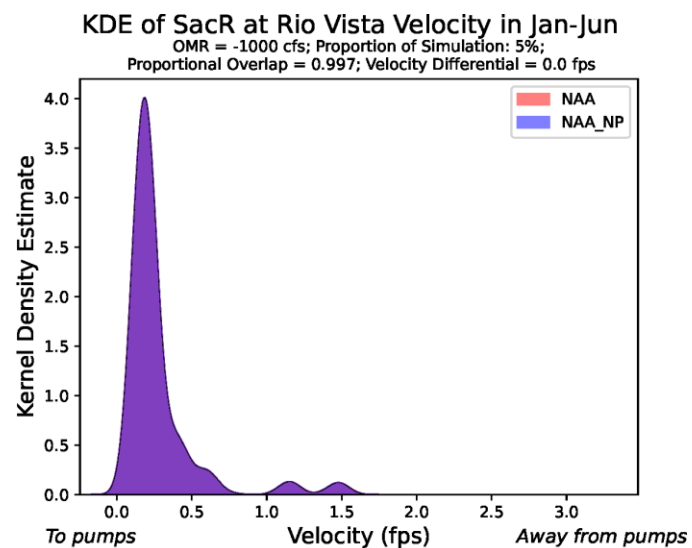
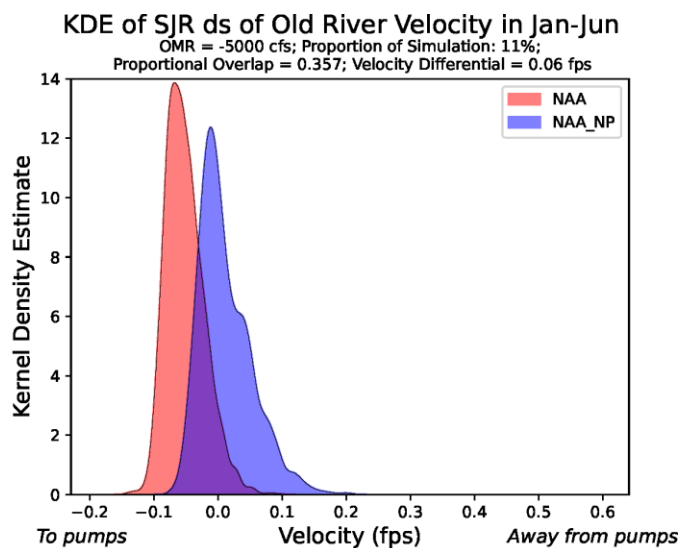






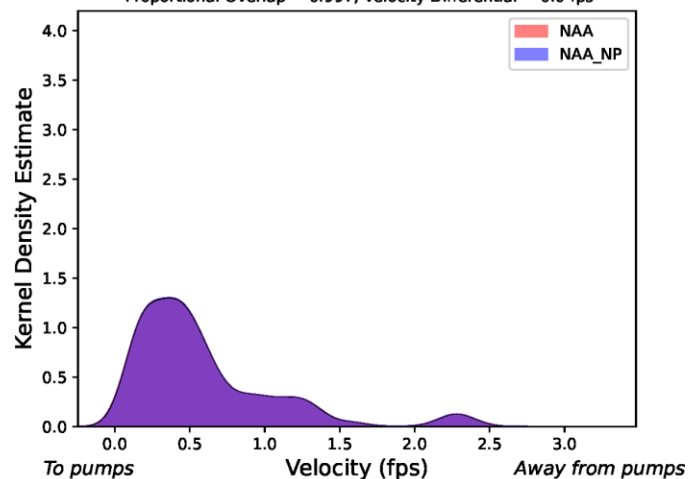






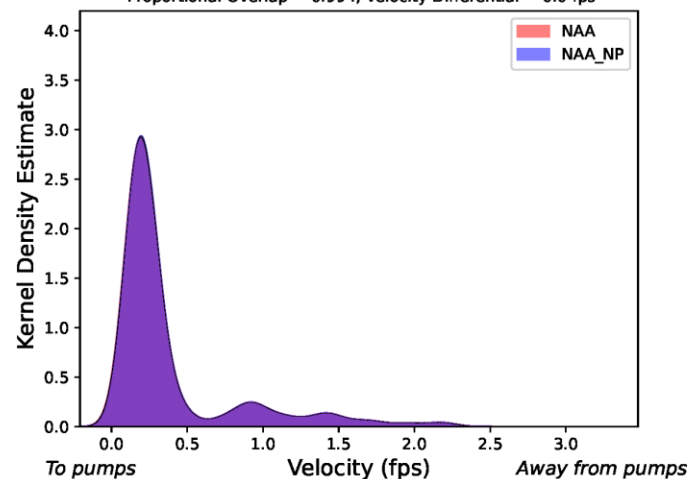
KDE of SacR at Rio Vista Velocity in Jan-Jun

OMR = -4000 cfs; Proportion of Simulation: 10%;  
Proportional Overlap = 0.997; Velocity Differential = 0.0 fps



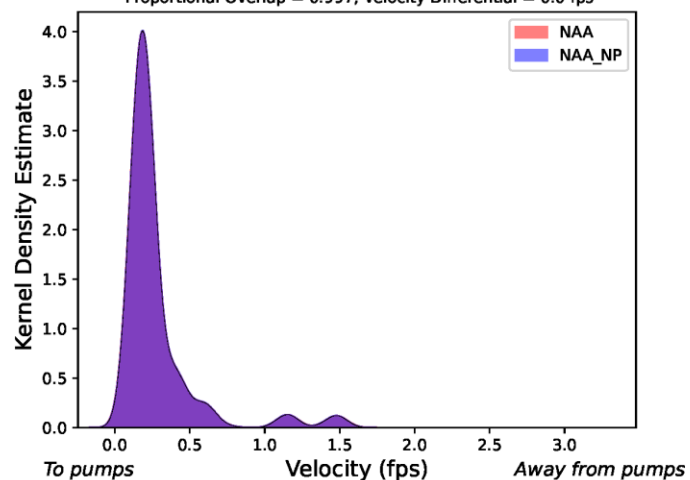
KDE of SacR at Rio Vista Velocity in Jan-Jun

OMR = -5000 cfs; Proportion of Simulation: 11%;  
Proportional Overlap = 0.994; Velocity Differential = 0.0 fps



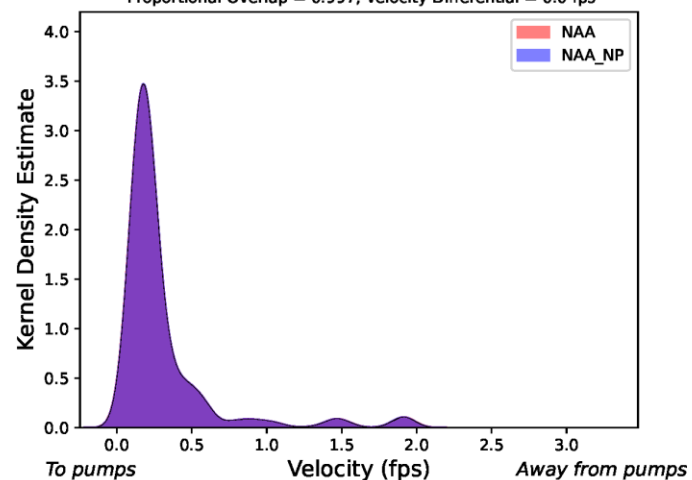
KDE of SacR at Emmatton Velocity in Jan-Jun

OMR = -1000 cfs; Proportion of Simulation: 5%;  
Proportional Overlap = 0.997; Velocity Differential = 0.0 fps



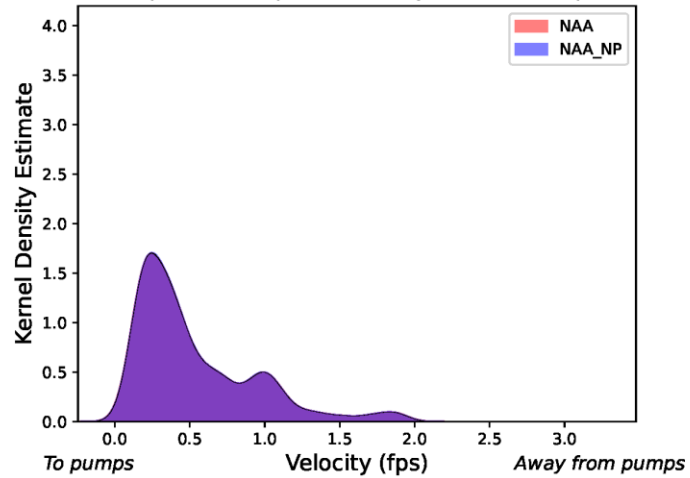
KDE of SacR at Emmatton Velocity in Jan-Jun

OMR = -2000 cfs; Proportion of Simulation: 10%;  
Proportional Overlap = 0.997; Velocity Differential = 0.0 fps



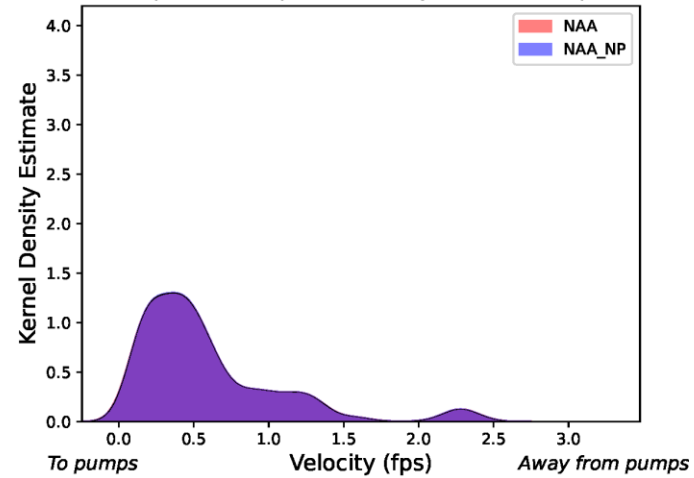
KDE of SacR at Emmaton Velocity in Jan-Jun

OMR = -3000 cfs; Proportion of Simulation: 10%;  
Proportional Overlap = 0.998; Velocity Differential = 0.0 fps



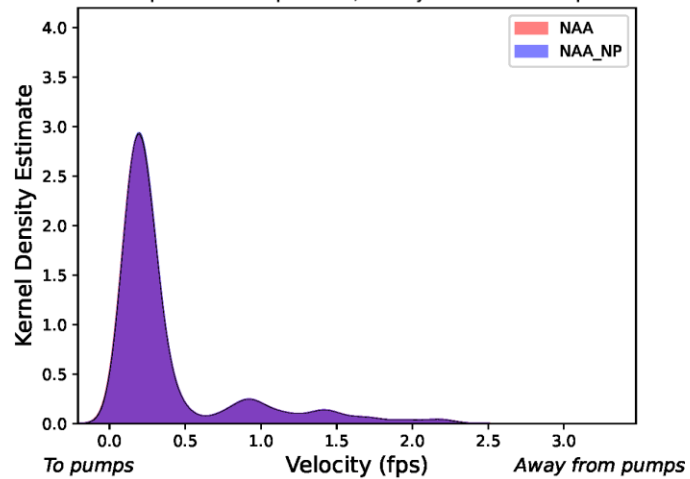
KDE of SacR at Emmaton Velocity in Jan-Jun

OMR = -4000 cfs; Proportion of Simulation: 10%;  
Proportional Overlap = 0.997; Velocity Differential = 0.0 fps

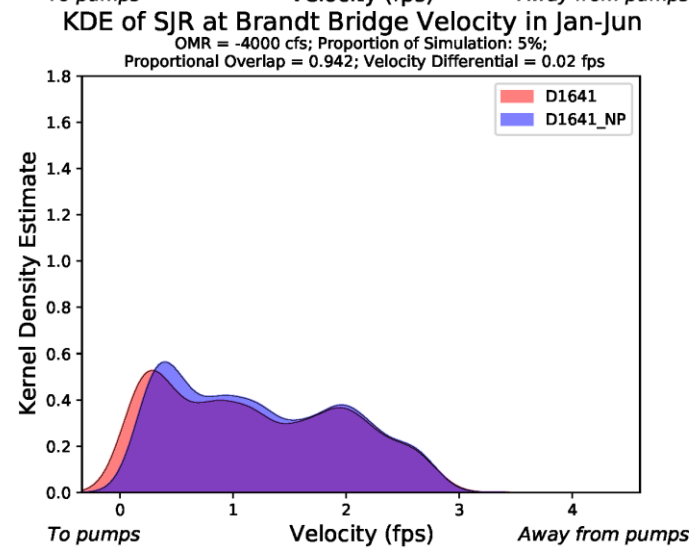
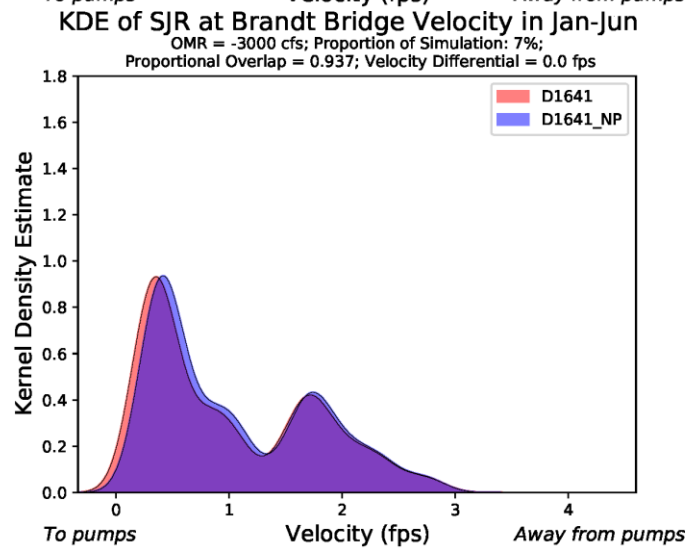
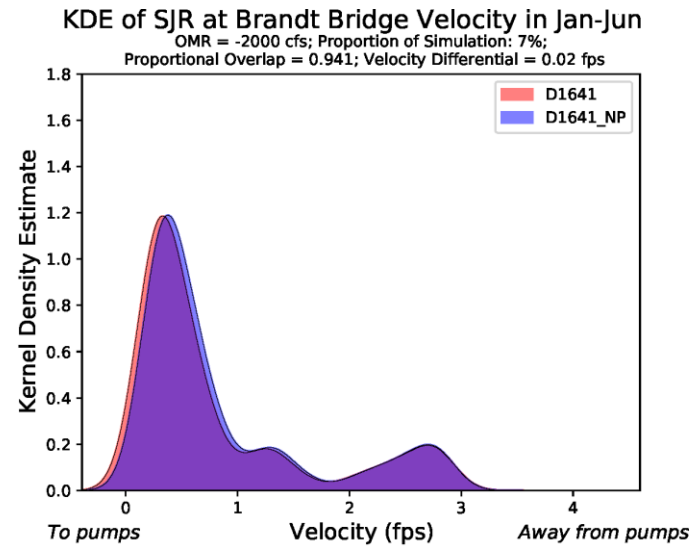
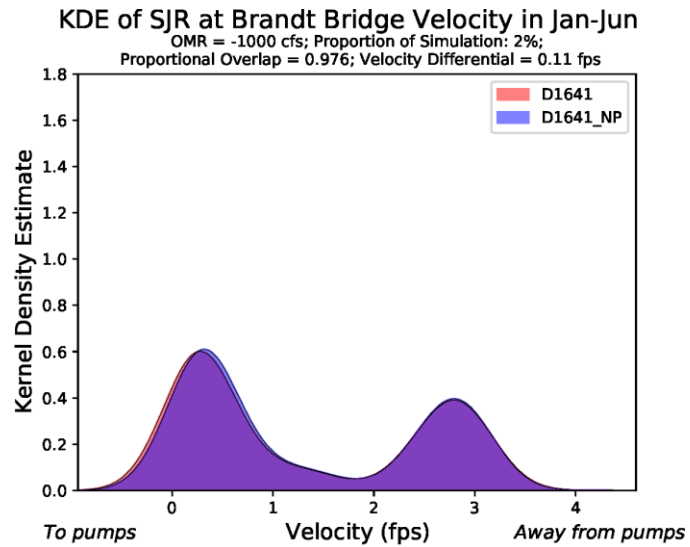


KDE of SacR at Emmaton Velocity in Jan-Jun

OMR = -5000 cfs; Proportion of Simulation: 11%;  
Proportional Overlap = 0.994; Velocity Differential = 0.0 fps

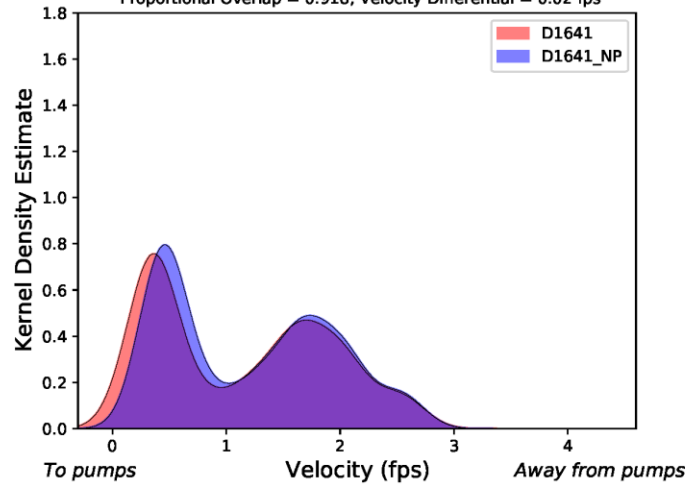


The set of figures below represent the D1641 results.



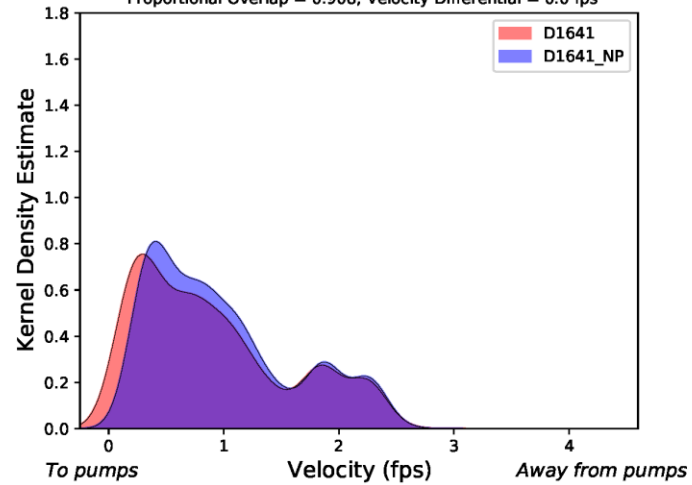
KDE of SJR at Brandt Bridge Velocity in Jan-Jun

OMR = -5000 cfs; Proportion of Simulation: 4%;  
Proportional Overlap = 0.918; Velocity Differential = 0.02 fps



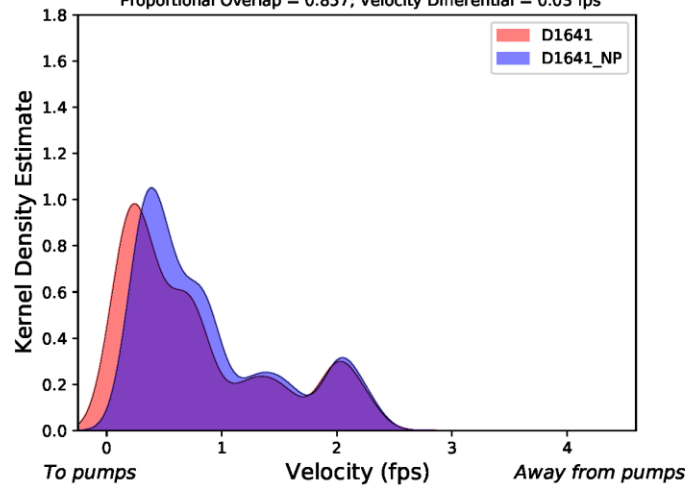
KDE of SJR at Brandt Bridge Velocity in Jan-Jun

OMR = -6000 cfs; Proportion of Simulation: 4%;  
Proportional Overlap = 0.908; Velocity Differential = 0.0 fps



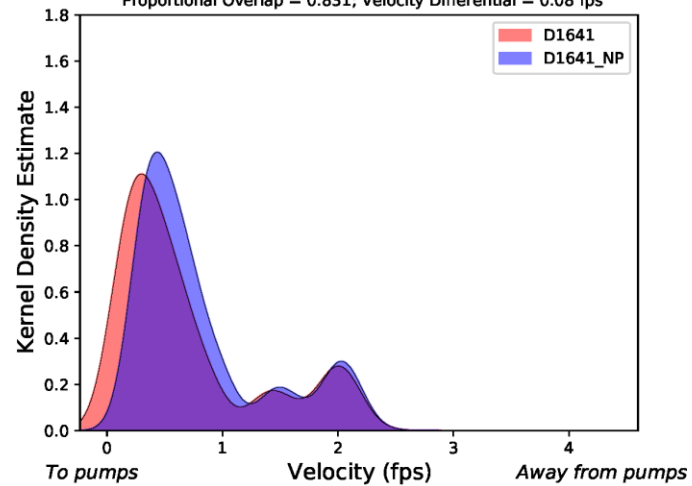
KDE of SJR at Brandt Bridge Velocity in Jan-Jun

OMR = -7000 cfs; Proportion of Simulation: 6%;  
Proportional Overlap = 0.857; Velocity Differential = 0.03 fps



KDE of SJR at Brandt Bridge Velocity in Jan-Jun

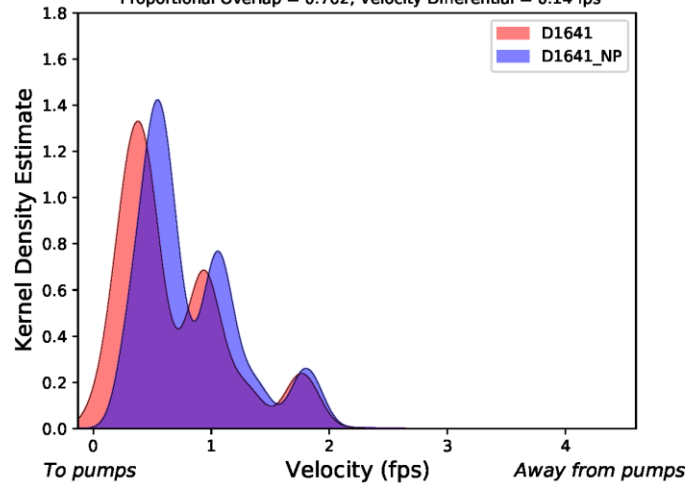
OMR = -8000 cfs; Proportion of Simulation: 4%;  
Proportional Overlap = 0.831; Velocity Differential = 0.08 fps





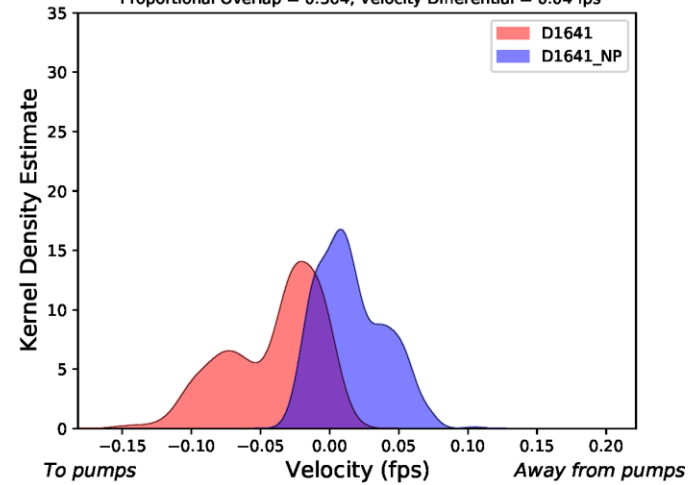
KDE of SJR at Brandt Bridge Velocity in Jan-Jun

OMR = -9000 cfs; Proportion of Simulation: 5%;  
Proportional Overlap = 0.762; Velocity Differential = 0.14 fps



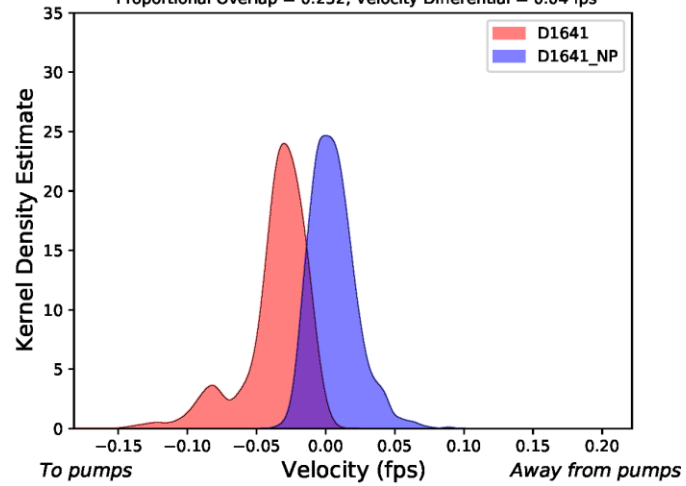
KDE of Turner Cut Velocity in Jan-Jun

OMR = -1000 cfs; Proportion of Simulation: 2%;  
Proportional Overlap = 0.364; Velocity Differential = 0.04 fps



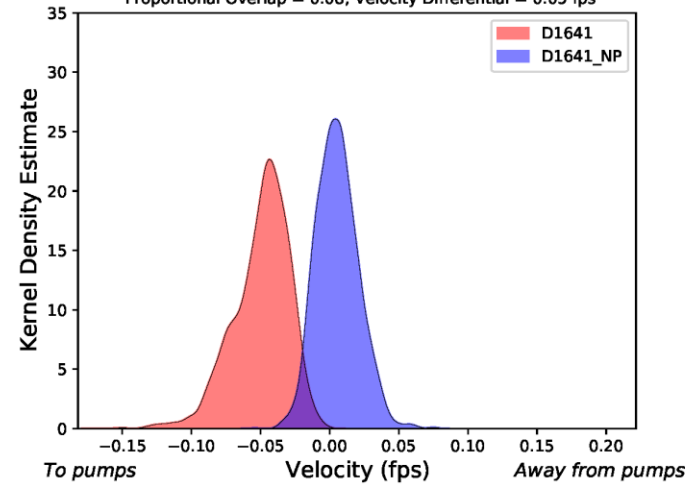
KDE of Turner Cut Velocity in Jan-Jun

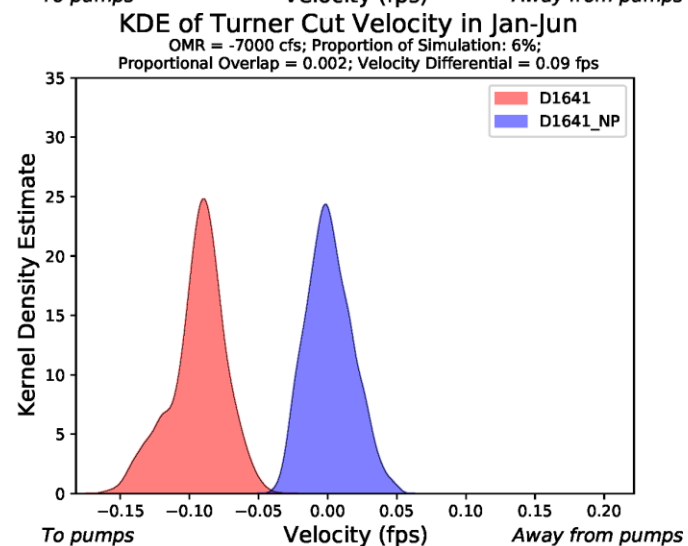
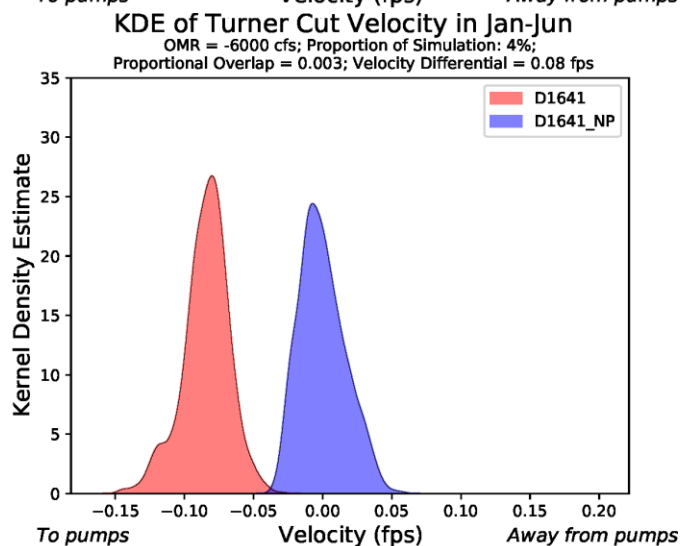
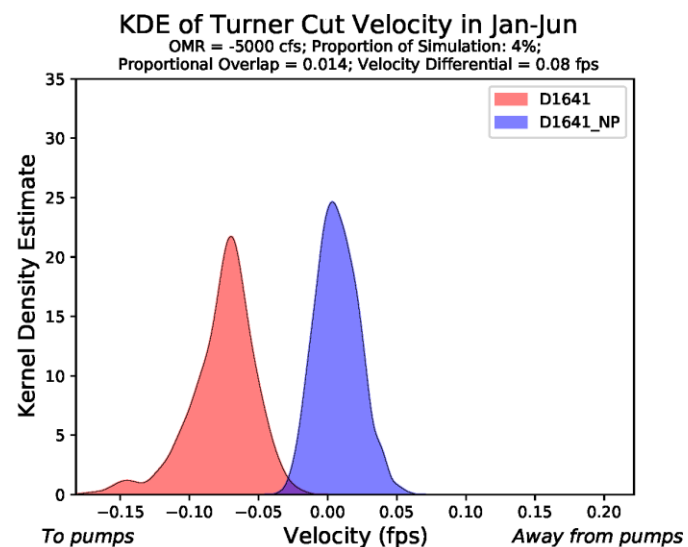
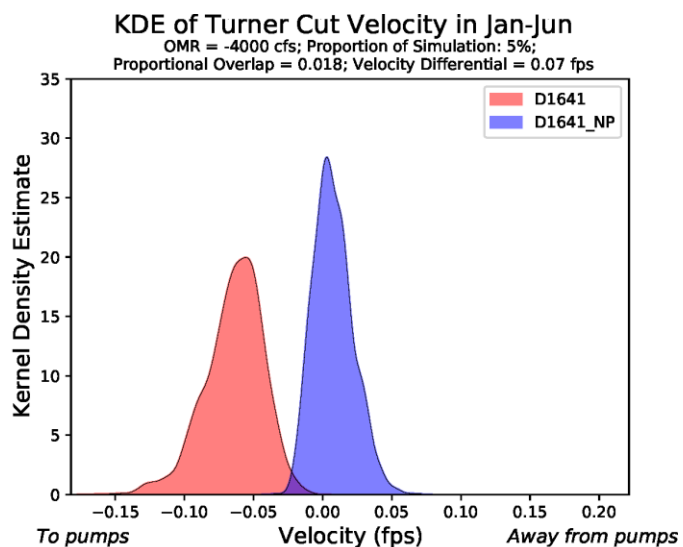
OMR = -2000 cfs; Proportion of Simulation: 7%;  
Proportional Overlap = 0.232; Velocity Differential = 0.04 fps

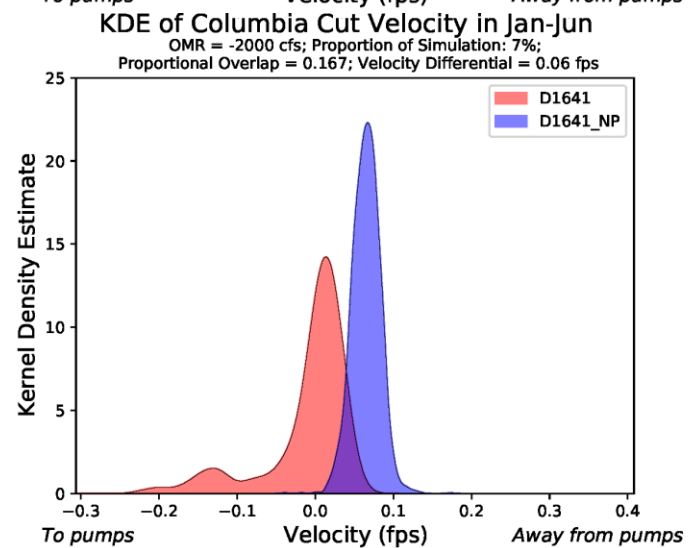
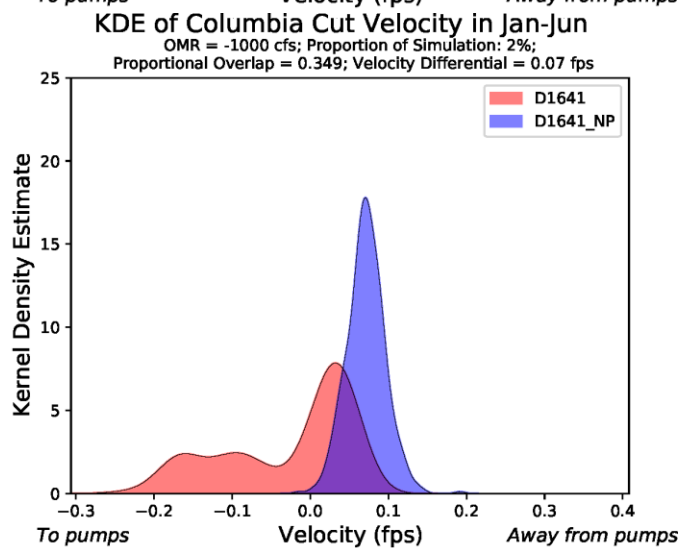
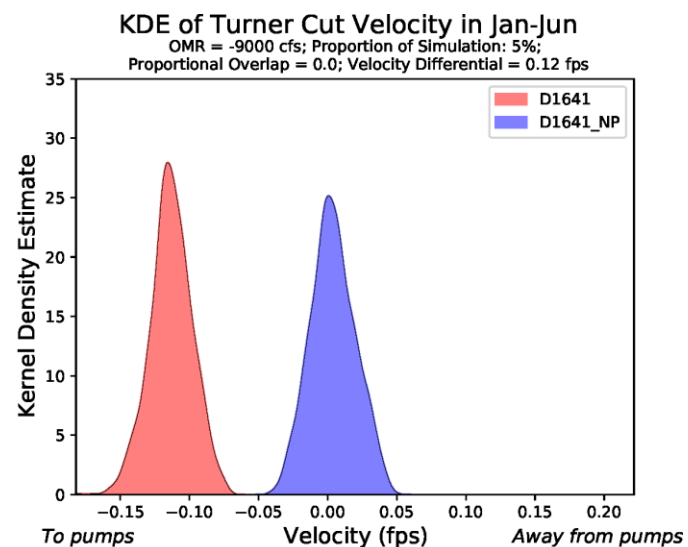
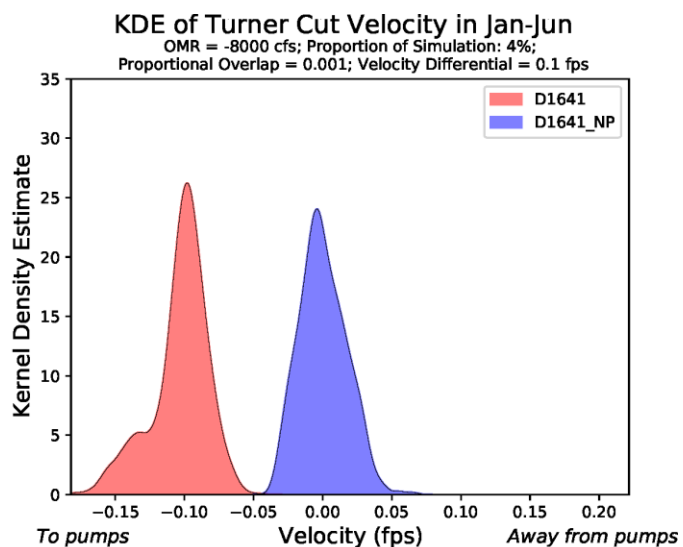


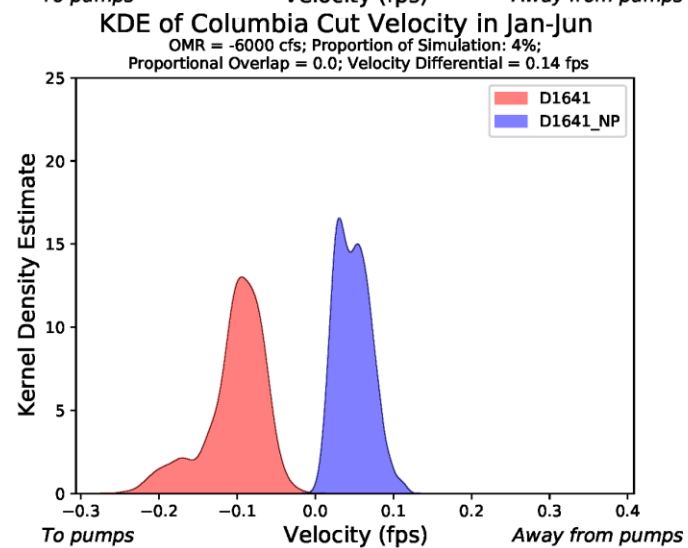
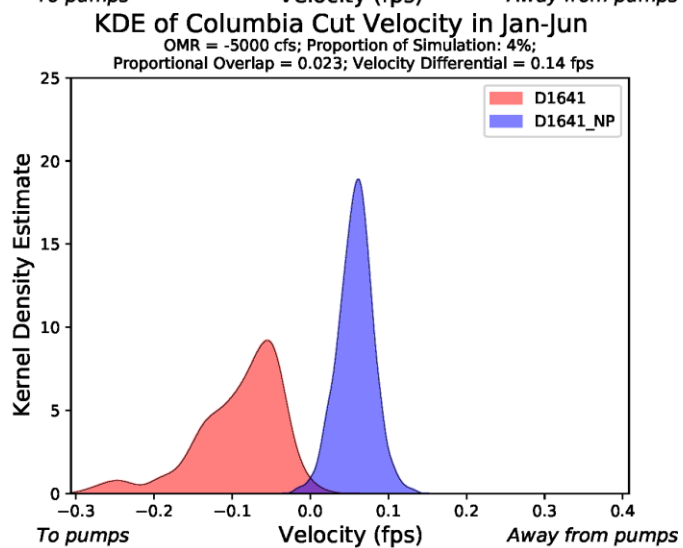
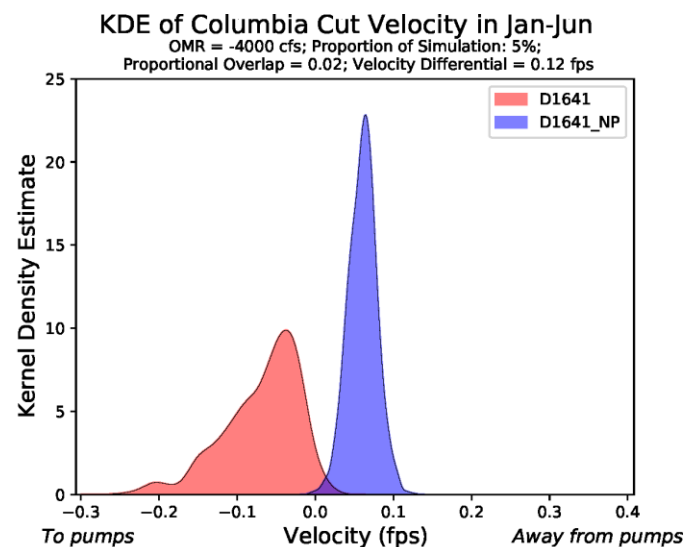
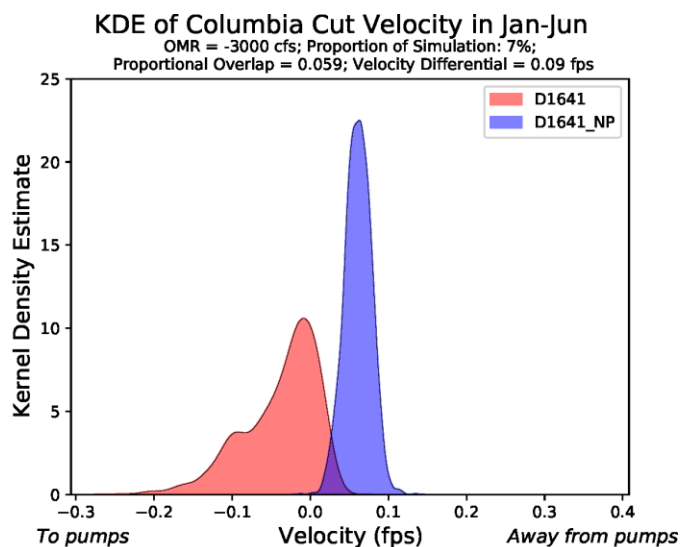
KDE of Turner Cut Velocity in Jan-Jun

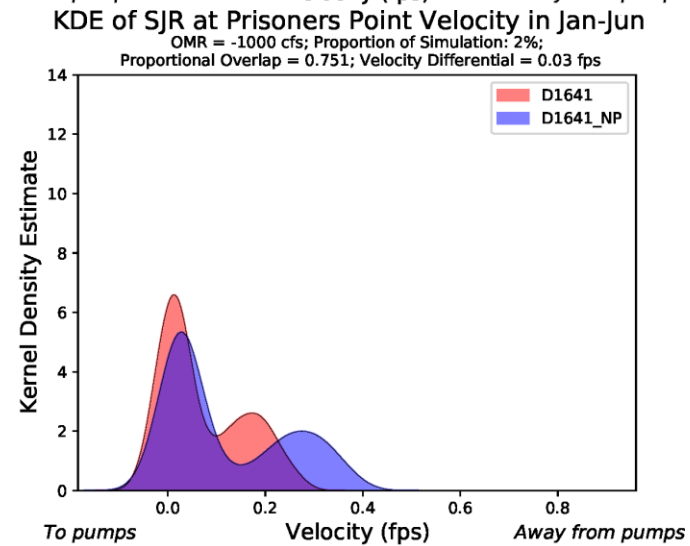
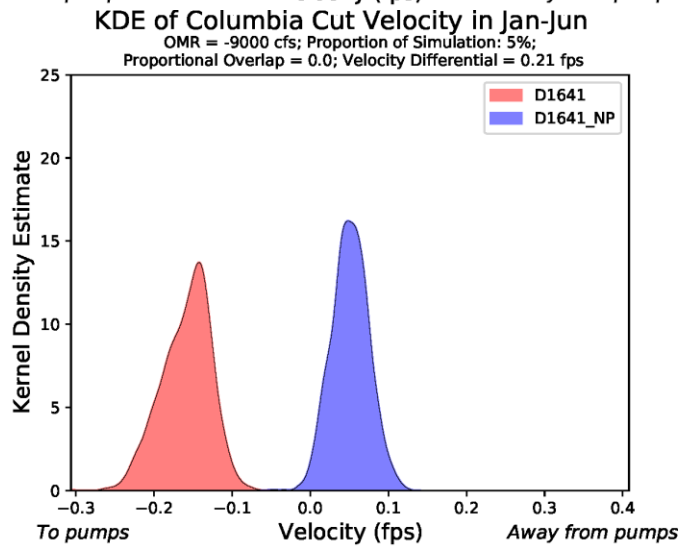
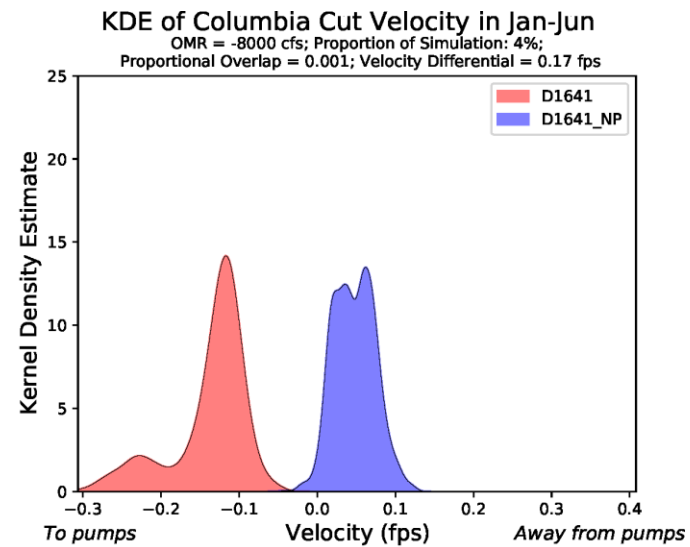
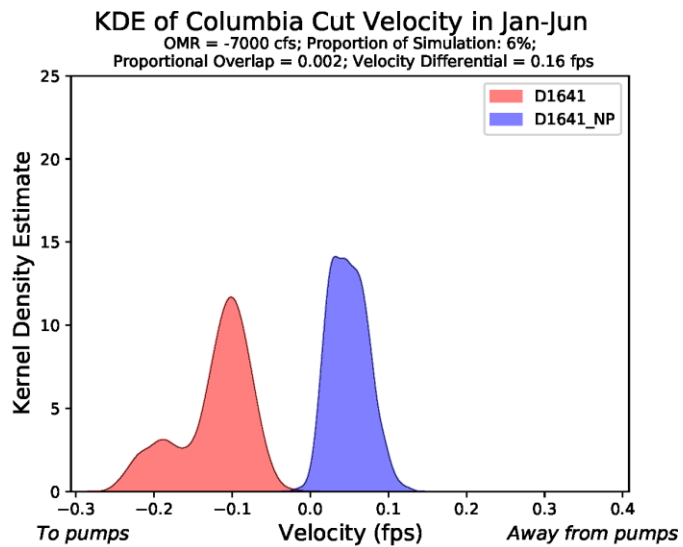
OMR = -3000 cfs; Proportion of Simulation: 7%;  
Proportional Overlap = 0.08; Velocity Differential = 0.05 fps

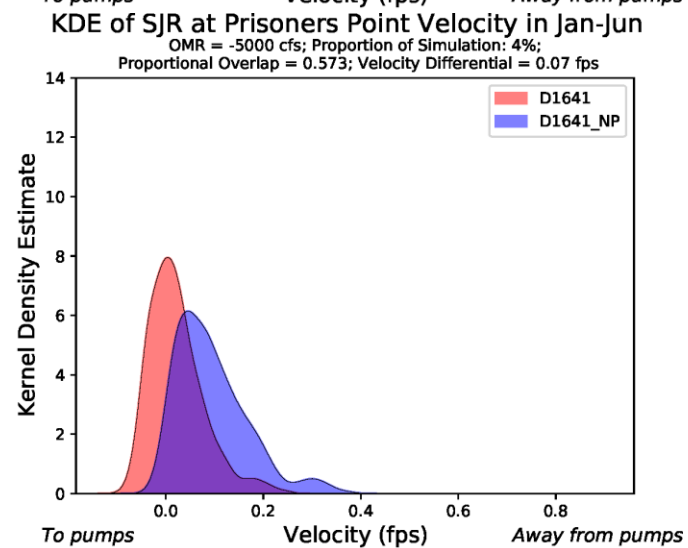
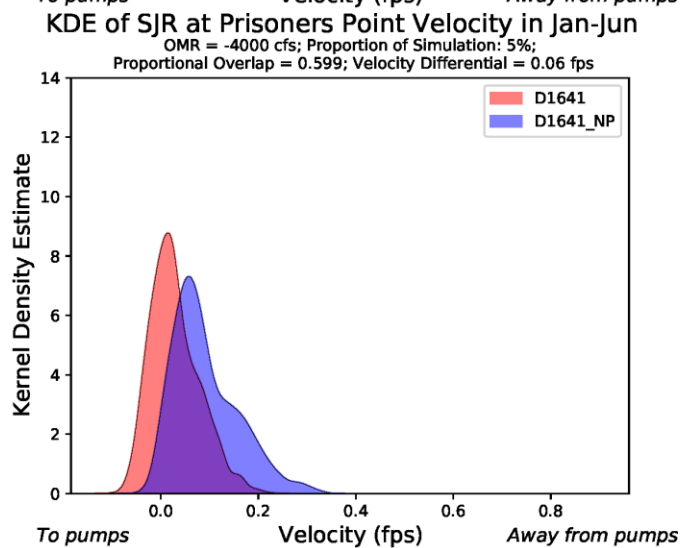
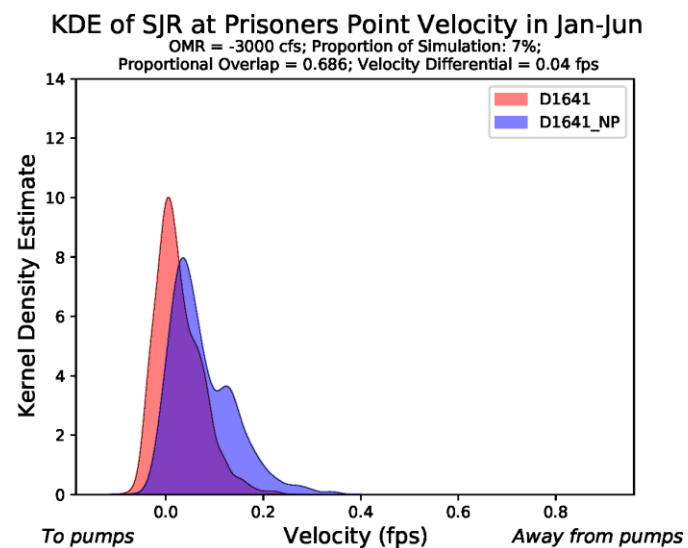
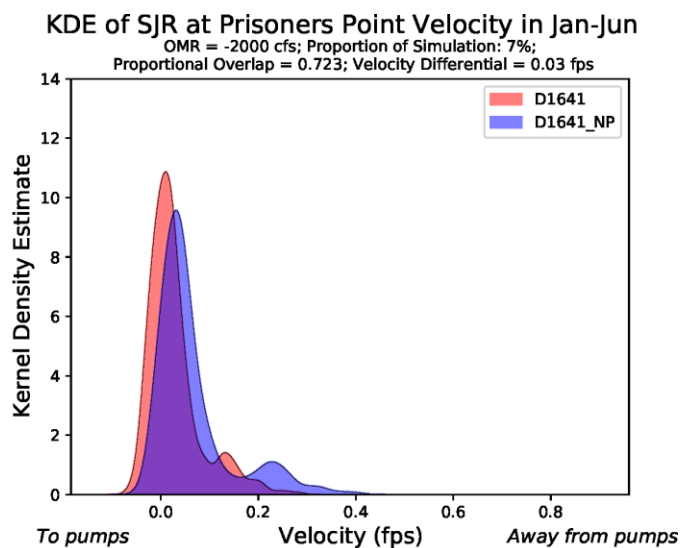


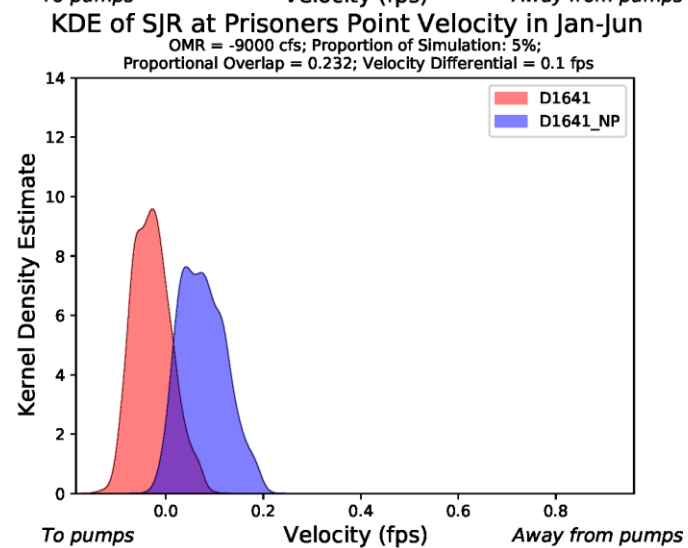
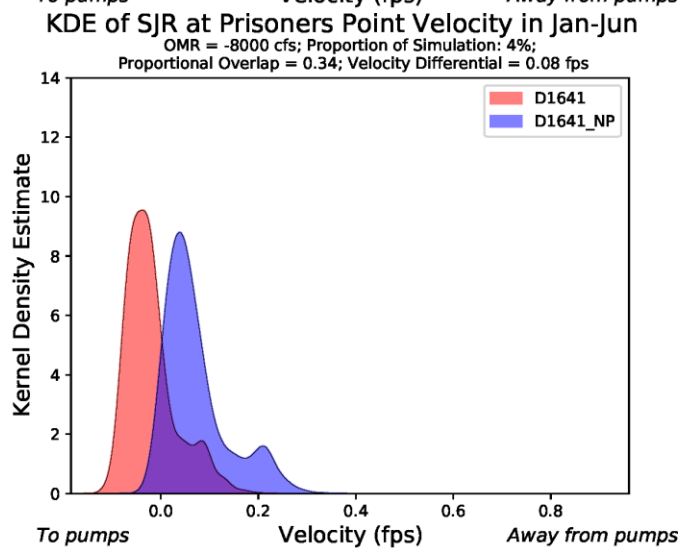
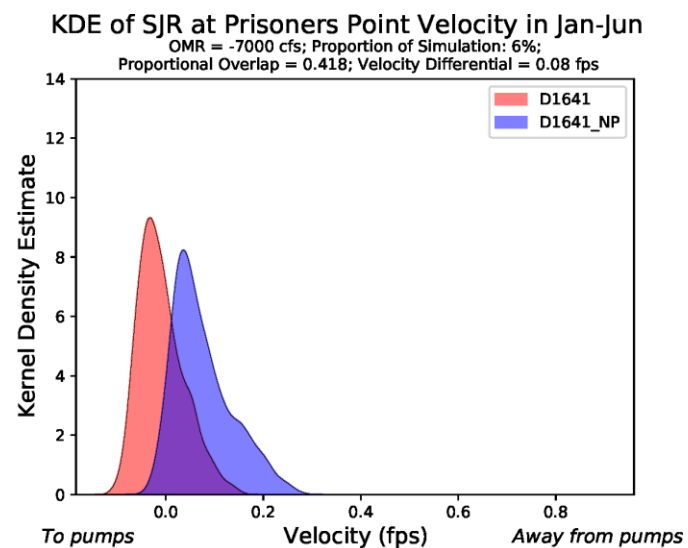
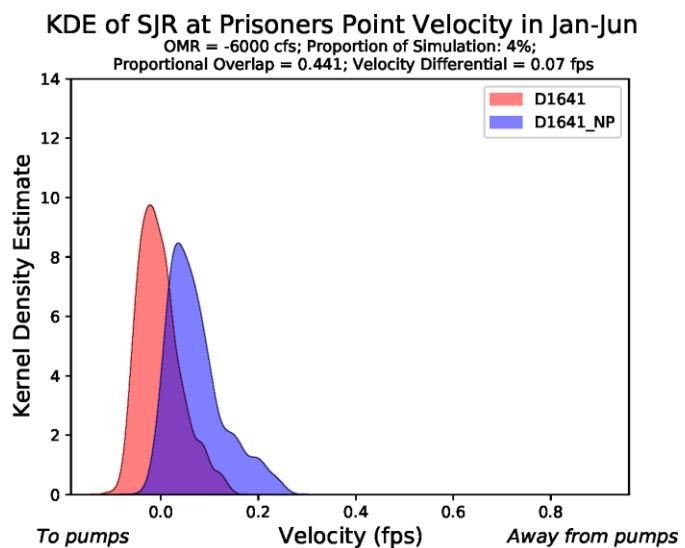


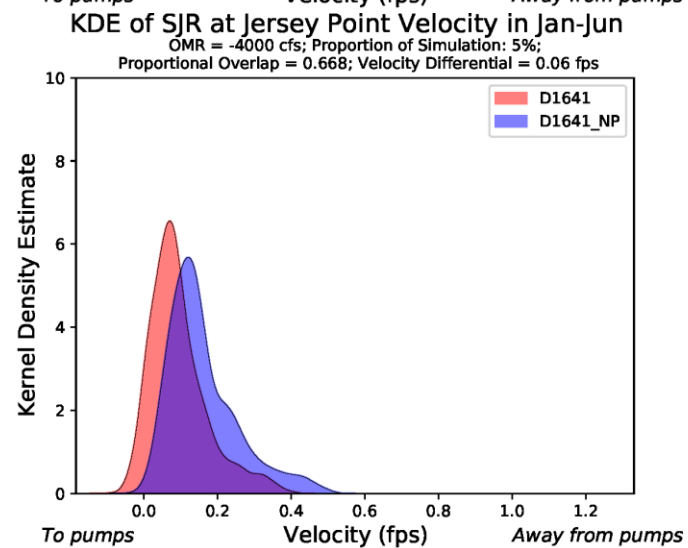
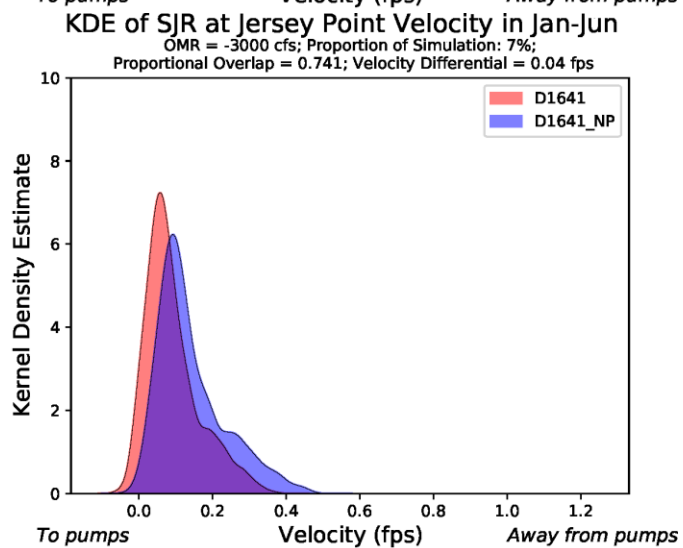
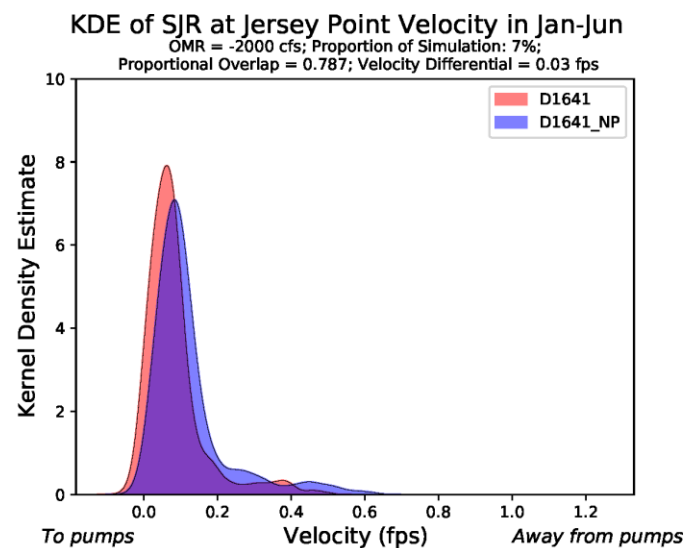
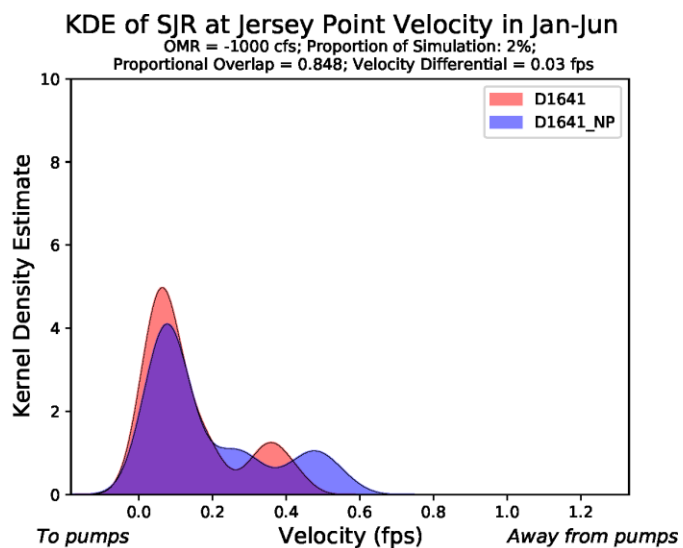




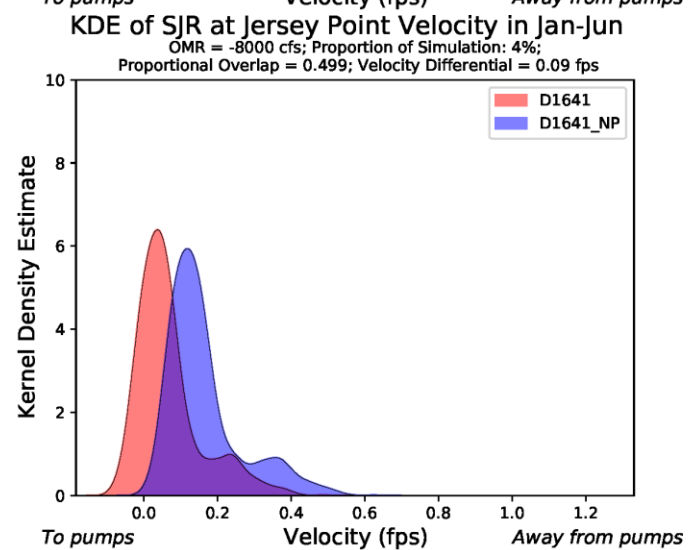
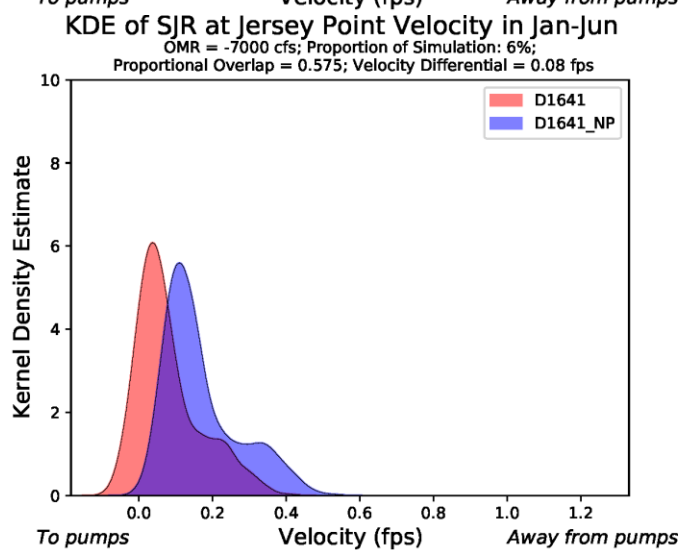
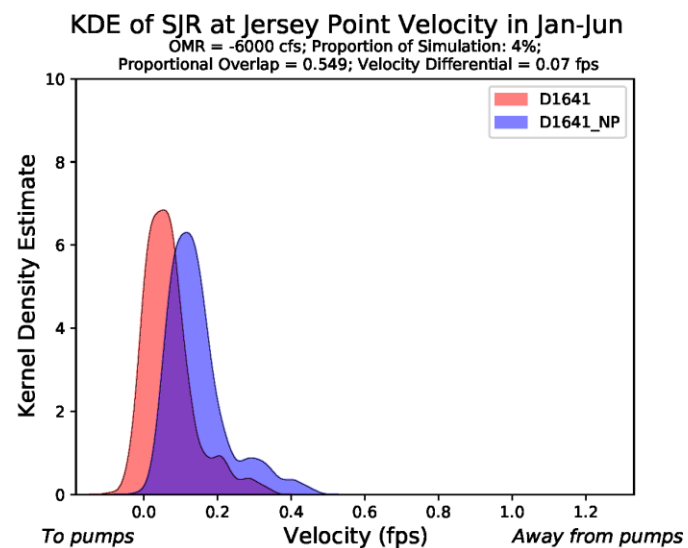
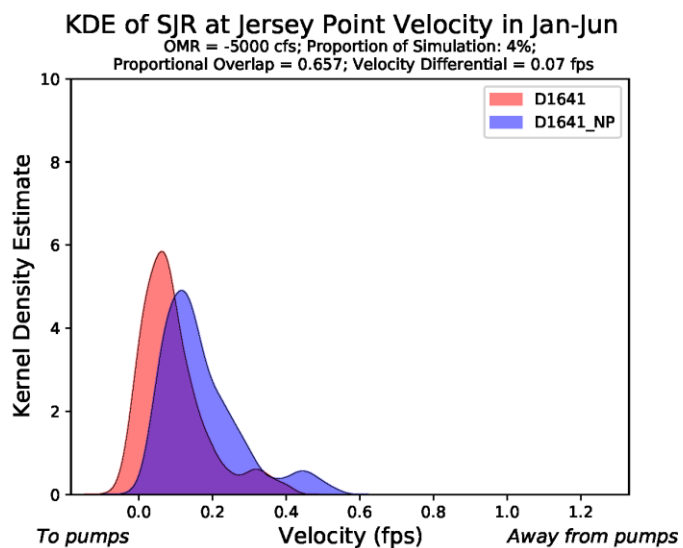






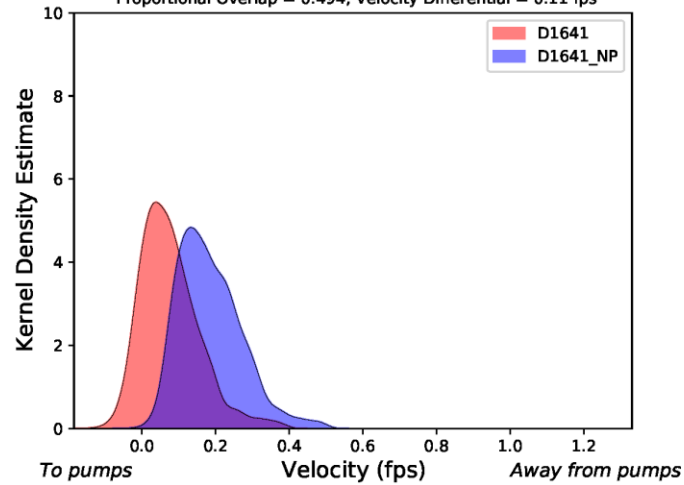






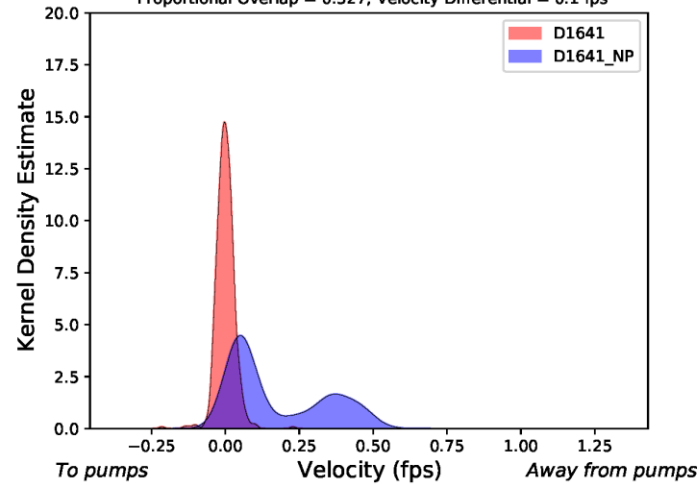
KDE of SJR at Jersey Point Velocity in Jan-Jun

OMR = -9000 cfs; Proportion of Simulation: 5%;  
Proportional Overlap = 0.494; Velocity Differential = 0.11 fps



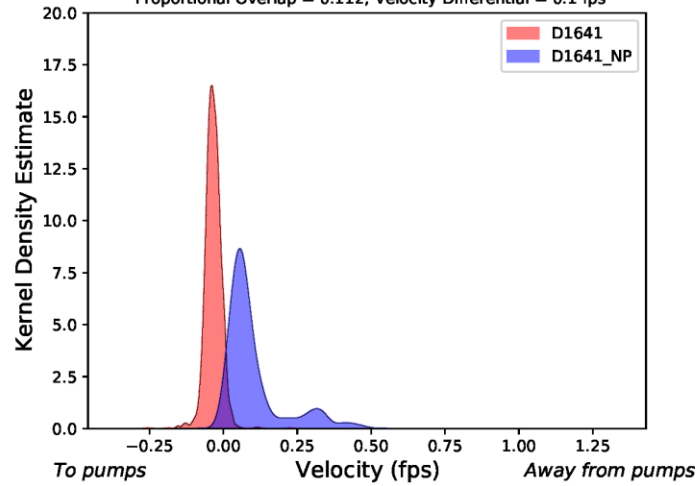
KDE of Old R at Bacon Island Velocity in Jan-Jun

OMR = -1000 cfs; Proportion of Simulation: 2%;  
Proportional Overlap = 0.327; Velocity Differential = 0.1 fps



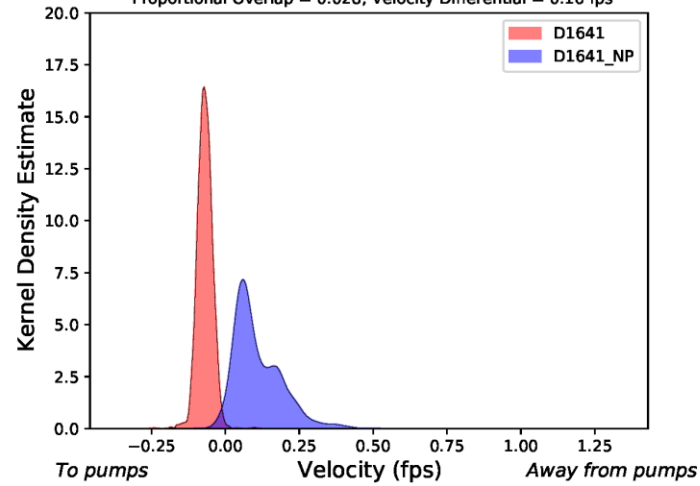
KDE of Old R at Bacon Island Velocity in Jan-Jun

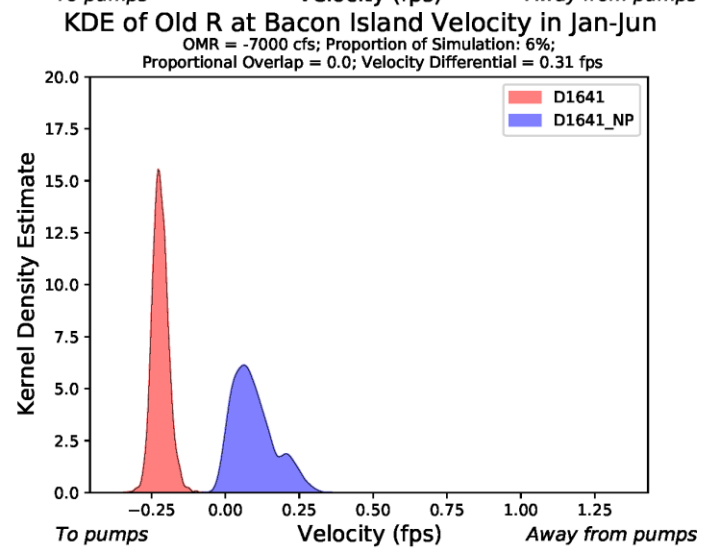
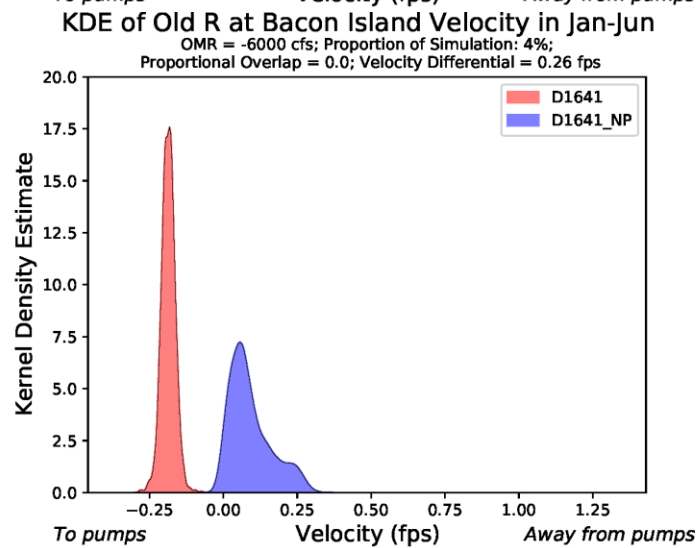
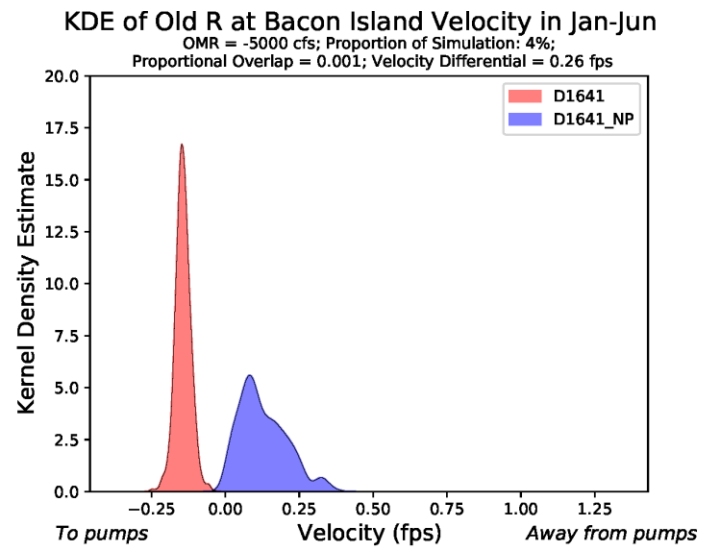
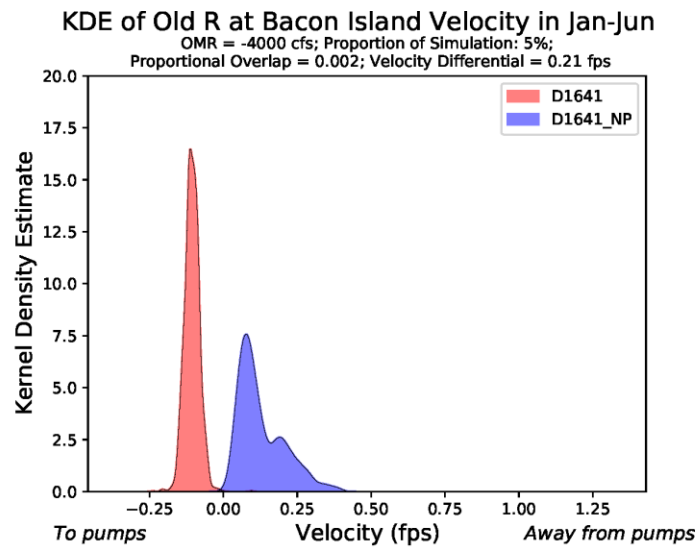
OMR = -2000 cfs; Proportion of Simulation: 7%;  
Proportional Overlap = 0.112; Velocity Differential = 0.1 fps

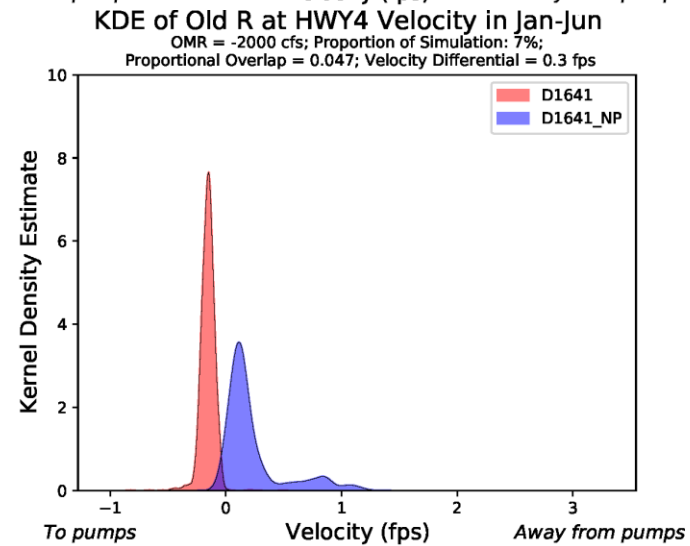
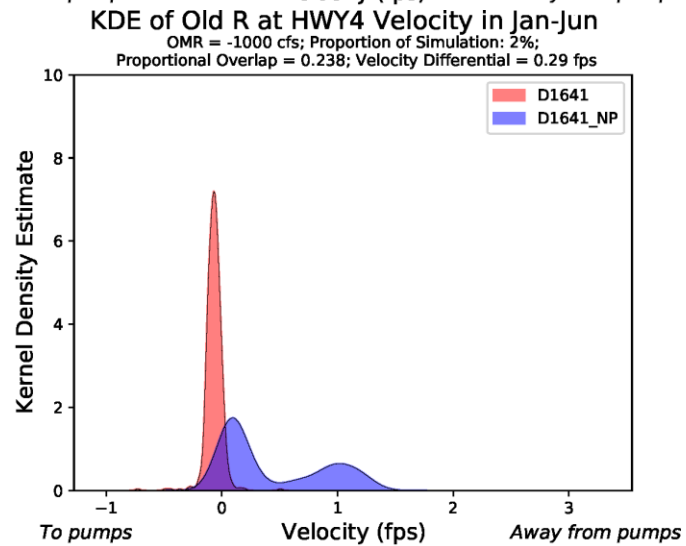
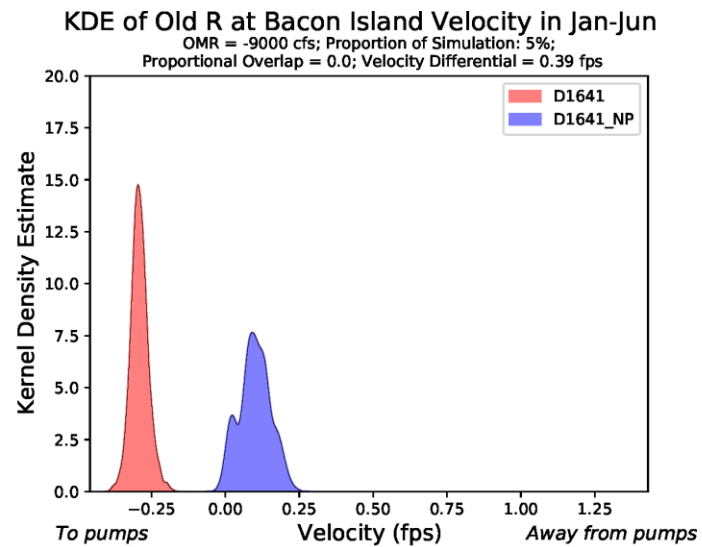
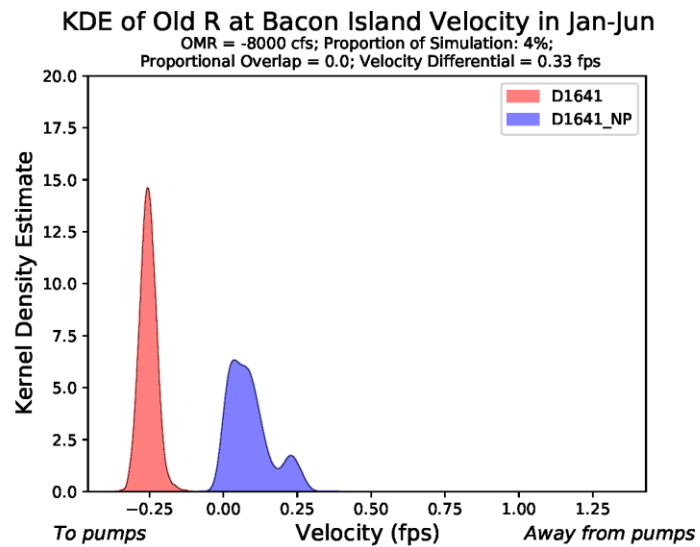


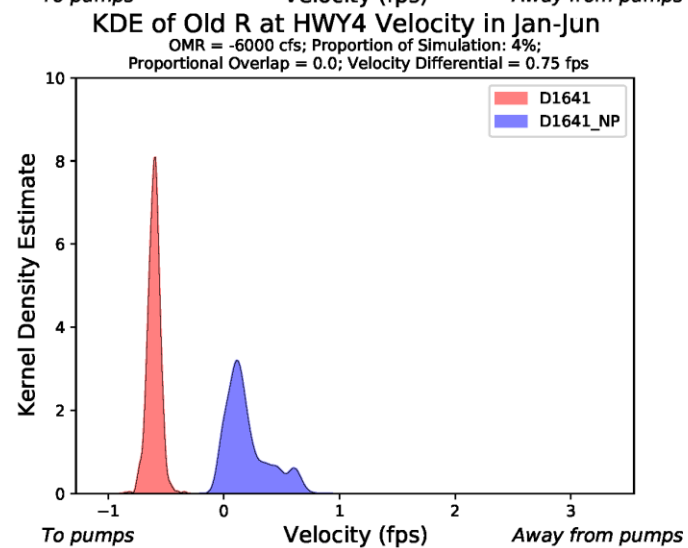
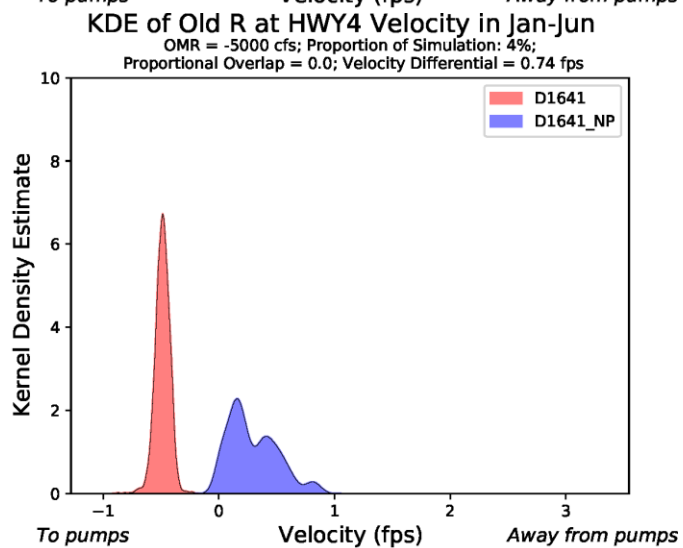
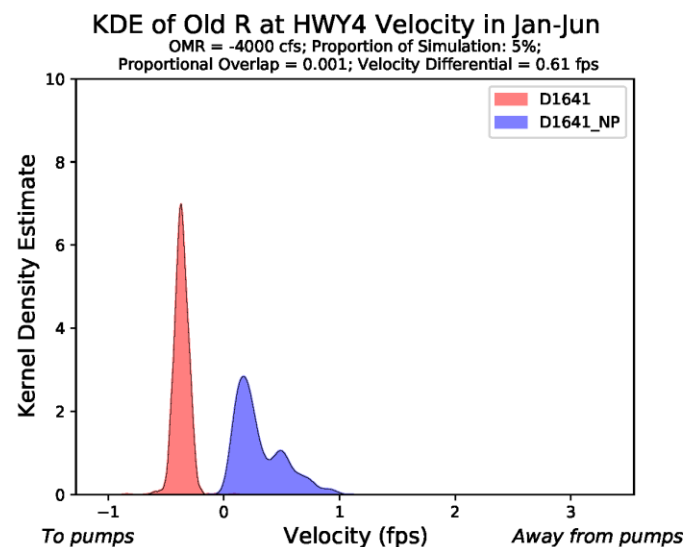
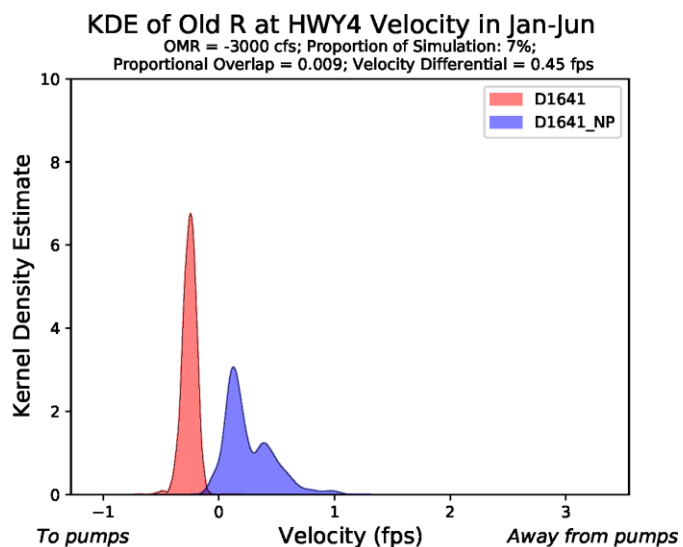
KDE of Old R at Bacon Island Velocity in Jan-Jun

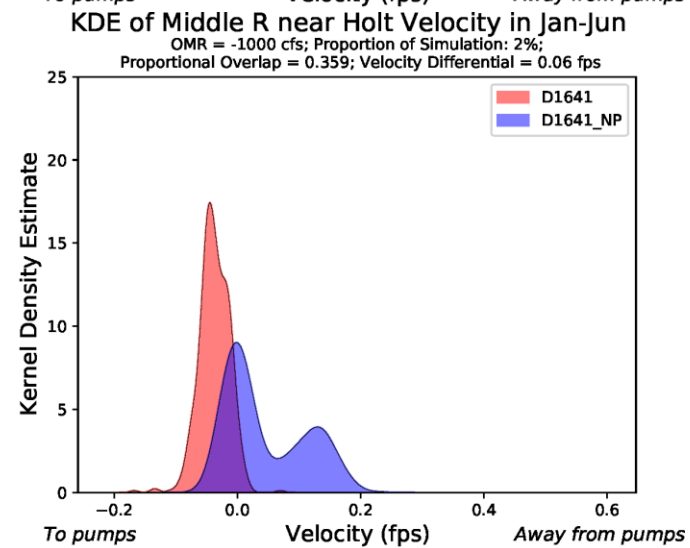
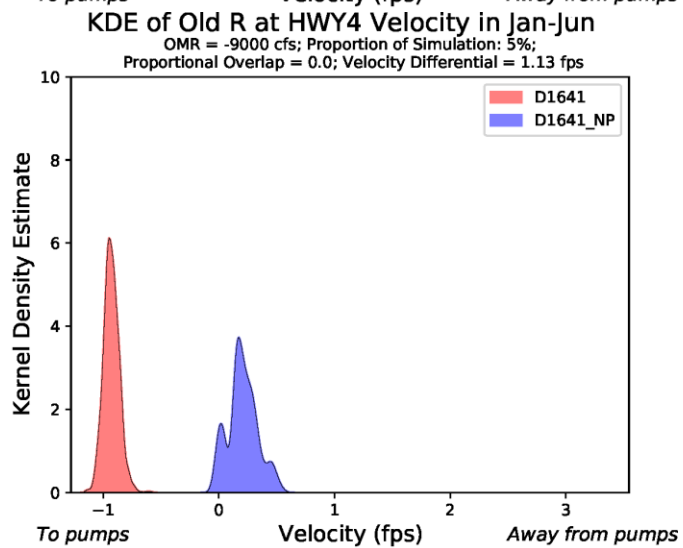
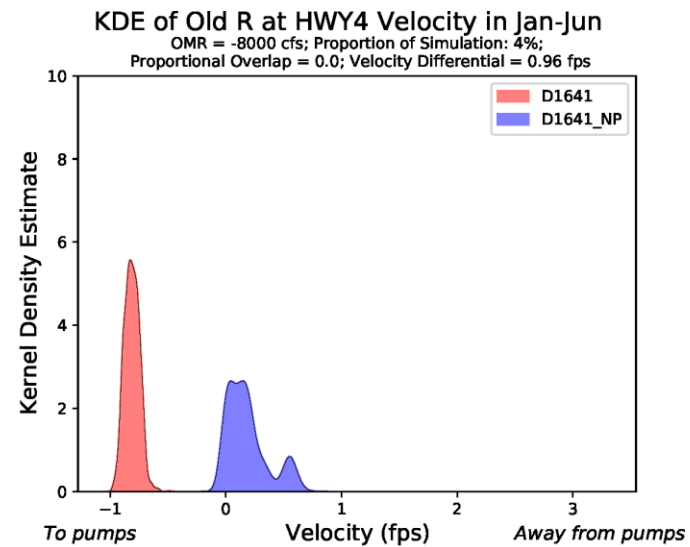
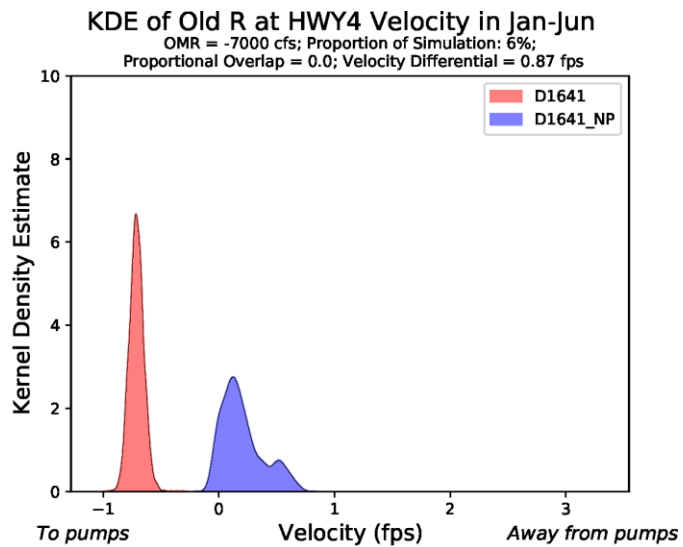
OMR = -3000 cfs; Proportion of Simulation: 7%;  
Proportional Overlap = 0.028; Velocity Differential = 0.16 fps

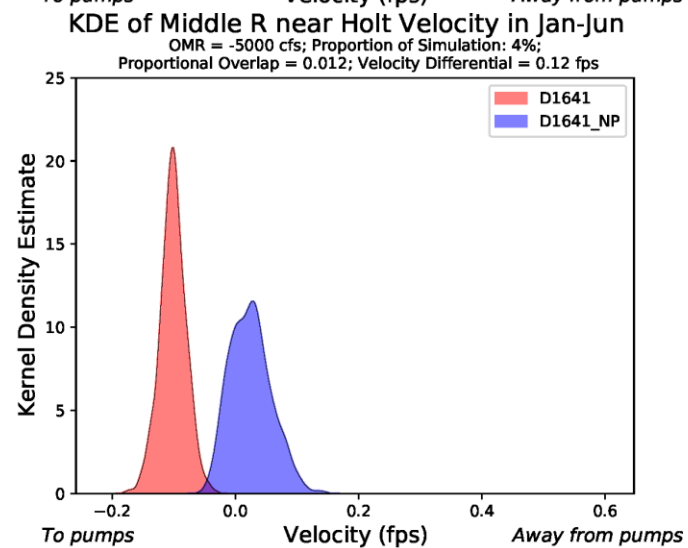
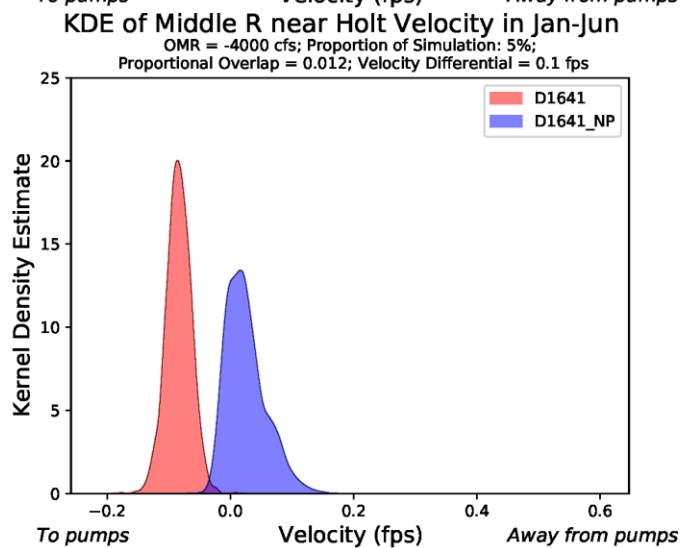
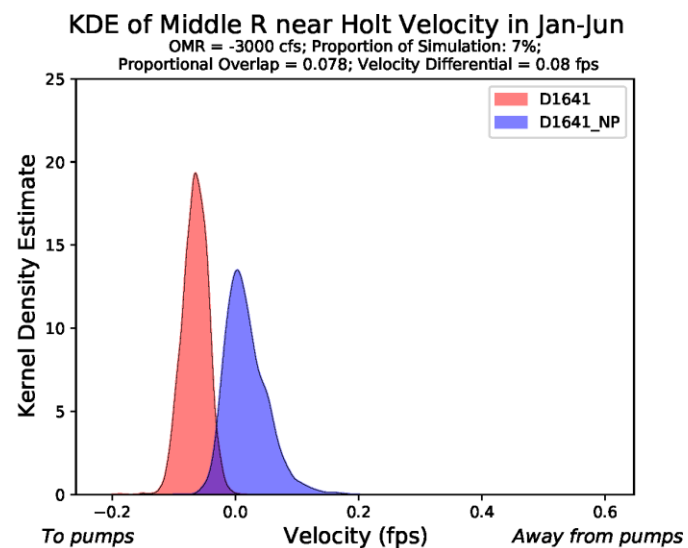
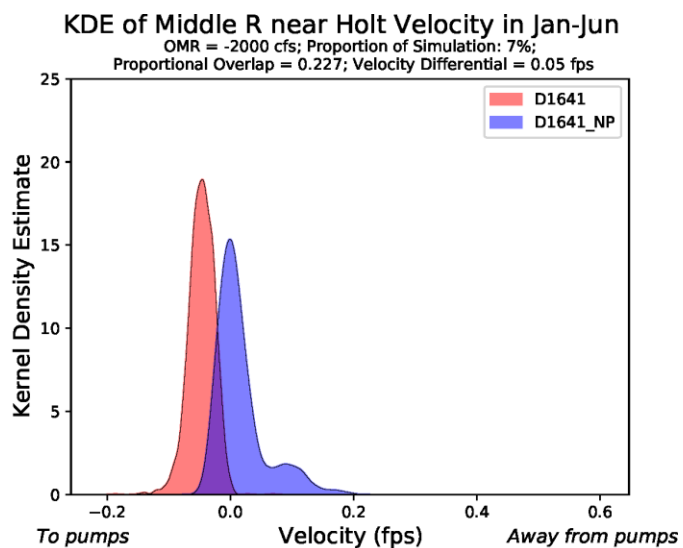


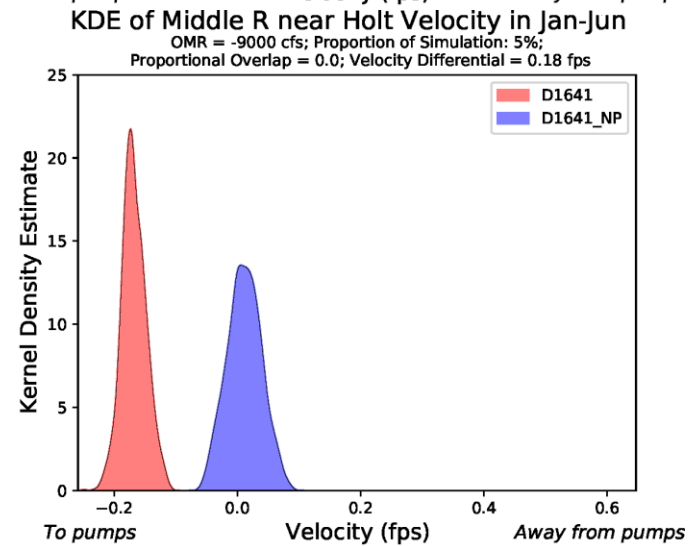
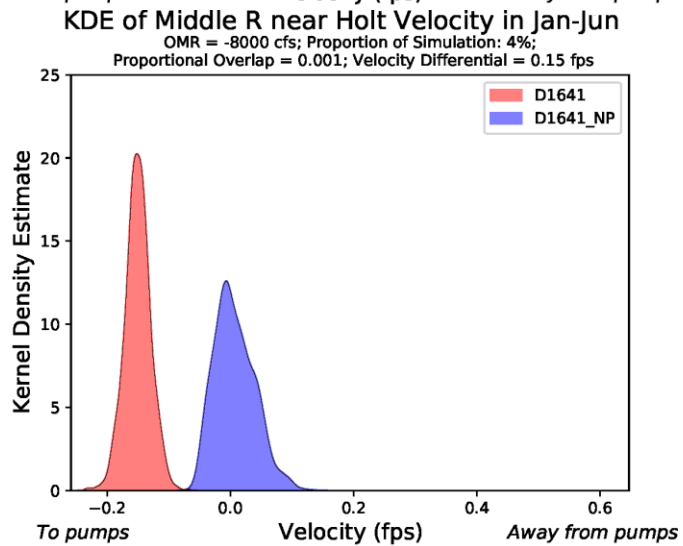
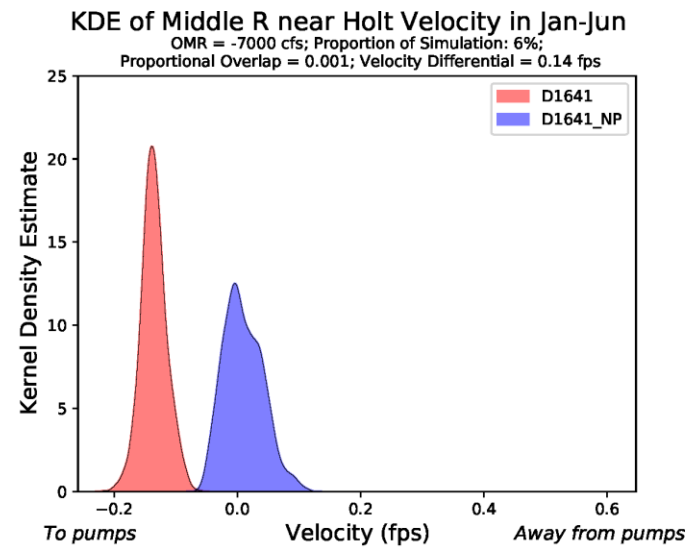
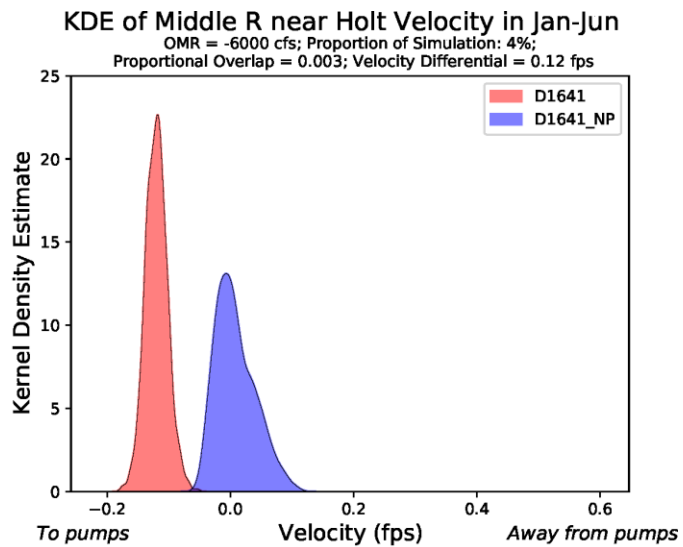








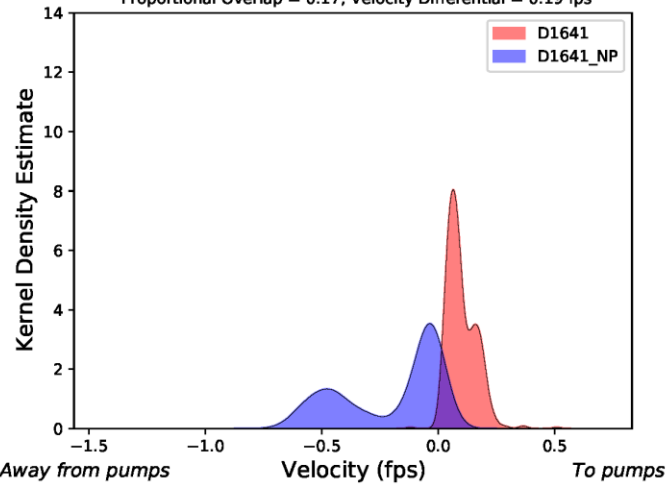






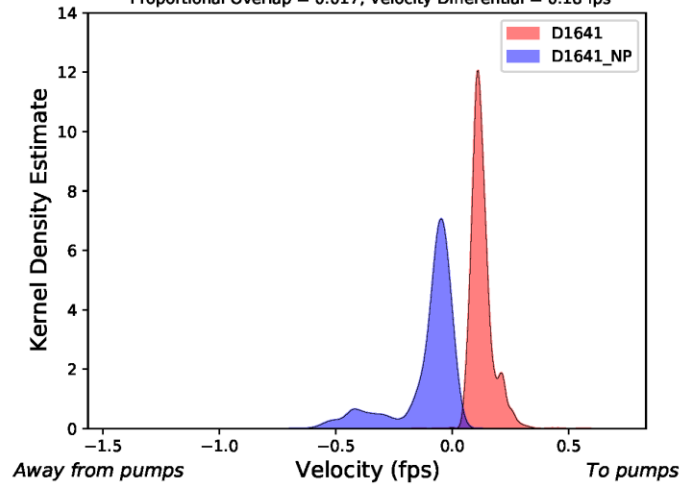
KDE of Victoria Canal near Byron Velocity in Jan-Jun

OMR = -1000 cfs; Proportion of Simulation: 2%;  
Proportional Overlap = 0.17; Velocity Differential = 0.19 fps



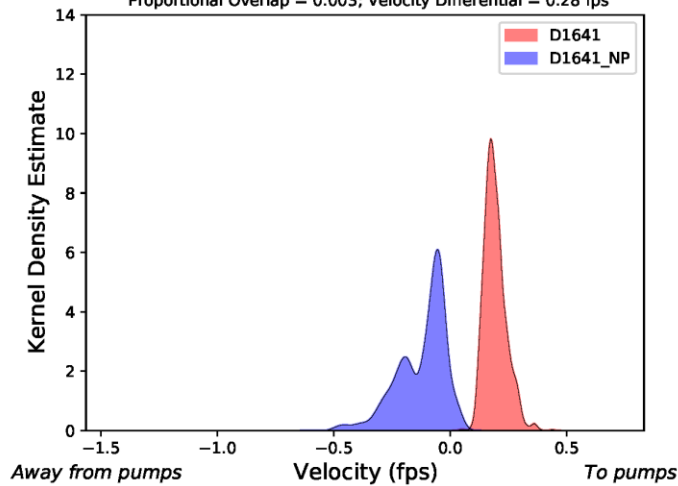
KDE of Victoria Canal near Byron Velocity in Jan-Jun

OMR = -2000 cfs; Proportion of Simulation: 7%;  
Proportional Overlap = 0.017; Velocity Differential = 0.18 fps



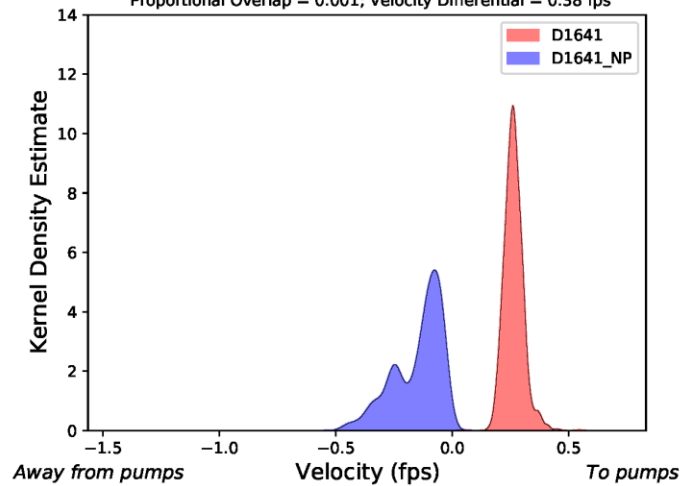
KDE of Victoria Canal near Byron Velocity in Jan-Jun

OMR = -3000 cfs; Proportion of Simulation: 7%;  
Proportional Overlap = 0.003; Velocity Differential = 0.28 fps



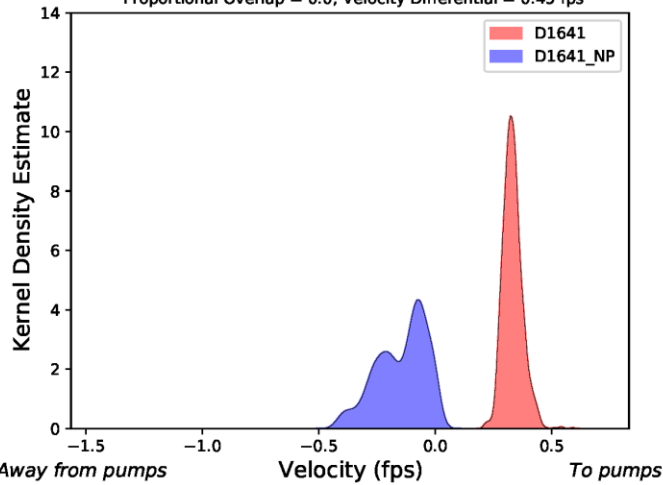
KDE of Victoria Canal near Byron Velocity in Jan-Jun

OMR = -4000 cfs; Proportion of Simulation: 5%;  
Proportional Overlap = 0.001; Velocity Differential = 0.38 fps



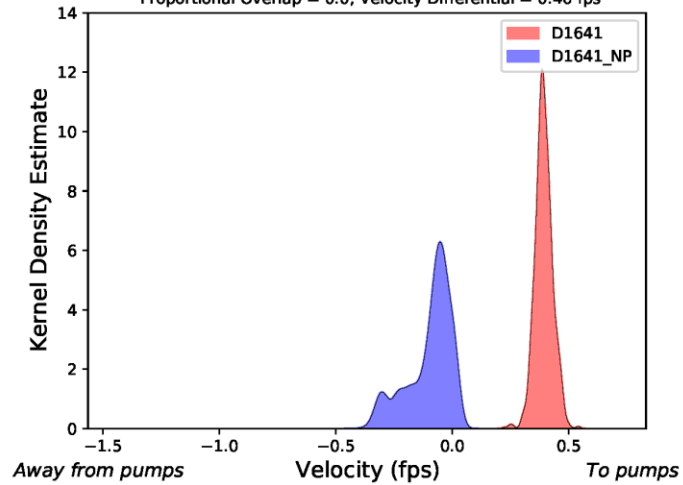
KDE of Victoria Canal near Byron Velocity in Jan-Jun

OMR = -5000 cfs; Proportion of Simulation: 4%;  
Proportional Overlap = 0.0; Velocity Differential = 0.45 fps



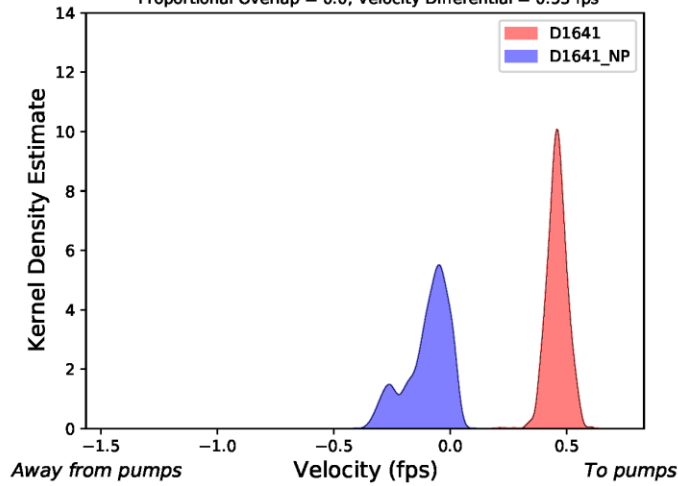
KDE of Victoria Canal near Byron Velocity in Jan-Jun

OMR = -6000 cfs; Proportion of Simulation: 4%;  
Proportional Overlap = 0.0; Velocity Differential = 0.46 fps



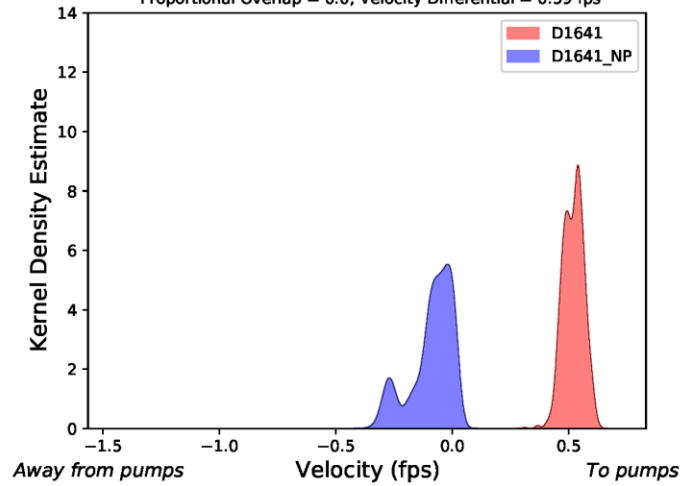
KDE of Victoria Canal near Byron Velocity in Jan-Jun

OMR = -7000 cfs; Proportion of Simulation: 6%;  
Proportional Overlap = 0.0; Velocity Differential = 0.53 fps



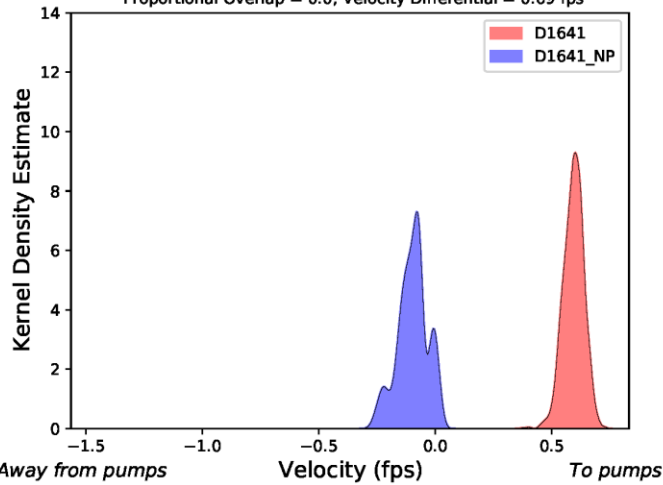
KDE of Victoria Canal near Byron Velocity in Jan-Jun

OMR = -8000 cfs; Proportion of Simulation: 4%;  
Proportional Overlap = 0.0; Velocity Differential = 0.59 fps



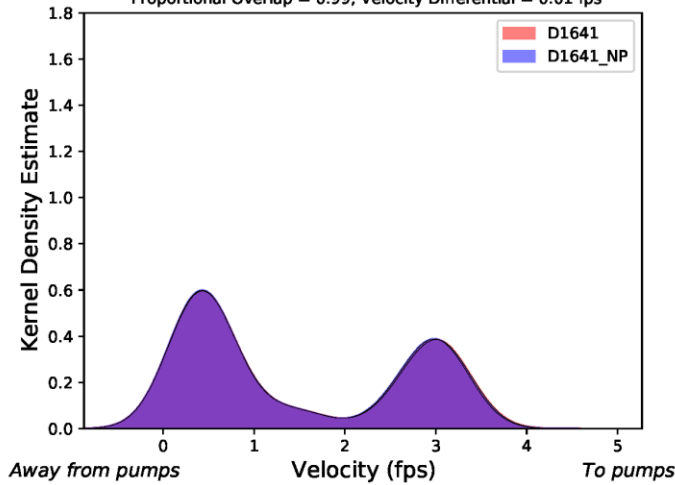
KDE of Victoria Canal near Byron Velocity in Jan-Jun

OMR = -9000 cfs; Proportion of Simulation: 5%;  
Proportional Overlap = 0.0; Velocity Differential = 0.69 fps



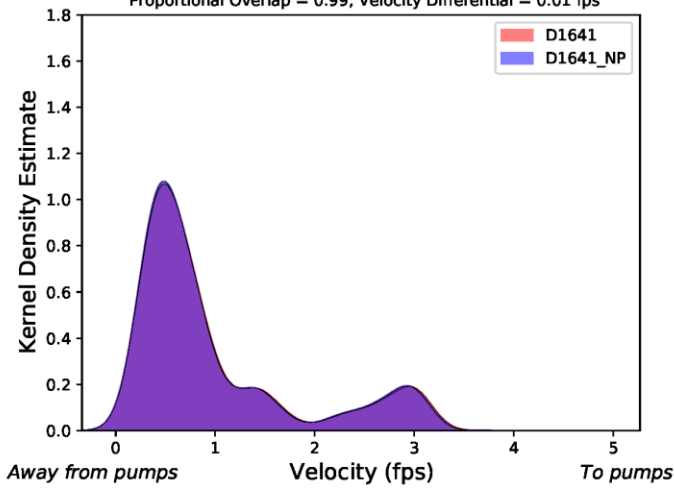
KDE of SJR US of Head of Old River Velocity in Jan-Jun

OMR = -1000 cfs; Proportion of Simulation: 2%;  
Proportional Overlap = 0.99; Velocity Differential = 0.01 fps



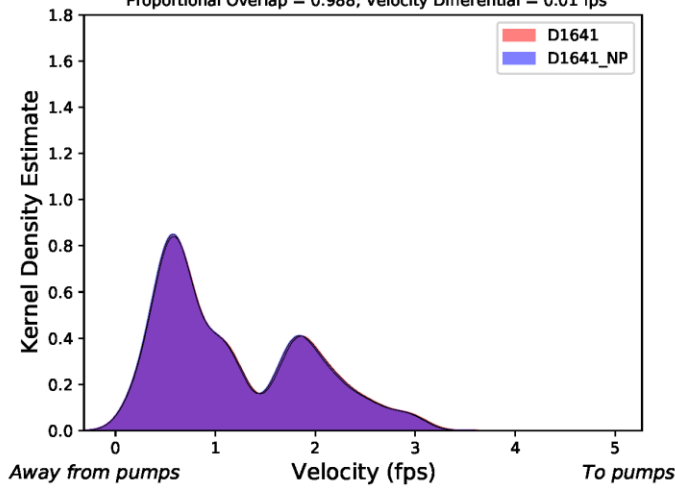
KDE of SJR US of Head of Old River Velocity in Jan-Jun

OMR = -2000 cfs; Proportion of Simulation: 7%;  
Proportional Overlap = 0.99; Velocity Differential = 0.01 fps



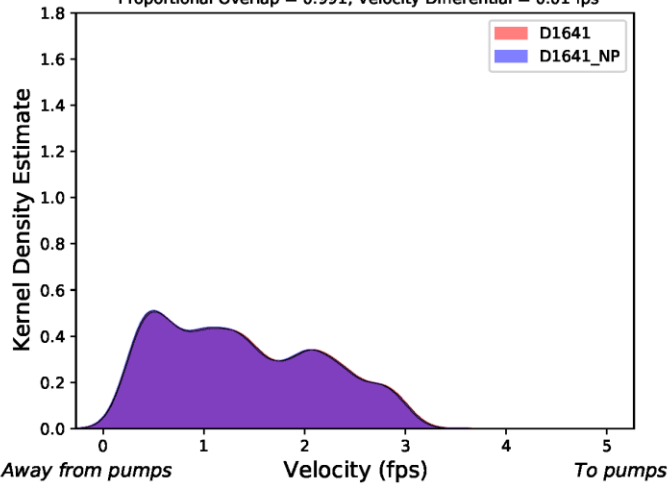
KDE of SJR US of Head of Old River Velocity in Jan-Jun

OMR = -3000 cfs; Proportion of Simulation: 7%;  
Proportional Overlap = 0.988; Velocity Differential = 0.01 fps



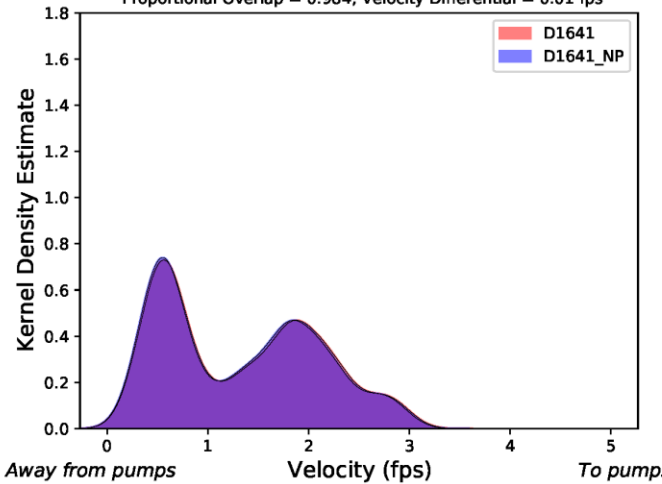
KDE of SJR US of Head of Old River Velocity in Jan-Jun

OMR = -4000 cfs; Proportion of Simulation: 5%;  
Proportional Overlap = 0.991; Velocity Differential = 0.01 fps



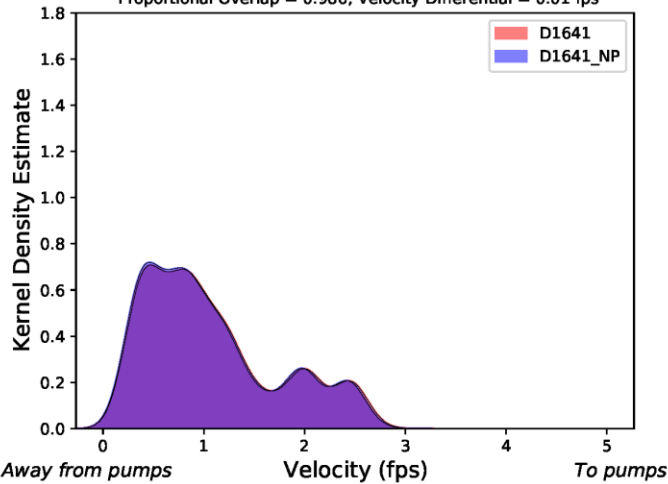
KDE of SJR US of Head of Old River Velocity in Jan-Jun

OMR = -5000 cfs; Proportion of Simulation: 4%;  
Proportional Overlap = 0.984; Velocity Differential = 0.01 fps



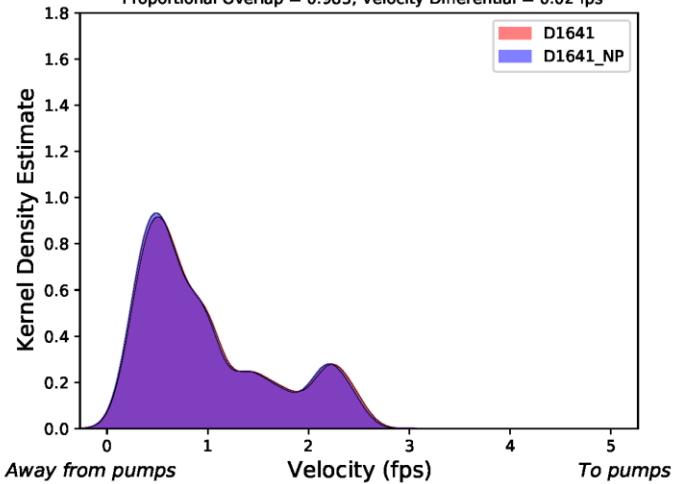
KDE of SJR US of Head of Old River Velocity in Jan-Jun

OMR = -6000 cfs; Proportion of Simulation: 4%;  
Proportional Overlap = 0.986; Velocity Differential = 0.01 fps



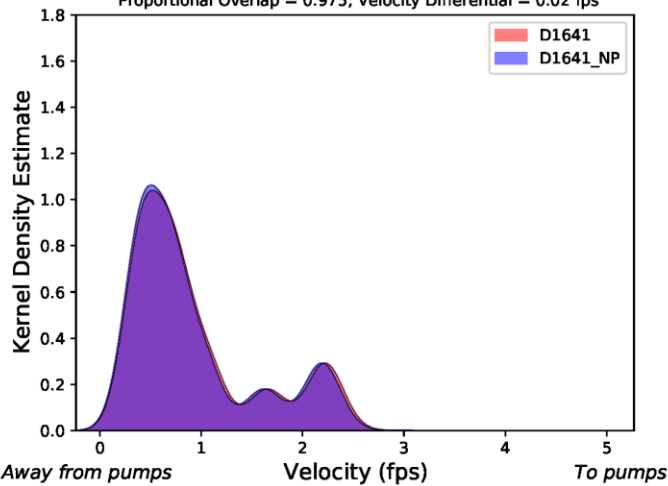
KDE of SJR US of Head of Old River Velocity in Jan-Jun

OMR = -7000 cfs; Proportion of Simulation: 6%;  
Proportional Overlap = 0.983; Velocity Differential = 0.02 fps



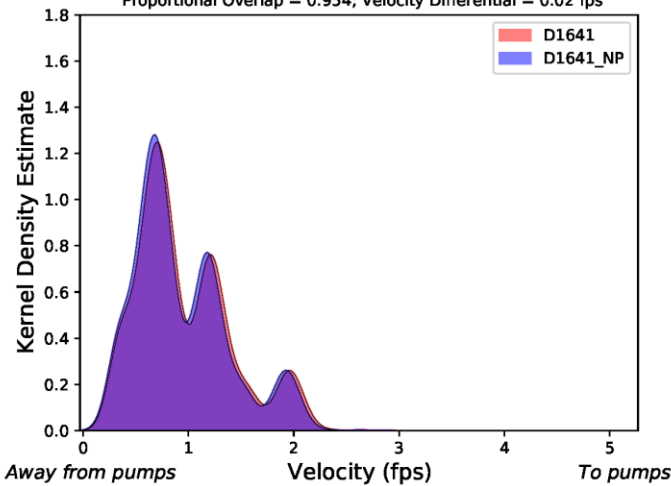
KDE of SJR US of Head of Old River Velocity in Jan-Jun

OMR = -8000 cfs; Proportion of Simulation: 4%;  
Proportional Overlap = 0.975; Velocity Differential = 0.02 fps



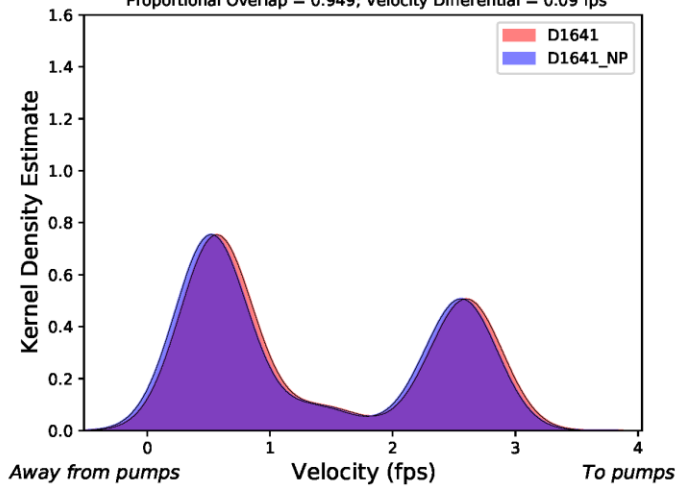
KDE of SJR US of Head of Old River Velocity in Jan-Jun

OMR = -9000 cfs; Proportion of Simulation: 5%;  
Proportional Overlap = 0.954; Velocity Differential = 0.02 fps



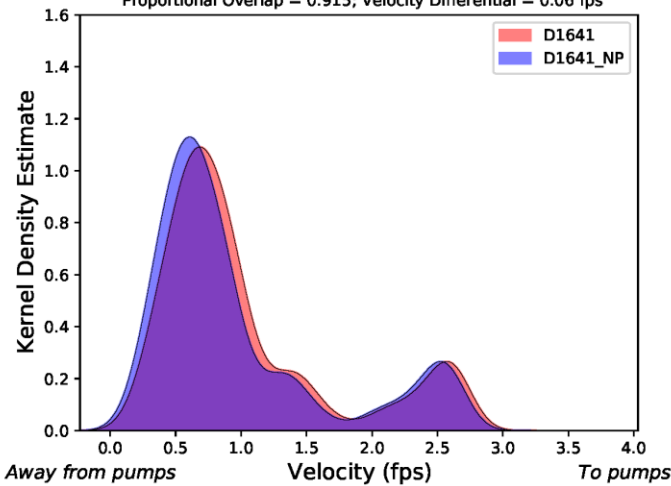
KDE of Old R at Head of Old River Velocity in Jan-Jun

OMR = -1000 cfs; Proportion of Simulation: 2%;  
Proportional Overlap = 0.949; Velocity Differential = 0.09 fps



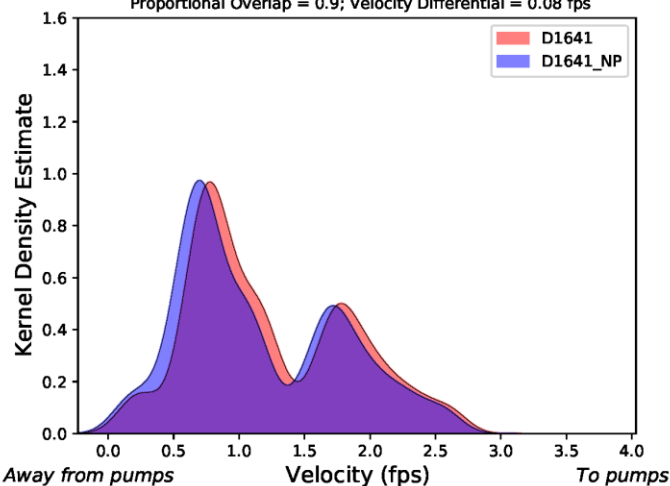
KDE of Old R at Head of Old River Velocity in Jan-Jun

OMR = -2000 cfs; Proportion of Simulation: 7%;  
Proportional Overlap = 0.915; Velocity Differential = 0.06 fps



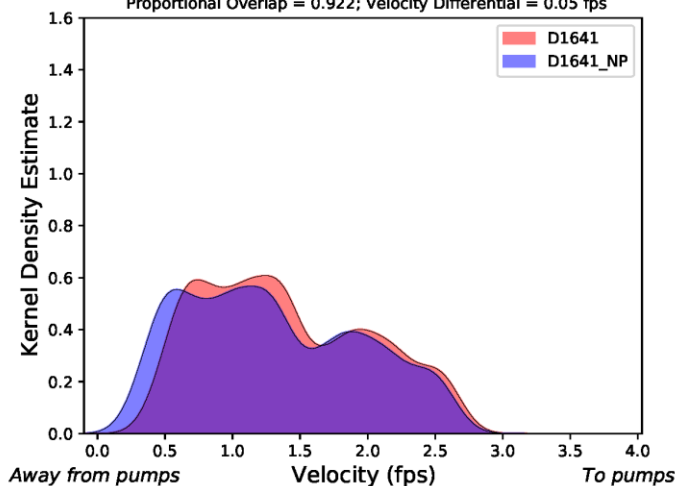
KDE of Old R at Head of Old River Velocity in Jan-Jun

OMR = -3000 cfs; Proportion of Simulation: 7%;  
Proportional Overlap = 0.9; Velocity Differential = 0.08 fps



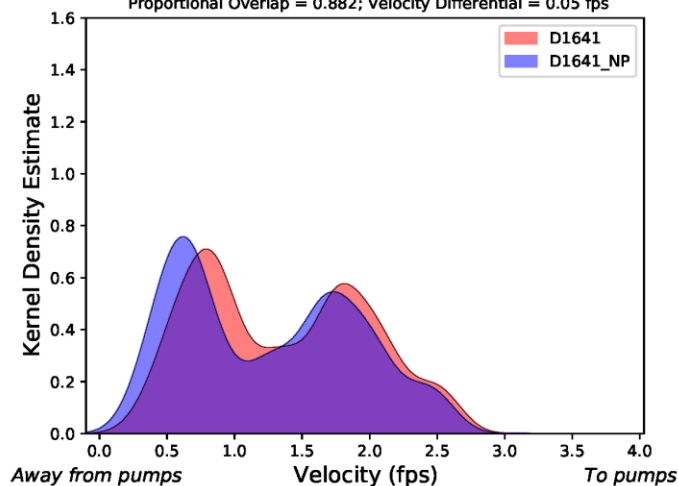
KDE of Old R at Head of Old River Velocity in Jan-Jun

OMR = -4000 cfs; Proportion of Simulation: 5%;  
Proportional Overlap = 0.922; Velocity Differential = 0.05 fps



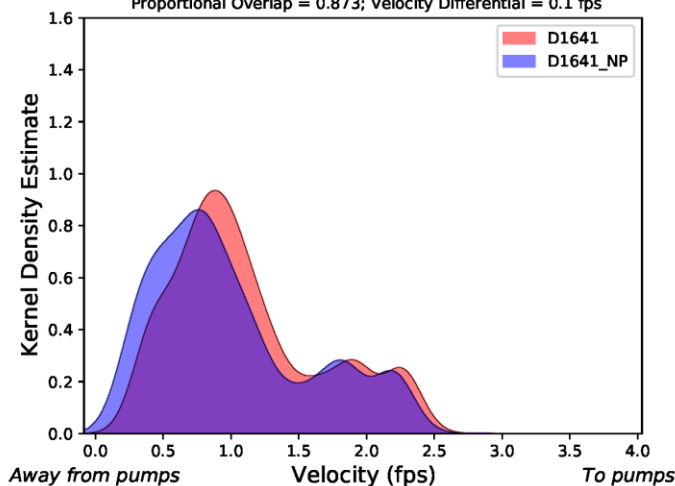
KDE of Old R at Head of Old River Velocity in Jan-Jun

OMR = -5000 cfs; Proportion of Simulation: 4%;  
Proportional Overlap = 0.882; Velocity Differential = 0.05 fps



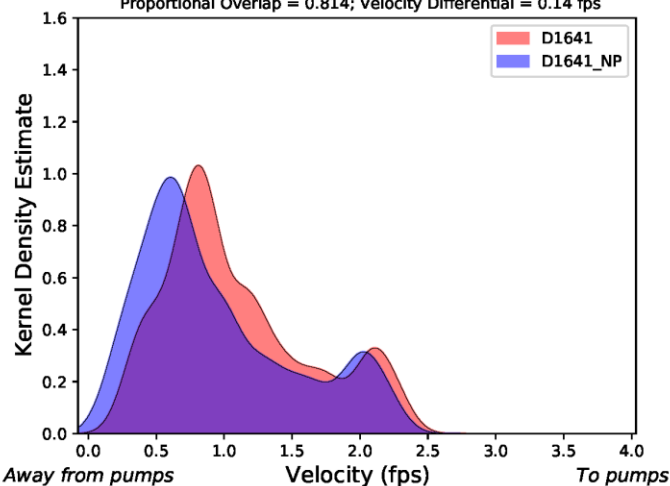
KDE of Old R at Head of Old River Velocity in Jan-Jun

OMR = -6000 cfs; Proportion of Simulation: 4%;  
Proportional Overlap = 0.873; Velocity Differential = 0.1 fps



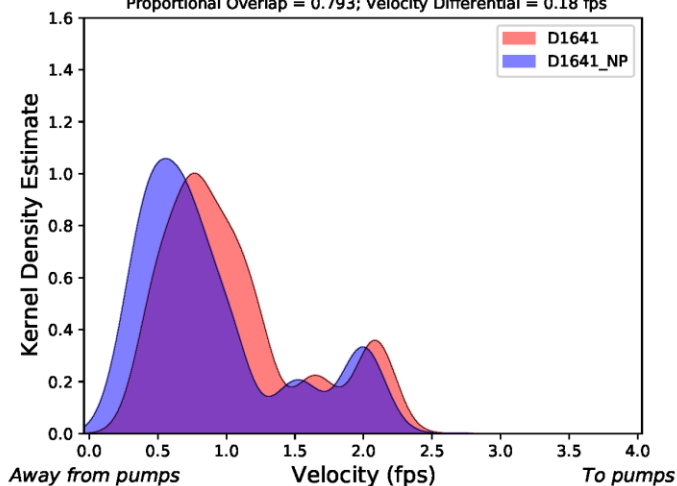
KDE of Old R at Head of Old River Velocity in Jan-Jun

OMR = -7000 cfs; Proportion of Simulation: 6%;  
Proportional Overlap = 0.814; Velocity Differential = 0.14 fps



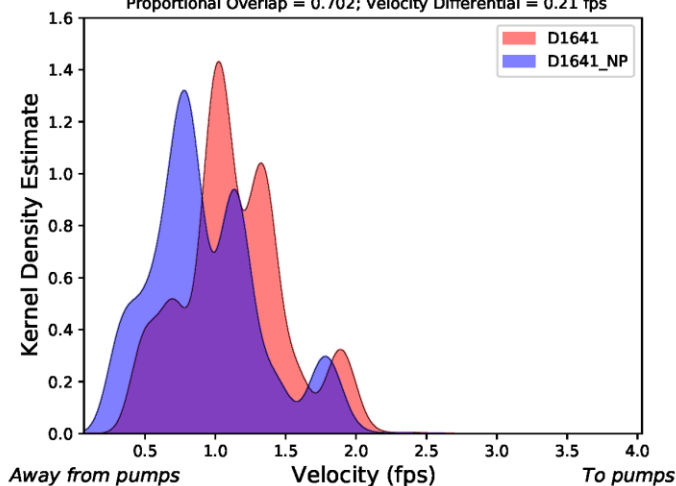
KDE of Old R at Head of Old River Velocity in Jan-Jun

OMR = -8000 cfs; Proportion of Simulation: 4%;  
Proportional Overlap = 0.793; Velocity Differential = 0.18 fps



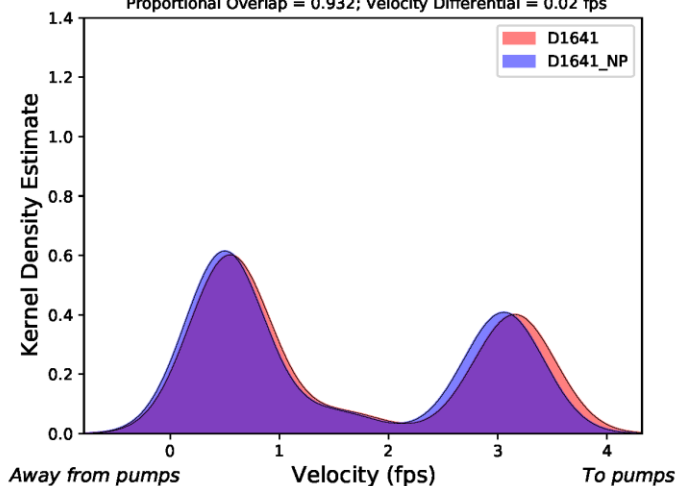
KDE of Old R at Head of Old River Velocity in Jan-Jun

OMR = -9000 cfs; Proportion of Simulation: 5%;  
Proportional Overlap = 0.702; Velocity Differential = 0.21 fps



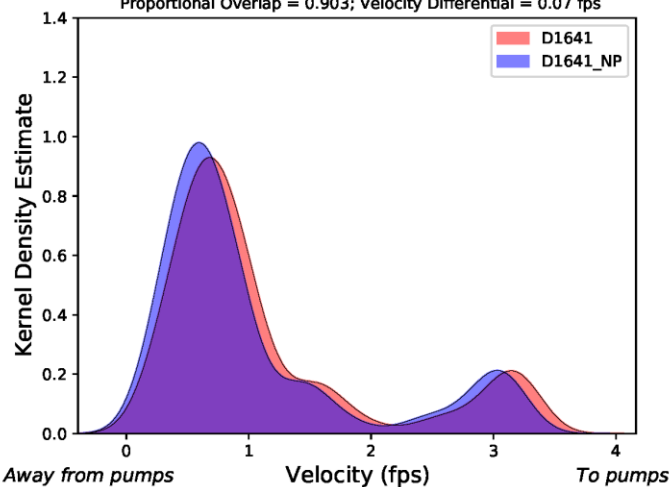
KDE of Old R at Middle River Velocity in Jan-Jun

OMR = -1000 cfs; Proportion of Simulation: 2%;  
Proportional Overlap = 0.932; Velocity Differential = 0.02 fps



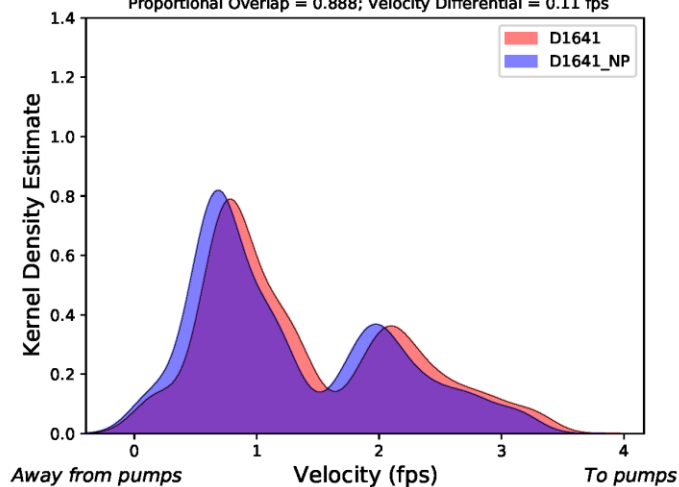
KDE of Old R at Middle River Velocity in Jan-Jun

OMR = -2000 cfs; Proportion of Simulation: 7%;  
Proportional Overlap = 0.903; Velocity Differential = 0.07 fps



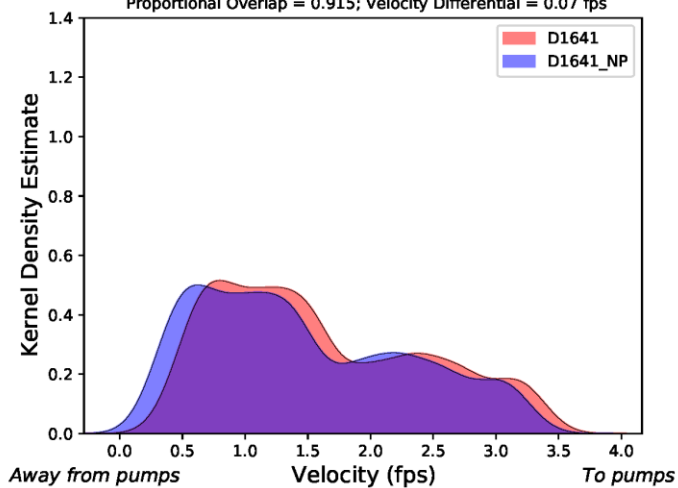
KDE of Old R at Middle River Velocity in Jan-Jun

OMR = -3000 cfs; Proportion of Simulation: 7%;  
Proportional Overlap = 0.888; Velocity Differential = 0.11 fps



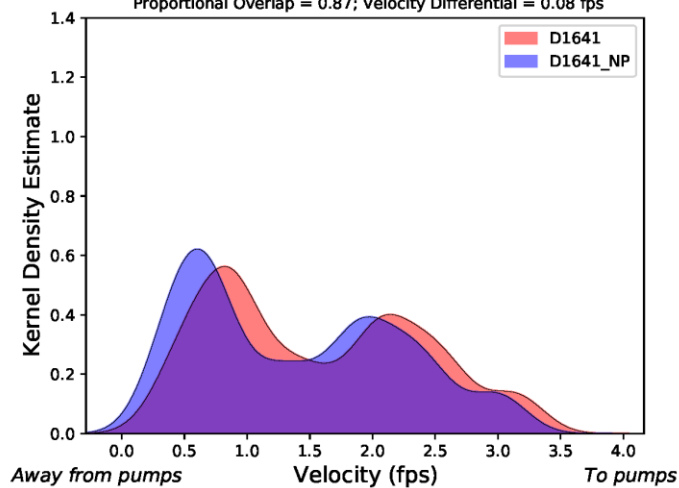
KDE of Old R at Middle River Velocity in Jan-Jun

OMR = -4000 cfs; Proportion of Simulation: 5%;  
Proportional Overlap = 0.915; Velocity Differential = 0.07 fps

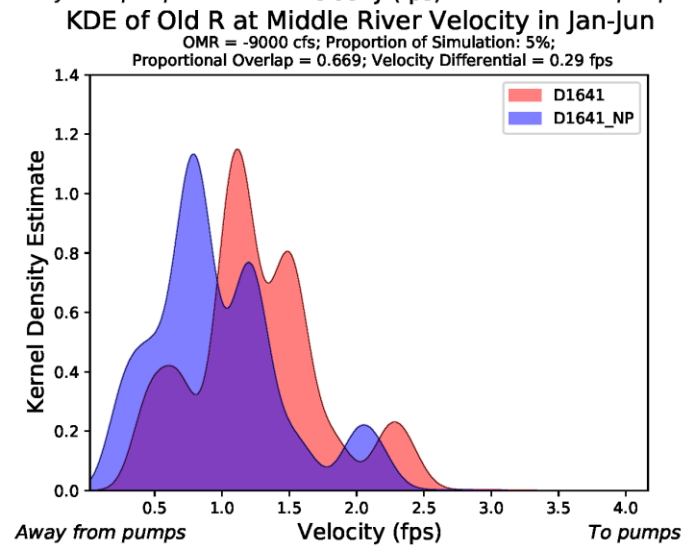
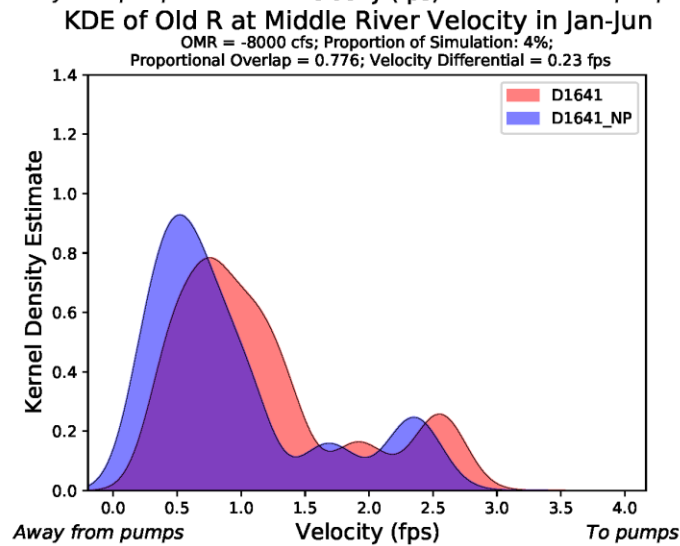
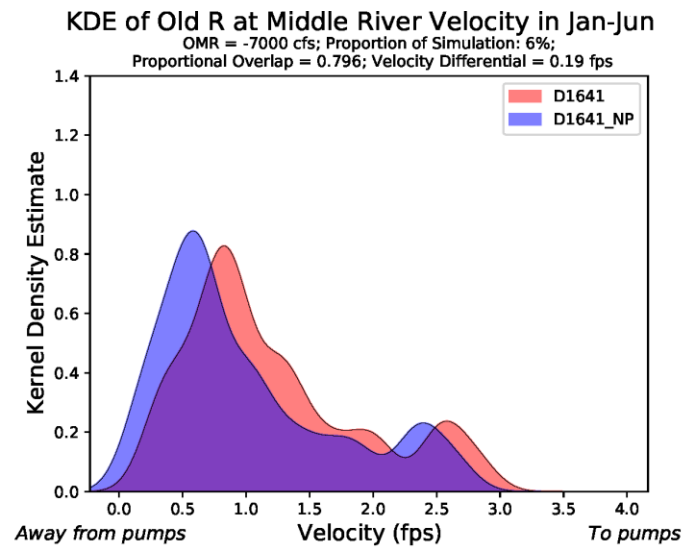
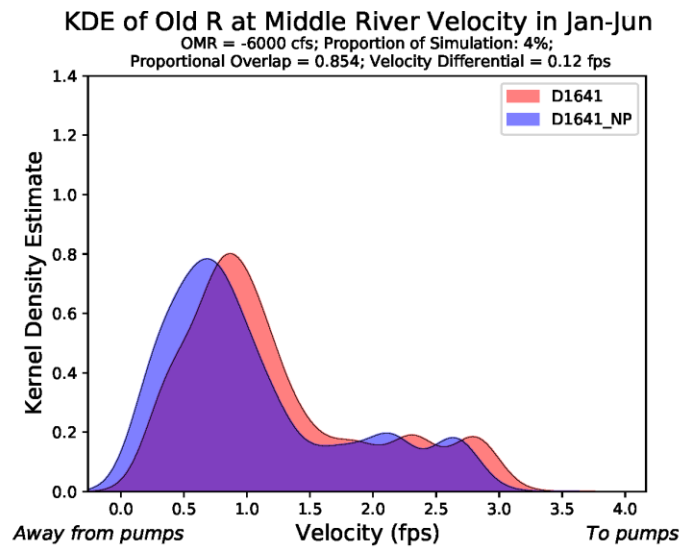


KDE of Old R at Middle River Velocity in Jan-Jun

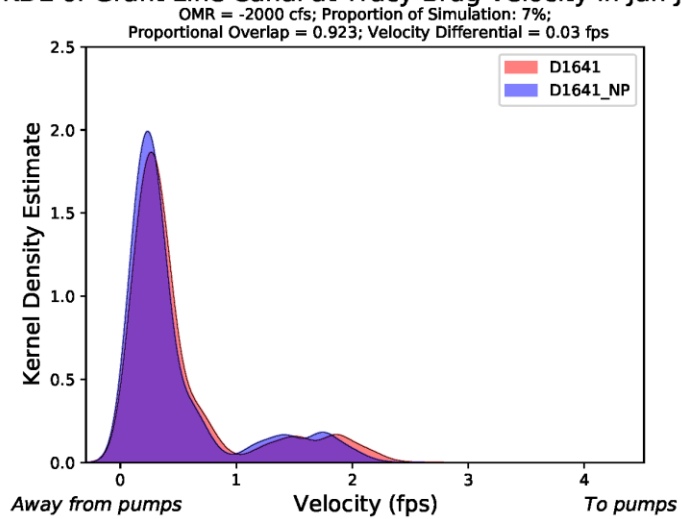
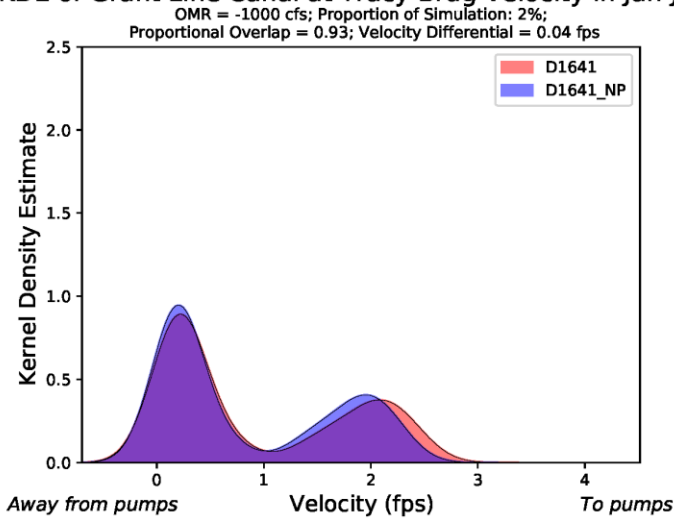
OMR = -5000 cfs; Proportion of Simulation: 4%;  
Proportional Overlap = 0.87; Velocity Differential = 0.08 fps



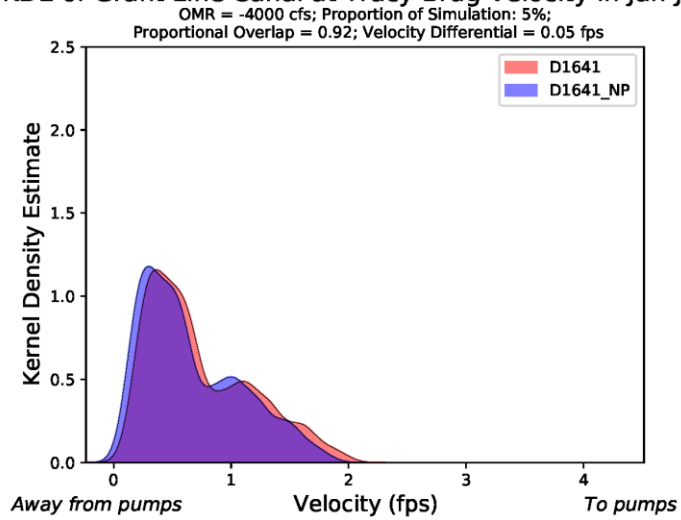
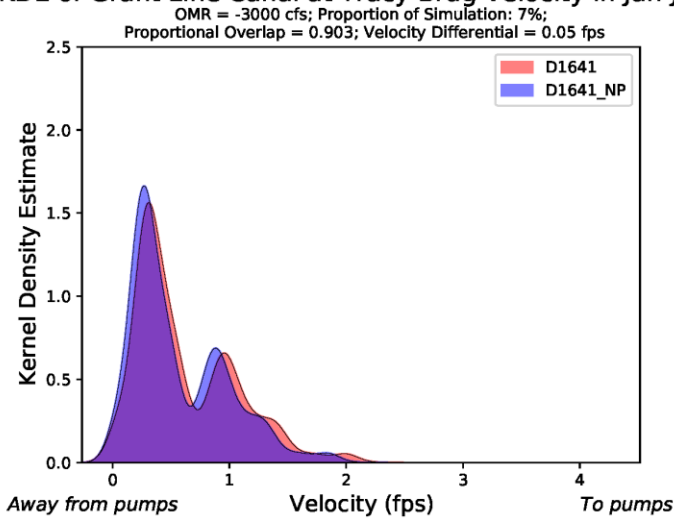




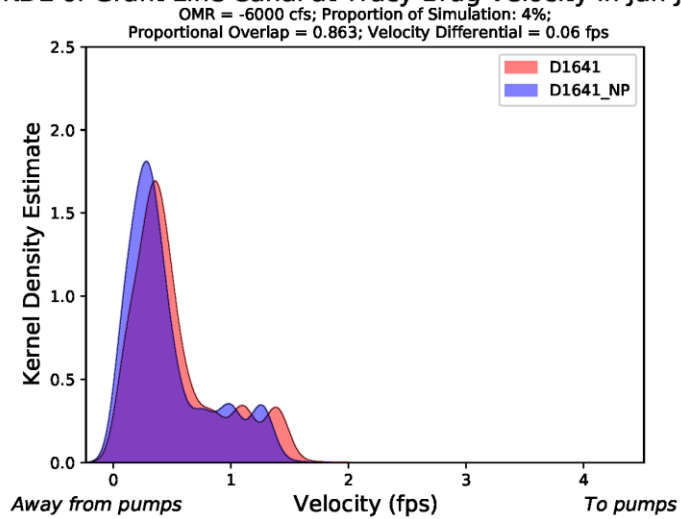
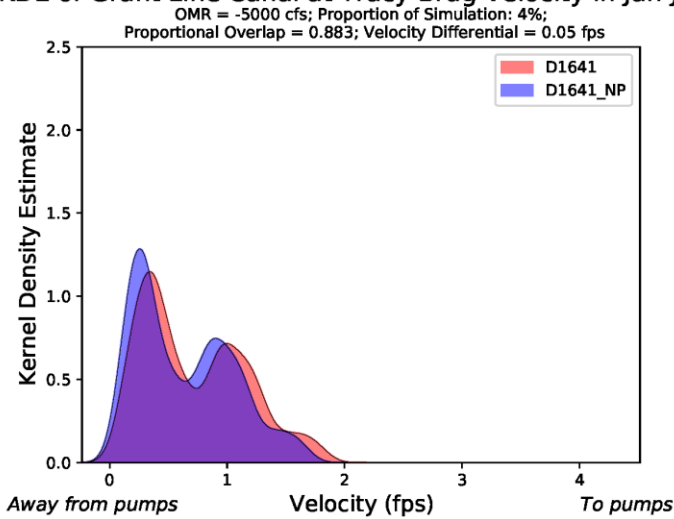
# KDE of Grant Line Canal at Tracy Brdg Velocity in Jan-Jun KDE of Grant Line Canal at Tracy Brdg Velocity in Jan-Jun



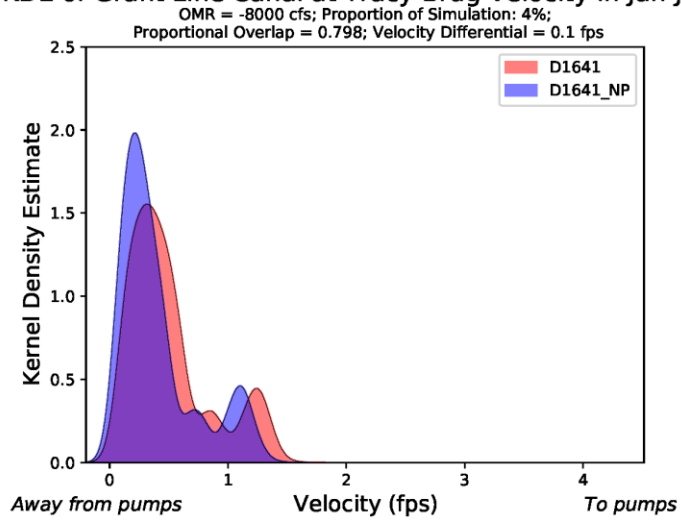
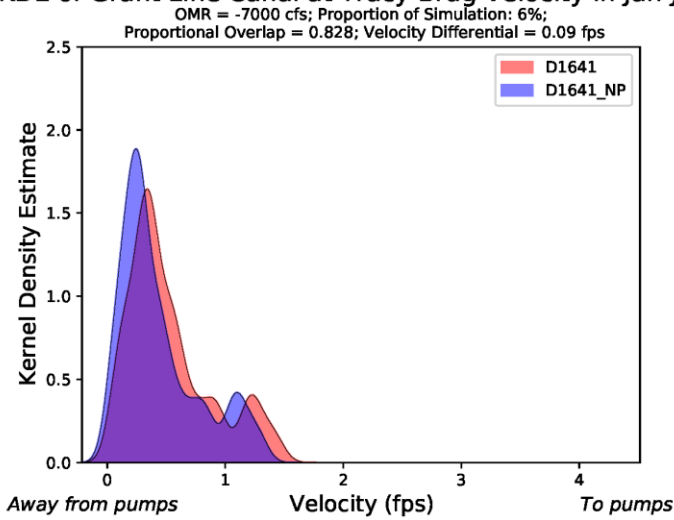
# KDE of Grant Line Canal at Tracy Brdg Velocity in Jan-Jun KDE of Grant Line Canal at Tracy Brdg Velocity in Jan-Jun



# KDE of Grant Line Canal at Tracy Brdg Velocity in Jan-Jun KDE of Grant Line Canal at Tracy Brdg Velocity in Jan-Jun

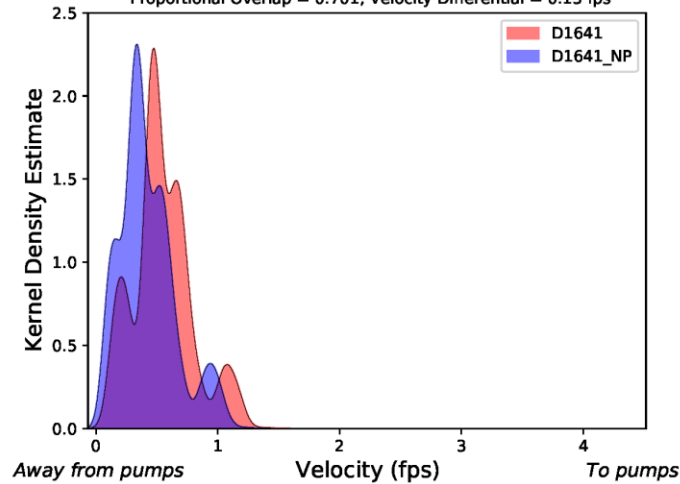


# KDE of Grant Line Canal at Tracy Brdg Velocity in Jan-Jun KDE of Grant Line Canal at Tracy Brdg Velocity in Jan-Jun



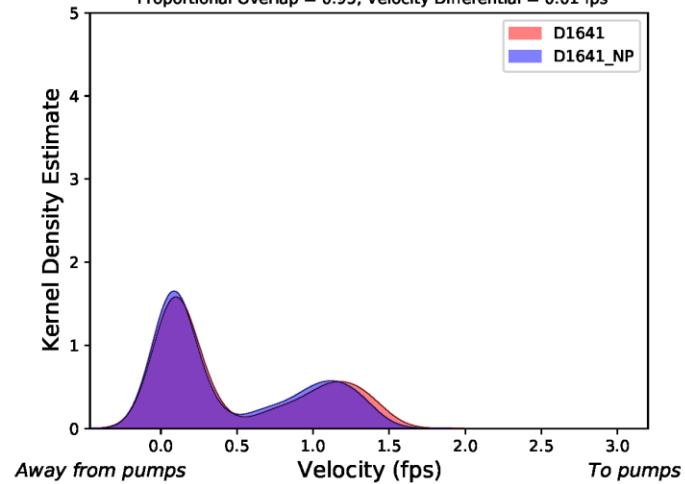
KDE of Grant Line Canal at Tracy Brdg Velocity in Jan-Jun

OMR = -9000 cfs; Proportion of Simulation: 5%;  
Proportional Overlap = 0.701; Velocity Differential = 0.13 fps



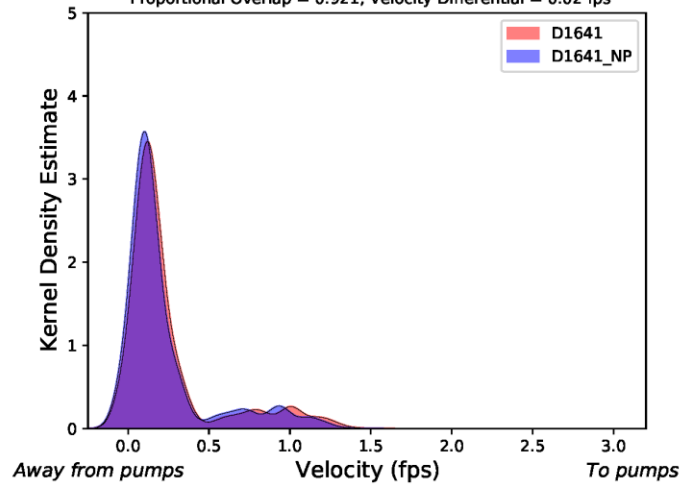
KDE of Old R near Tracy Velocity in Jan-Jun

OMR = -1000 cfs; Proportion of Simulation: 2%;  
Proportional Overlap = 0.95; Velocity Differential = 0.01 fps



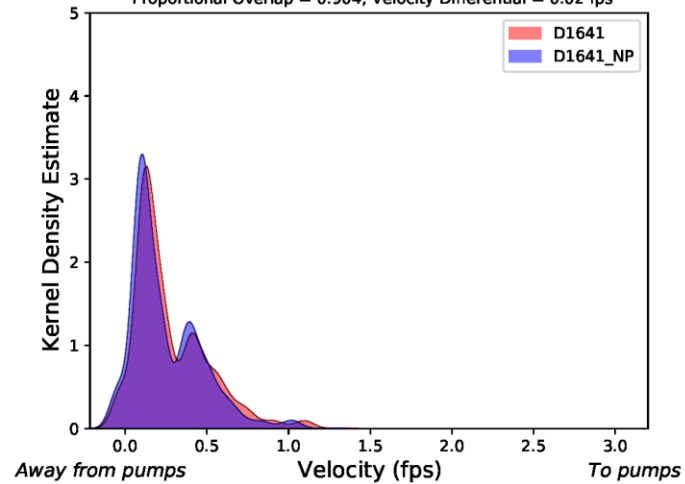
KDE of Old R near Tracy Velocity in Jan-Jun

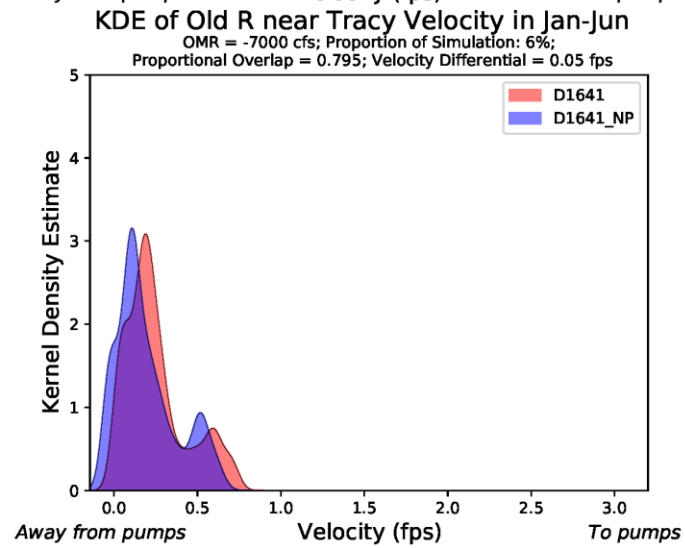
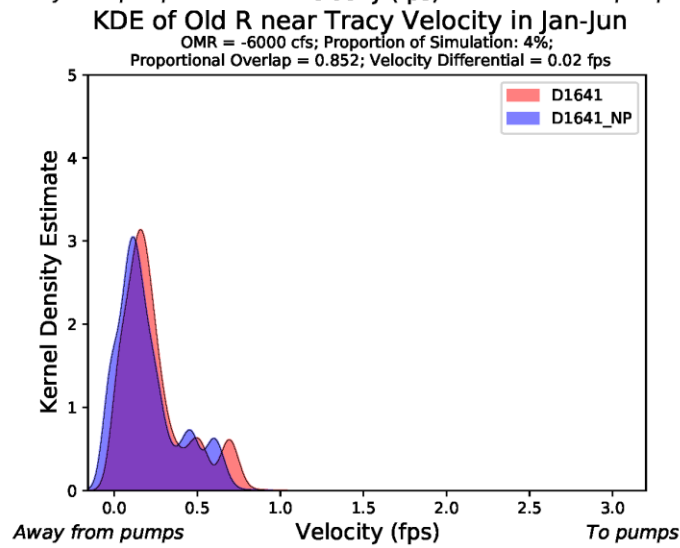
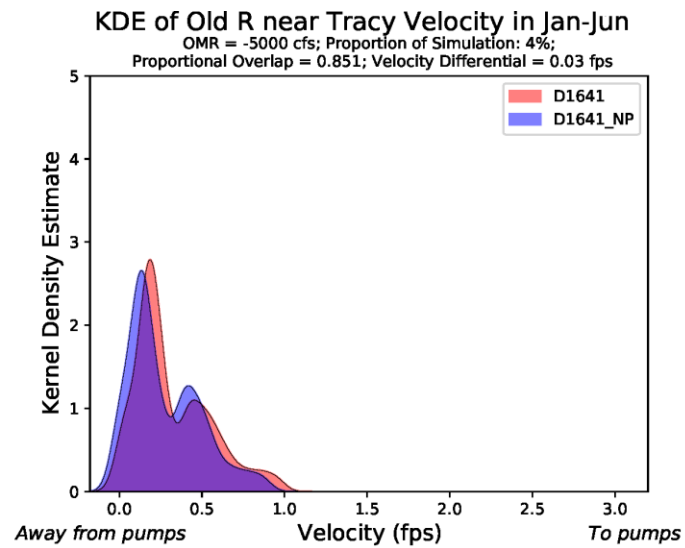
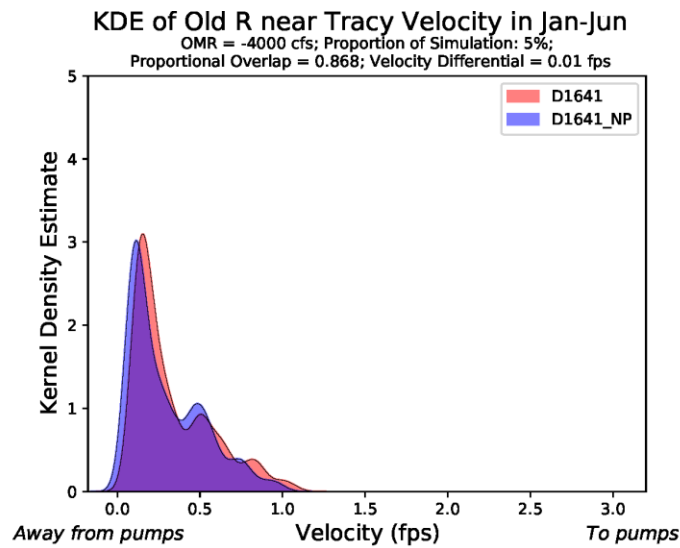
OMR = -2000 cfs; Proportion of Simulation: 7%;  
Proportional Overlap = 0.921; Velocity Differential = 0.02 fps

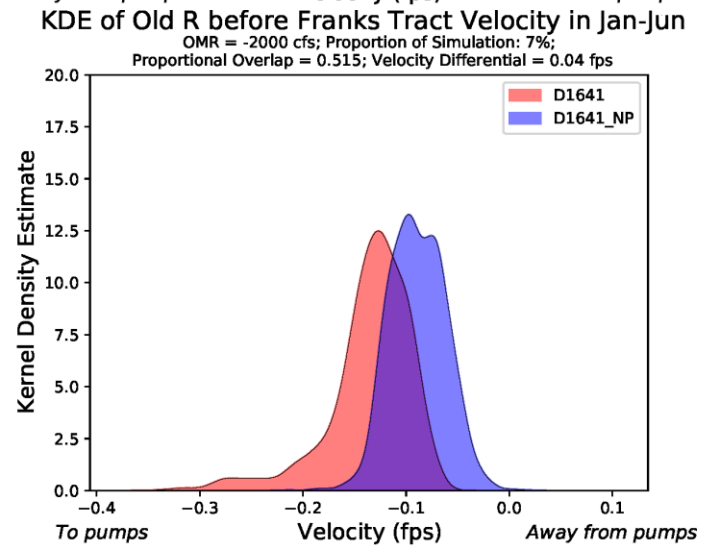
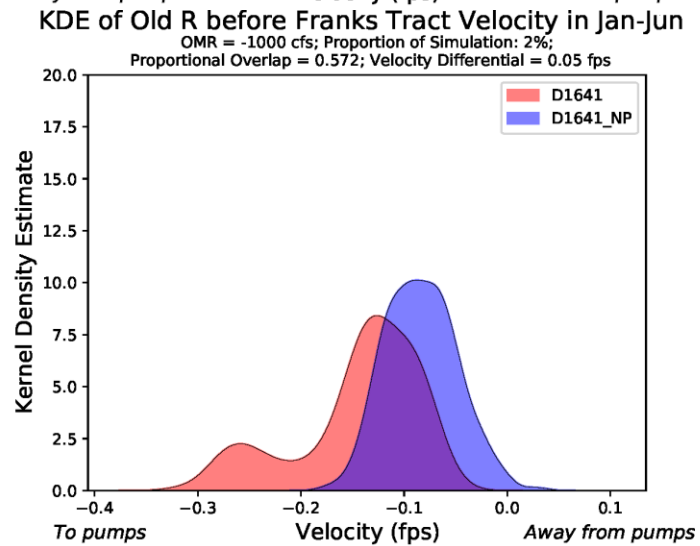
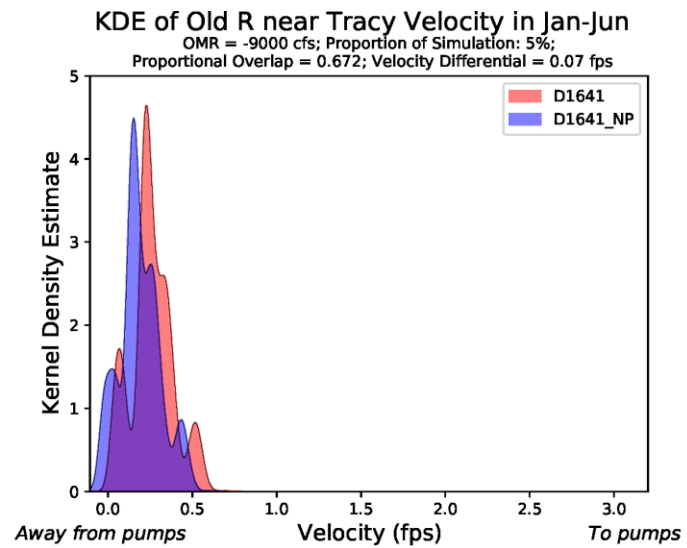
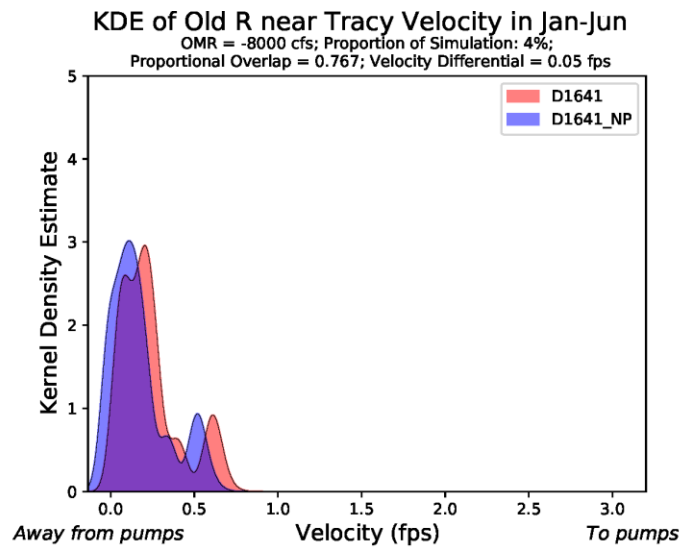


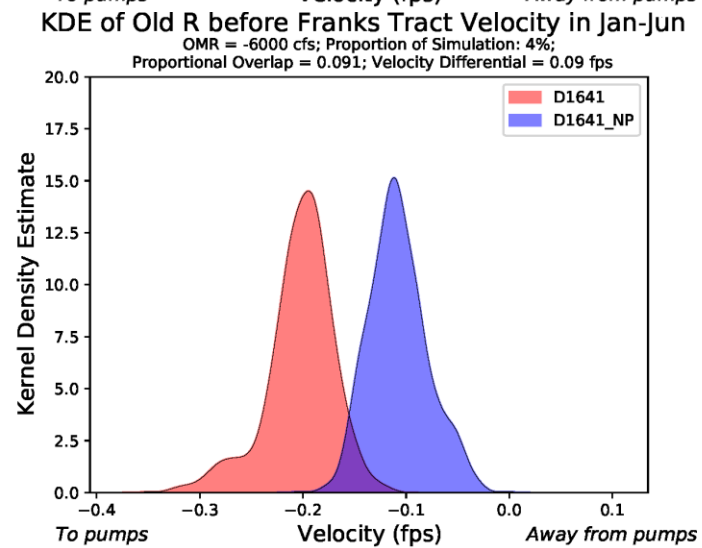
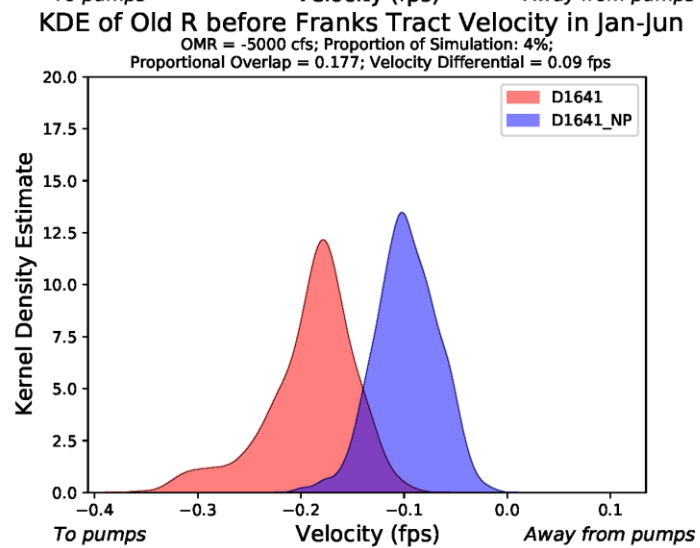
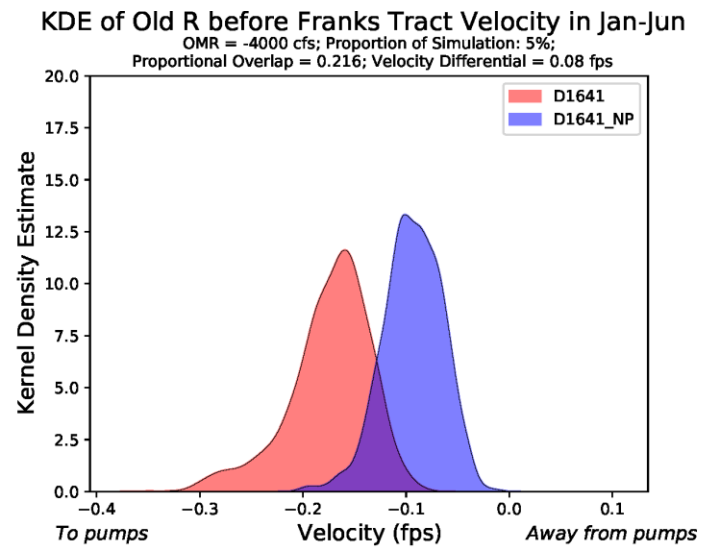
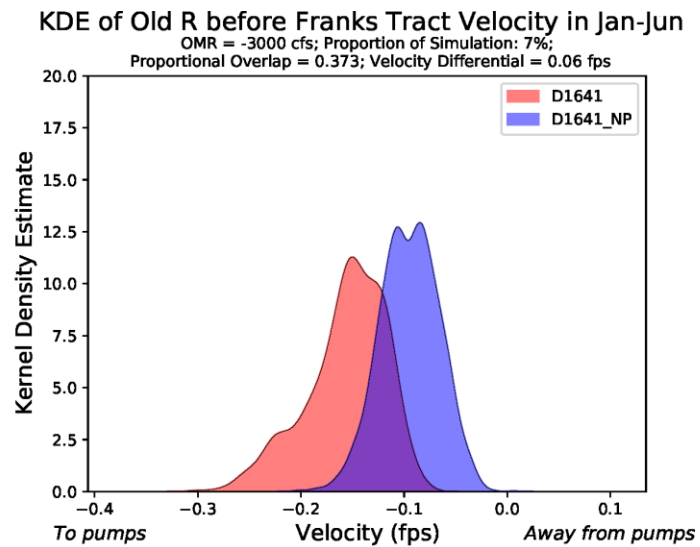
KDE of Old R near Tracy Velocity in Jan-Jun

OMR = -3000 cfs; Proportion of Simulation: 7%;  
Proportional Overlap = 0.904; Velocity Differential = 0.02 fps



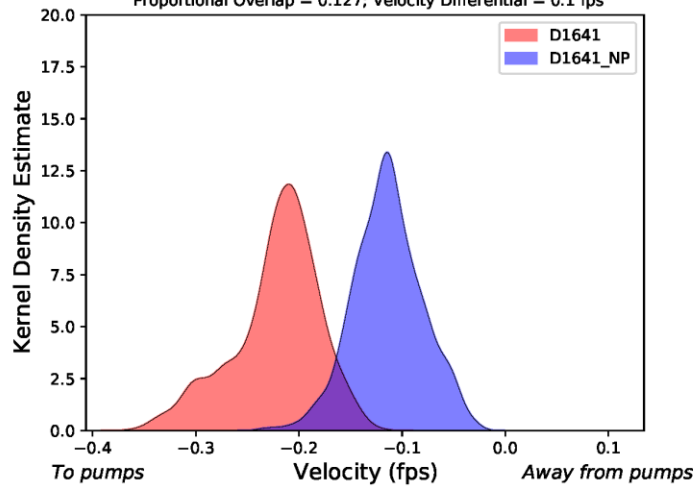






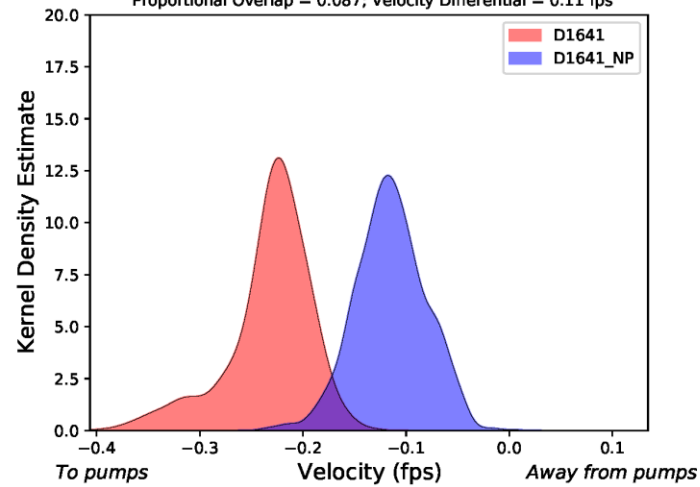
KDE of Old R before Franks Tract Velocity in Jan-Jun

OMR = -7000 cfs; Proportion of Simulation: 6%;  
Proportional Overlap = 0.127; Velocity Differential = 0.1 fps



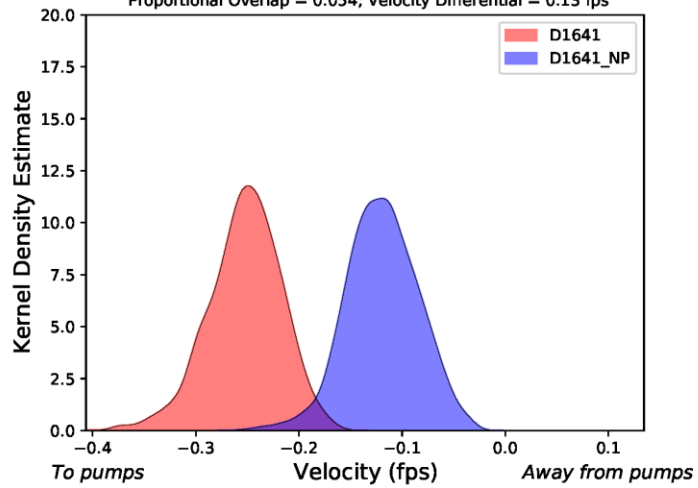
KDE of Old R before Franks Tract Velocity in Jan-Jun

OMR = -8000 cfs; Proportion of Simulation: 4%;  
Proportional Overlap = 0.087; Velocity Differential = 0.11 fps



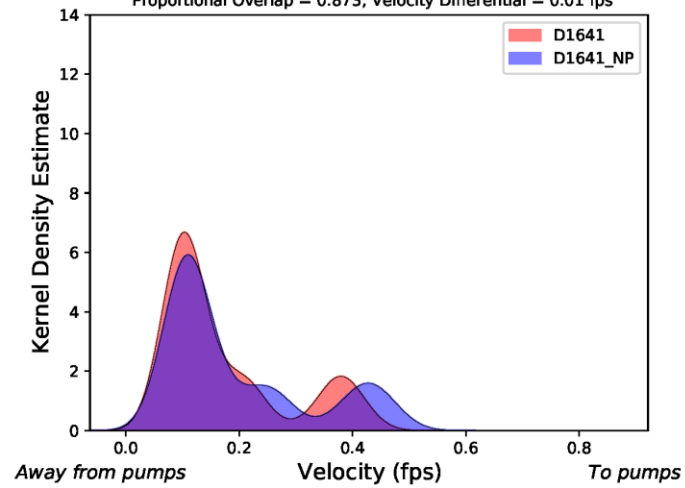
KDE of Old R before Franks Tract Velocity in Jan-Jun

OMR = -9000 cfs; Proportion of Simulation: 5%;  
Proportional Overlap = 0.054; Velocity Differential = 0.13 fps

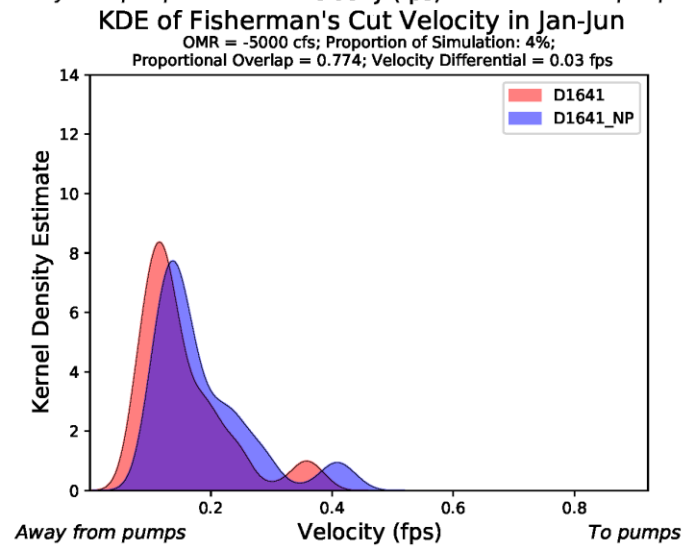
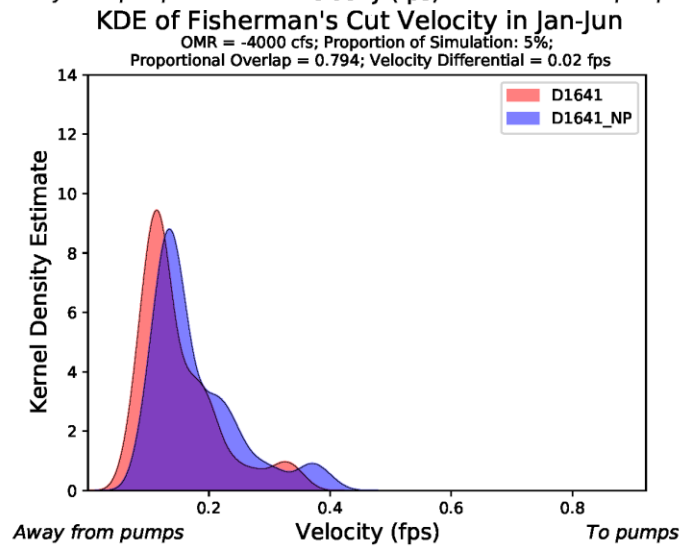
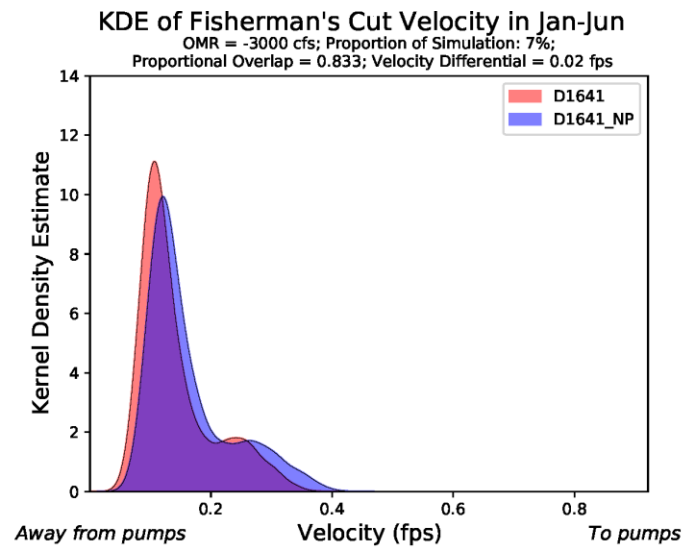
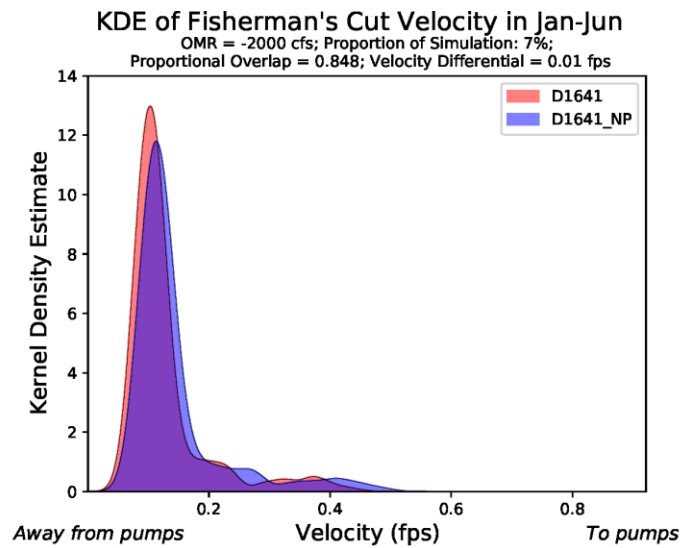


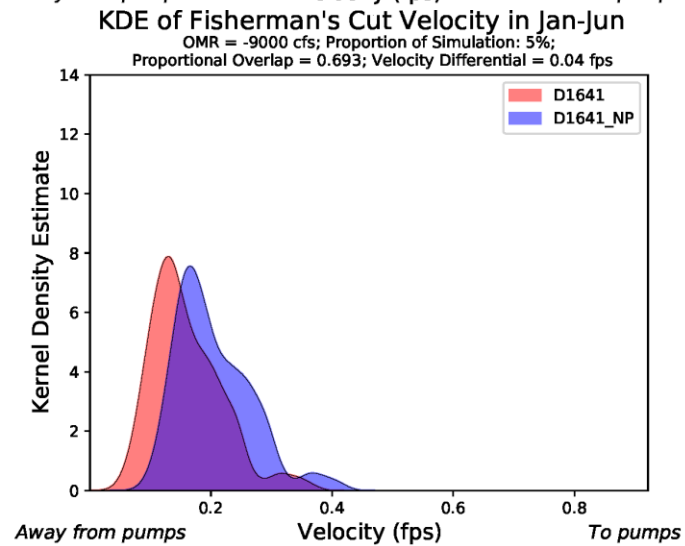
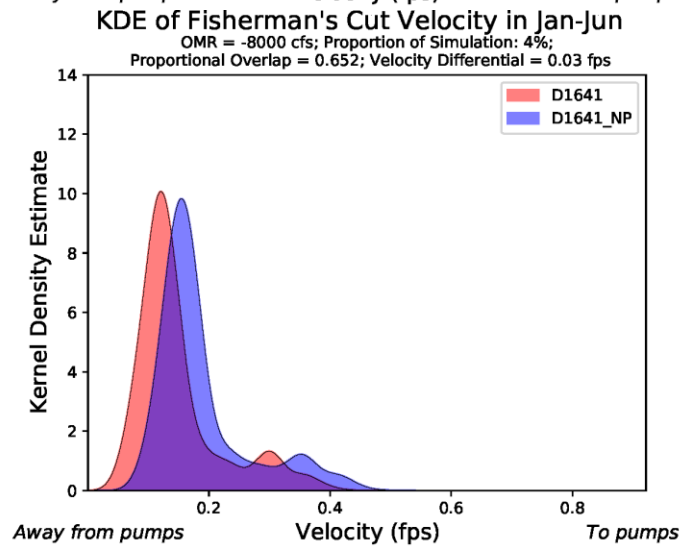
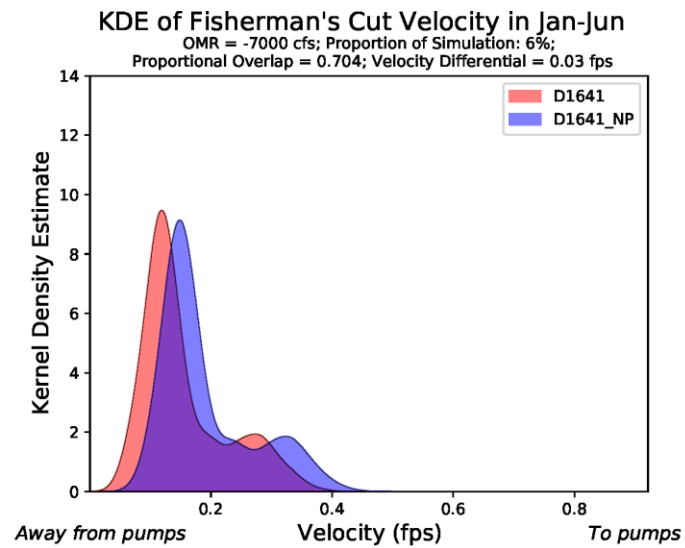
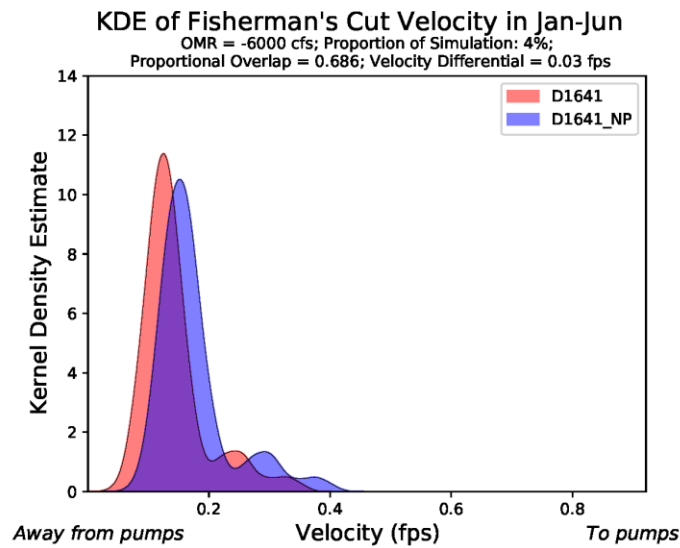
KDE of Fisherman's Cut Velocity in Jan-Jun

OMR = -1000 cfs; Proportion of Simulation: 2%;  
Proportional Overlap = 0.873; Velocity Differential = 0.01 fps

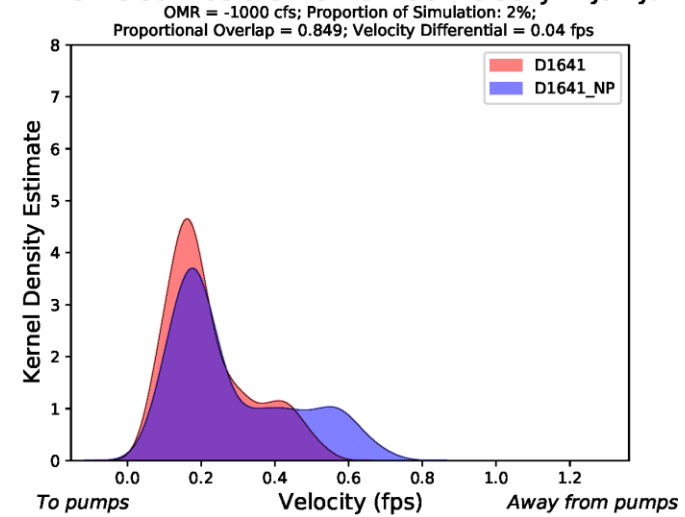




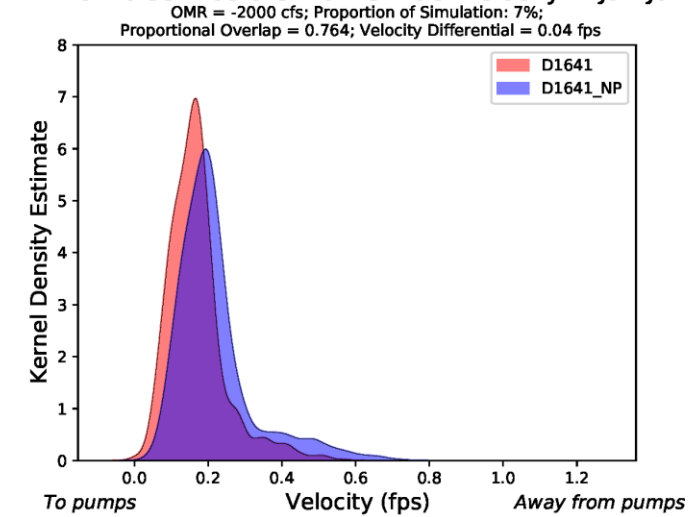




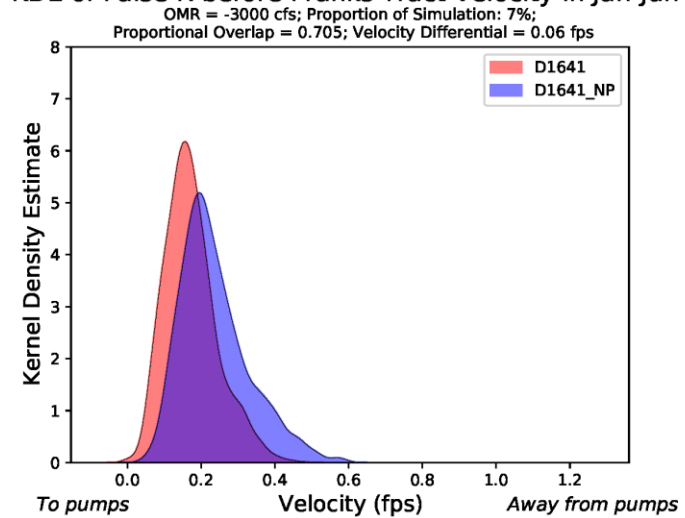
KDE of False R before Franks Tract Velocity in Jan-Jun



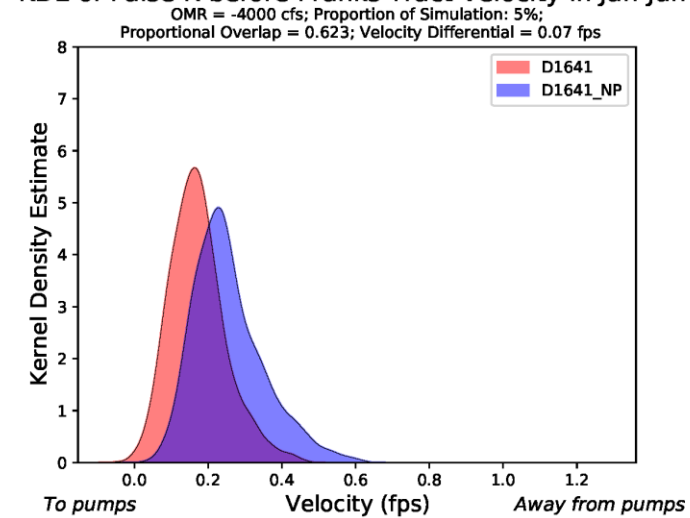
KDE of False R before Franks Tract Velocity in Jan-Jun



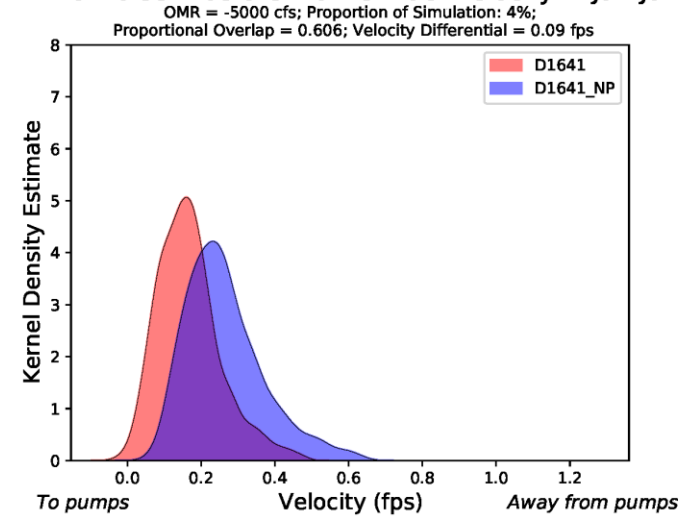
KDE of False R before Franks Tract Velocity in Jan-Jun



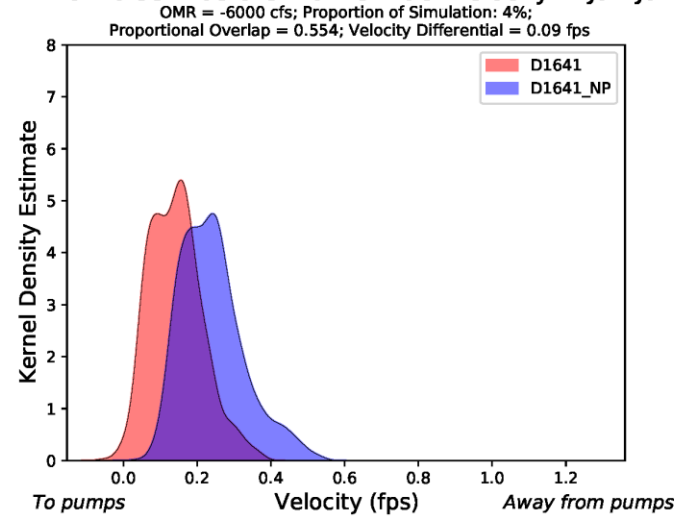
KDE of False R before Franks Tract Velocity in Jan-Jun



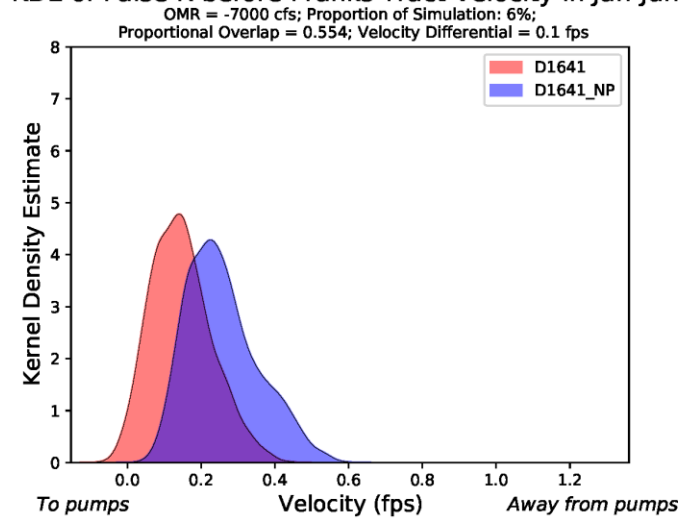
KDE of False R before Franks Tract Velocity in Jan-Jun



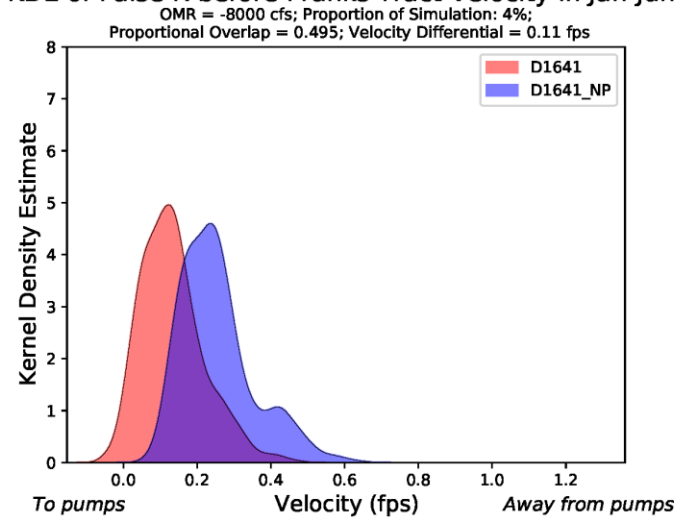
KDE of False R before Franks Tract Velocity in Jan-Jun



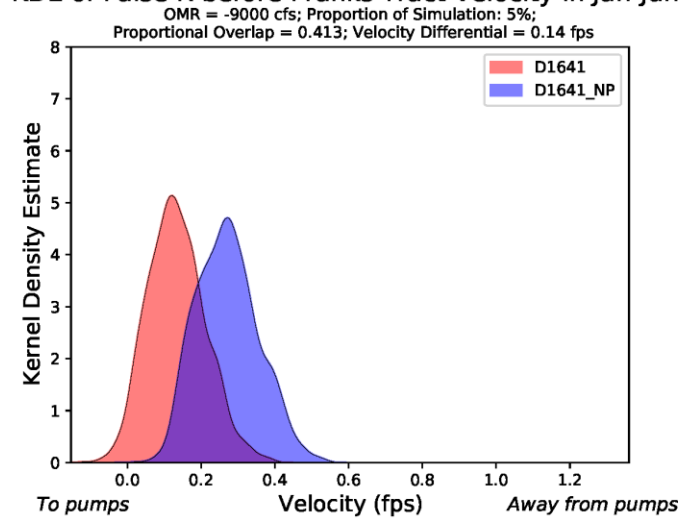
KDE of False R before Franks Tract Velocity in Jan-Jun



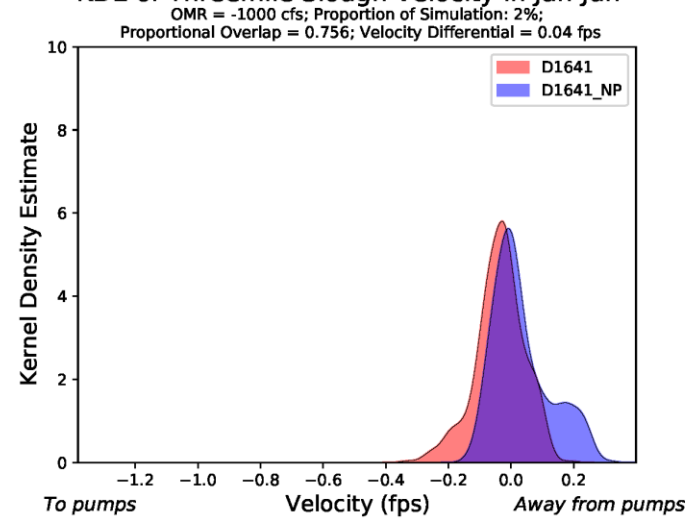
KDE of False R before Franks Tract Velocity in Jan-Jun



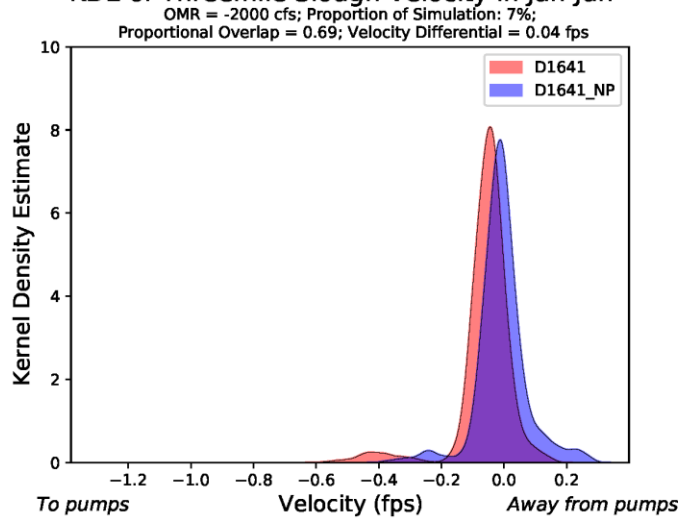
KDE of False R before Franks Tract Velocity in Jan-Jun



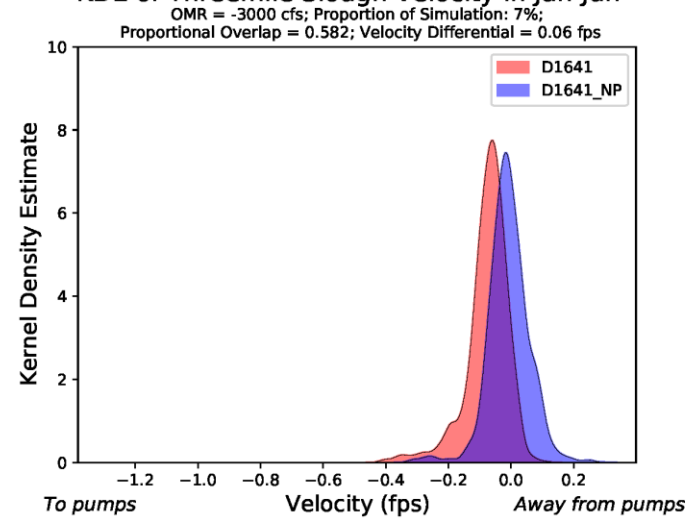
KDE of Threemile Slough Velocity in Jan-Jun

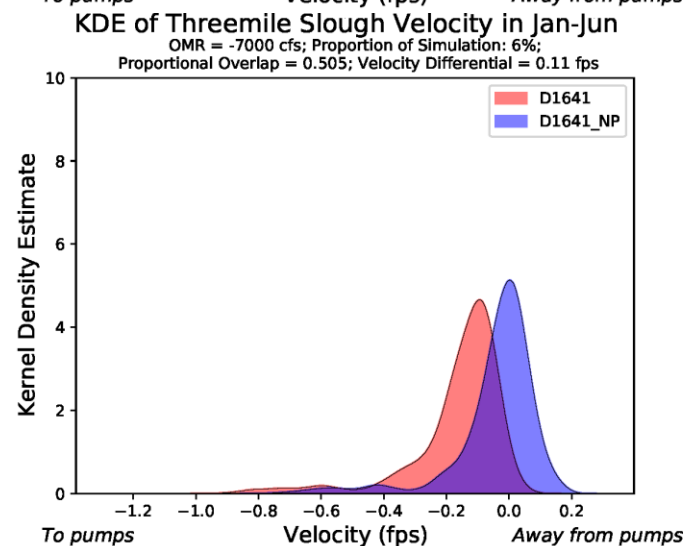
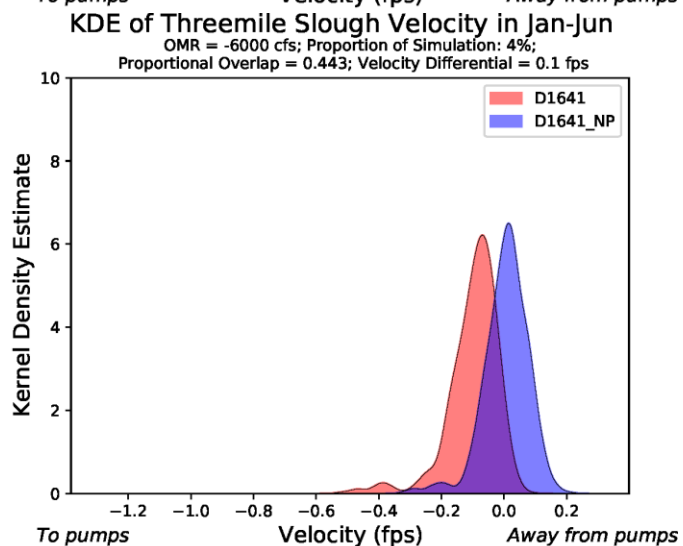
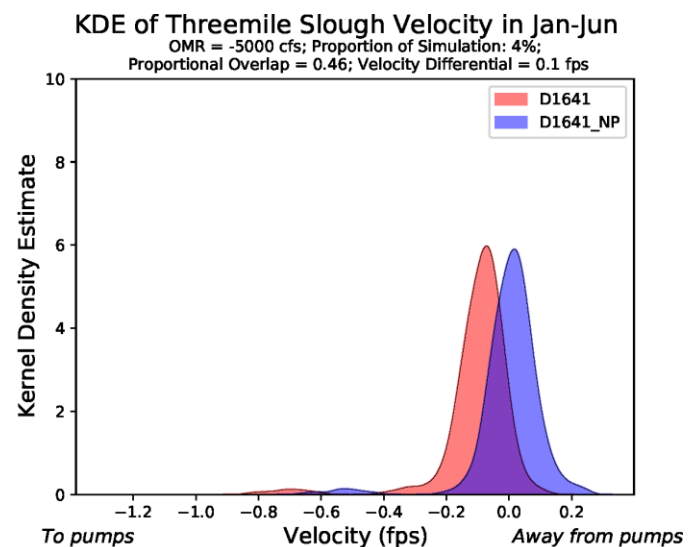
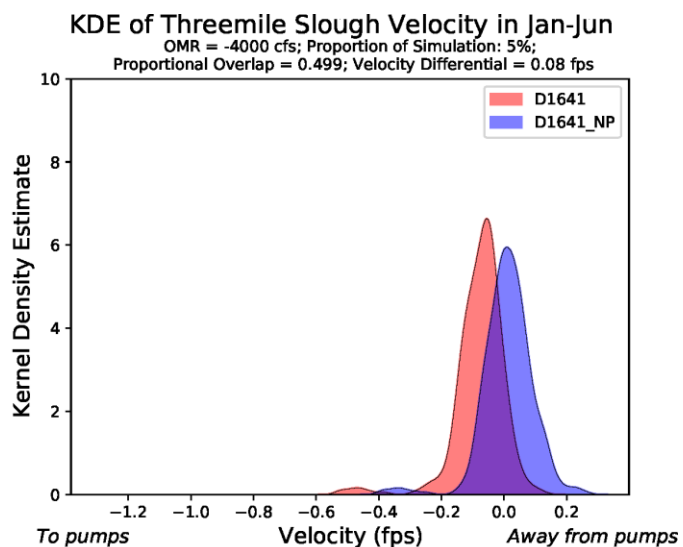


KDE of Threemile Slough Velocity in Jan-Jun



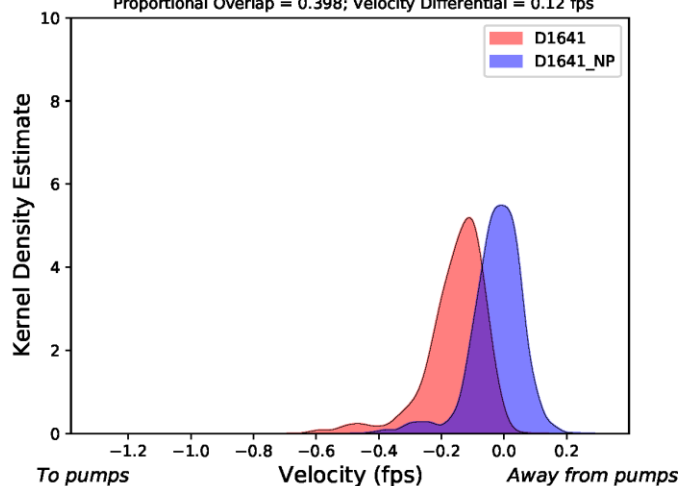
KDE of Threemile Slough Velocity in Jan-Jun





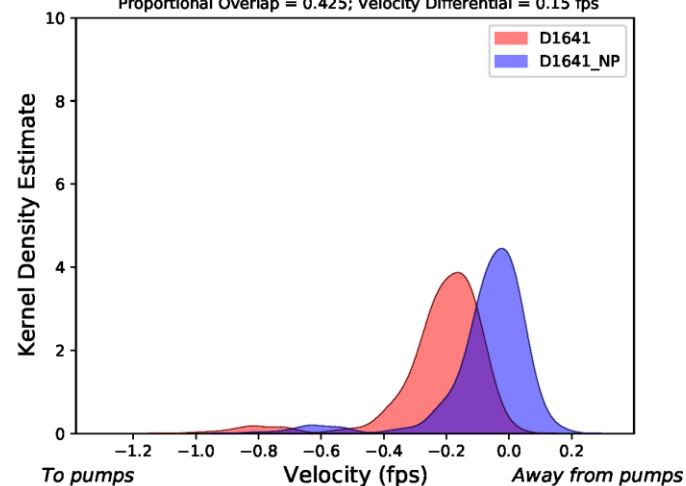
KDE of Threemile Slough Velocity in Jan-Jun

OMR = -8000 cfs; Proportion of Simulation: 4%;  
Proportional Overlap = 0.398; Velocity Differential = 0.12 fps



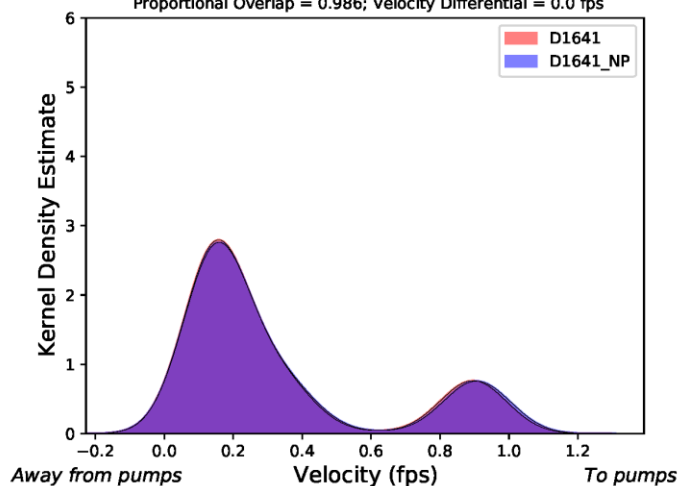
KDE of Threemile Slough Velocity in Jan-Jun

OMR = -9000 cfs; Proportion of Simulation: 5%;  
Proportional Overlap = 0.425; Velocity Differential = 0.15 fps



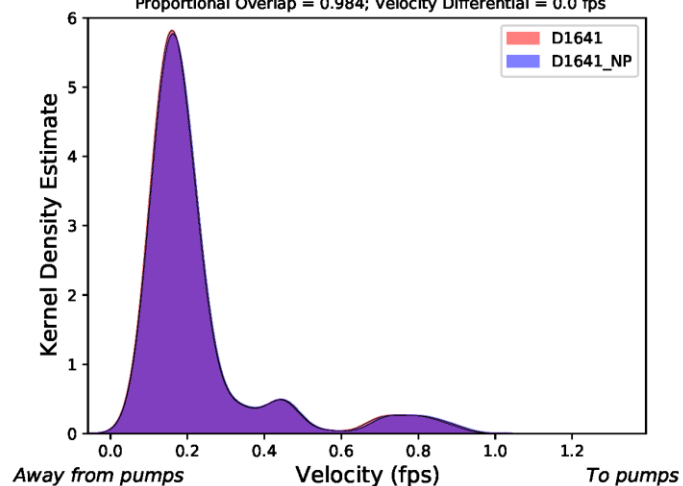
KDE of Mokelumne R Velocity in Jan-Jun

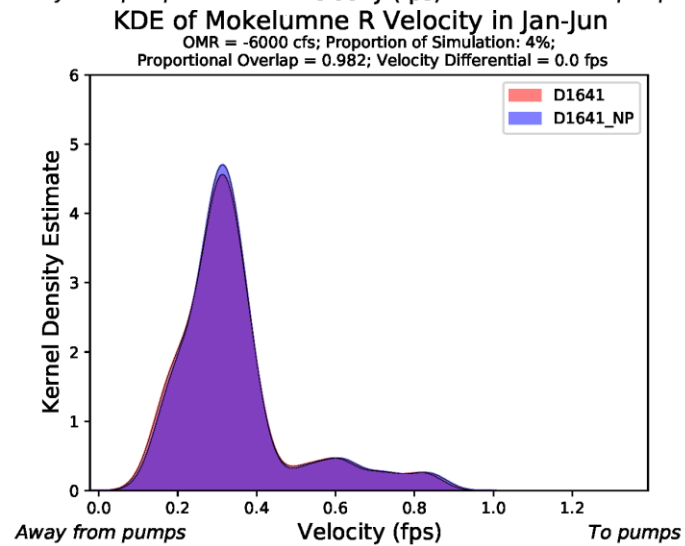
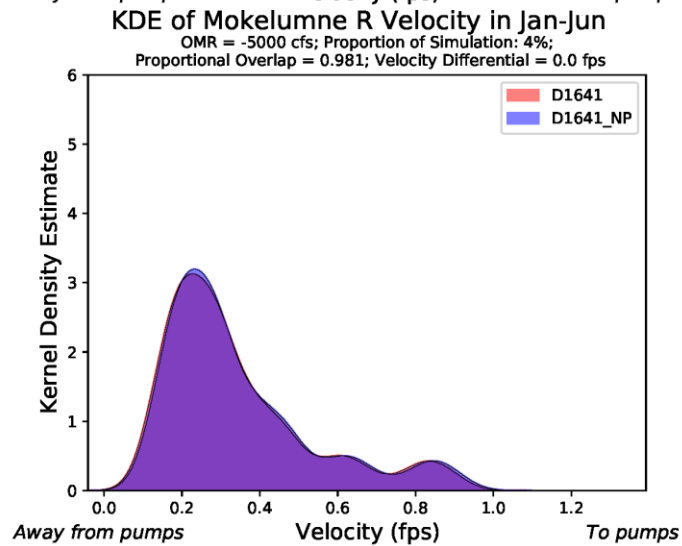
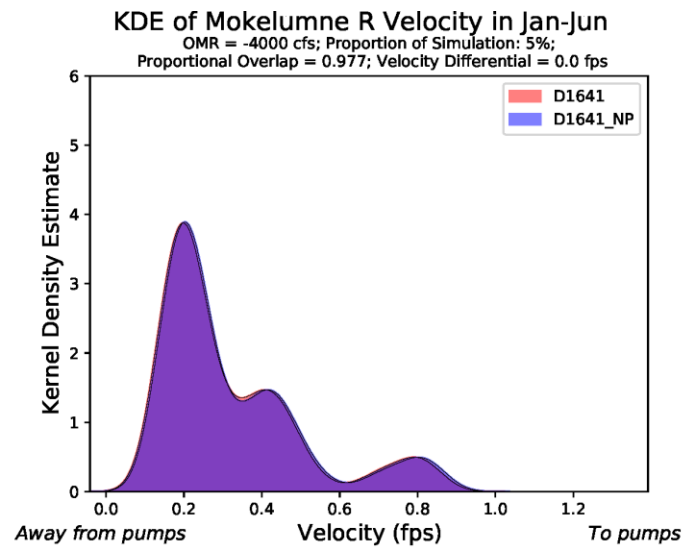
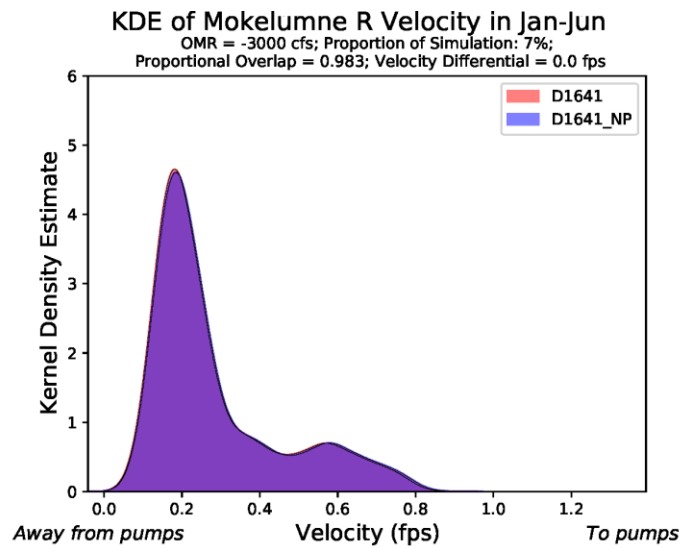
OMR = -1000 cfs; Proportion of Simulation: 2%;  
Proportional Overlap = 0.986; Velocity Differential = 0.0 fps



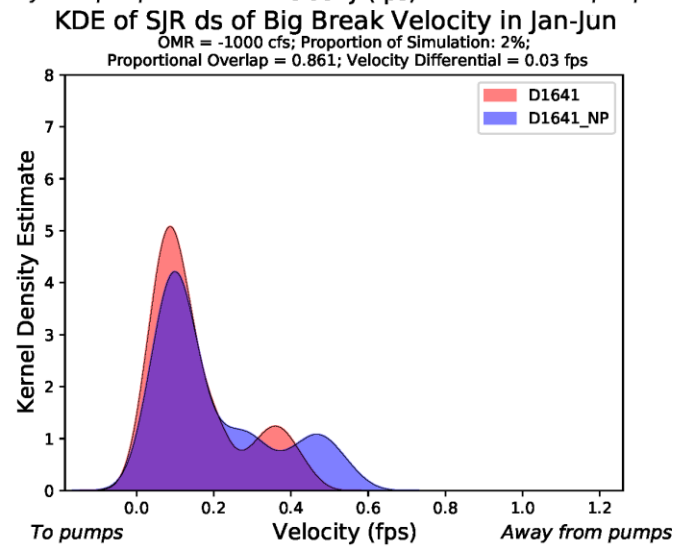
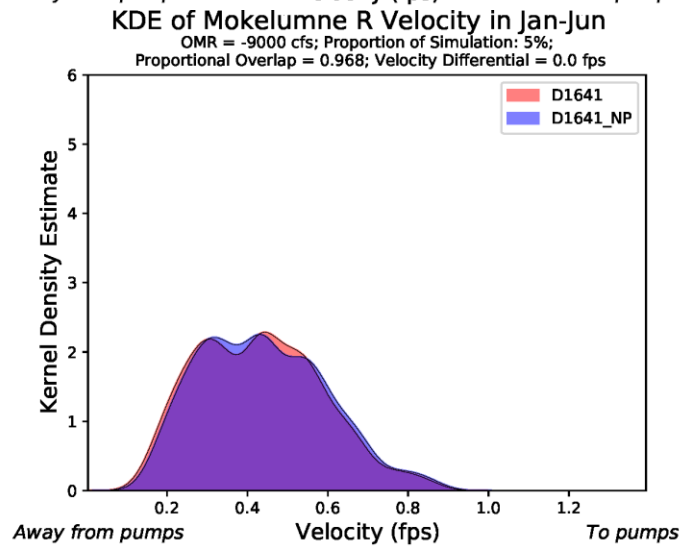
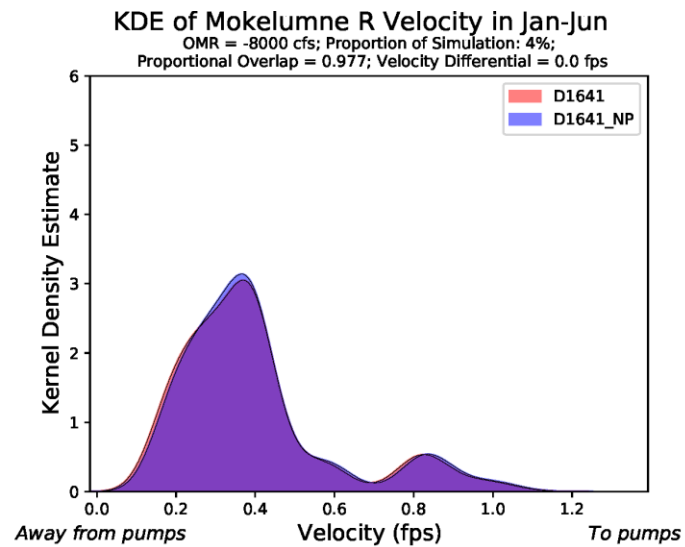
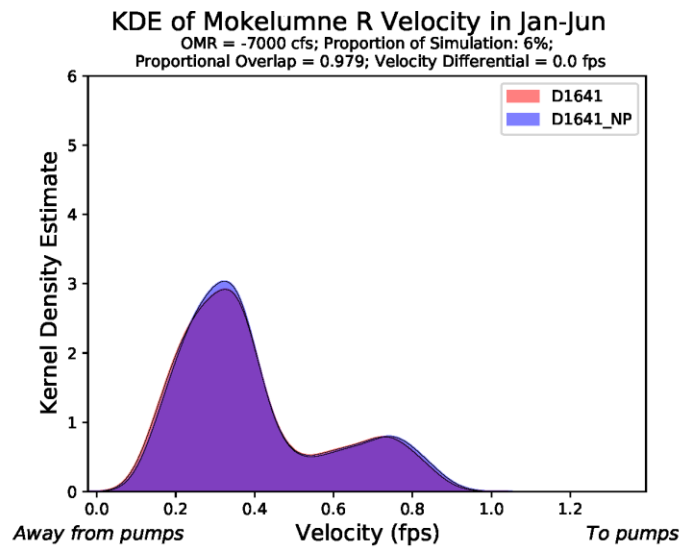
KDE of Mokelumne R Velocity in Jan-Jun

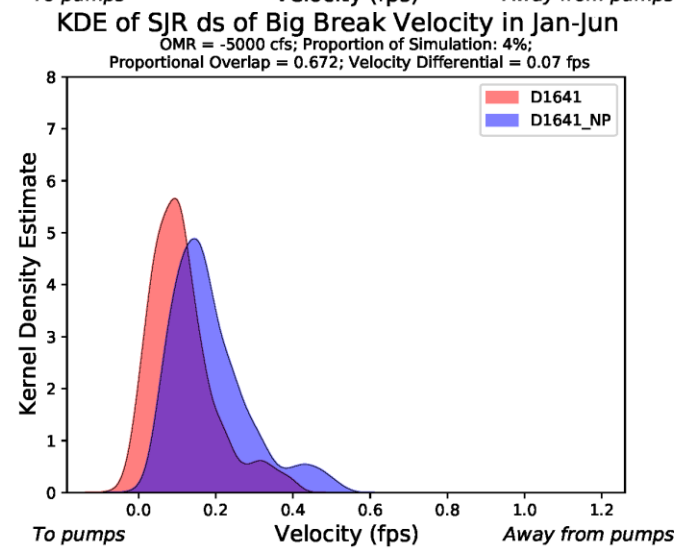
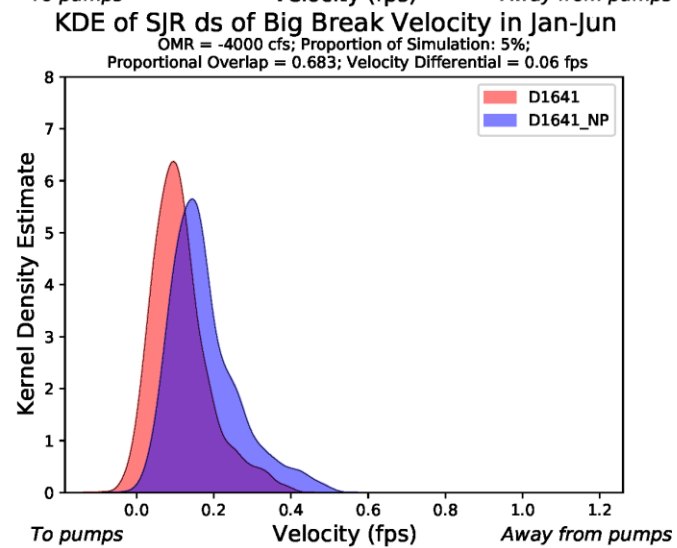
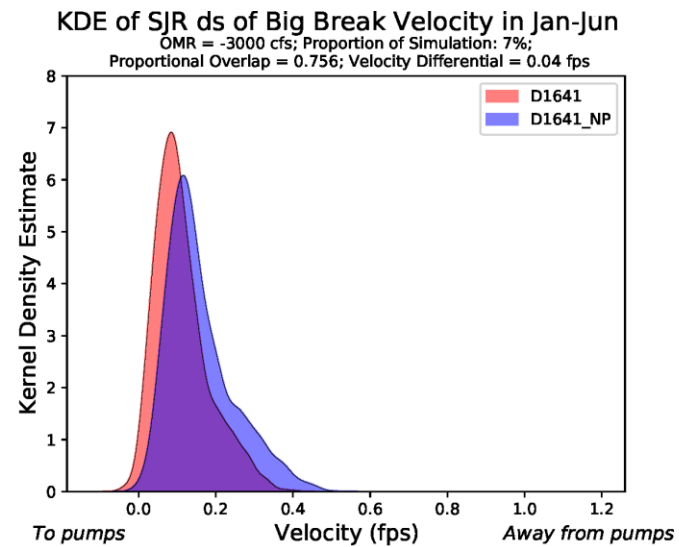
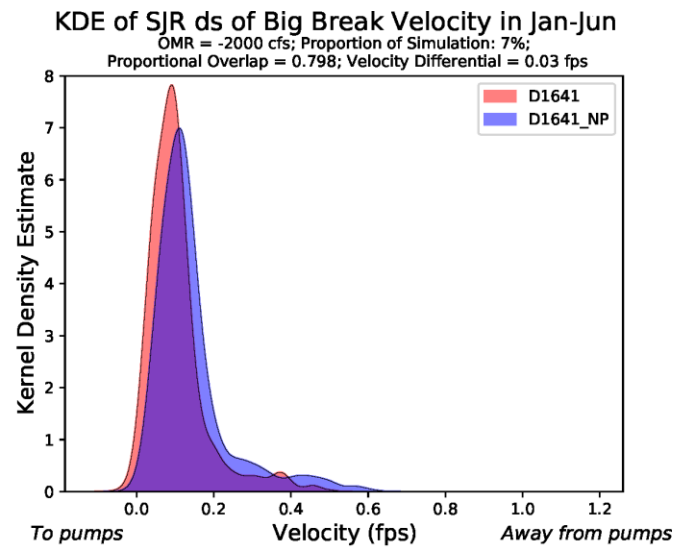
OMR = -2000 cfs; Proportion of Simulation: 7%;  
Proportional Overlap = 0.984; Velocity Differential = 0.0 fps

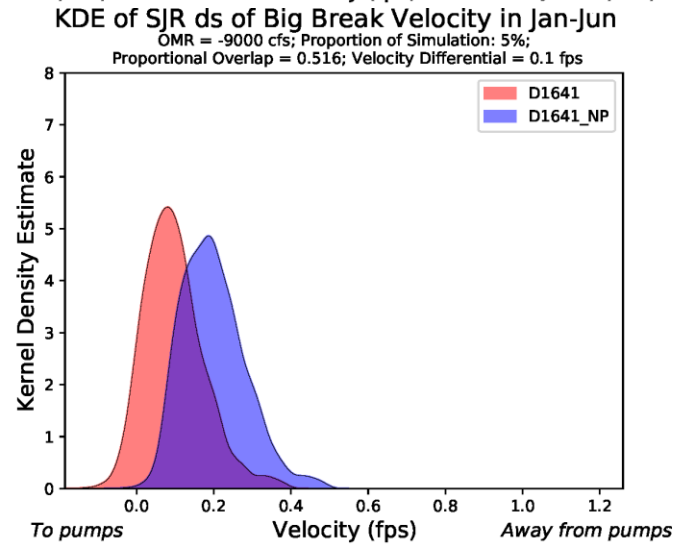
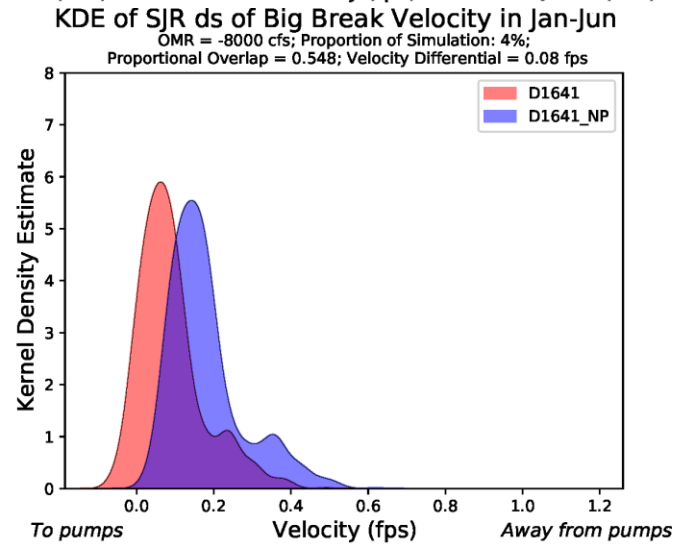
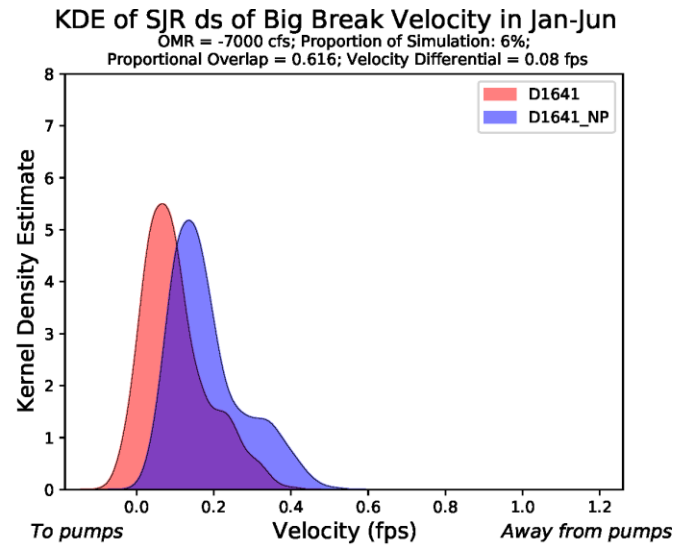
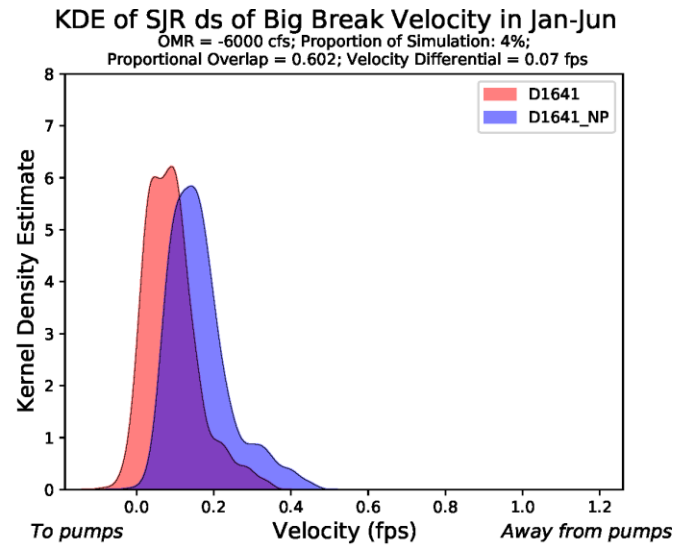


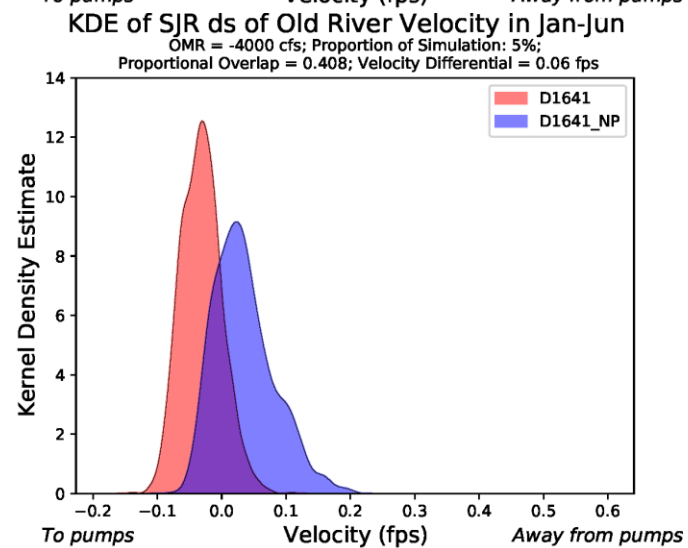
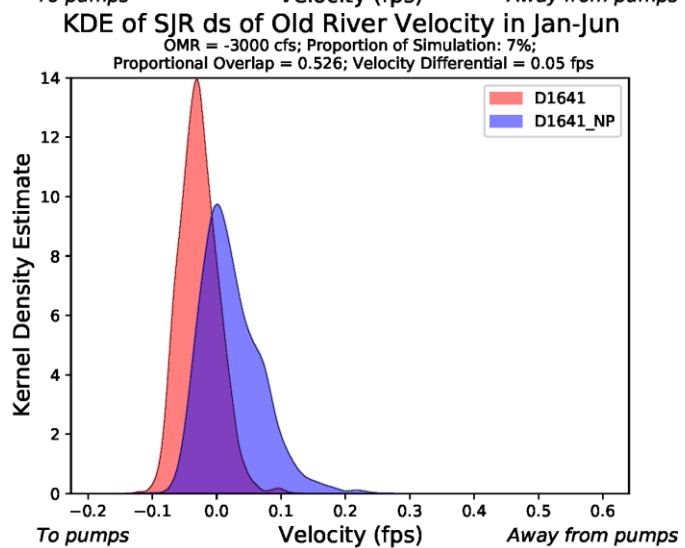
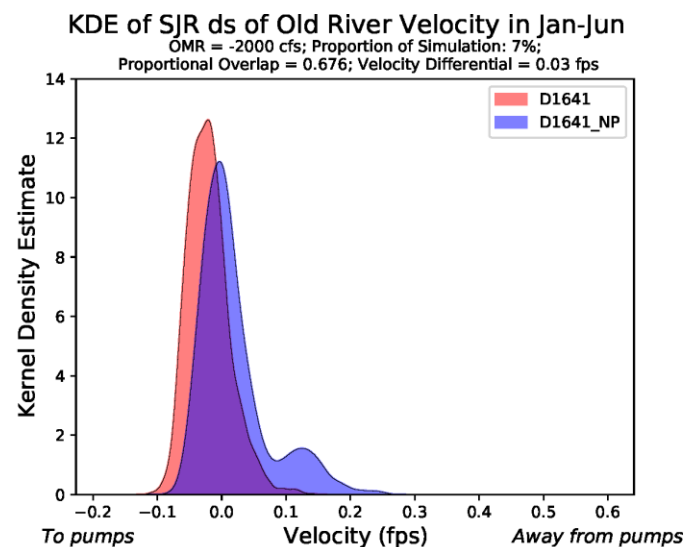
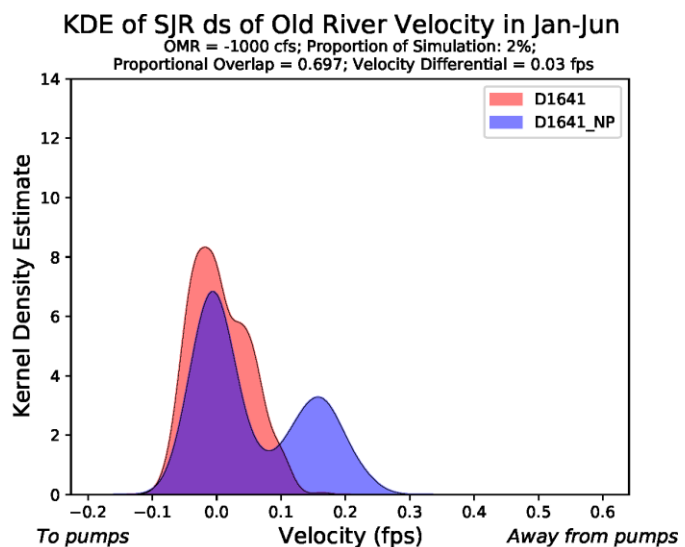


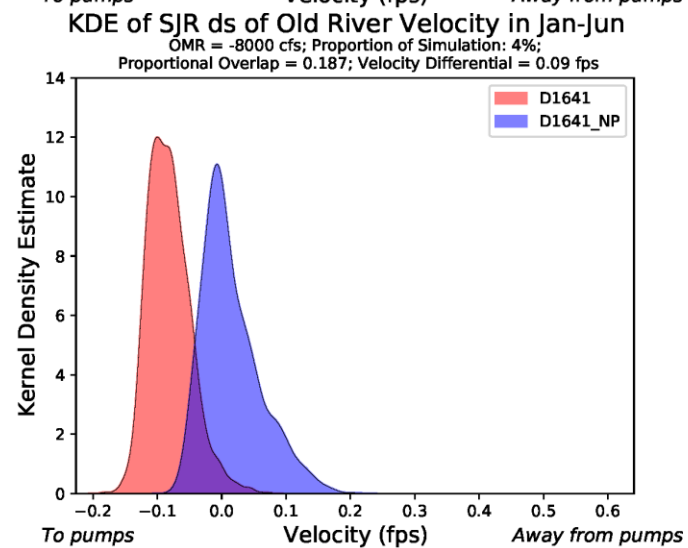
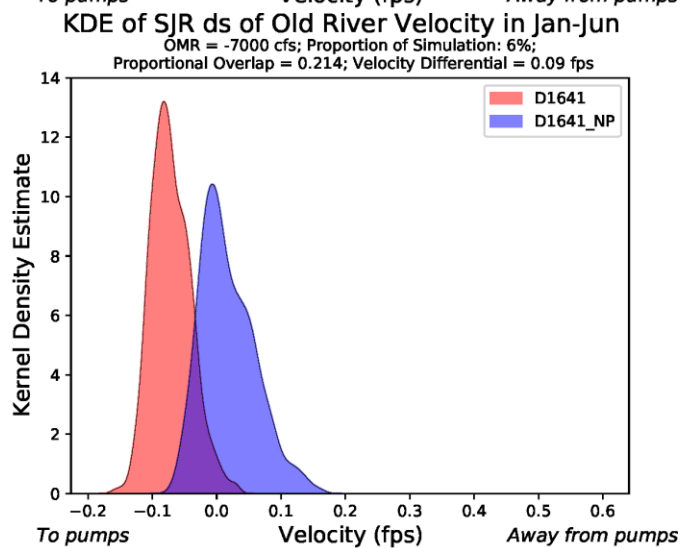
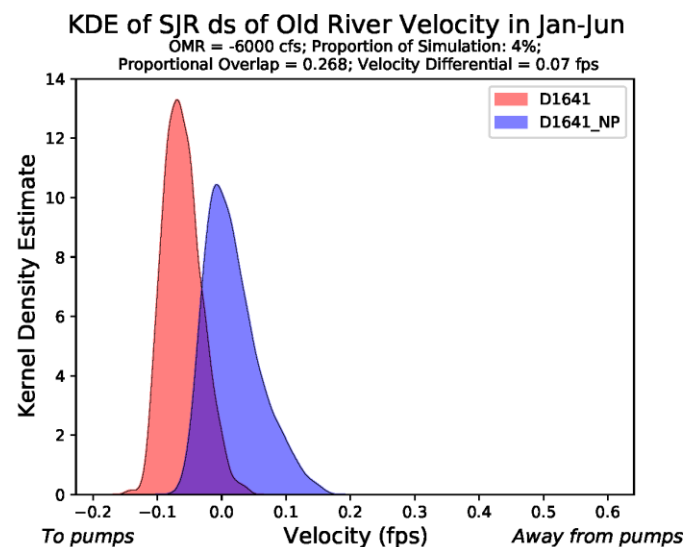
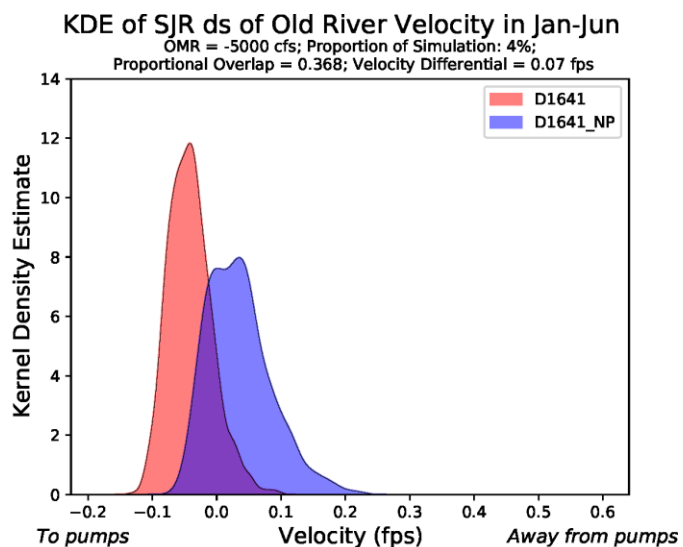


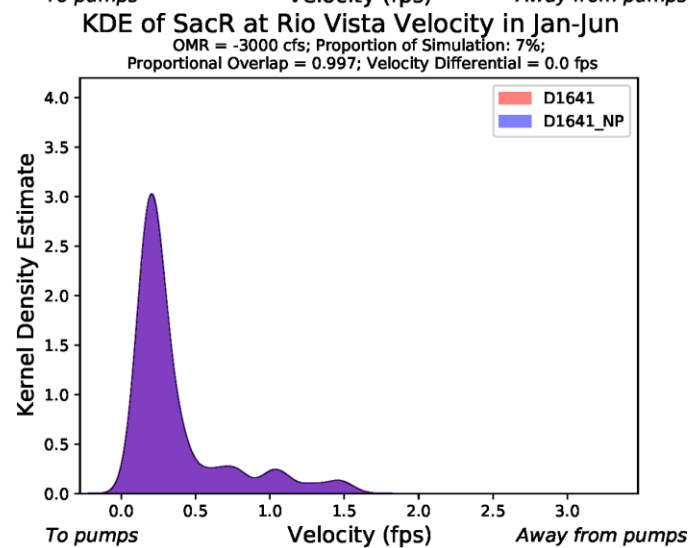
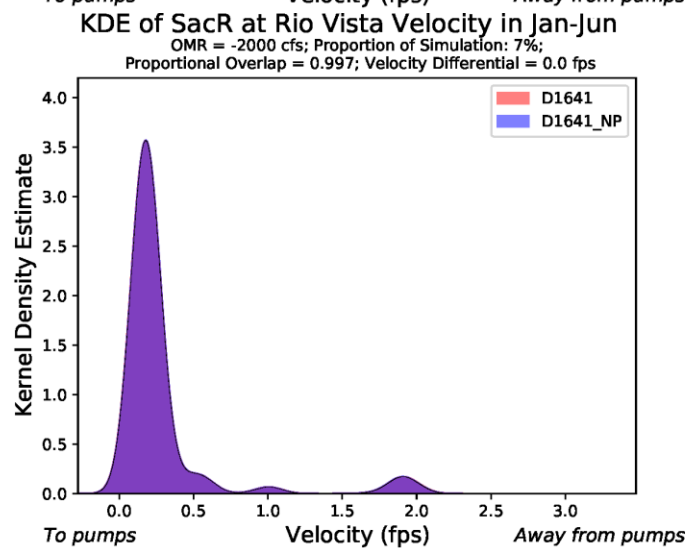
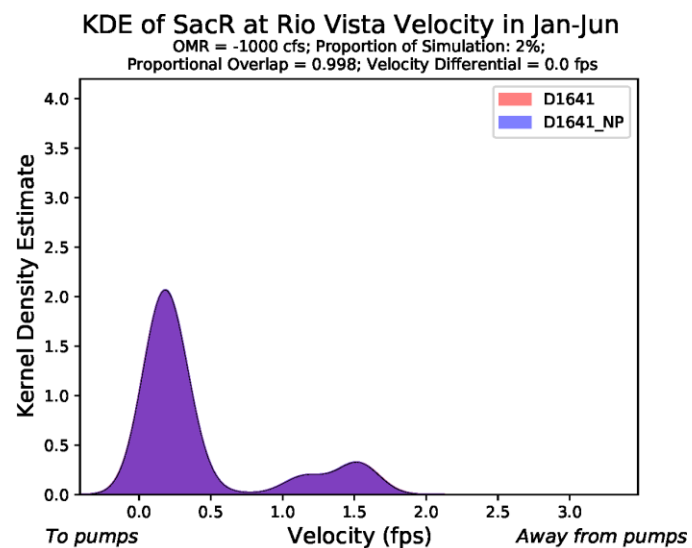
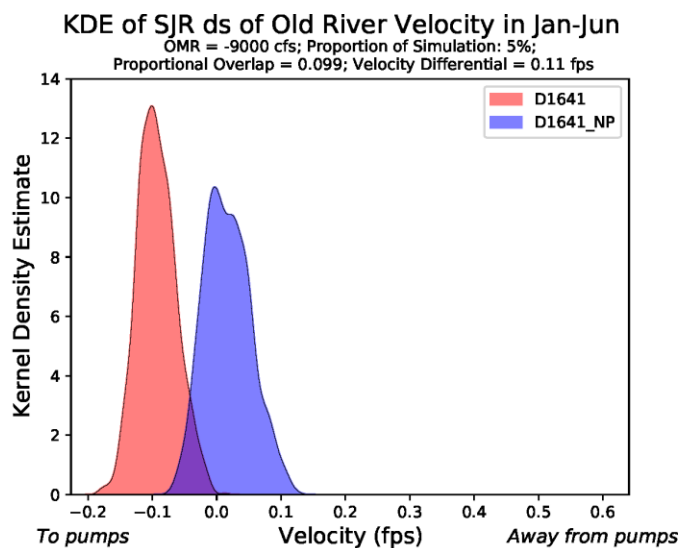






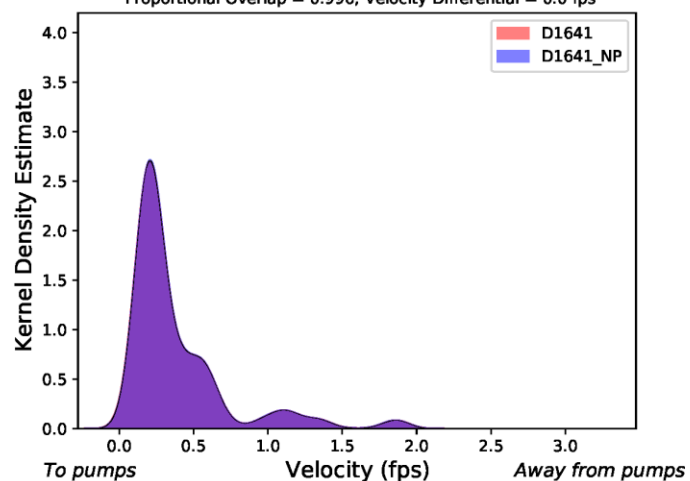






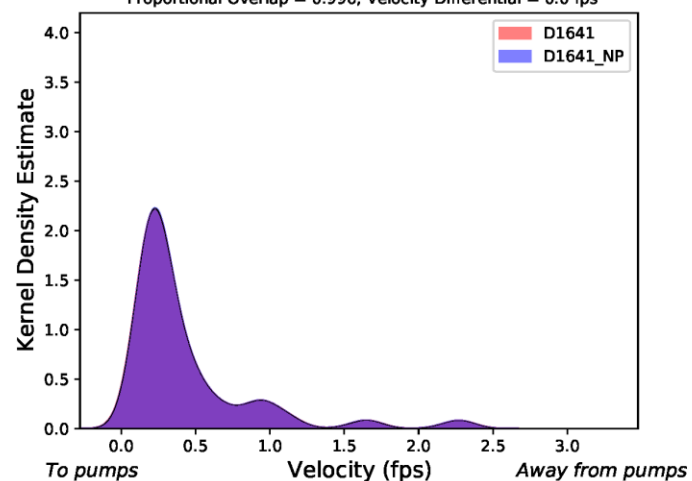
KDE of SacR at Rio Vista Velocity in Jan-Jun

OMR = -4000 cfs; Proportion of Simulation: 5%;  
Proportional Overlap = 0.996; Velocity Differential = 0.0 fps



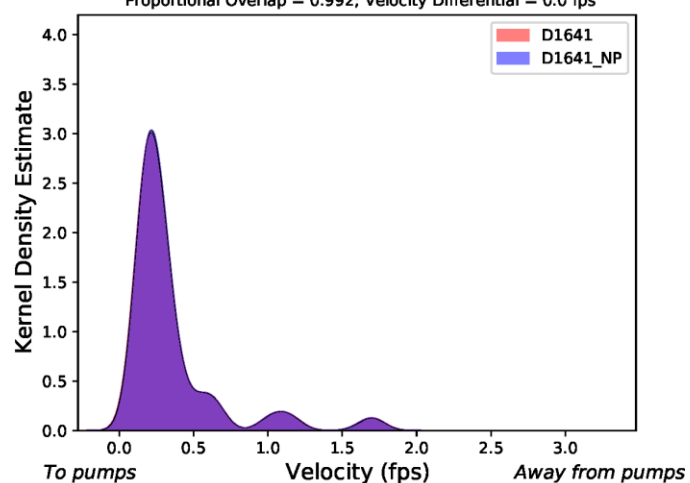
KDE of SacR at Rio Vista Velocity in Jan-Jun

OMR = -5000 cfs; Proportion of Simulation: 4%;  
Proportional Overlap = 0.996; Velocity Differential = 0.0 fps



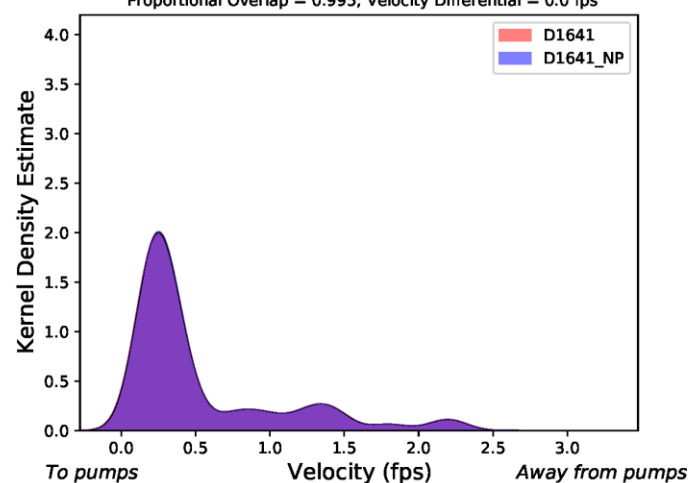
KDE of SacR at Rio Vista Velocity in Jan-Jun

OMR = -6000 cfs; Proportion of Simulation: 4%;  
Proportional Overlap = 0.992; Velocity Differential = 0.0 fps



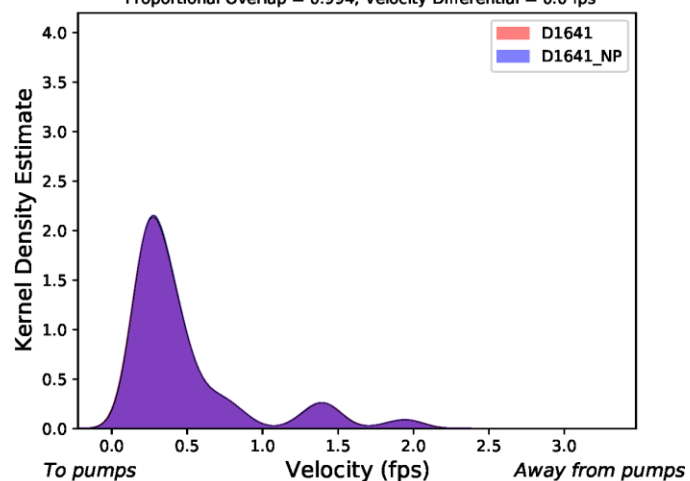
KDE of SacR at Rio Vista Velocity in Jan-Jun

OMR = -7000 cfs; Proportion of Simulation: 6%;  
Proportional Overlap = 0.995; Velocity Differential = 0.0 fps



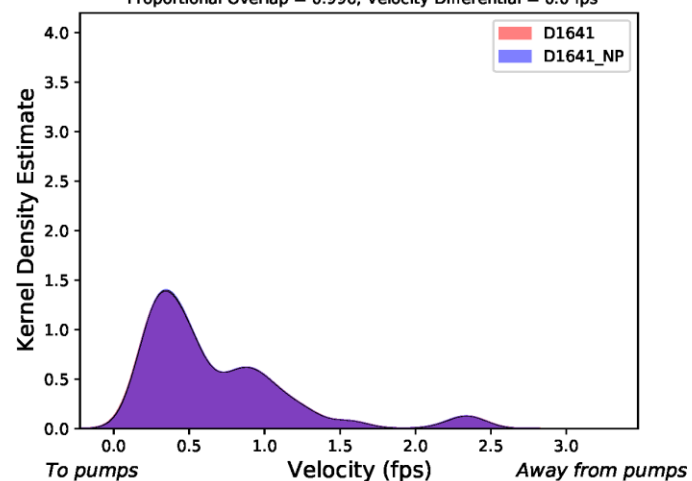
KDE of SacR at Rio Vista Velocity in Jan-Jun

OMR = -8000 cfs; Proportion of Simulation: 4%;  
Proportional Overlap = 0.994; Velocity Differential = 0.0 fps



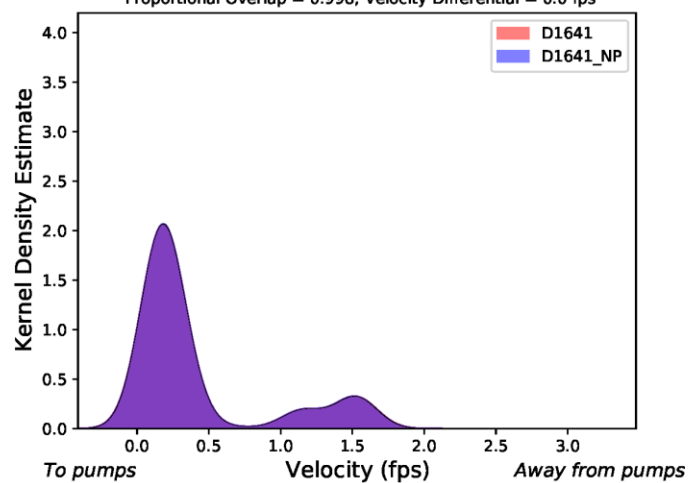
KDE of SacR at Rio Vista Velocity in Jan-Jun

OMR = -9000 cfs; Proportion of Simulation: 5%;  
Proportional Overlap = 0.996; Velocity Differential = 0.0 fps



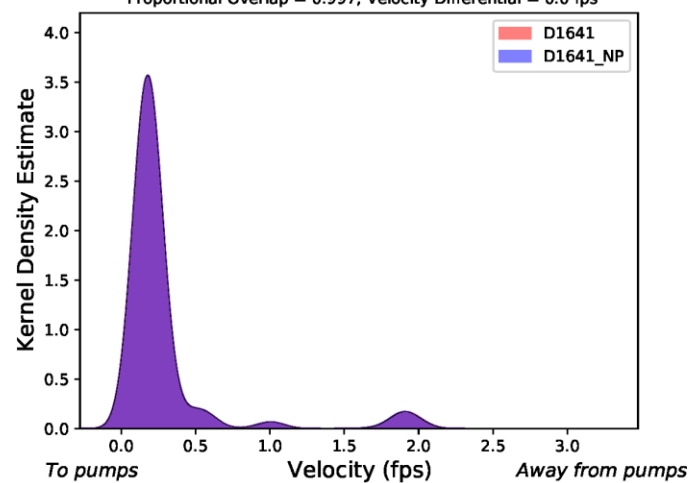
KDE of SacR at Emmatton Velocity in Jan-Jun

OMR = -1000 cfs; Proportion of Simulation: 2%;  
Proportional Overlap = 0.998; Velocity Differential = 0.0 fps



KDE of SacR at Emmatton Velocity in Jan-Jun

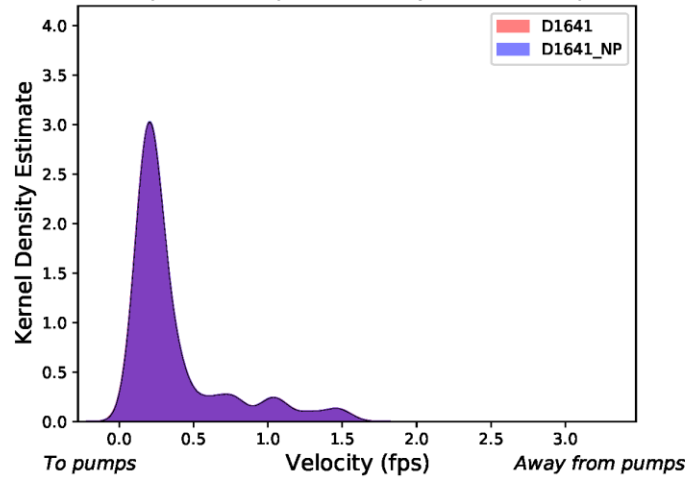
OMR = -2000 cfs; Proportion of Simulation: 7%;  
Proportional Overlap = 0.997; Velocity Differential = 0.0 fps





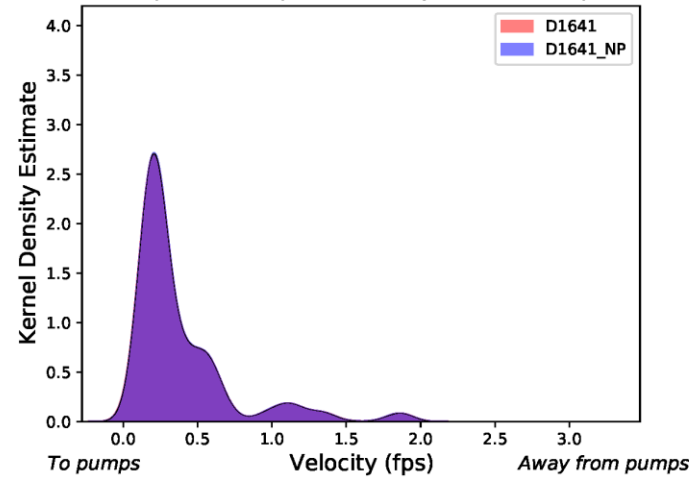
KDE of SacR at Emmaton Velocity in Jan-Jun

OMR = -3000 cfs; Proportion of Simulation: 7%;  
Proportional Overlap = 0.997; Velocity Differential = 0.0 fps



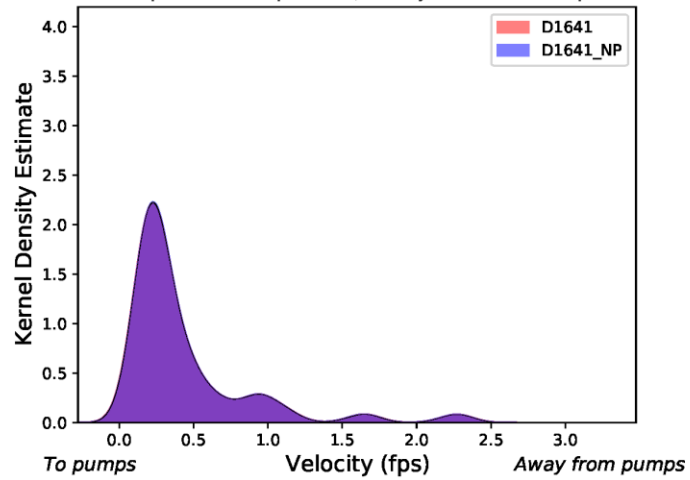
KDE of SacR at Emmaton Velocity in Jan-Jun

OMR = -4000 cfs; Proportion of Simulation: 5%;  
Proportional Overlap = 0.996; Velocity Differential = 0.0 fps



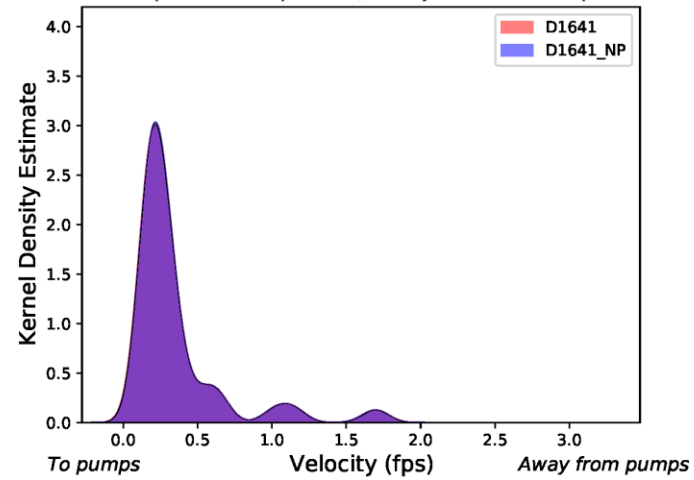
KDE of SacR at Emmaton Velocity in Jan-Jun

OMR = -5000 cfs; Proportion of Simulation: 4%;  
Proportional Overlap = 0.996; Velocity Differential = 0.0 fps



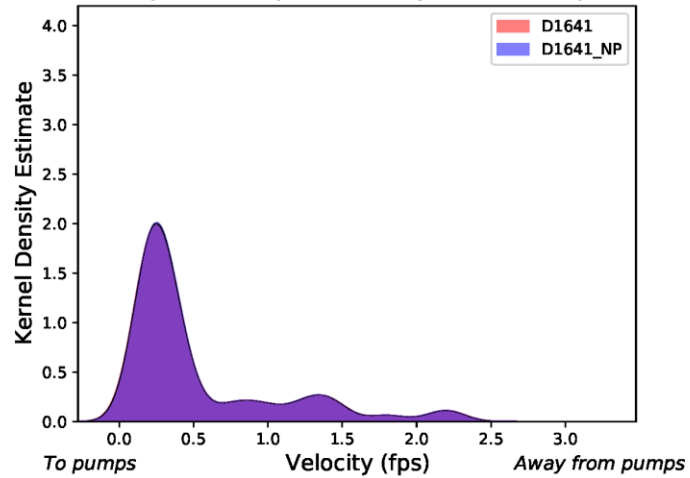
KDE of SacR at Emmaton Velocity in Jan-Jun

OMR = -6000 cfs; Proportion of Simulation: 4%;  
Proportional Overlap = 0.992; Velocity Differential = 0.0 fps



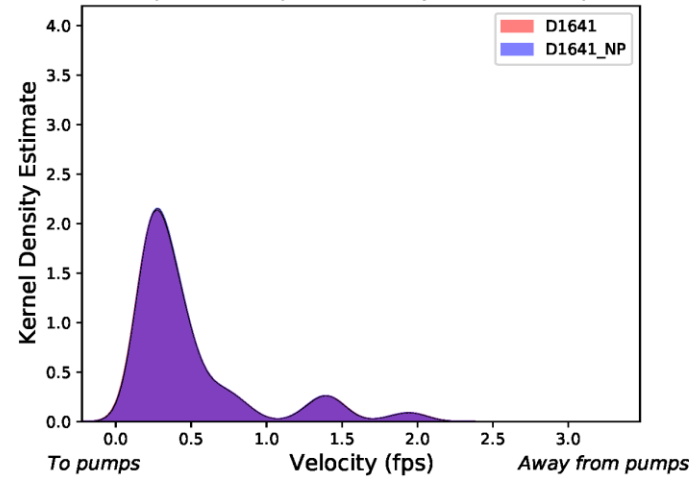
KDE of SacR at Emmaton Velocity in Jan-Jun

OMR = -7000 cfs; Proportion of Simulation: 6%;  
Proportional Overlap = 0.995; Velocity Differential = 0.0 fps



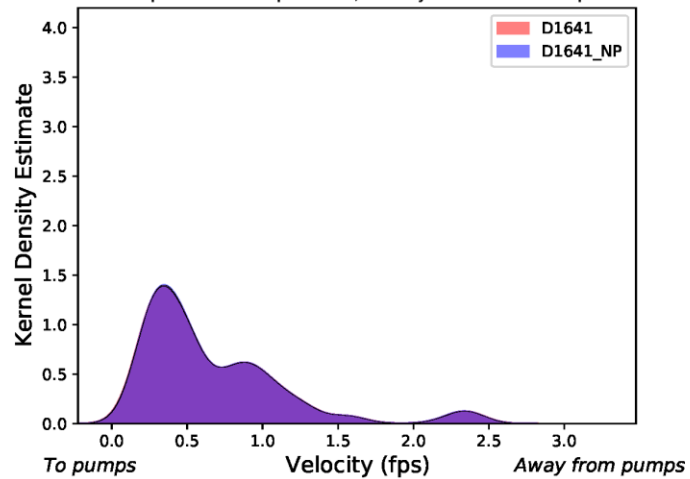
KDE of SacR at Emmaton Velocity in Jan-Jun

OMR = -8000 cfs; Proportion of Simulation: 4%;  
Proportional Overlap = 0.994; Velocity Differential = 0.0 fps



KDE of SacR at Emmaton Velocity in Jan-Jun

OMR = -9000 cfs; Proportion of Simulation: 5%;  
Proportional Overlap = 0.996; Velocity Differential = 0.0 fps



Although there are a wider range of OMR conditions in the D1641 results, the proportional overlap value for a given location and OMR condition does not vary significantly between NAA and D1641 results.

Table I.2-2. Locations for Velocity KDE Plots

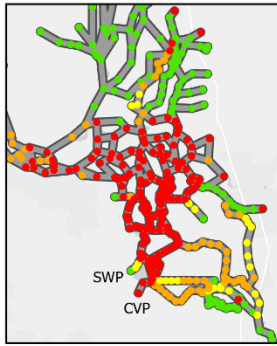
<b>Locations</b>
San Joaquin River downstream of Old River (Brandt Bridge)
Turner Cut
Columbia Cut
San Joaquin River at Prisoners Point
San Joaquin River at Jersey Point
Old River at Bacon Island
Old River at HWY 4
Middle River near Holt
Victoria Canal near Byron
San Joaquin River upstream of Old River
Old River at Head of Old River
Old River at Middle River
Grant Line Canal at Tracy Bridge
Old River near Tracy
Old River before Franks Tract
Fisherman's Cut
False River before Franks Tract
Threemile Slough
Mokelumne River
San Joaquin River downstream of Big Break
Sacramento River at Rio Vista
Sacramento River at Emmaton

#### **I.2.4.3 Zone of Influence Maps**

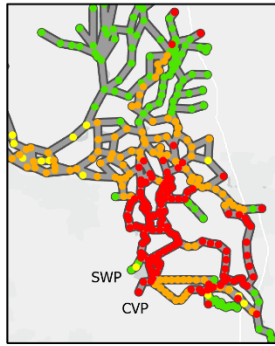
Maps depicting the proportional overlap, an indicator of zone of influence, were developed for each month (December through June) and OMR condition. These maps are below.

# Zone Of Influence - OMR NAA vs NAA No Pumps

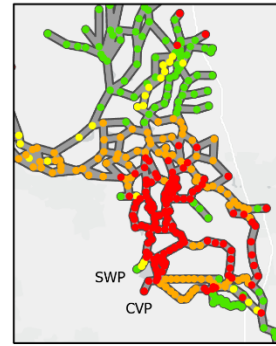
December



-1000 cfs (0.1%)



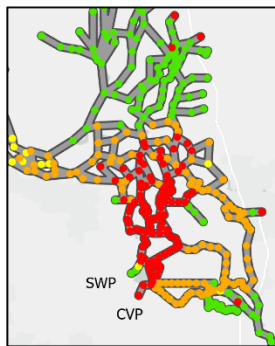
-2000 cfs (0.1%)



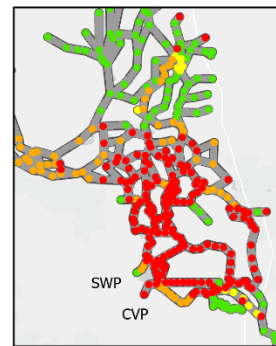
-3000 cfs (0.5%)



-4000 cfs (0.4%)



-5000 cfs (3.4%)



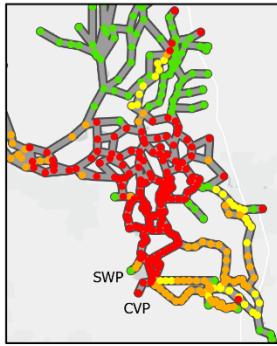
-6000 cfs (0.6%)

Proportional Overlap

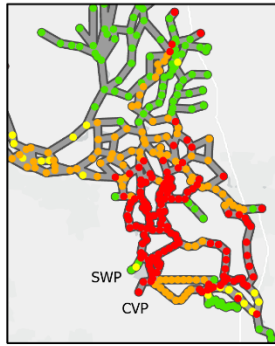


# Zone Of Influence - OMR NAA vs NAA No Pumps

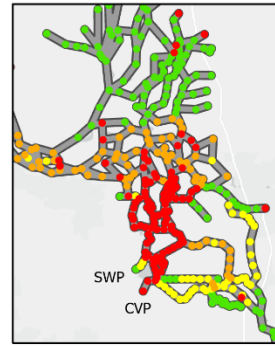
January



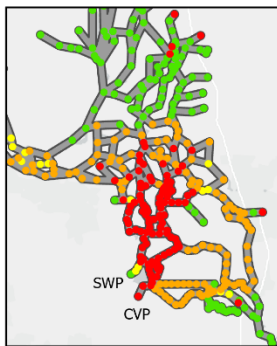
-1000 cfs (0.1%)



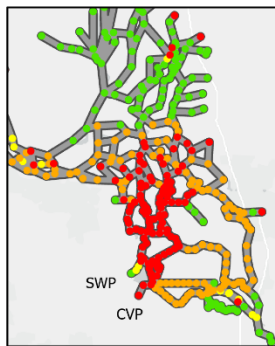
-2000 cfs (0.1%)



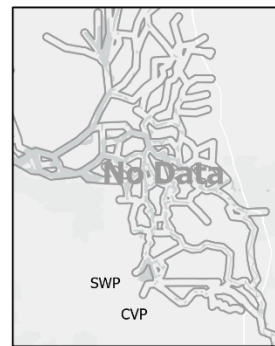
-3000 cfs (0.3%)



-4000 cfs (3.6%)

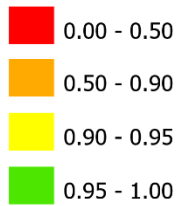


-5000 cfs (3.7%)



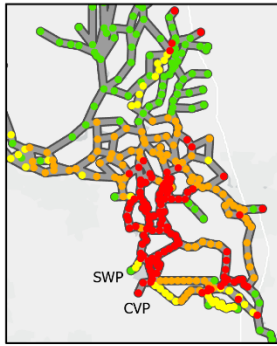
-6000 cfs (0.0%)

Proportional Overlap

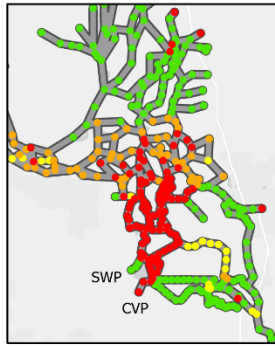


# Zone Of Influence - OMR NAA vs NAA No Pumps

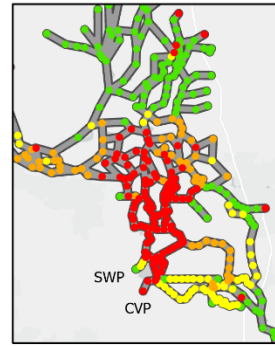
February



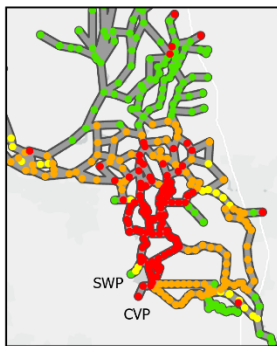
-1000 cfs (0.1%)



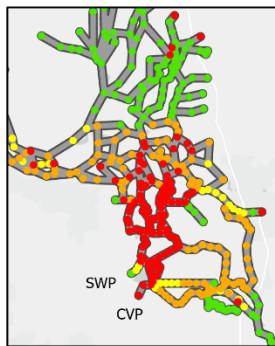
-2000 cfs (0.3%)



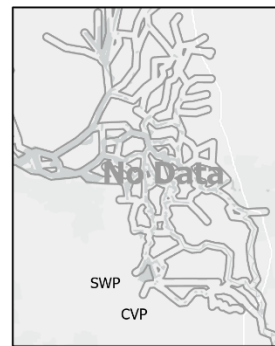
-3000 cfs (0.4%)



-4000 cfs (3.6%)



-5000 cfs (2.6%)



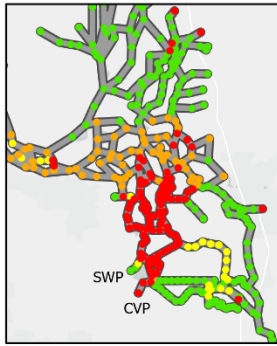
-6000 cfs (0.0%)

Proportional Overlap

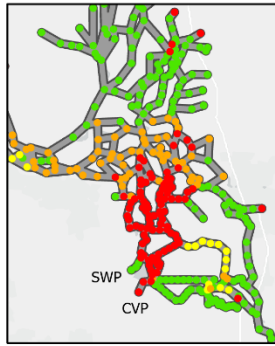


# Zone Of Influence - OMR NAA vs NAA No Pumps

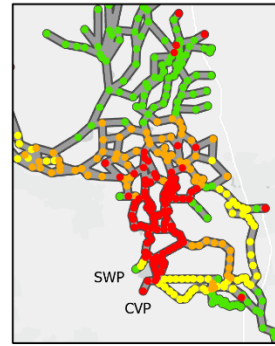
March



-1000 cfs (0.2%)



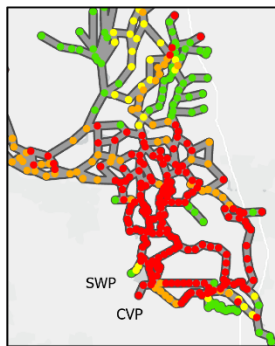
-2000 cfs (0.4%)



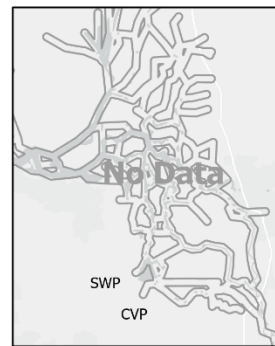
-3000 cfs (6.1%)



-4000 cfs (0.8%)



-5000 cfs (0.1%)



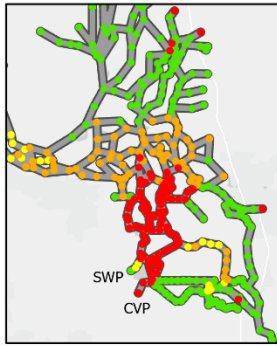
-6000 cfs (0.0%)

Proportional Overlap

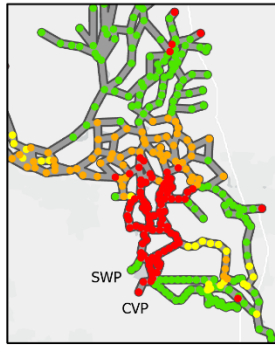


# Zone Of Influence - OMR NAA vs NAA No Pumps

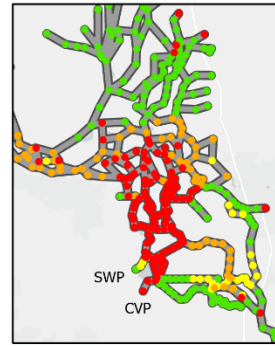
April



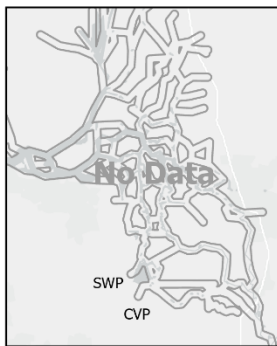
-1000 cfs (3.0%)



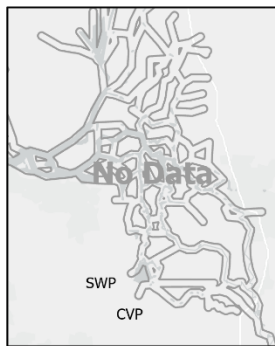
-2000 cfs (3.0%)



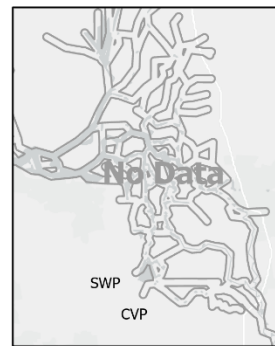
-3000 cfs (0.9%)



-4000 cfs (0.0%)



-5000 cfs (0.0%)



-6000 cfs (0.0%)

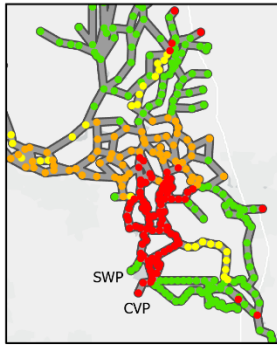
Proportional Overlap



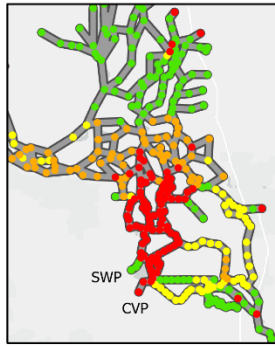


# Zone Of Influence - OMR NAA vs NAA No Pumps

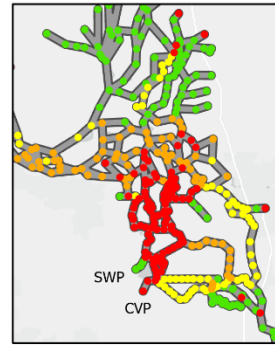
May



-1000 cfs (0.8%)



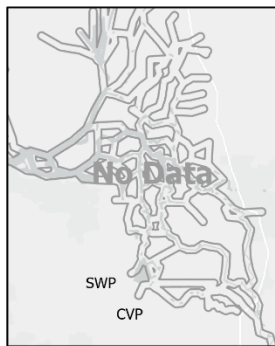
-2000 cfs (4.9%)



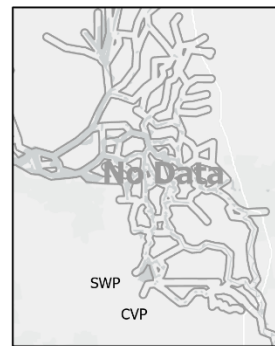
-3000 cfs (1.6%)



-4000 cfs (0.3%)



-5000 cfs (0.0%)



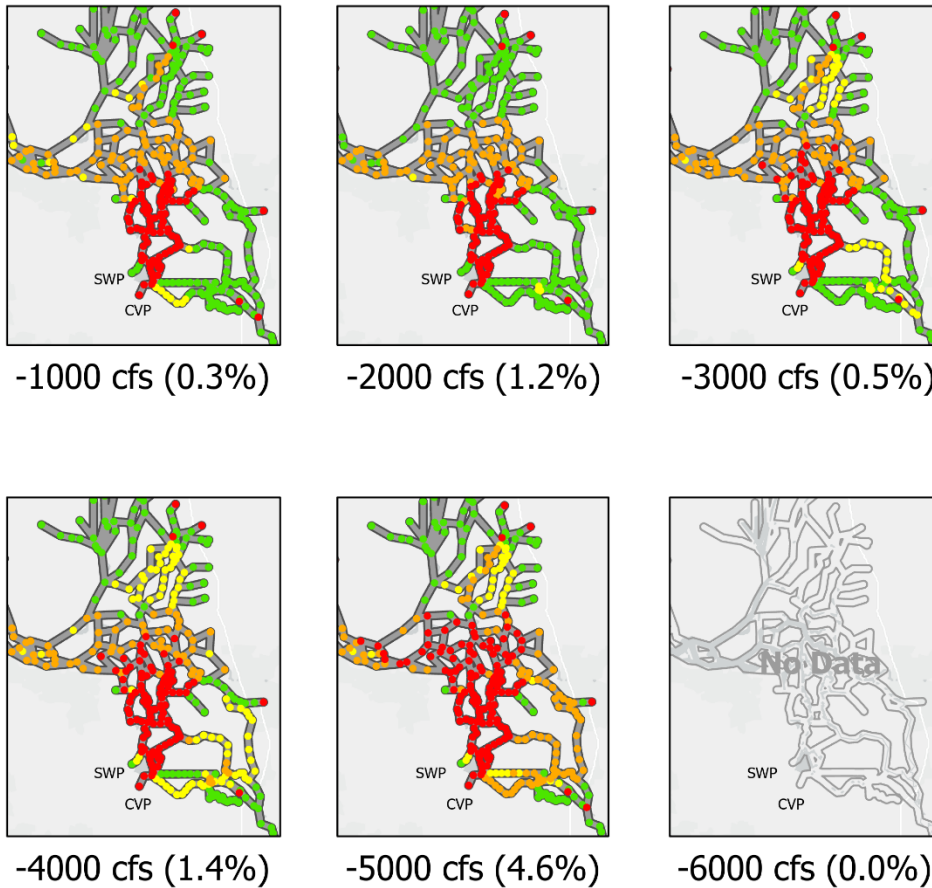
-6000 cfs (0.0%)

Proportional Overlap



## Zone Of Influence - OMR NAA vs NAA No Pumps

June



### I.2.4.4 Contour Maps

We removed missing data from the zone of influence analysis by Jacobs, then interpolated proportional overlap values between DSM2 nodes for each month-OMR flow scenario

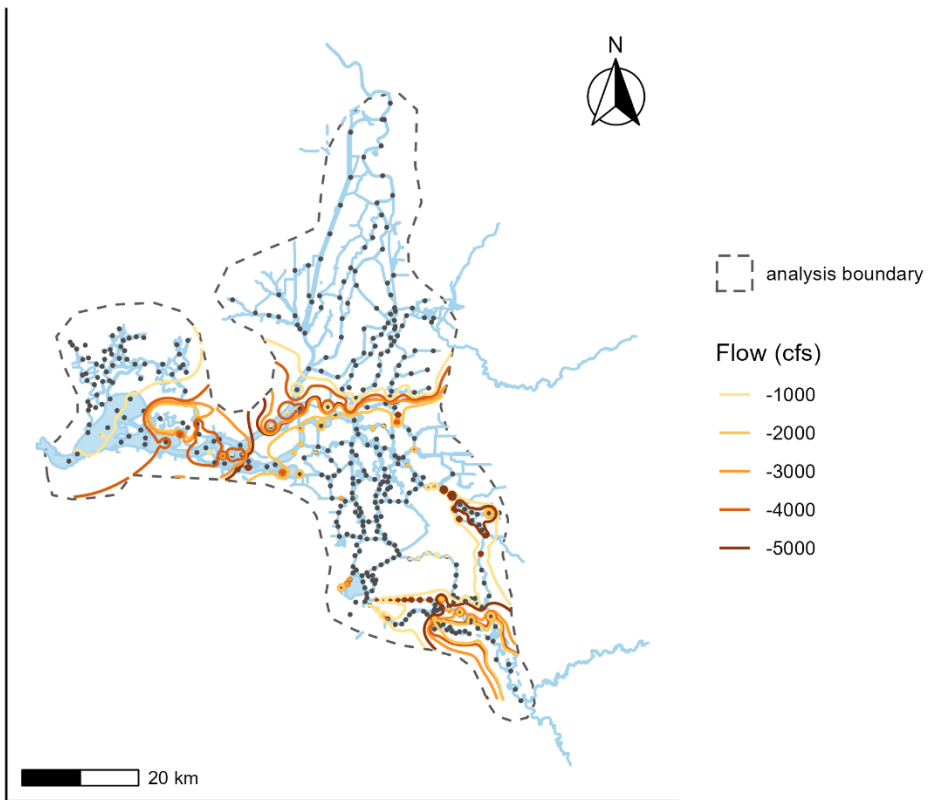
(December–June, -1000 to -5000 cfs). Each value reflects the overlap in velocity distribution between a pumping (CVP exports) and no pumping scenario, with higher values indicating greater similarity in distribution and lower values indicating lesser similarity in distribution. We used the interpolations to create contour lines at the 0.75 overlap level, and layered contour lines from each OMR flow onto one monthly map. Some months did not have modeled data for every OMR flow.

In order to reduce the noise in contour lines, we removed DSM2 nodes that were sufficiently different from neighboring nodes to create isolated contours at several OMR flows (Removed nodes: 146, 147, 148, 206, 242, 246). It was unclear whether the values associated with these DSM2 nodes were artifacts of the model output and/or assumptions, or due to unique hydrodynamics characteristics at that node location.

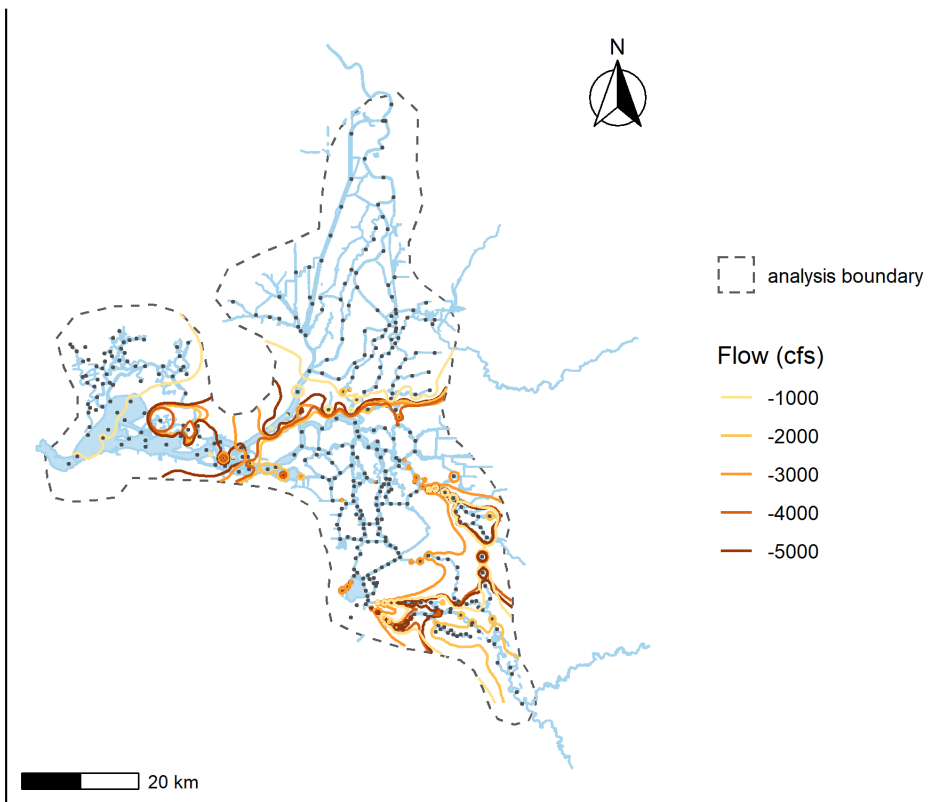
Caveats associated with contour maps:

- Contours have been mapped across land to visualize the relative spatial extent of the zone of influence at each OMR flow. We assume that changes in the Delta's channels and channel configuration (e.g., new channels constructed) would impact regional hydrodynamics, and therefore the zone of influence would need to be recalculated. In other words, this map does not suggest that a new channel added within the current zone of influence would have the same impacts of pumping as existing waterways within that contour. The addition of new waterways would require an update to the current DSM2 models and recalculation of the zone of influence.
- The proportional overlap values do not reflect the magnitude of velocity differences, only that there were differences. Thus, two locations with the same value of proportional overlap might actually experience very different magnitudes of velocity difference. These figures also do not directly reflect biological implications, as we are not analyzing velocity differences and do not know the values of velocity change that would alter fish movements.
- We examined 75% and 95% contour maps. We chose to visualize 75% proportional overlap rather than 95% proportional overlap because 95% contours extended to most of the Delta at all OMR flows, with only small pockets excluded from the zone of influence.

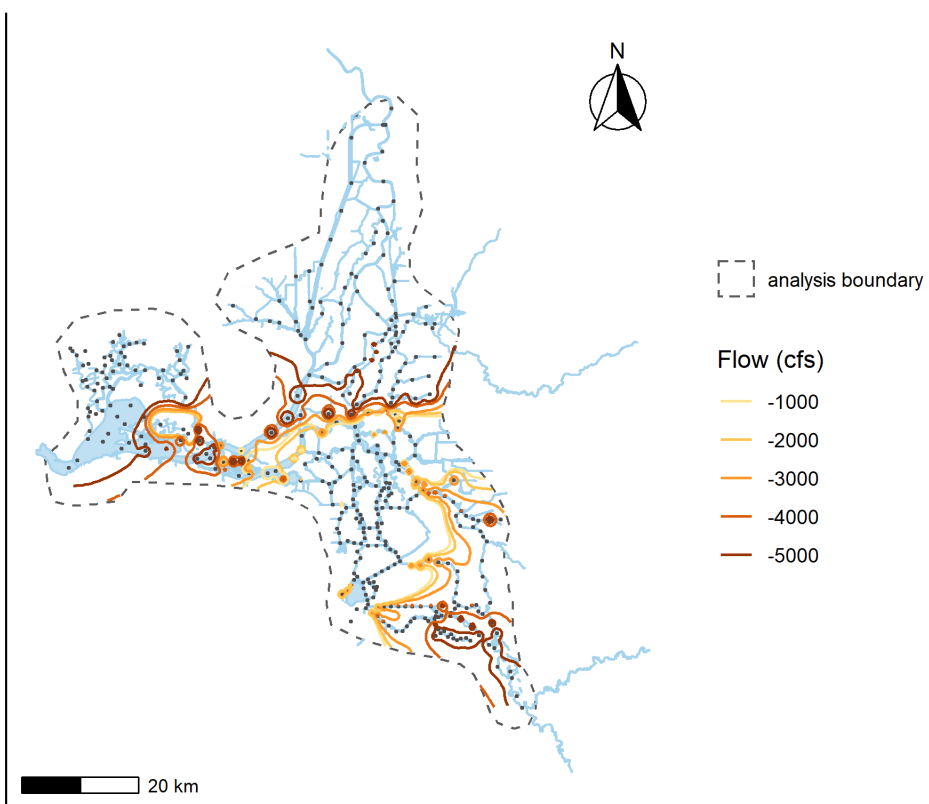
dec contour 0.75



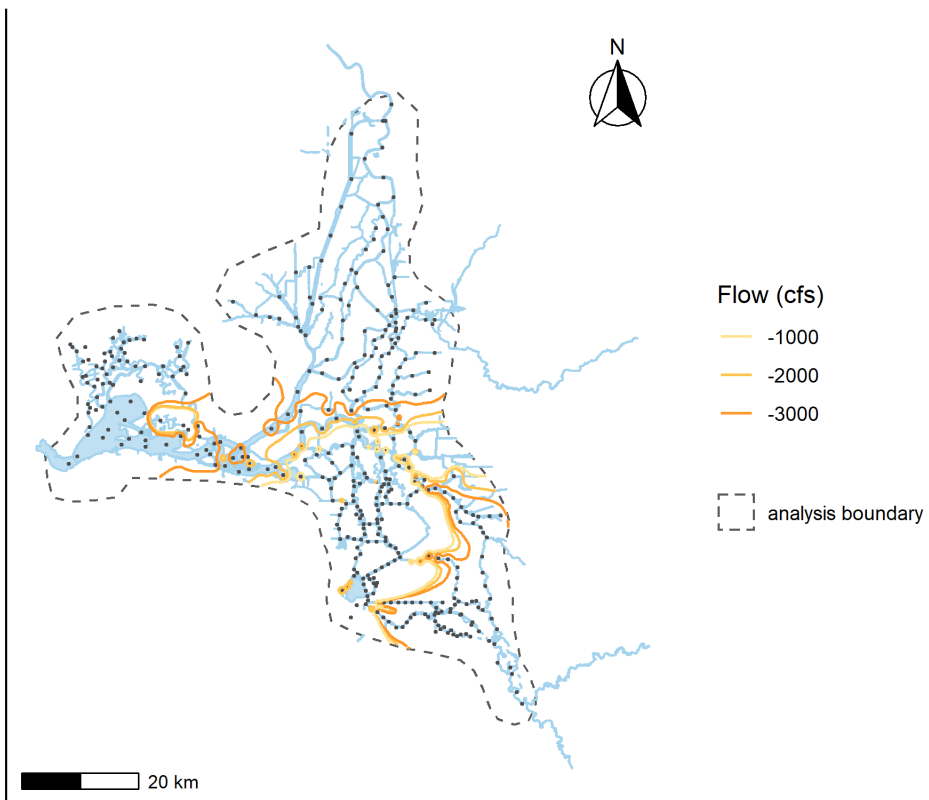
jan contour 0.75



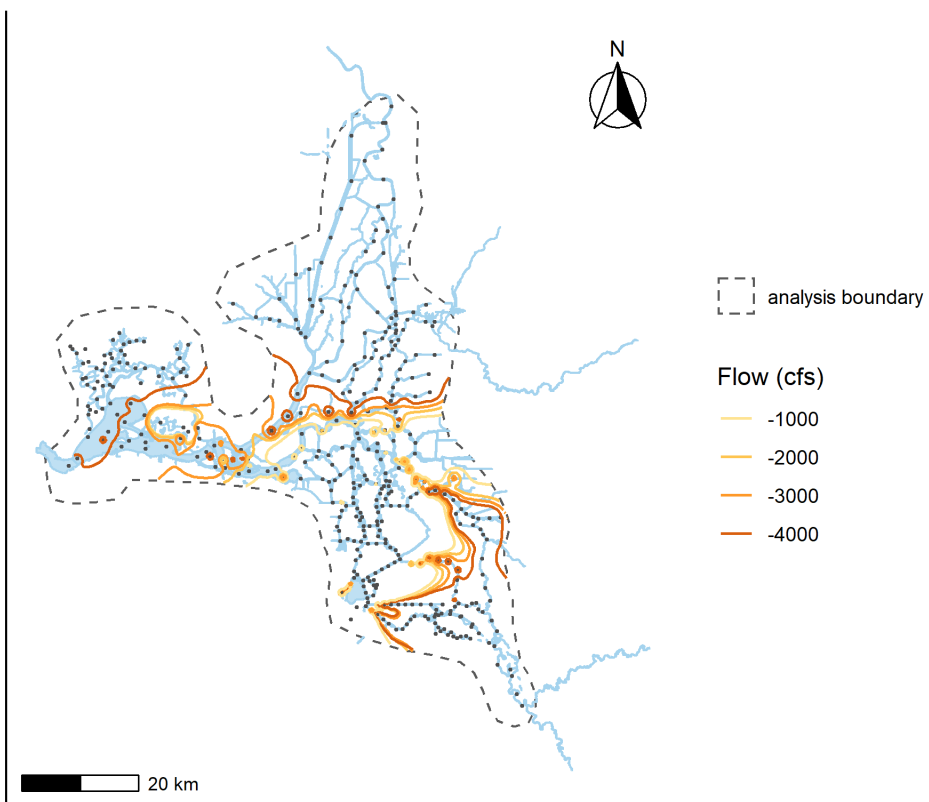
mar contour 0.75



apr contour 0.75



may contour 0.75





jun contour 0.75

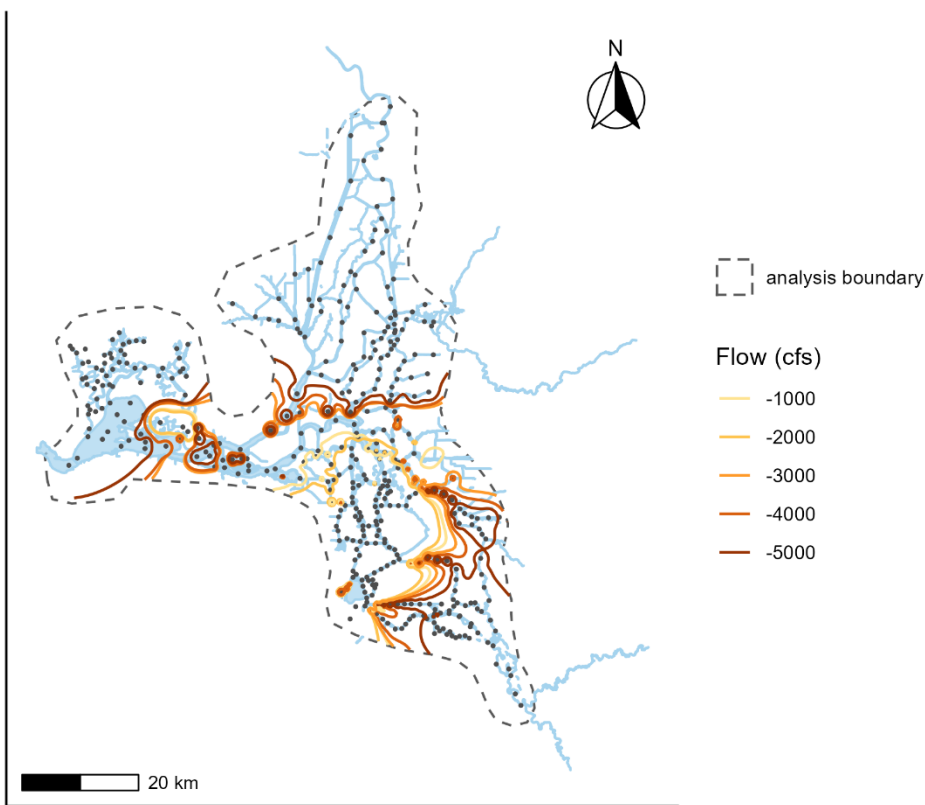


Figure I.2-4. Monthly (December-June) Maps of Generalized 75% Contours at Varying OMR Flows (-5000 To -1000) between the No Action Alternative With and Without Pumping (The contours identify where there is 75% overlap in velocity distribution with and without CVP exports. Dashed black line shows the analysis boundary and points represent the locations of DSM2 nodes)

## I.2.5 Discussion

The first four locations above depict flows along the San Joaquin River in the Delta, moving from upstream to downstream. Old River is the first location in the Delta where flows could be affected by pumping. Therefore, change to velocity in the San Joaquin River at Brandt Bridge demonstrates the influence of the Old River on the San Joaquin River. Then, Turner and Columbia Cuts are the next locations at which the San Joaquin River could be affected by pumping. Subsequently, San Joaquin River at Prisoner's Point demonstrates effects of pumping downstream from Turner and Columbia Cuts. With incremental increases to pumping, proportional overlap at these four locations decreases. Changes to proportional overlap are more subtle along the San Joaquin River (Brandt Bridge and Prisoners Point) as compared to Turner and Columbia Cuts. Since Turner and Columbia Cuts are less influenced by riverine flow, they are more susceptible to changes in pumping. Effects of pumping are smallest at the upstream-most location (San Joaquin River at Brandt Bridge). At this point, the pumps have only diverted

San Joaquin River flow through Old River. As we move downstream on the San Joaquin River, the pumps divert additional San Joaquin River flow through Turner and Columbia Cuts. Therefore, the effect of pumping is greater at Prisoners Point as compared to Brandt Bridge.

Due to proximity, channel connectivity, and/or flow/velocity patterns, proportional overlap values change significantly with pumping at Jones and Banks: Old River at Bacon Island, Old River at Highway 4, Old River before Franks Tract, Middle River near Holt, San Joaquin River downstream of Old River, Victoria Canal near Byron, and Threemile Slough. At each of these locations, the range of velocities (presented on the x-axis) is much narrower (ranging from -0.25 to 0.25 fps) compared to the rest of the Delta. As such, despite a small change in the velocity at these locations, the proportional overlap value is more sensitive to pumping, relative to other locations in the Delta.

Conversely, there are several locations in the south and central Delta where proportional overlap values are less sensitive to pumping at Jones and Banks: Old River at Head of Old River, Old River near Middle River, Old River near Tracy, and Grant Line Canal at Tracy Bridge. At these locations, the velocity distribution is much greater (ranging from 0 fps to 4 fps). The change in proportional overlap of Gaussian KDEs is reduced as there is a greater range of preexisting velocities at these locations. The change in velocity due to pumping remains within this preexisting range.

Finally, there are locations where, due to distance from pumping facilities and channel connectivity, Gaussian KDEs remain similar: Sacramento River at Rio Vista, Sacramento River at Emmaton, and Mokelumne River.

The Gaussian KDE plots and proportional overlap maps demonstrate the effects of pumping under a range of OMR flow conditions. Several factors affect the proportional overlap and velocity differential values, including proximity to the pumps, orientation of the flow (relative to the pumps), influence of riverine flow, and preexisting flow/velocity patterns in the channel. Each location and output parameter (proportional overlap and velocity differential) must be examined to understand the influence of pumping at a given location.

#### **1.2.5.1 Next Steps**

This effort provides insight into the potential capacity for entrainment at various levels of pumping. In review of the results, additional analysis could consider: (1) south Delta pumping rates, (2) Delta inflow conditions, (3) more discrete timesteps, (4) review of changes when the Delta is in excess conditions, and (5) a review of multi-modal plots to ascertain influencing conditions/operations. This analysis focuses to changes in velocity at differing levels of OMR flow, which typically reflects south Delta pumping. However, it should be noted that Delta inflow (especially from the San Joaquin River) influences OMR flow as well. A large range of pumping conditions may exist within a given OMR flow condition. Isolating the pumping rates and Delta inflow from the OMR bin may better demonstrate the direct effect of south Delta pumping. This analysis only observes the change in velocity at a daily average time step. More discrete, sub-tidal timesteps could demonstrate the range of effect at a given pumping level. There are several multi-model plots in Attachments 2-1 and 2-2. Detailed review of these plots may elucidate additional variables for consideration.

### **I.3. Attachment 3: OMR Flow Management CalSim Analysis**

Old and Middle River (OMR) flow management addresses entrainment of salmonids and smelt into the central Delta, south Delta, and/or into salvage facilities. The following analysis compares the effects of OMR flow management in Initial Alternative 1 (IA1), Initial Alternative 2 (IA2), and Initial Alternative 3 (IA3) to the No Action Alternative (NAA).

In addition to these two sensitivity studies, three 82-year simulations were conducted using CalSim II, DSM2, and DPM to assess water supply effects and near- and far-field entrainment effects under the operations described for Initial Alternative 1, Initial Alternative 2, and Initial Alternative 3, described above. Initial Alternative 4 was evaluated qualitatively using all of the available analyses.

## **I.3.1 Assumptions**

### **I.3.1.1 No Action Alternative**

The NAA is described as Revised Alternative 1 in Appendix F1 of the 2019 Reinitiation of Consultation on Long-Term Operation of the CVP and SWP, with additional SWP operations for implementing the 2020 ITP. The NAA uses hydrology projected at 2035 (2035 Central Tendency). Information on the updated modeling can be found on the CalSim Model Maintenance Management repository at [github.com/usbr/cm3](https://github.com/usbr/cm3). In addition, full Sacramento River Settlement Contractors (SRSC) contract amounts were assumed, and there are no daily components to the Wilkin's Slough flow requirement. For the OMR, the NAA includes the following:

- Onset of OMR Management
- First Flush
- Turbidity Bridge Avoidance
- Storm Flex
- Species-Specific Cumulative Salvage or Loss Thresholds

Each of the following alternatives were built on top of the NAA, and all other assumptions besides OMR management actions are the same across all the alternatives.

### **I.3.1.2 Initial Alternative 1**

IA1 includes a fixed schedule for the onset and offramp of OMR with high-magnitude OMR constraint criteria:

- The First Flush and Turbidity Bridge Avoidance actions were implemented in the same way as the NAA.
- A fixed start and end date for the OMR Management season from December 1 – June 30 which represents the historical presence of fish that can be entrained.
- A baseline OMR constraint no more negative than -3,500 cfs that represents a hydraulic footprint westward of the Head of Old River.

- Positive OMR upon fish salvage, subject to public health and safety. For modeling purposes, it is assumed that 7 days each month will be subject to this action.

### **I.3.1.3 Initial Alternative 2**

IA2 includes a fixed schedule for the onset and offramp of OMR with an intermediate-magnitude OMR constraint criterion:

- The First Flush and Turbidity Bridge Avoidance actions were implemented in the same way as the NAA.
- Fixed start and end date for the OMR Management season from December 1 – June 30, which represents the historical presence of fish that can be entrained.
- OMR no more negative than -5,000 cfs, which represents a hydraulic footprint south of the San Joaquin River.
- No response upon salvage and mitigation would rely on non-flow actions.

### **I.3.1.4 Initial Alternative 3**

IA3 includes a variable onset of OMR management based on real-time species risk assessment and an initial lower-magnitude OMR constraint criterion that may be made more restrictive in real-time:

- The First Flush and Turbidity Bridge Avoidance actions were implemented in the same way as the NAA.
- Flexible start and end December 1 – June 30. The flexible start date is based on real-time presence of fish and/or suitable water temperatures. In CalSim, the onset of OMR management is either triggered by the First Flush action or in January, whichever happens first.
- OMR no more negative than -6,250 cfs.
- Additional constraints on OMR upon fish salvage or in anticipation of salvage. In CalSim, this is triggered in wet, above normal (AN), below normal (BN), and dry water year types in April and May. When triggered, OMR flows are constrained to be no more negative than -3,500 cfs over the entire month.

Each alternative has different regulatory requirements for negative OMR flows, and therefore affects how much water can be delivered to the south Delta.

## **I.3.2 Results**

### **I.3.2.1 OMR Flow**

In CalSim, the OMR management season potentially starts as early as December and ends in June. For the NAA and IA3, the onset of OMR Management is flexible, starting after the First Flush action is triggered or in January. IA1 and IA2 have a fixed start date of December 1.

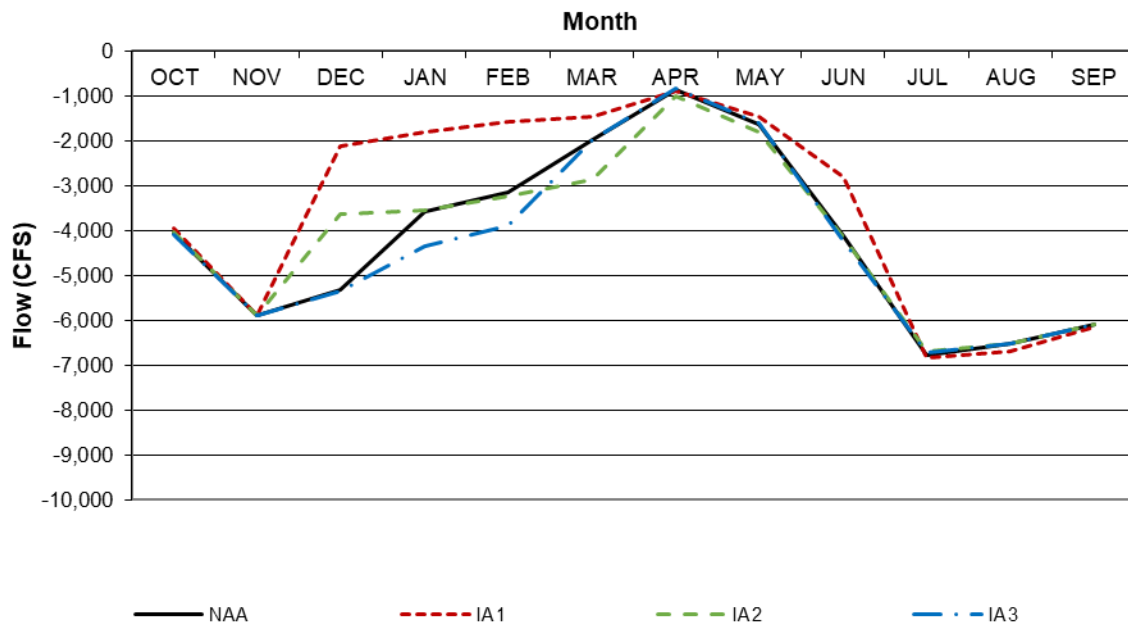


Figure I.3-1: Long-Term Average Monthly Pattern of OMR Flow

Figure I.3-1 shows for all alternatives, that there is no limitation on negative OMR flows from July through November. In December, the fixed start date in IA1 and IA2 flow patterns show the effect of OMR action starting in December all the time; while in the NAA and IA3, OMR flow management is not triggered in approximately 58% of Decembers. In IA1, it was assumed that actions triggered by fish salvage occur for 7 days in each month from December to June. For those 7 days, OMR is constrained to positive flows, subject to health and safety pumping. When compared to the NAA, this requirement combined with the background -3,500 cfs constraint keeps OMR flows in IA1 more positive throughout the OMR management season. Despite IA2 and the NAA having the same background -5,000 cfs constraint during the OMR management season, IA2 is allowed to be more negative in March through May than the NAA because IA2 does not have a flow action triggered by fish salvage while the NAA does. IA3 has a less export-restrictive seasonal OMR limit of -6,250 cfs, which accounts for more negative flows in January and February than the NAA.

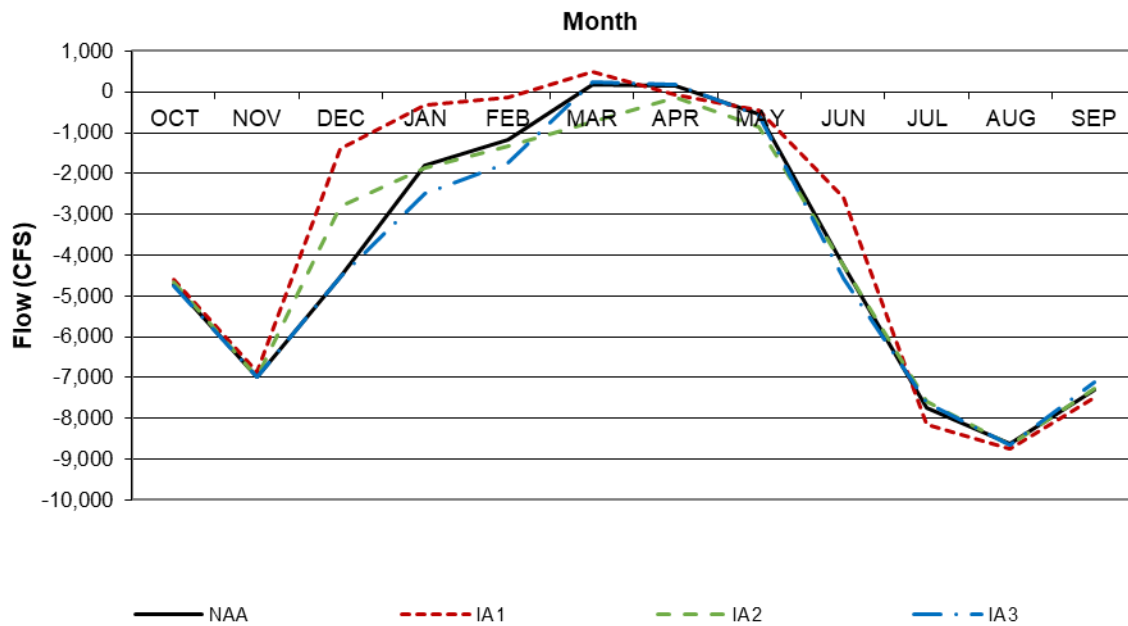


Figure I.3-2: Average Monthly Pattern of OMR Flow for Wet Years

Figure I.3-2 shows that for the most part, the same trends occur in wet years as were in the long-term average, but with more positive flows during December through May and more negative flows during June through September. Significantly higher inflows in wet years during December through May account for more positive flows during those months. However, during June through September, higher south of Delta (SOD) allocations require higher exports to meet those allocations, which results in more negative OMR flows.

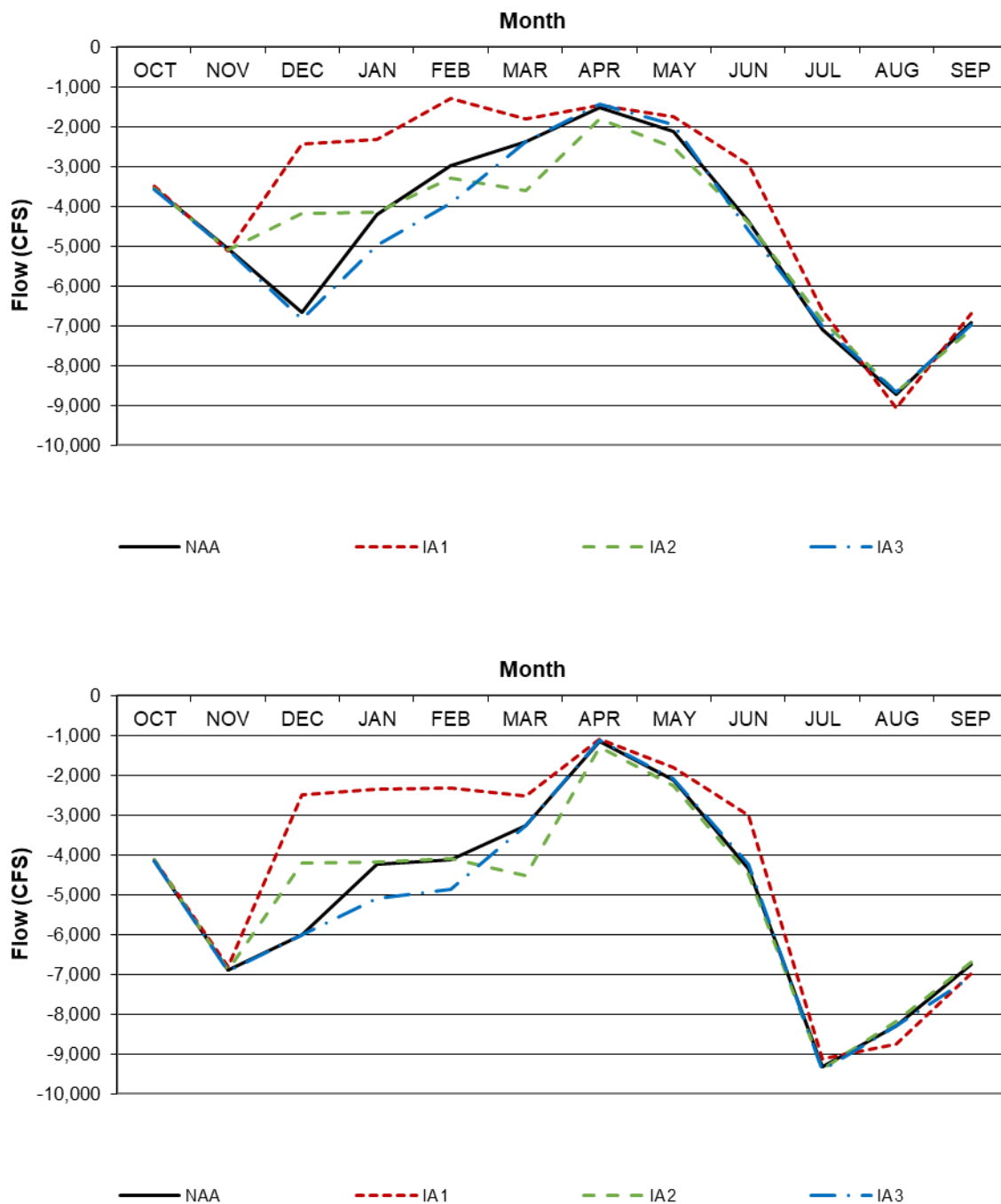


Figure I.3-3: Average Monthly Pattern of OMR Flow for AN (Above) and BN (Below) Years



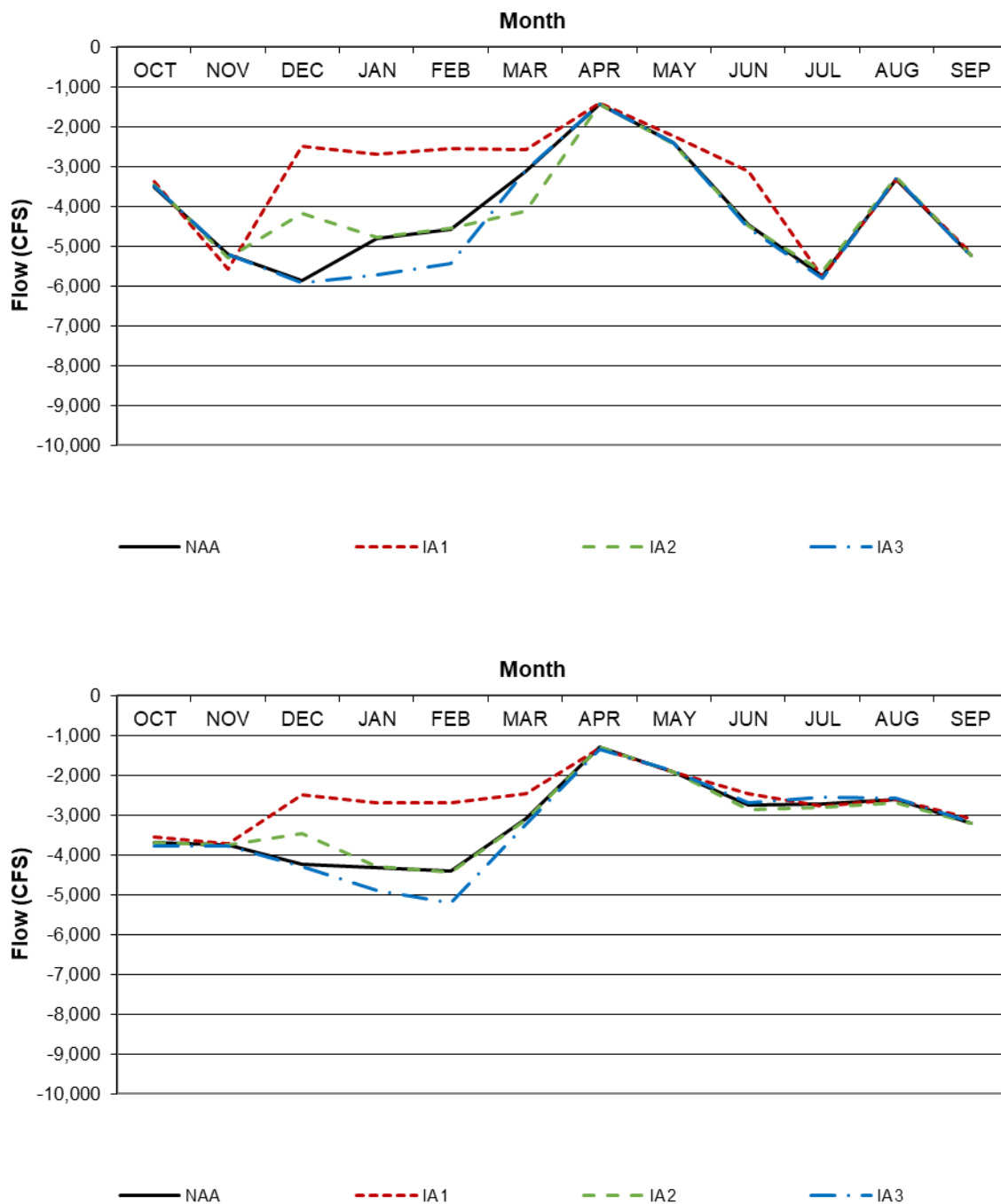


Figure I.3-4: Average Monthly Patterns of OMR Flows for Dry (Above) and Critically Dry (Below) Years

Again, the trends in Figure I.3-3 for AN and BN years resemble that of the long-term average except for more negative flows in June through September. In dry and critically dry years, exports are greatly reduced because SOD allocations are greatly reduced. Figure I.3-4 shows

much more positive flows during June through September than the long-term average because there is much less pumping to cause those negative flows on the OMR.

### I.3.2.2 Exports

In general, the more constrained the limits on negative OMR flows during the OMR management season, the less pumping is allowed, which results in lower exports. For the most part, IA1 had the most export-restrictive seasonal OMR limit, which resulted in the least exports, while IA3 had the least export-restrictive seasonal OMR limit, which allowed for the most exports.

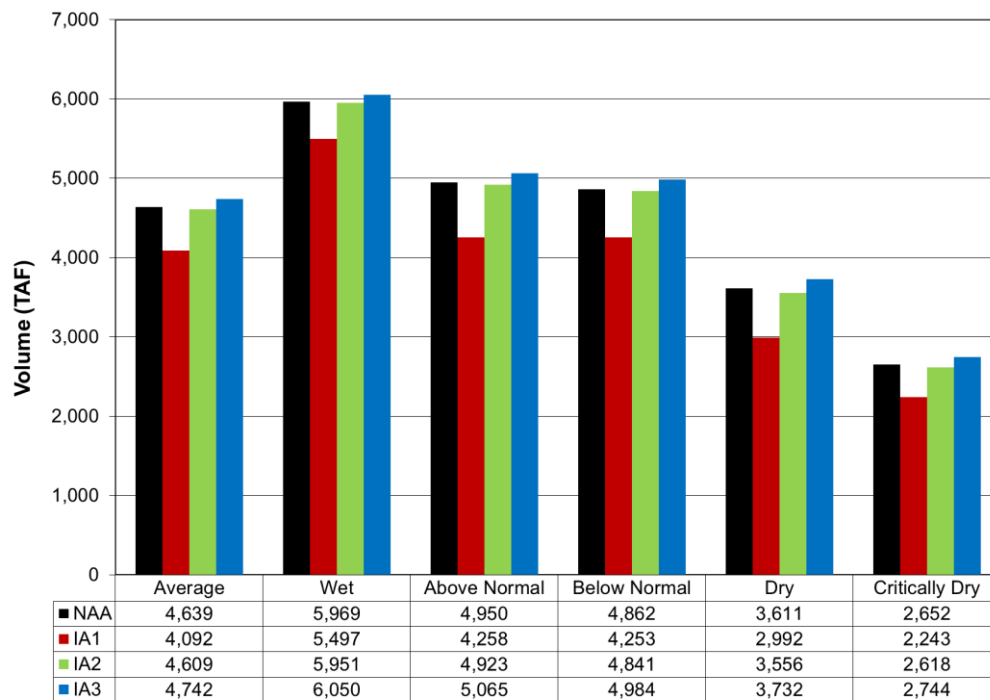


Figure I.3-5: Annual Total Exports by Water Year Type (Oct – Sep)

Figure I.3-5 shows that the constraints on negative OMR flow in the NAA and IA2 result in similar exports across all water year types, while IA1 is more export-restrictive and IA3 is less export-restrictive across all water year types. However, pumping at Jones and Banks responded differently to the constraints of IA2 relative to the NAA.

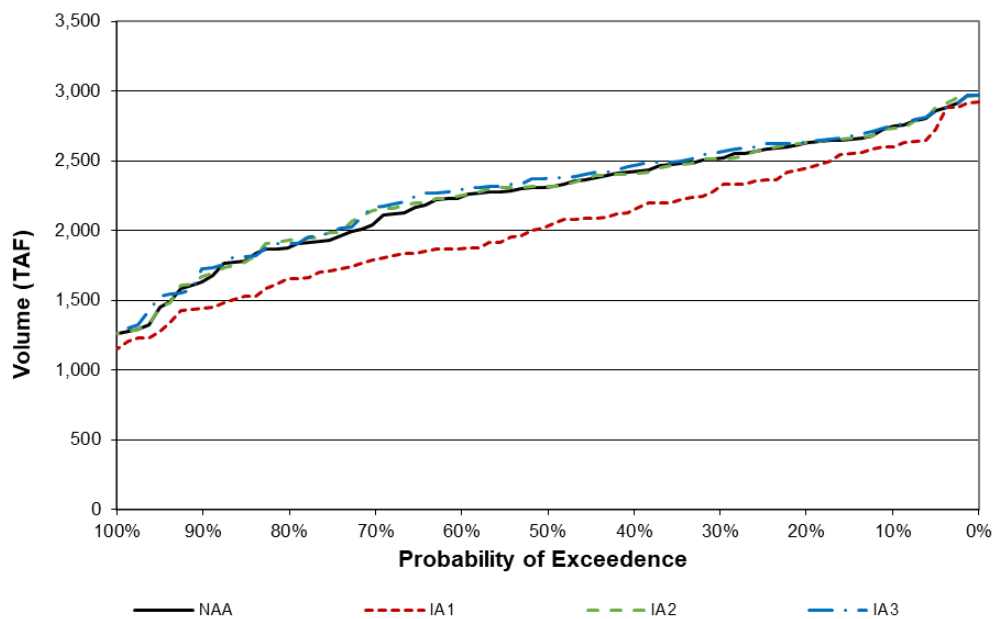


Figure I.3-6: Annual Exceedance of Jones Pumping for Exports (Oct – Sep)

Figure I.3-6 shows that annual Jones pumping for IA2 and NAA are very similar, despite the NAA having the additional actions triggered by fish salvage in March through May.

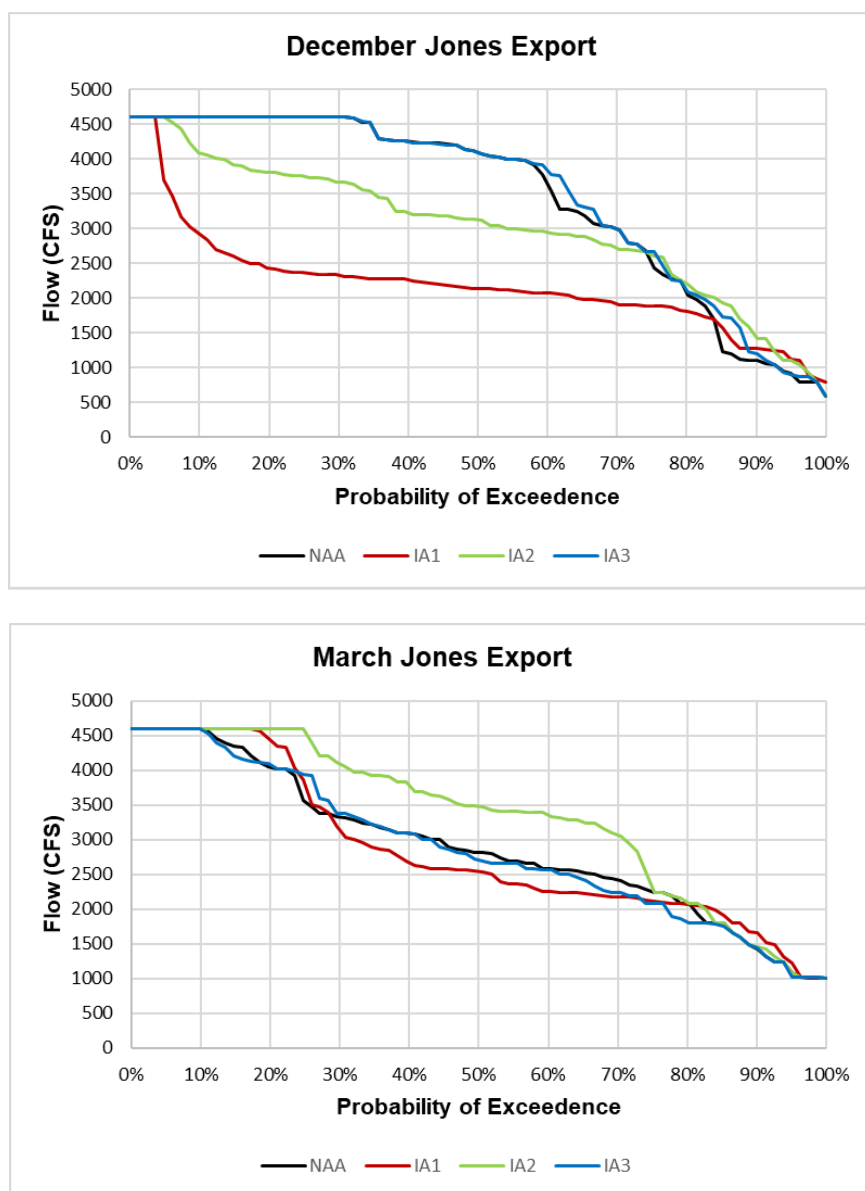


Figure I.3-7: Exceedance for December (Above) and March (Below) Jones Pumping

When looking at the individual monthly exceedances, IA2 and the NAA have similar exports for most months. However, Figure I.3-7 shows a distinct difference in December and March. In December, the IA2 has significantly lower Jones export than the NAA because IA2 has a fixed start date in December for the onset of OMR management while the NAA has a flexible start date. In March, on the other hand, IA2 has higher Jones export than the NAA because IA2 does not have flow actions due to fish salvage triggers. For Jones pumping, these two differences counteract each other, resulting in similar annual exports from Jones.

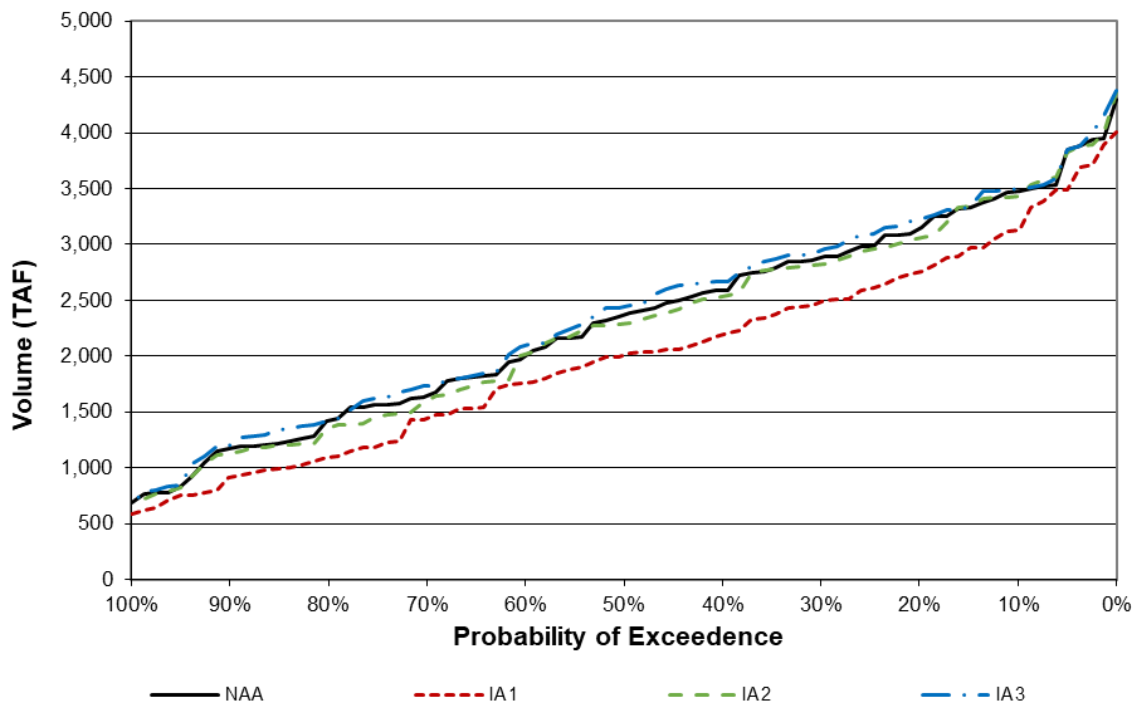


Figure I.3-8: Annual Exceedance of Banks Pumping for Exports (Oct – Sep)

Figure I.3-8 shows slightly lower Banks pumping in IA2 than in the NAA. For Banks, the effects of the fixed start date for the onset of OMR management are slightly larger than the cumulative effect of the additional action triggered by fish salvage in March through May.

### I.3.2.3 Deliveries

For both the CVP and SWP, constraints on negative OMR flow directly affect how much can be delivered to SOD while not having much of an effect on NOD deliveries.

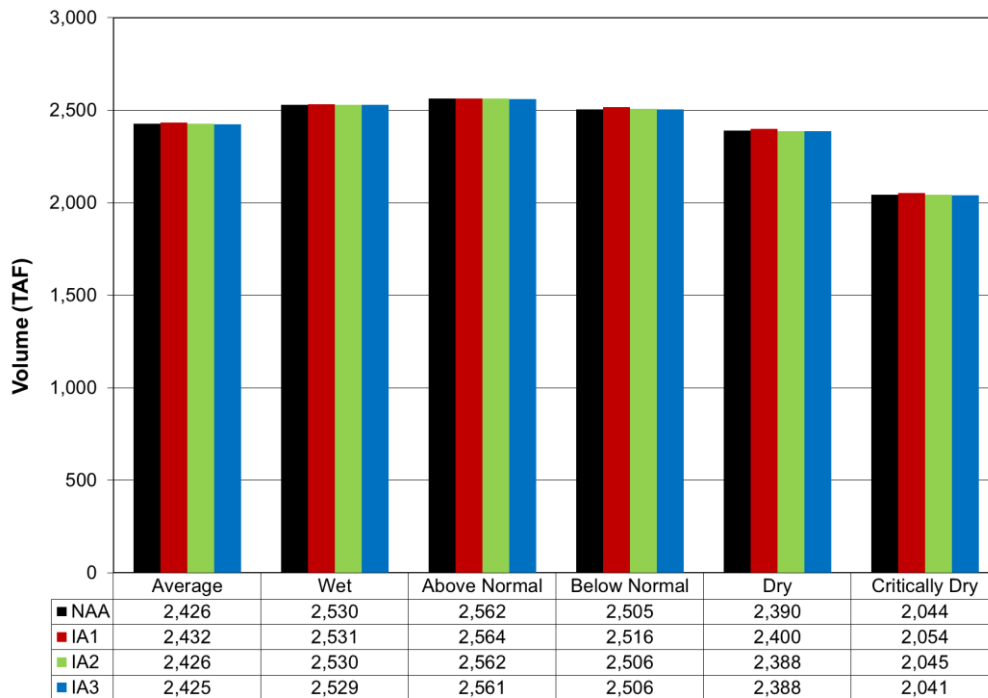


Figure I.3-9: Annual CVP NOD Deliveries by Water Year Type (Mar – Feb)

In Figure I.3-9, the total NOD deliveries are similar across all the alternatives because varying constraints on negative OMR flow does not directly affect NOD deliveries. The differences in deliveries by water year type reflect the differences in demand and allocation by water year type.

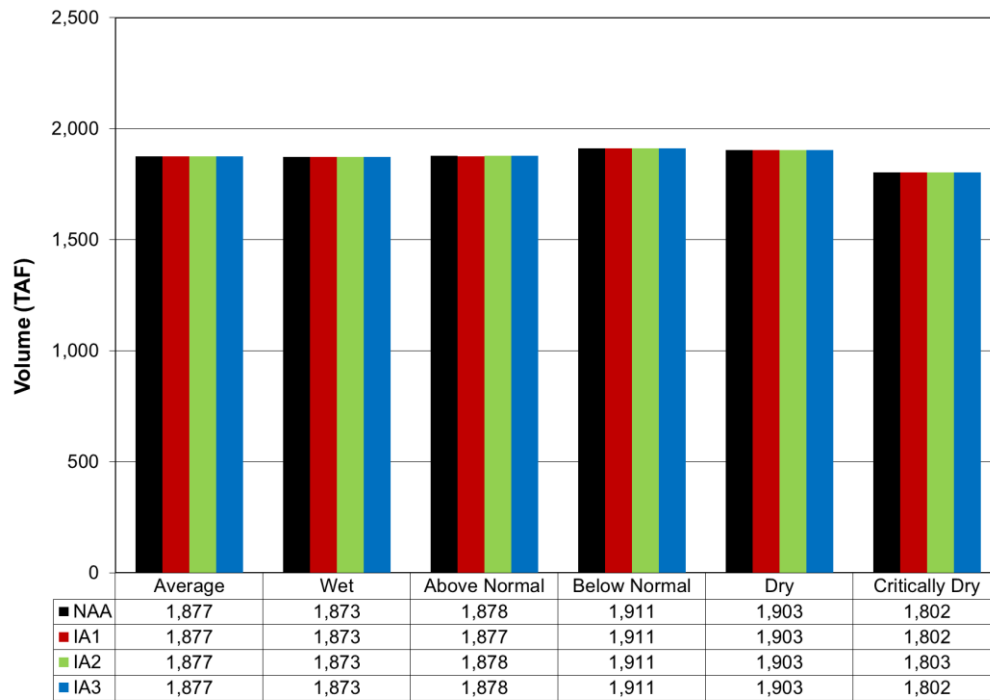


Figure I.3-10: Annual CVP NOD Settlement Contract Deliveries by Water Year Type (Mar - Feb)

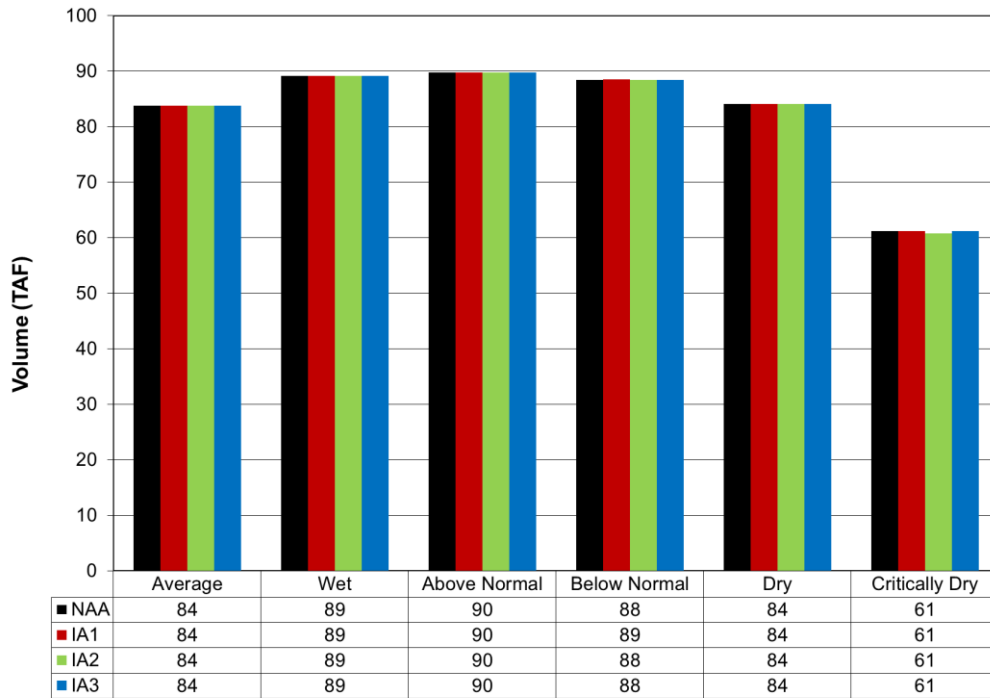


Figure I.3-11: Annual CVP NOD Refuge Deliveries by Water Year Type (Mar - Feb)

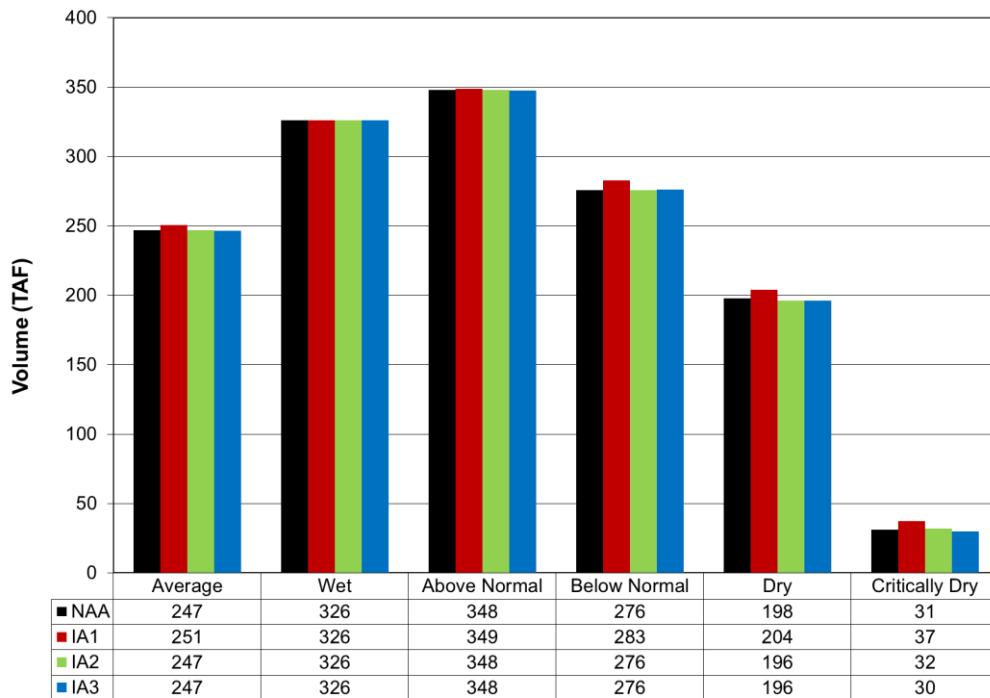


Figure I.3-12: Annual CVP NOD Project Ag Deliveries by Water Year Type (Mar - Feb)



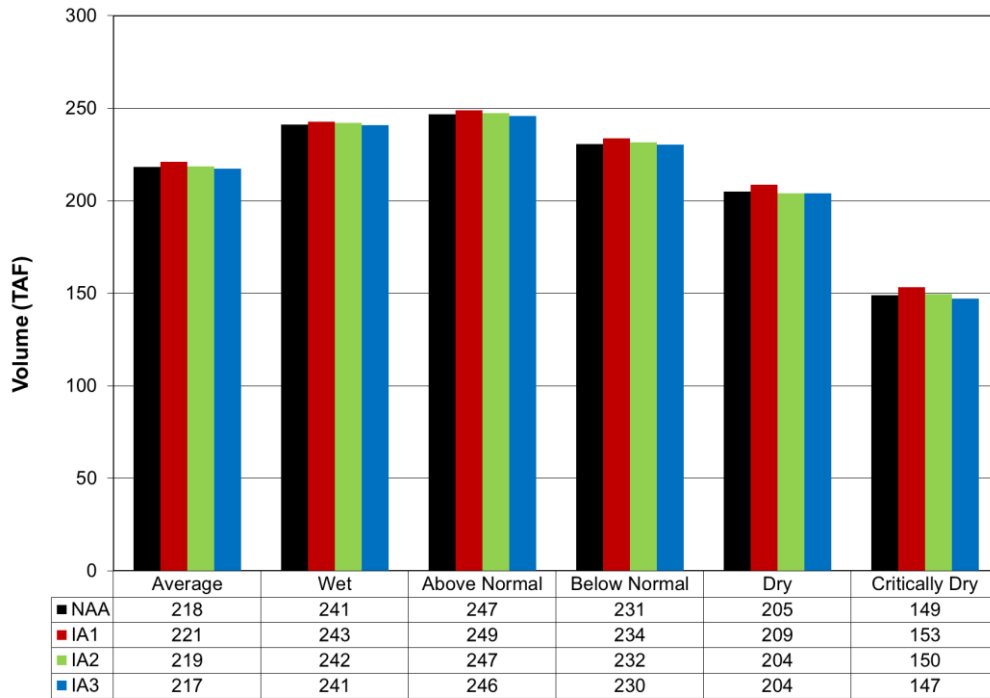


Figure I.3-13: Annual CVP NOD Project M&I Deliveries by Water Year Type (Mar - Feb)

Figures I.3-10 through I.3-13 split out the NOD deliveries by contract type. All contract types show little difference between the alternatives.

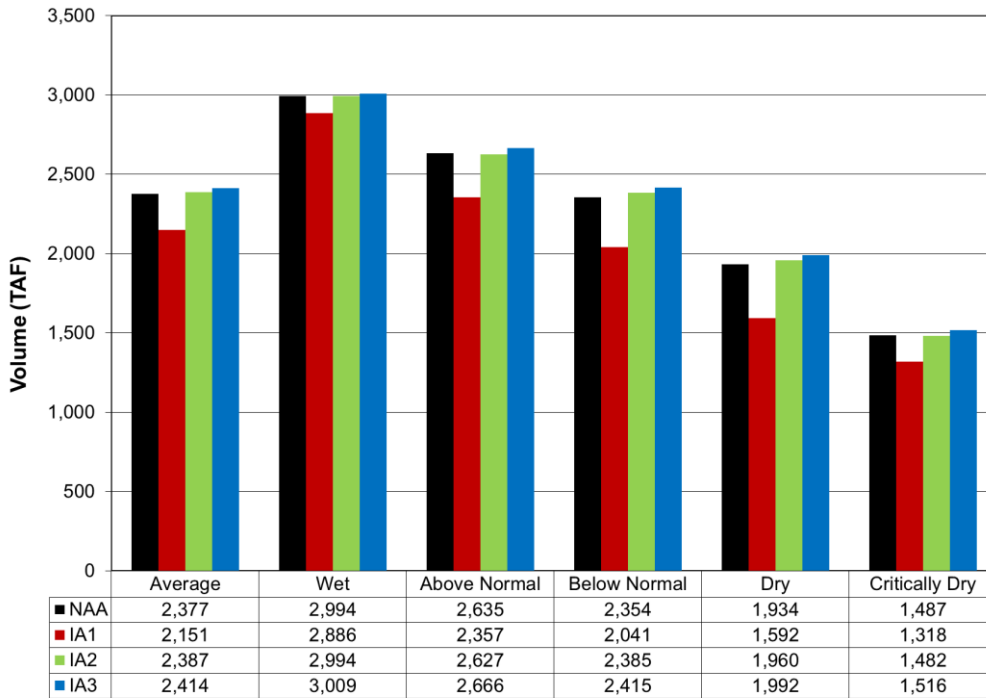


Figure I.3-14: Annual CVP SOD Deliveries by Water Year Type (Mar - Feb)

Figure I.3-14 shows the constraints on negative OMR flow in IA1 has a noticeable effect on SOD deliveries across all water year types. The other three alternatives show minimal differences in wet years, and IA2 has slightly more SOD deliveries in the other water year types. When initially run, SOD shortages in those three alternatives were very similar, but IA1 had significantly more and larger shortages.

In CalSim, a seasonal export estimate based on the Sac River Index is one component of the logic used to determine CVP SOD allocations. IA1 reduced export capability for a broad range of hydrologic conditions, so the export estimate curve in IA1 was adjusted to better represent export capacity and lead to determination of appropriate CVP allocations, which did not produce high levels of shortage.

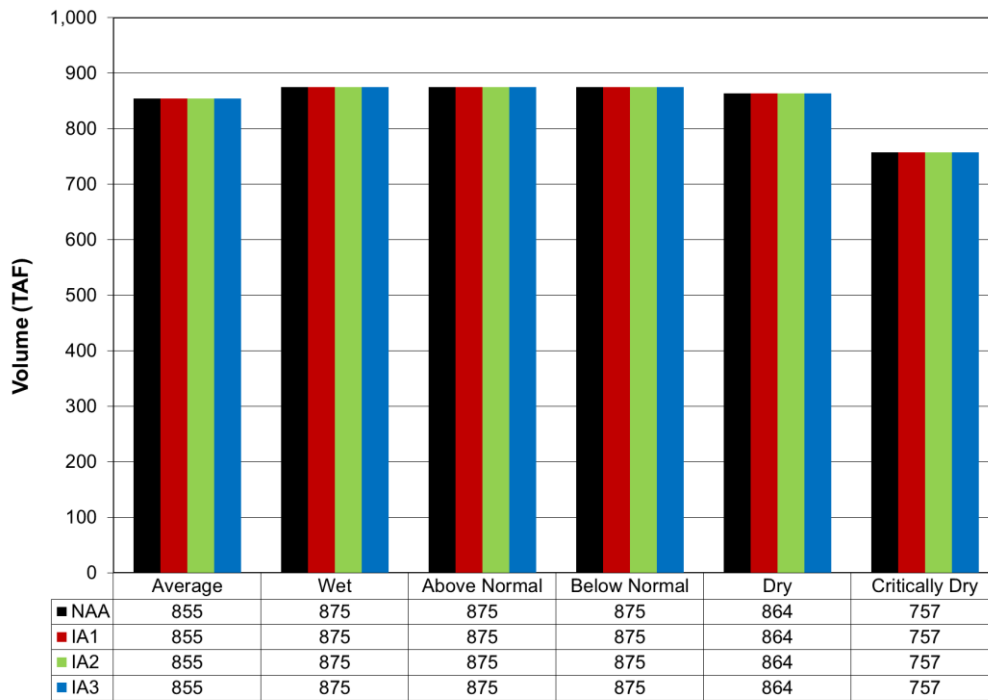


Figure I.3-15: Annual CVP SOD Exchange Contract Deliveries by Water Year Type (Mar - Feb)

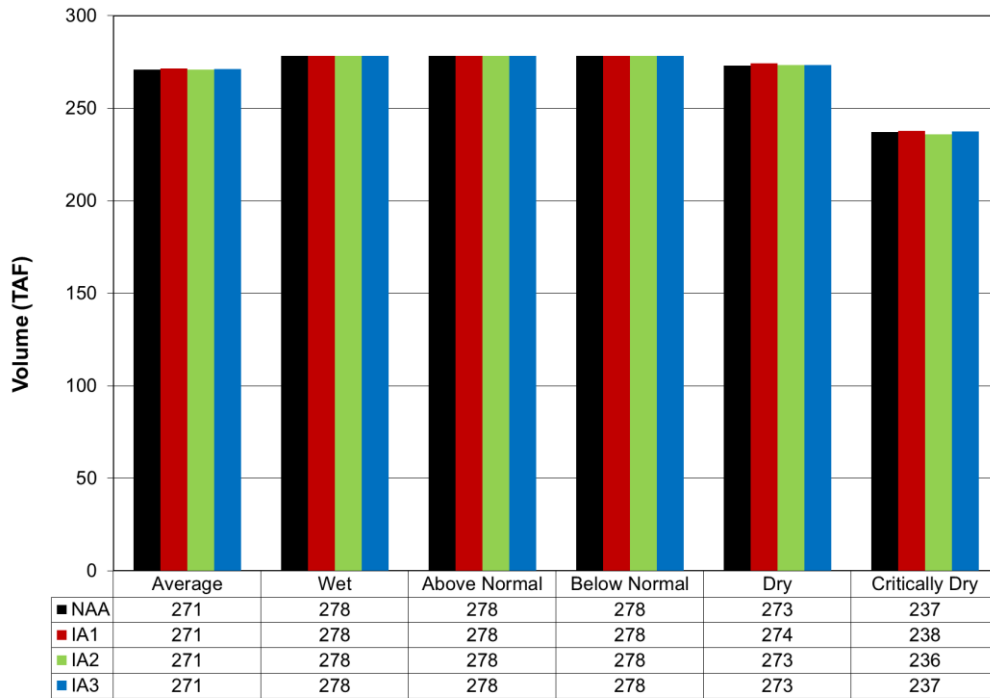


Figure I.3-16: Annual CVP SOD Refuge Deliveries by Water Year Type (Mar - Feb)

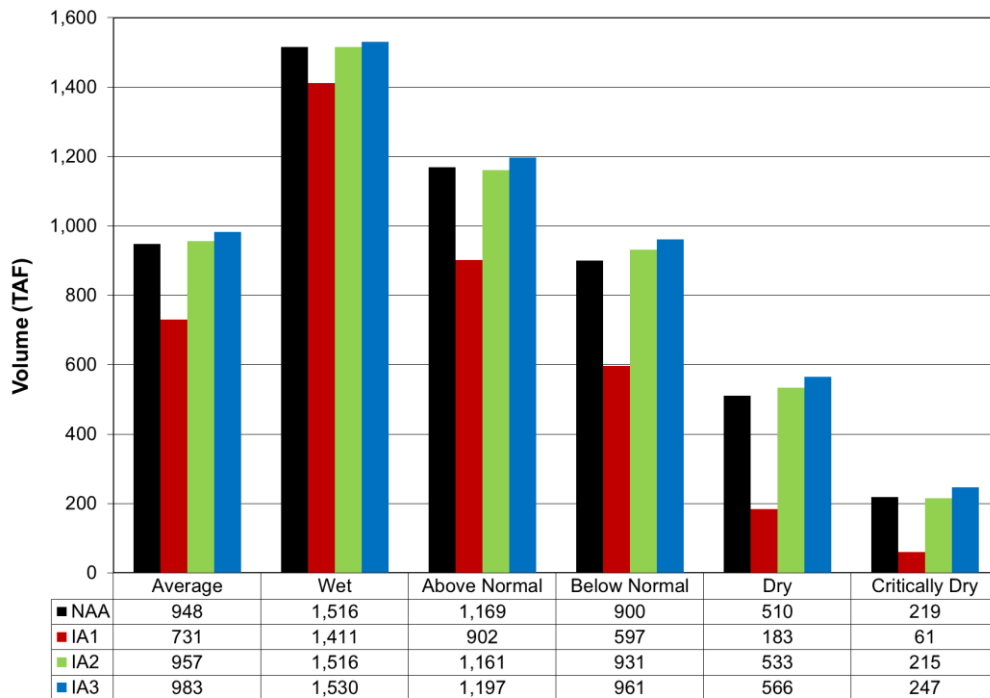


Figure I.3-17: Annual CVP SOD Project Ag Deliveries by Water Year Type (Mar - Feb)

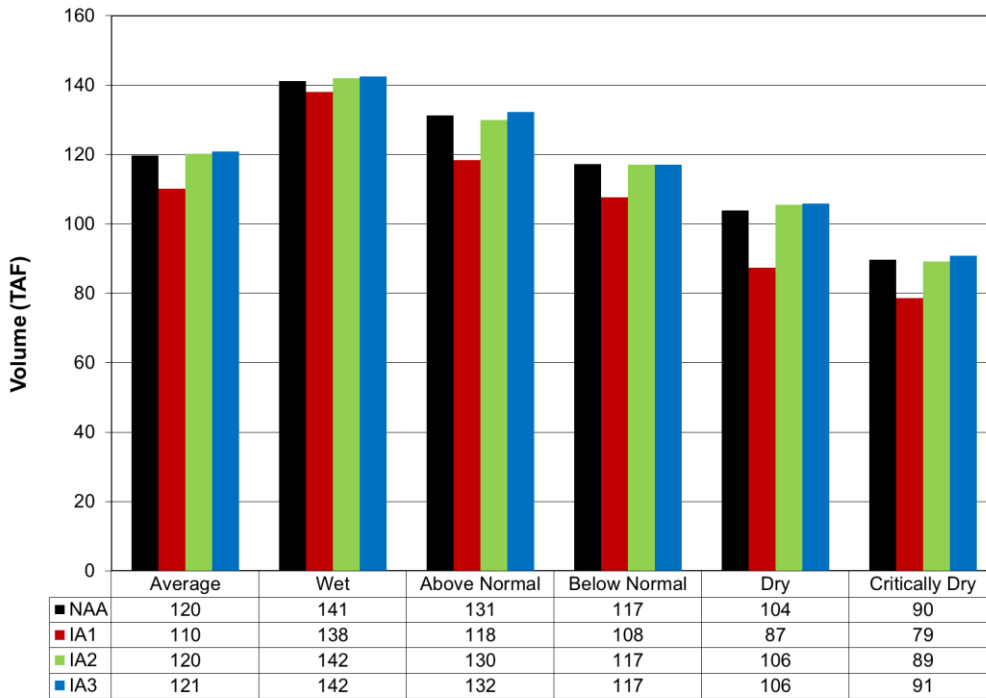


Figure I.3-18: Annual CVP SOD Project M&I Deliveries by Water Year Type (Mar - Feb)

Figures I.3-15 through I.3-18 split out SOD deliveries by contract type. Exchange and refuge deliveries are similar across all the alternatives, and only Project Agricultural (Ag) and Municipal and Industrial (M&I) deliveries show the effects of reduced exports in IA1.

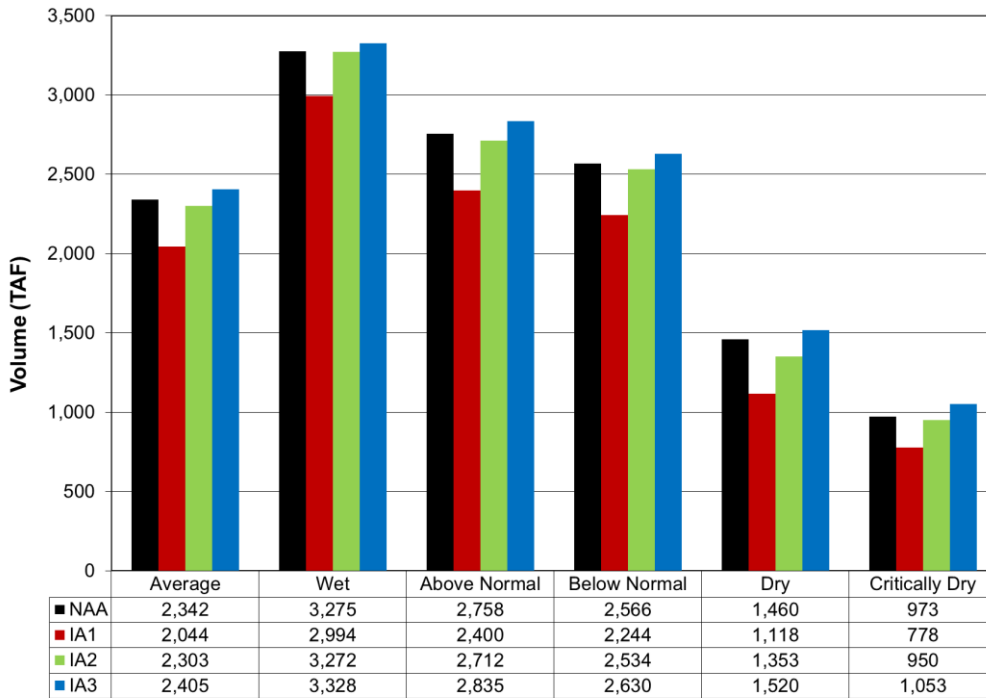


Figure I.3-19: Annual SWP Total Deliveries by Water Year Type (Jan - Dec)

SWP deliveries between alternatives shows the same trends as the CVP. IA1 has noticeably decreased deliveries, while IA3 has slightly increased deliveries due to the respective constraints on negative OMR flows.

#### I.3.2.4 Delta Outflow

The differences in constraints on negative OMR flow across the alternatives can affect how much water is going to exports instead of Delta outflow.

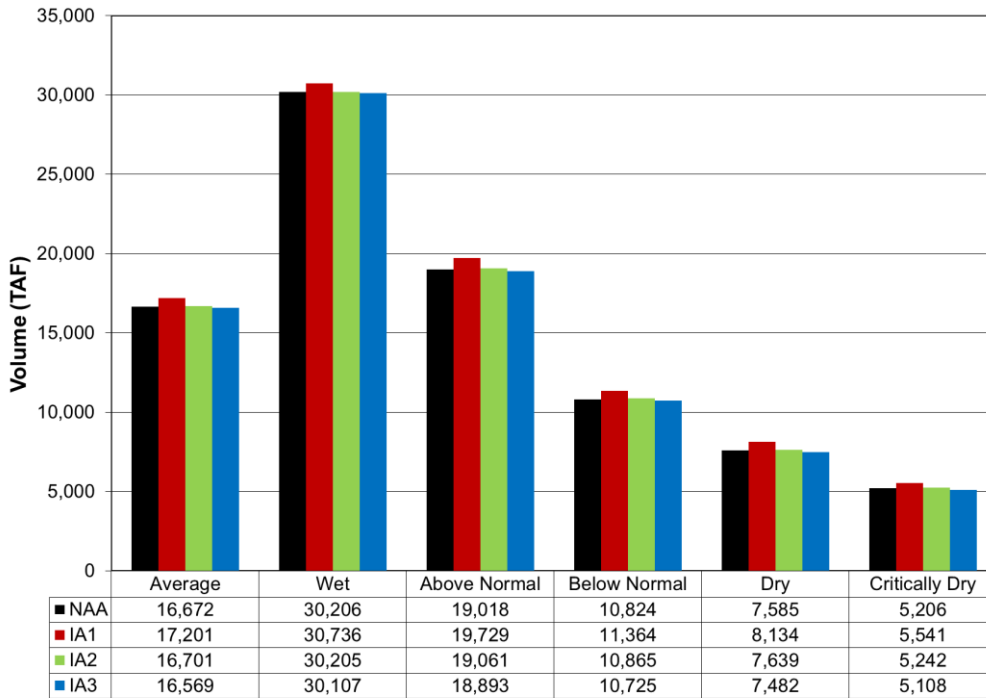


Figure I.3-20: Annual Delta Outflow by Water Year Type (Oct - Sep)

Figure I.3-20 shows that only IA1 and IA3 show any noticeable difference from the NAA. The more export-restrictive seasonal OMR limit in IA1 results in more of the excess water in the Delta going to Delta outflow rather than being exported. When compared to the NAA, this is about 400 to 600 TAF additional water going to Delta outflow annually, depending on the water year type. Inversely, IA3 has the least export-restrictive seasonal OMR limit, and when compared to the NAA, has up to 100 TAF less water going to Delta outflow annually.

### I.3.2.5 Reservoir Storage

When reservoirs make additional releases for exports, they only release as much as can be exported, which is limited by the pumping capacities and regulatory constraints on negative OMR flow. A more export-restrictive OMR requirement, such as the one applied in IA1, can reduce releases for exports and therefore increase reservoir storage. This effect can be cumulative across months and even years, but any cumulative gains are lost when the reservoir is forced to release due to flood control.

**Shasta:** Shasta can make releases for all regulatory requirements and deliveries along the Sacramento River and Delta, including for export.

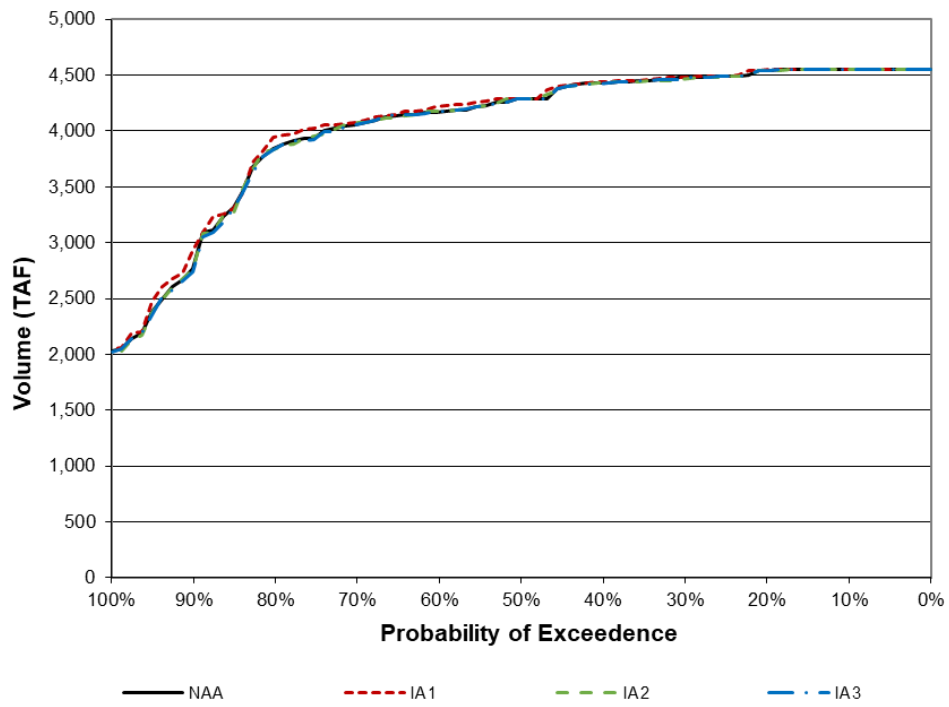


Figure I.3-21: Exceedance of End of April Shasta Storage

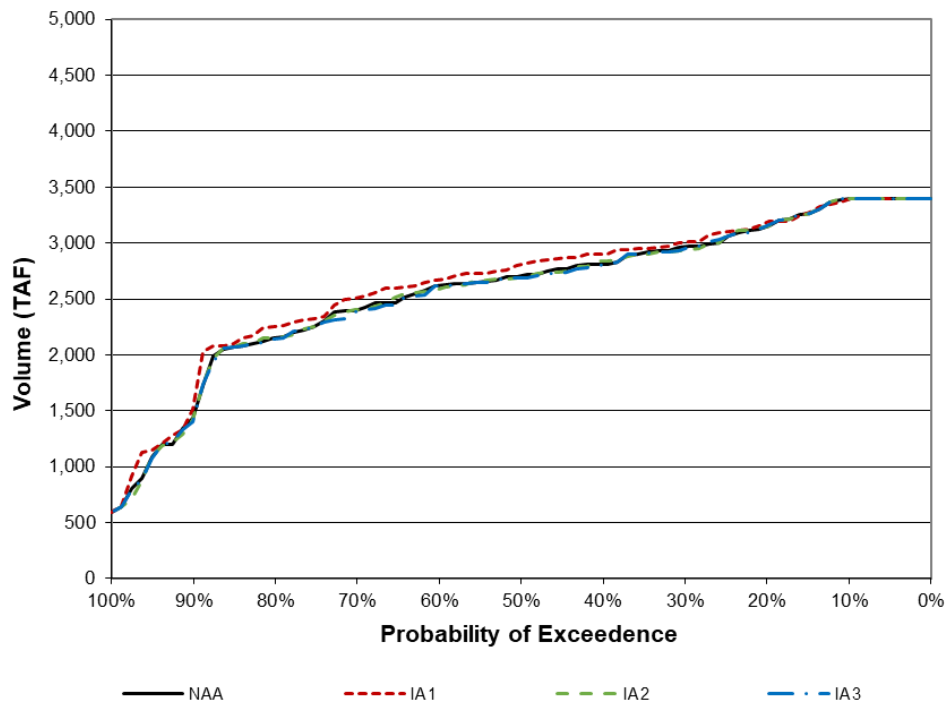


Figure I.3-22: Exceedance of End of September Shasta Storage



Figures I.3-21 and I.3-22 are exceedance plots of end of April and end of September Shasta storage, which represent Shasta fill and carryover, respectively. Except for IA1, all the alternatives are similar for both Shasta fill and carryover. IA1 has slightly increased fill about 50% of the time because spills are common during the months of November through April, which reset any gains made by reducing releases for exports. Additional gains in storage for IA1 can be seen in Shasta carryover; less water is released for exports due to lower allocations.

**Trinity:** Imports from the Trinity Basin are primarily used to supplement Shasta in providing water for exports. The volume of imports is controlled by the relative water supply in the respective basins. Higher water supply in the Trinity Basin and lower water supply in the Sacramento Basin results in higher imports.

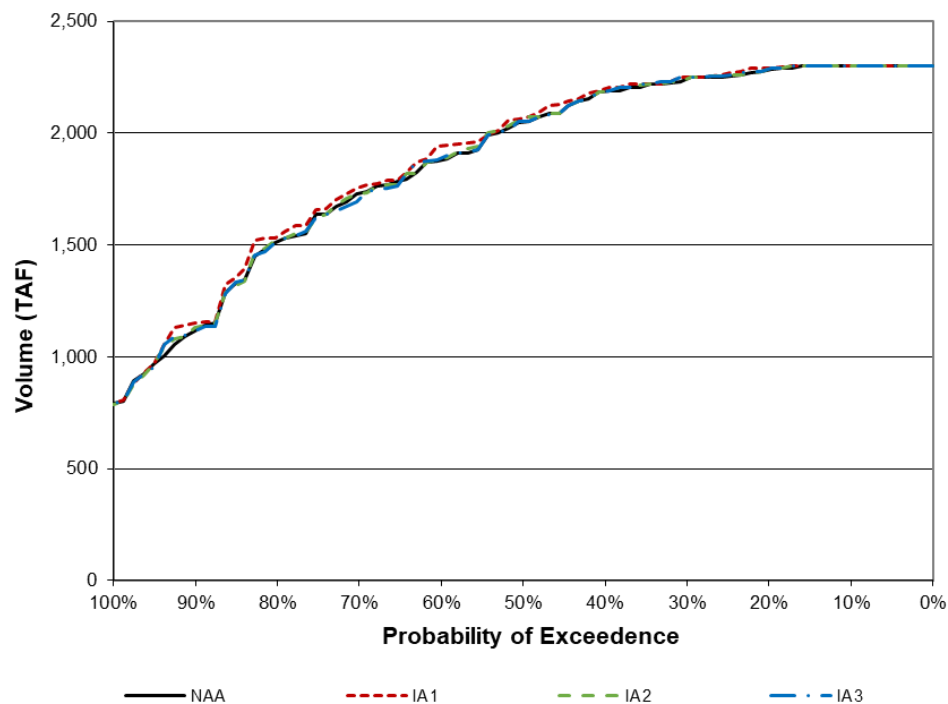


Figure I.3-23: Exceedance of End of April Trinity Storage

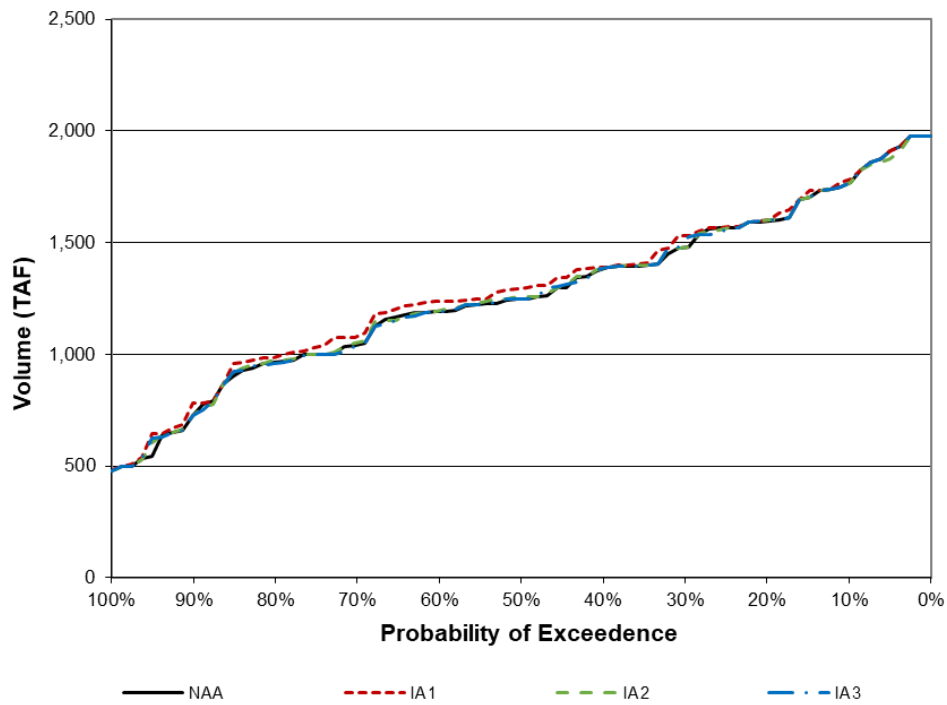


Figure I.3-24: Exceedance of End of September Trinity of Storage

Figures I.3-23 and I.3-24 are exceedance plots of end of April and end of September Trinity storage, which represent Trinity fill and carryover, respectively. Again, IA1 is the only alternative that shows noticeable differences in Trinity fill and carryover. It has increased fill and carryover in about 70% of years.

**Folsom:** Similar to Shasta and Trinity, Folsom storage trends slightly higher for IA1 but is little changed from the NAA distribution in IA2 and IA3.

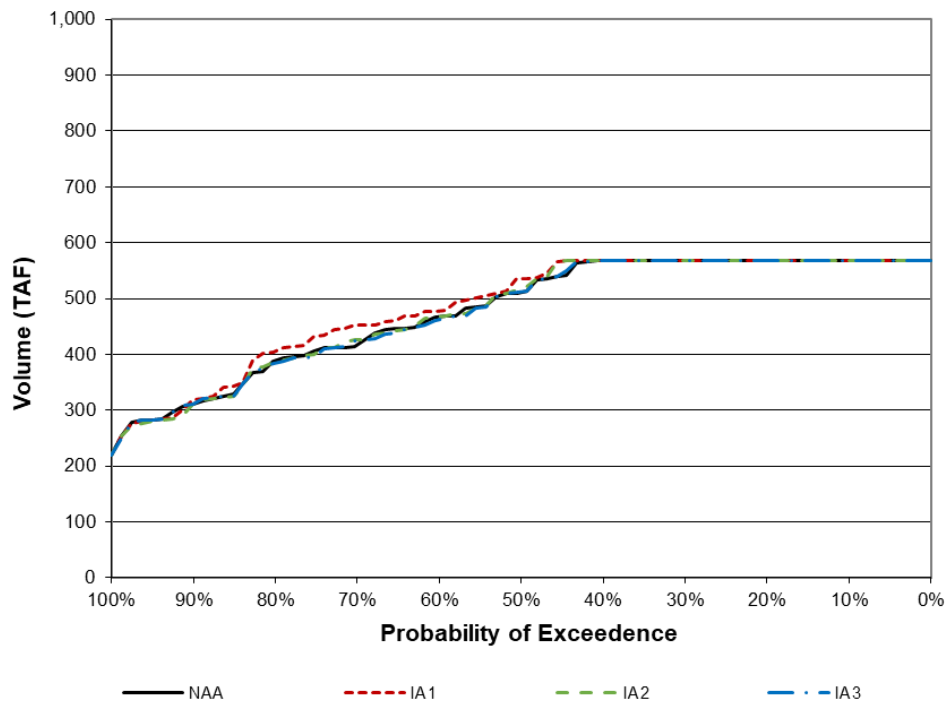


Figure I.3-25: Exceedance of End of December Folsom Storage

Figure I.3-25 shows an exceedance of end of December Folsom Storage. At the lower end, when the December Folsom target of 275 TAF, based on the American River Flow Management Standard, influences storage levels, all the alternatives are similar. However, IA1 again shows that between the December Flow target controlling releases and flood control, it has more storage than the other alternatives.

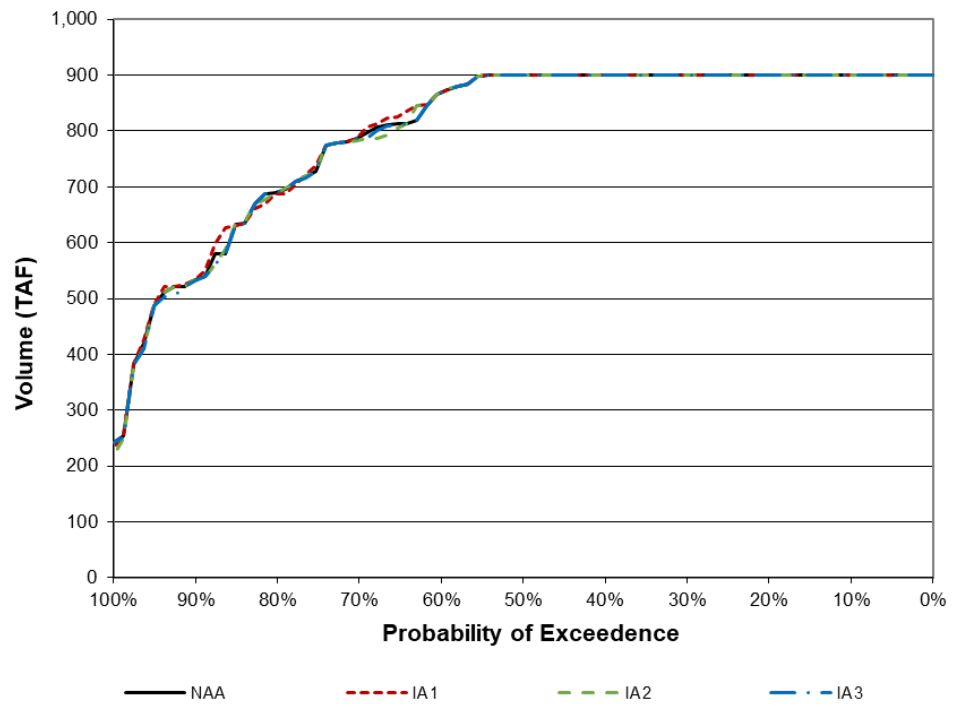


Figure I.3-26: Exceedance of End of April Folsom Storage

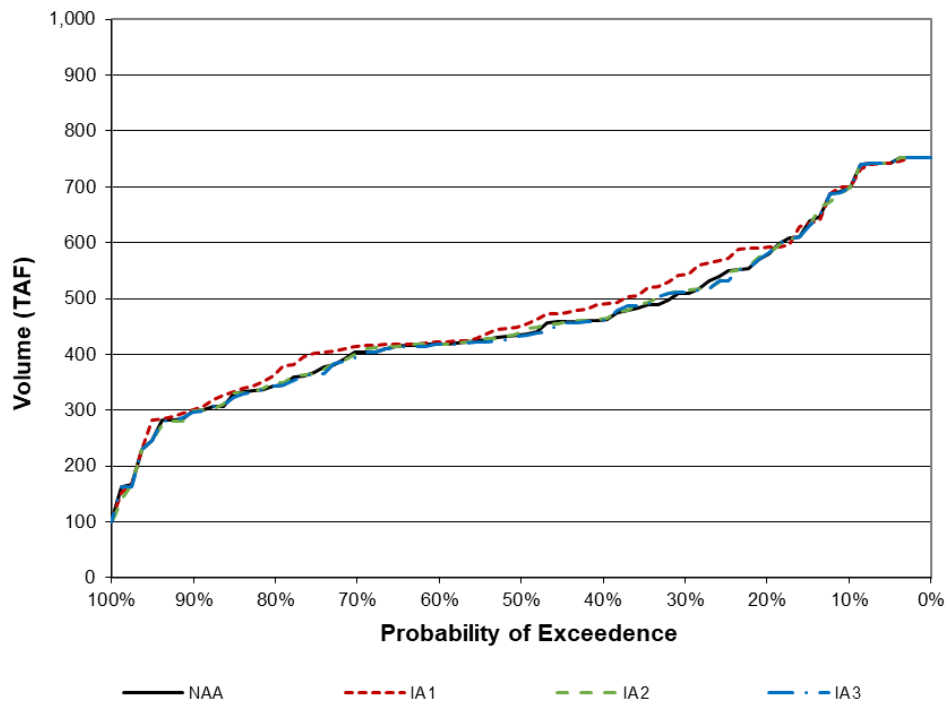


Figure I.3-27: Exceedance of End of September Folsom Storage

Figures I.3-26 and I.3-27 are exceedance plots of end of April and end of September Folsom storage, which represent Folsom fill and carryover, respectively. Since Folsom fully fills and therefore spills more often, IA1 does not have many opportunities to show increased fill due to less releases for exports. However, between the months of May and September when there are more releases for exports, IA1 shows the influence of the reduced SOD allocation on Folsom releases.

**Oroville:** Oroville serves State Water Project responsibilities.

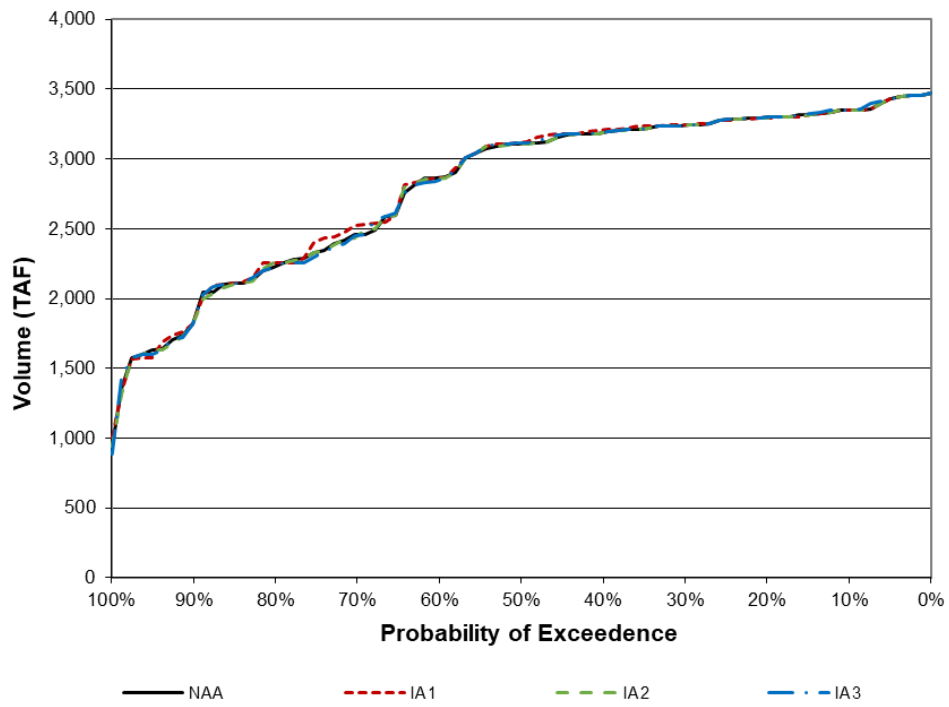


Figure I.3-28: Exceedance of End of April Oroville Storage

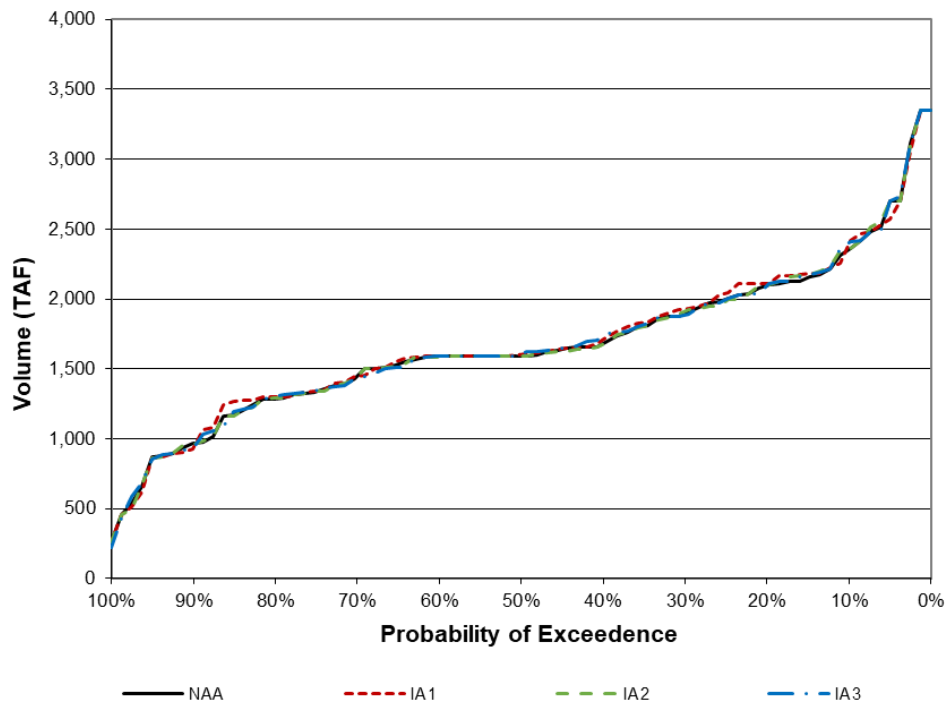


Figure I.3-29: Exceedance of End of September Oroville Storage

Figures I.3-28 and I.3-29 are exceedance plots of end of April and end of September Oroville storage, which represent Oroville fill and carryover, respectively. Oroville does have some limited additional fill and carryover in IA1 relative to the NAA, and the other alternatives see virtually no impact. The combination of SWP obligations under the 2020 Incidental Take Permit (ITP), controlling flow standards in the Feather River, reduced Table A delivery, and increased drawdown of SWP San Luis reserves collectively blunt the impact of IA1 on Oroville.

Page Intentionally Left Blank



# **I.4. Attachment 4: Delta Passage Model: A Simulation Model of Chinook Salmon Survival, Routing, and Travel Time in the Sacramento–San Joaquin Delta.**

## I.4.1 Model Overview

The (Delta Passage Model) DPM is based on migratory pathways and reach-specific mortality as Chinook Salmon smolts travel through a simplified network of reaches and junctions (Figure I.4-1). The biological functionality of the DPM is based on releases of acoustically tagged Chinook salmon performed between 2007 and 2017. The previous version of the DPM primarily relied on releases of large ( $> 140$  mm) acoustically tagged late fall–run Chinook salmon performed by Perry (2010) and coded wire tag releases of late fall–run Chinook salmon reported by Newman and Brandes (2010). There was considerable uncertainty about the transferability of those relationships to other runs that migrate at different times of year and at smaller sizes. The revised model is based on acoustically tagged winter run, spring run, fall run and late fall–run individuals ( $\geq 80$  mm) released in the upper reaches of the Sacramento River and within the Delta. These releases are primarily comprised of hatchery fish. However, wild spring and fall run are included in the dataset. These releases cover a wide range of environmental conditions, including extreme drought in 2014 and 2015 and high flow years. Uncertainty is explicitly modeled in the DPM by incorporating environmental stochasticity and estimation error whenever available.

The major model functions in the DPM are as follows.

1. Delta Entry Timing, which models the temporal distribution of smolts entering the Delta for each race of Chinook salmon.
2. Fish Behavior at Junctions, which models fish movement as they approach river junctions.
3. Migration Speed, which models reach-specific smolt migration speed and travel time.
4. Route-Specific Survival, which models route-specific survival response to non-flow factors.
5. Flow-Dependent Survival, which models reach-specific survival response to flow.
6. Export-Dependent Survival, which models survival response to water export levels in the interior Delta reach (see Table I.4-1 for reach description).

Functional relationships are described in detail in the Section *Model Functions*.

## I.4.2 Model Timestep

The DPM operates on a daily timestep using simulated daily average flows and south Delta exports as model inputs. The DPM does not attempt to represent sub-daily flows or diel salmon smolt behavior in response to the interaction of tides, flows, and specific channel features. The DPM is intended to represent the net outcome of migration and mortality occurring over one day, not three-dimensional movements occurring over minutes or hours (e.g., Blake and Horn 2003). It is acknowledged that finer scale modeling with a shorter timestep may match the biological processes governing fish movement better than a daily timestep (e.g., because of diel activity patterns; Plumb et al. 2015) and that sub-daily differences in flow proportions into junctions make daily estimates somewhat coarse (Cavallo et al. 2015).

### I.4.3 Spatial Framework

The DPM is composed of 10 reaches and three junctions (Figure I.4-1; Table I.4-1) selected to represent primary salmonid migration corridors for fish originating from the Sacramento River basin where high-quality data were available for fish and hydrodynamics. For simplification, Sutter Slough and Steamboat Slough are combined as the reach “SS,” and Georgiana Slough and the Delta Cross Channel (DCC) are a combined junction. Sacramento Chinook salmon that enter the DCC migrate through the Forks of the Mokelumne River, and fish entering Georgiana Slough migrate only through that route. The interior Delta reach can be entered from the Mokelumne River or Georgiana Slough route. The entire interior Delta region is treated as a single model reach. The three distributary junctions (channel splits) depicted in the DPM are (A) Sacramento River at Fremont Weir (head of Yolo Bypass), (B) Sacramento River at head of Sutter and Steamboat Sloughs, and (C) Sacramento River at the combined junction with Georgiana Slough and DCC (Figure I.4-1, Table I.4-1).

Table I.4-1. Description of Modeled Reaches and Junctions in the Delta Passage Model (Yolo and interior Delta reach lengths are not defined because multiple migration pathways are possible)

Reach/ Junction	Description	Approximate Reach Length (km)	Final Receiver name/location
Verona	Sacramento River between Fremont Weir and Freeport	57	Freeport
Sac_1	Sacramento River between Freeport and the combined junction of Steamboat and Sutter Slough	19	Sacramento River below Steamboat Slough
Sac_2	Sacramento River from Sutter/Steamboat Sloughs junction to junction with Delta Cross Channel/Georgiana Slough	11	Sacramento River below Georgiana Slough
Sac_3	Sacramento River from below Georgiana Slough to Rio Vista	16	Chippis Island
SS	Steamboat and Sutter Sloughs from their junction with the Sacramento River to Chippis Island	21	Chippis Island
Yolo Bypass	Fremont Weir to Highway 84 Ferry	NA	Highway 84 Ferry
Sac_4	Rio Vista to Chippis Island	30	Chippis Island
Geo/DCC	Georgiana Slough from the junction with the Sacramento River to the base of the Mokelumne River. Includes fish that migrate through the Mokelumne River via the Delta Cross Channel	25	Mokelumne Base
Interior Delta	Confluence of Mokelumne and San Joaquin Rivers to Chippis Island	NA	Chippis Island

<b>Reach/ Junction</b>	<b>Description</b>	<b>Approximate Reach Length (km)</b>	<b>Final Receiver name/location</b>
A	Junction of Yolo Bypass and Sacramento River	NA	NA
B	Combined junction of Sutter Slough and Steamboat Slough with the Sacramento River	NA	NA
C	Combined junction of the Delta Cross Channel and Georgiana Slough with the Sacramento River	NA	NA

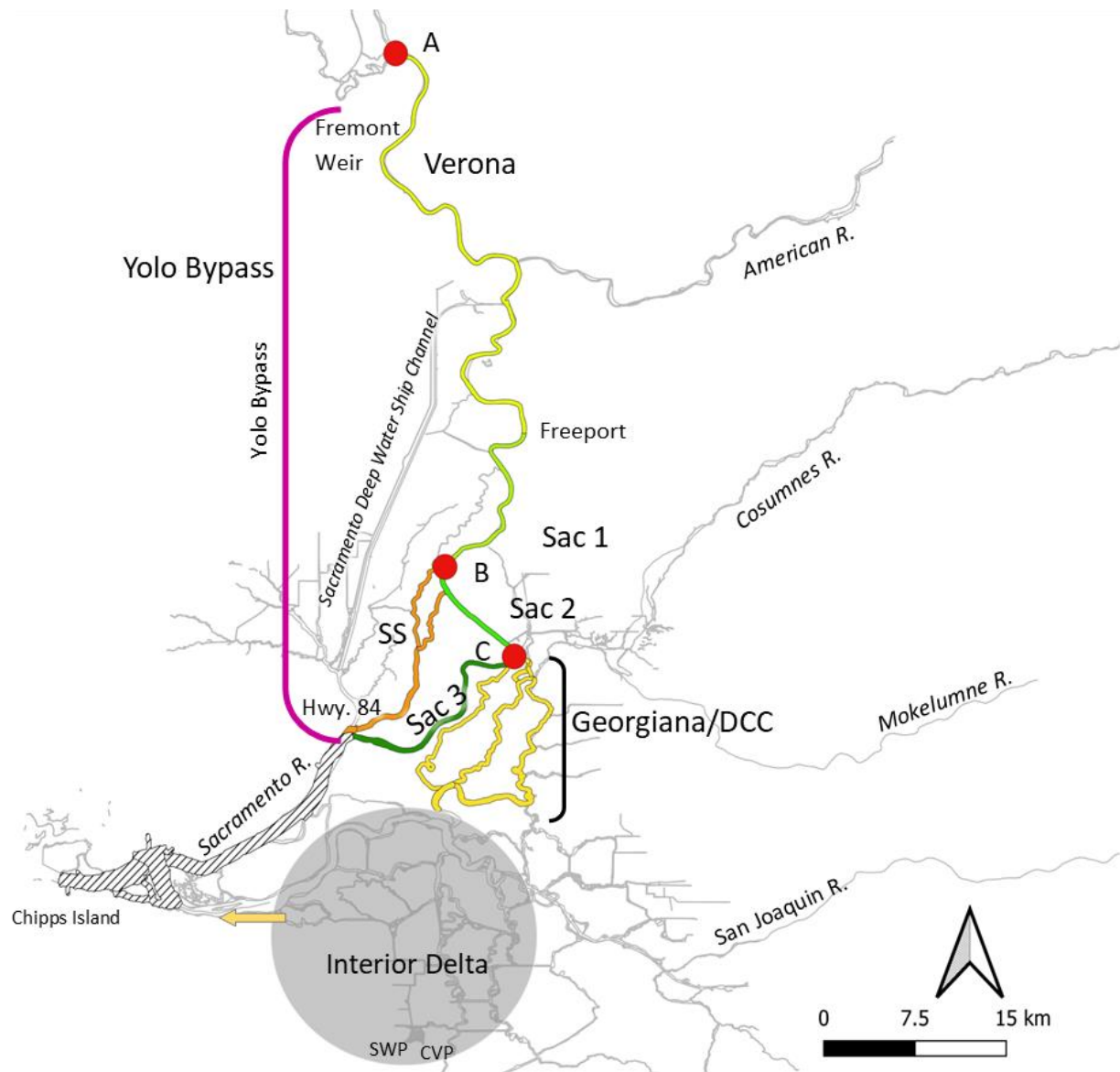


Figure I.4-1. Map of the Sacramento–San Joaquin River Delta Showing the Modeled Reaches and Junctions of the Delta Applied in the Delta Passage Model

#### I.4.4 Flow Input Data

Water movement through the Delta as input to the DPM is derived from daily (tidally averaged) flow output produced by the hydrology module of the Delta Simulation Model II (DSM2-HYDRO; <<http://baydeltaoffice.water.ca.gov/modeling/deltamodeling/>>) or from CalSim -II.

The nodes in the DSM2-HYDRO and CalSim II models that were used to provide flow for specific reaches in the DPM are shown in Table I.4-2.

Table I.4-2. Delta Passage Model Reaches and Associated Output Locations from DSM2-HYDRO and CalSim II Models

DPM Reach or Model Component	DSM2 Output Locations	CalSim Node
Sac1	rsac155	
Sac2	rsac128	
Sac3	rsac123	
Sac4	rsac101	
Yolo		d160a+d166aa
Verona		C160a
SS	slsbt011	
Geo/DCC	dcc+georg_sl	
South Delta Export Flow	Clifton Court Forebay + Delta Mendota Canal	
Sacramento River flow at Fremont Weir		C129a

#### I.4.4.1 Delta Entry Timing

Catch data for emigrating juvenile smolts for five Central Valley Chinook salmon runs were used to inform the daily proportion of juveniles entering the Delta for each run (Table I.4-3). Because the DPM models the survival of smolt-sized juvenile salmon, pre-smolts were removed from catch data before creating entry timing distributions. The lower 95th percentile of the range of salmon fork lengths visually identified as smolts by the USFWS in Sacramento trawls was used to determine the lower length cutoff for smolts. A lower fork length cutoff of 70 mm for smolts was applied, and all catch data of fish smaller than 70 mm were eliminated. To isolate wild production, all fish identified as having an adipose-fin clip (hatchery production) were eliminated, recognizing that most (75%) of the fall-run hatchery fish released upstream of Sacramento are not marked. Daily catch data for each brood year were divided by total annual catch to determine the daily proportion of smolts entering the DPM for each run (Figure I.4-2). Sampling was not conducted daily at most stations and catch was not expanded for fish caught but not measured. Finally, a generic probability density function was fit to the data using the package “sm” in R software (R Core Team 2012). The R fitting procedure estimated the best-fit probability distribution of the daily proportion of fish entering the DPM.

For the current analysis, the most recent data from the Sacramento Trawl survey was added to the previous data to determine if entry distributions had shifted since the original fitting. Only late fall–run Chinook Salmon exhibited substantial change from the original fit and the entry distribution for that race was updated.

Table I.4-3. Sampling Gear Used to Create Juvenile Delta Entry Timing Distributions for Each Central Valley Run of Chinook Salmon

Chinook Salmon Run	Gear	Agency	Brood Years
Sacramento River Winter Run	Trawls at Sacramento	USFWS	1995–2009
Sacramento River Spring Run	Trawls at Sacramento	USFWS	1995–2005
Sacramento River Fall Run	Trawls at Sacramento	USFWS	1995–2005
Sacramento River Late Fall Run	Trawls at Sacramento	USFWS	1995–2018

Agencies that conducted sampling are listed

USFWS = U.S. Fish and Wildlife Service; EBMUD = East Bay Municipal District; CDFW = California Department of Fish and Wildlife.

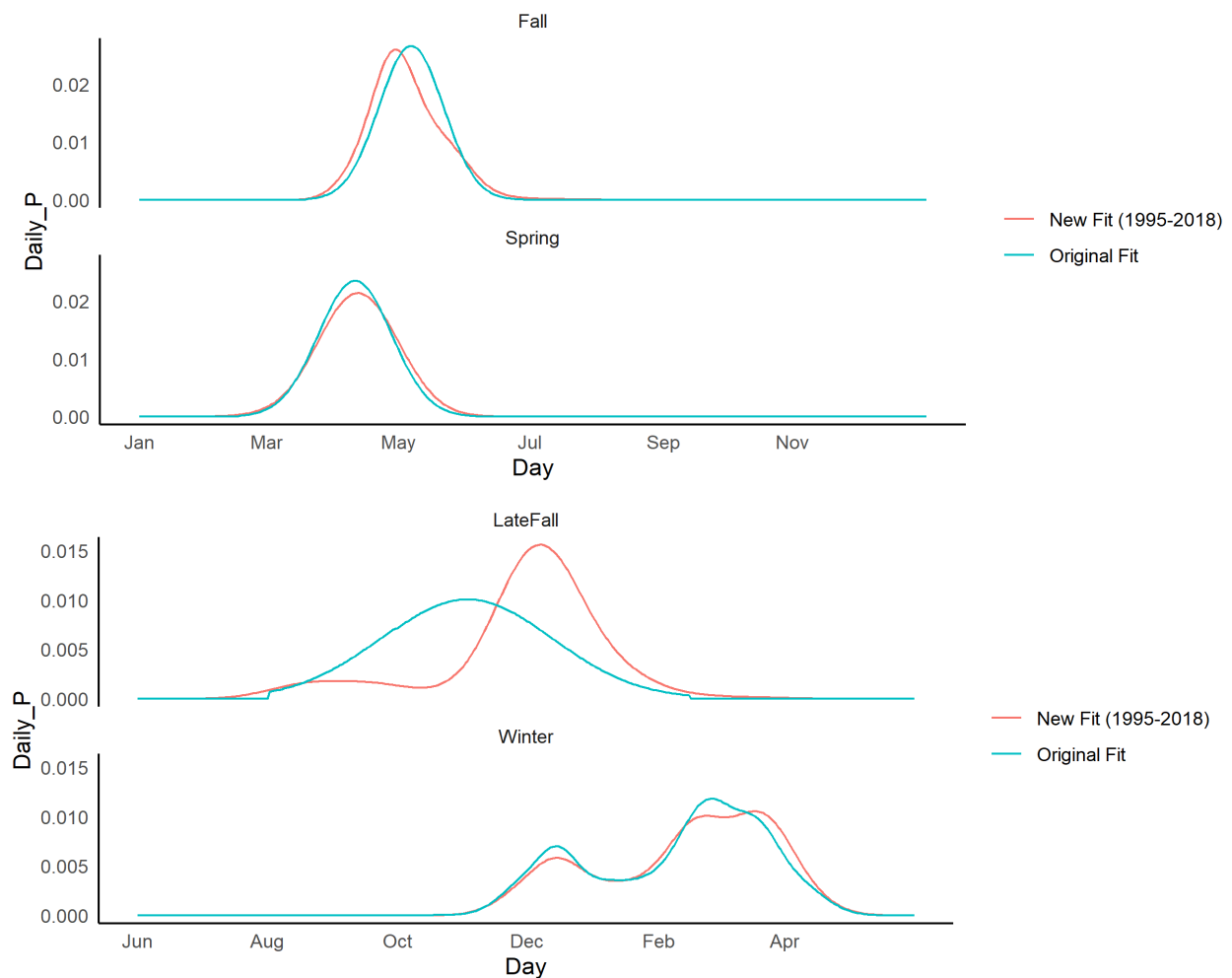


Figure I.4-2. Delta Entry Distributions for Chinook Salmon Smolts Applied in the Delta Passage Model for Sacramento River Winter-Run, Central Valley Spring-Run

(Sacramento River), Central Valley Fall-Run (Sacramento River), and Central Valley Late Fall-Run (Note the change in x axes between the upper and lower panel)

#### **I.4.4.2 Migration Speed**

The DPM assumes a net daily movement of smolts in the downstream direction. The rate of smolt movement in the DPM affects the timing of arrival at Delta junctions and reaches, which can affect route selection and survival as flow conditions or water project operations change.

Smolt movement in all reaches except Yolo Bypass and the interior Delta is a function of reach-specific length and migration speed, as observed from acoustic-tagging results. Reach-specific length (kilometers [km]) is divided by reach migration speed (km/day) the day smolts enter the reach to calculate the number of days smolts will take to travel through the reach.

For north Delta reaches Verona, Sac1, Sac2, SS, and Geo/DCC, mean migration speed through the reach is predicted as a function of flow. Many studies have found a positive relationship between juvenile Chinook salmon migration rate and flow in the Columbia River Basin (Raymond 1968; Berggren and Filardo 1993; Schreck et al. 1994), with Berggren and Filardo (1993) finding a logarithmic relationship for Snake River yearling Chinook salmon. Ordinary least squares regression was used to test for a logarithmic relationship between reach-specific migration speed (km/day) and average daily reach-specific flow (cubic meters per second [m<sup>3</sup>/sec]) for the first day smolts entered a particular reach for reaches where acoustic-tagging data was available (Sac1, Sac2, Sac3, Sac4, Geo/DCC, and SS):

$$Speed = \beta_0 \ln(flow) + \beta_1;$$

Where  $\beta_0$  is the slope parameter and  $\beta_1$  is the intercept.

Individual smolt reach-specific travel times were calculated from detection histories of releases of acoustically-tagged smolts conducted in December and January for three consecutive winters (2006/2007, 2007/2008, and 2008/2009) (Perry 2010). Reach-specific migration speed (km/day) for each smolt was calculated by dividing reach length by travel days. Flow data was queried from the DWR's California Data Exchange website (<<http://cdec.water.ca.gov/>>).

Migration speed was significantly related to flow for reaches Sac1 (df = 450, F = 164.36, P < 0.001), Sac2 (df = 292, F = 4.17, P = 0.042), and Geo/DCC (df = 84, F = 13.74, P < 0.001). Migration speed increased as flow increased for all three reaches (Table I.4-4, Figure I.4-3). Therefore, for reaches Sac1, Sac2, and Geo/DCC, the regression coefficients shown in Table I.4-4 are used to calculate the expected average migration rate given the input flow for the reach; and the associated standard error of the regressions is used to inform a normal probability distribution that is sampled from the day that smolts enter the reach to determine their migration speed throughout the reach. The minimum migration speed for each reach is set at the minimum reach-specific migration speed observed from the acoustic-tagging data. The flow-migration rate relationship that was used for Sac1 also was applied for the Verona reach.



Table I.4-4. Sample Size and Slope ( $\beta_0$ ) and Intercept ( $\beta_1$ ) Parameter Estimates with Associated Standard Error (in Parenthesis) for the Relationship between Migration Speed and Flow for Reaches Sac1, Sac2, and Geo/DCC

Reach	N	$\beta_0$	$\beta_1$
Sac1	452	21.34 (1.66)	-105.98 (9.31)
Sac2	294	3.25 (1.59)	-8.00 (8.46)
Geo/DCC	86	11.08 (2.99)	-33.52 (12.90)

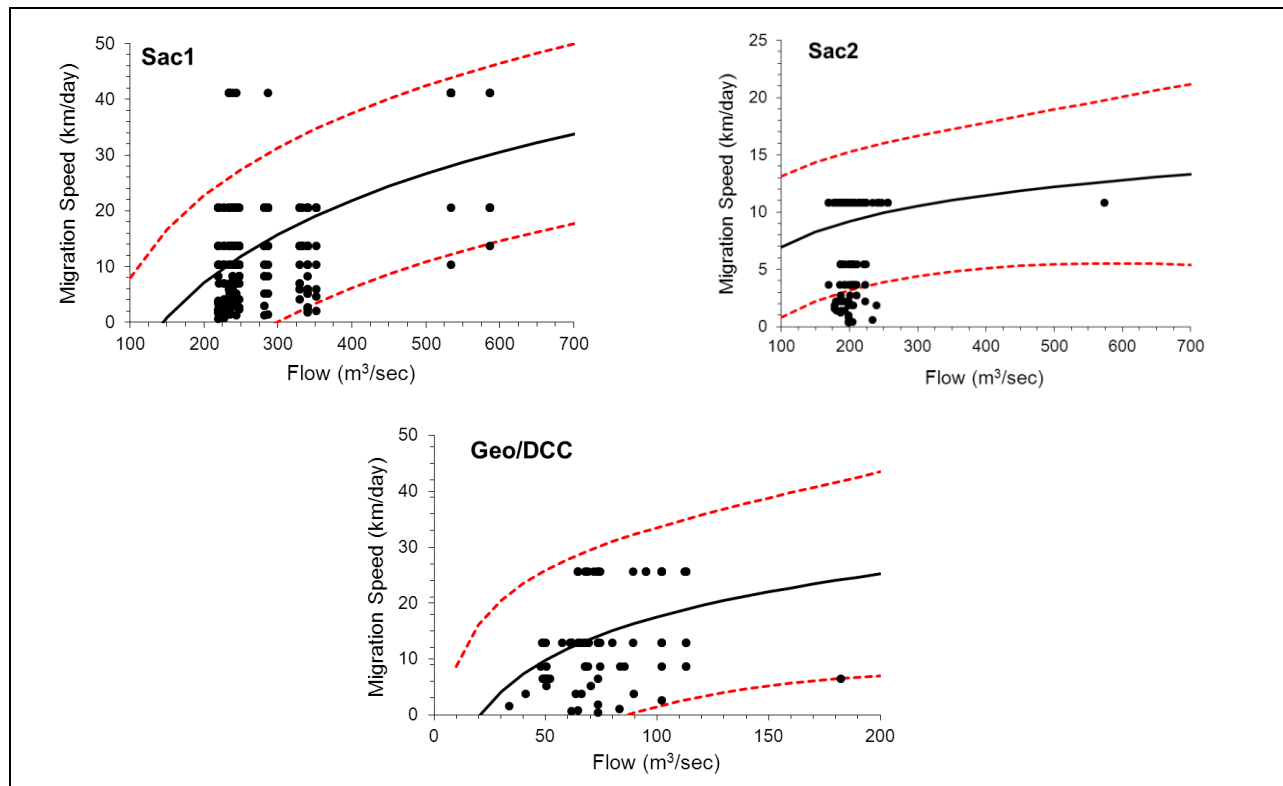


Figure I.4-3. Reach-Specific Migration Speed (km/day) as a Function of Flow (m³/sec) Applied in Reaches Sac1, Sac2, and Geo/DCC

No significant relationship between migration speed and flow was found for reaches Sac3 ( $df = 100$ ,  $F = 1.13$ ,  $P = 0.29$ ), Sac4 ( $df = 60$ ,  $F = 0.33$ ,  $P = 0.57$ ), and SS ( $df = 28$ ,  $F = 0.86$ ,  $P = 0.36$ ). Therefore, for these reaches the observed mean migration speed and associated standard deviation is used to inform a normal probability distribution that is sampled from the day smolts enter the reach to determine their migration speed throughout the reach. As applied for reaches Sac1, Sac2, and Geo/DCC, the minimum migration speed for reaches Sac3, Sac4, and SS is set at the minimum reach-specific migration speed observed from the acoustic-tagging data.

Yolo Bypass travel time data from Sommer et al. (2005) for coded wire-tagged, fry-sized (mean size = 57 mm fork length [FL]) Chinook salmon were used to inform travel time through the

Yolo Bypass in the DPM. Because the DPM models the migration and survival of smolt-sized juveniles, the range of the shortest travel times observed across all three years (1998–2000) by Sommer et al. (2005) was used to inform the bounds of a uniform distribution of travel times (range = 4–28 days), on the assumption that smolts would spend less time rearing and would travel faster than fry. On the day smolts enter the Yolo Bypass, their travel time through the reach is calculated by sampling from this uniform distribution of travel times.

The travel time of smolts migrating through the interior Delta in the DPM is informed by observed mean travel time (7.95 days) and associated standard deviation (6.74) from north Delta acoustic-tagging studies (Perry 2010). However, the timing of smolt passage through the interior Delta does not affect Delta survival because there are no Delta reaches located downstream of the interior Delta.

#### **I.4.4.3 Fish Behavior at Junctions (Channel Splits)**

Perry (2010) and Cavallo et al. (2015) found that acoustically-tagged smolts arriving at Delta junctions exhibited inconsistent movement patterns in relation to the flow being diverted. For Junction A (entry into the Yolo Bypass at Fremont Weir), the following relationships were used.

- Proportion of smolts entering Yolo Bypass = Fremont Weir spill/ (Fremont Weir spill + Sacramento River at Verona flows).

As noted above in *Flow Input Data*, the flow data informing Yolo Bypass entry were obtained by disaggregating CalSim estimates using historical daily patterns of variability because DSM2 does not provide daily flow data for these locations.

For Junction B (Sacramento River-Sutter/Steamboat Sloughs), both Perry (2010) and Cavallo et al. (2015) found that smolts consistently entered downstream distributaries in proportion to the flow being diverted. Therefore, smolts arriving at Junction B in the model move proportionally with flow according to the linear relationship found in Cavallo et al. (2015):

$$P_{SS} = -0.00203 + P_{flowSS} * 0.775344$$

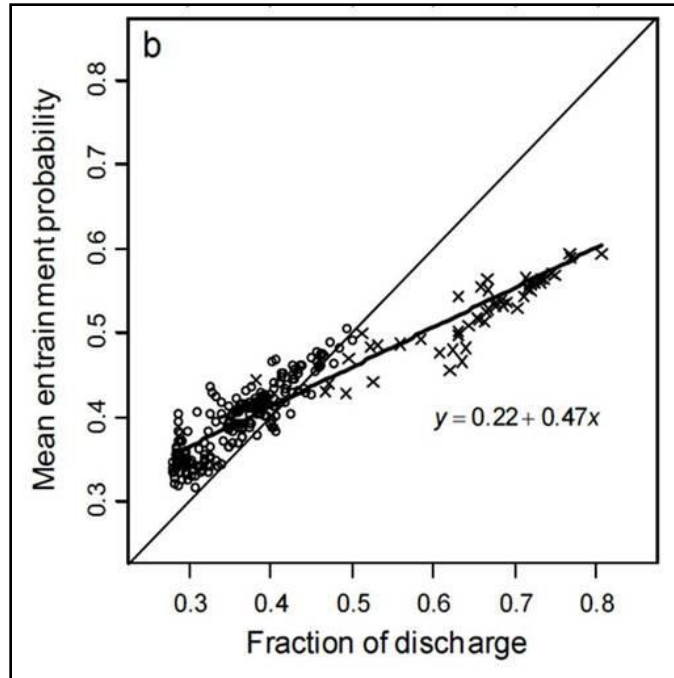
Where  $P_{SS}$  is the proportion of fish entering the SS reach, and  $P_{flowSS}$  is the proportion of flow entering Sutter/Steamboat Slough distributaries from the total flow in the mainstem Sacramento River.

For Junction C (Sacramento River–Georgiana Slough/DCC), Perry (2010) found a linear, nonproportional relationship between flow and fish movement. His relationship for Junction C was applied in the DPM:

$$y = 0.22 + 0.47x;$$

where y is the proportion of fish diverted into Geo/DCC and x is the proportion of flow diverted into Geo/DCC (Figure I.4-4).

In the DPM, this linear function is applied to predict the daily proportion of fish movement into Geo/DCC as a function of the proportion of flow into Geo/DCC.



Circles Depict DCC Gates Closed, Crosses Depict DCC Gates Open.

Figure I.4-4. Figure from Perry (2010) Depicting the Mean Entrainment Probability (Proportion of Fish Being Diverted into Reach Geo/DCC) as a Function of Fraction of Discharge (Proportion of Flow Entering Reach Geo/DCC)

#### **I.4.4.4 Reach-Specific Survival**

To update survival estimates in the DPM, we analyzed a dataset of detections from >2000 acoustically-tagged (JSATS) fish recorded in the DPM region of the Sacramento–San Joaquin Delta from 2013-2019. To estimate survival from such a large and heterogeneous dataset (receiver combinations, monitored reaches, and release locations differed from year to year), we used only detections from receivers at the endpoint of reaches in the DPM and constructed binary detection histories along DPM routes. Moving downstream from receiver to receiver along a route, we assumed that if a fish was not seen again in the route after a given receiver, the fish did not survive. The probability of being detected again downstream (assumed to be a direct proxy for survival) was then modeled as a function of an individual’s detection history and time-specific covariates associated with reach entry. From this analysis, four reaches were associated with a consistent relationship between flow and survival: Sac1, Sac2, Sac3, and Sac4; all other reaches had no consistent flow-survival relationship, and survival in those reaches of the DPM is drawn from a normal distribution derived from a reach-specific, intercept-only model of survival and standard deviation from the JSATS data.

##### **I.4.4.4.1 Flow-Dependent Survival**

Survival through a given reach is estimated and applied the first day smolts enter that reach. For reaches where analysis of the JSATS detections supported a consistent flow-survival relationship, flow on the day fish enter the reach is used to predict survival through the entire reach even if migration through the reach takes place over more than one day.

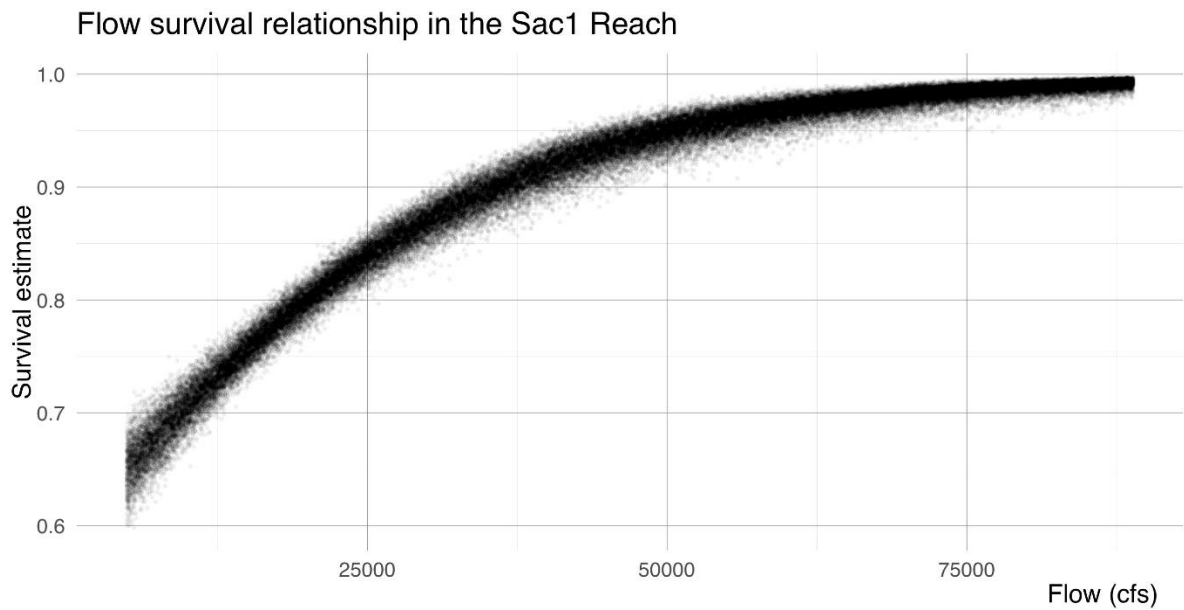


Figure I.4-5. Relationship between Sacramento River Discharge and Survival through the Sac 1 Reach Modeled with JSATS Releases of Multiple Runs of Chinook Salmon

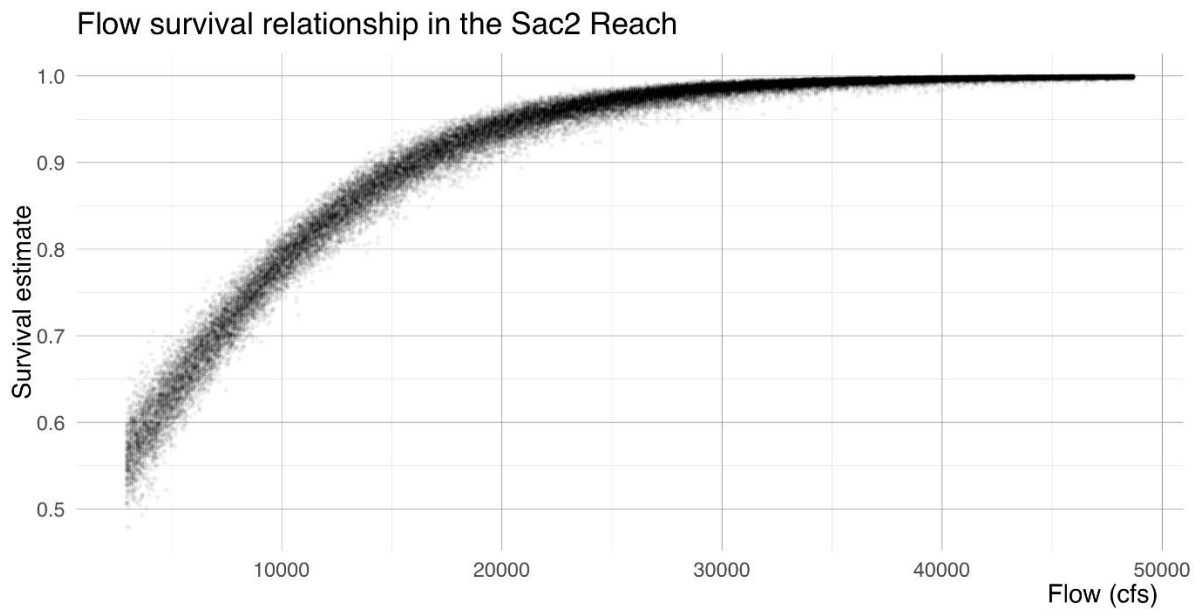


Figure I.4-6. Relationship between Sacramento River Discharge and Survival through the Sac 2 Reach Modeled with JSATS Releases of Multiple Runs of Chinook Salmon

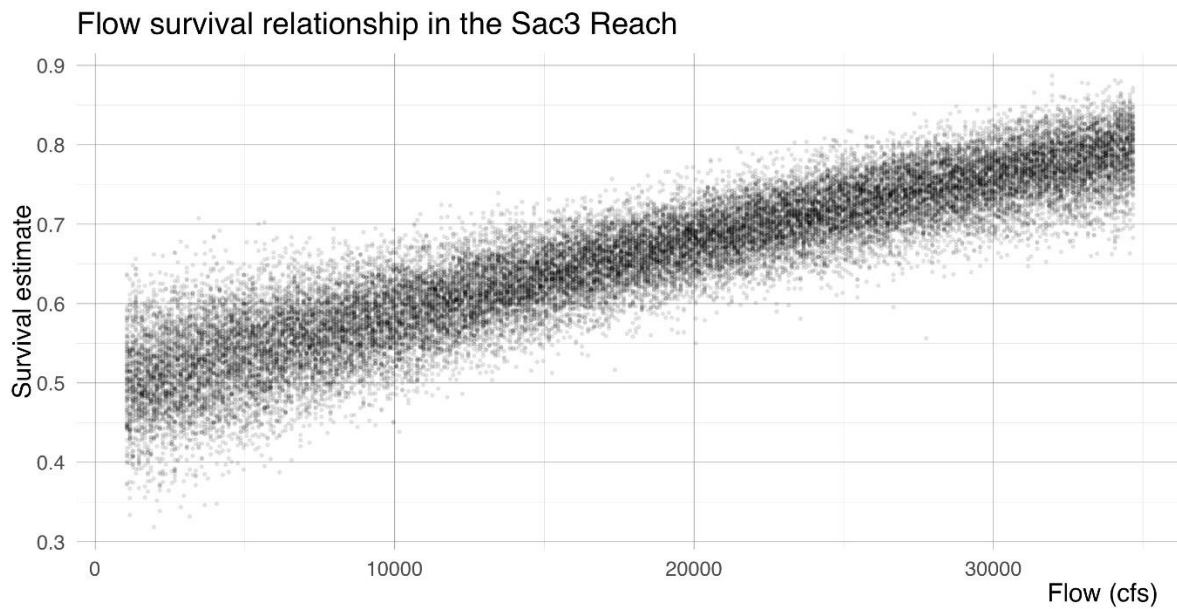


Figure I.4-7. Relationship between Sacramento River Discharge and Survival through the Sac 3 Reach Modeled with JSATS Releases of Multiple Runs of Chinook Salmon

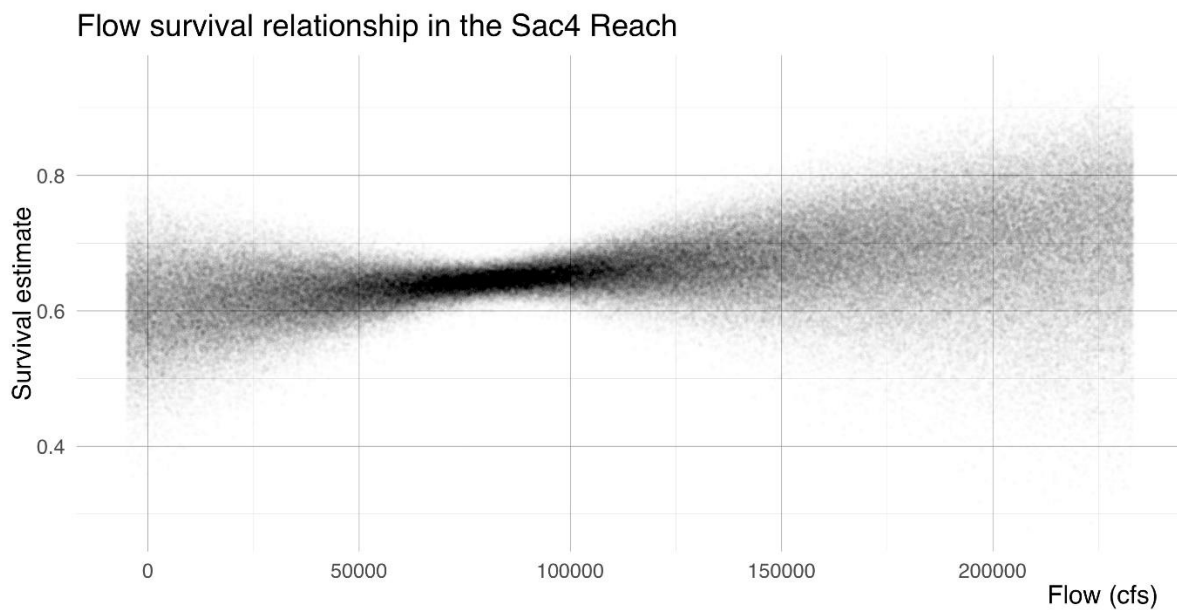


Figure I.4-8. Relationship between Sacramento River Discharge and Survival through the Sac 4 Reach Modeled with JSATS Releases of Multiple Runs of Chinook Salmon

#### I.4.4.5 Export-Dependent Survival

An export-survival relationship was tested for fish entering the interior Delta from the

Mokelumne River and Georgiana Slough. Hydrodynamic data for exports covering the period of JSATS detection data (2013 – 2019) was queried from Dayflow (<https://data.cnra.ca.gov/dataset/dayflow/resource/21c377fe-53b8-4bd6-9e1f-2025221be095>). A model that included exports and Freeport flow was also tested. Exports observed over the data period ranged from 1038 to 14650 cfs. For the interior Delta route, the export value (in cfs) on the day the fish enters the reach and the effect of exports from the JSATs model is used to predict survival through the entire reach, even if migration through the reach takes place over more than one day.

For the model that included exports only, the coefficient for the export effect was positive and well-supported, indicating higher survival probabilities with greater exports. In the model including both exports and flow, the export coefficient remained positive but was not well-supported with a mean effect that included zero in the distribution. This positive effect of exports may seem contradictory based on coded wire tag studies used in the previous model version that includes a weak, yet negative effect (Newman and Brandes 2010). The effect of exports on Sacramento River-origin Chinook salmon was a source of uncertainty identified in the previous version. Hydrodynamic analysis indicates that there is little effect of exports on hydrodynamics in the Sacramento River (Cavallo et al. 2015), and only fish entering the interior Delta, and the Old-Middle River corridor specifically, are likely to be exposed to the hydrodynamic effects of exports (Reclamation 2019). Previous studies of export effects relied on the relative survival of coded wire tagged salmon released into Georgiana Slough relative to the Sacramento River (Newman and Brandes 2010). Thus, export effects in the coded wire tag studies are not directly estimated for fish in the area of interest. In previous workshops and comments, it was suggested that modeling potential effects of exports on individually tagged fish would be a superior approach. The JSATS data analyzed here represents the best dataset available and covers a wide range of export conditions. Thus, the data strongly suggest the absence of a negative effect of exports on survival of Sacramento River-origin Chinook salmon that enter the interior Delta.

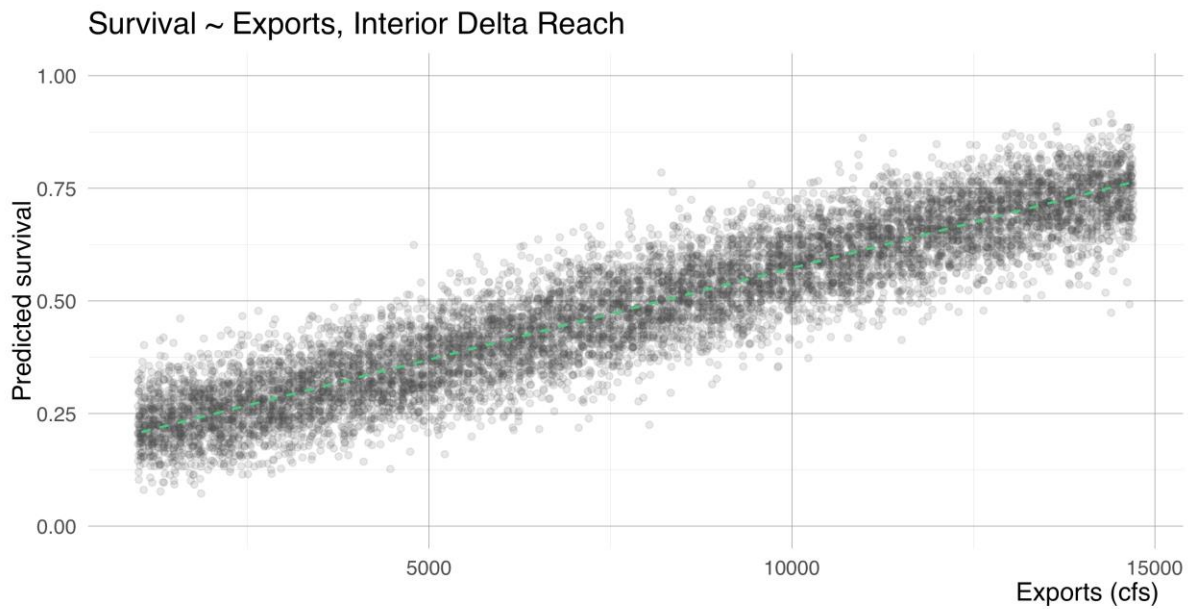


Figure I.4-9. Relationship between Exports and Survival of JSATS-Tagged Juvenile Chinook Salmon (The coefficient for the effect of exports was well-supported with a credible interval that did not include zero)

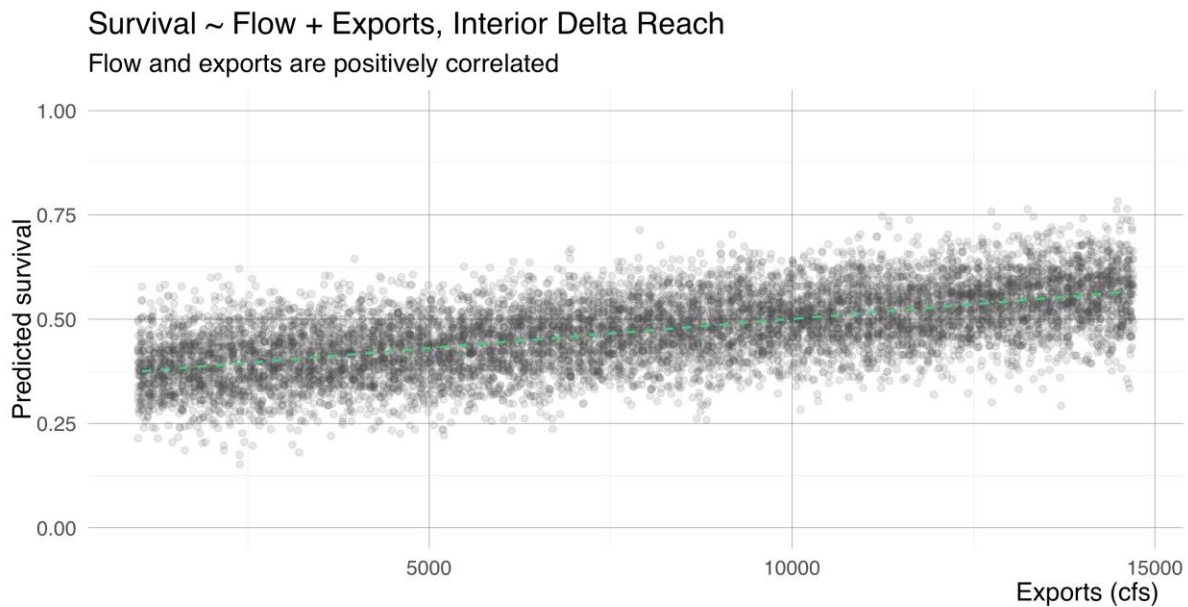


Figure I.4-10. Relationship between Exports and Survival of JSATS-Tagged Juvenile Chinook Salmon with Freeport Flow Was Held at the Mean Value (When flow is included in the model, the effect of exports on survival remains positive but is no longer well-supported)

## I.4.5 Results

Survival to Chipps Island for winter-run Chinook salmon and spring-run Chinook salmon varied by water year type, but not Old and Middle River management as described in the CalSim alternative descriptions (Attachment 3).

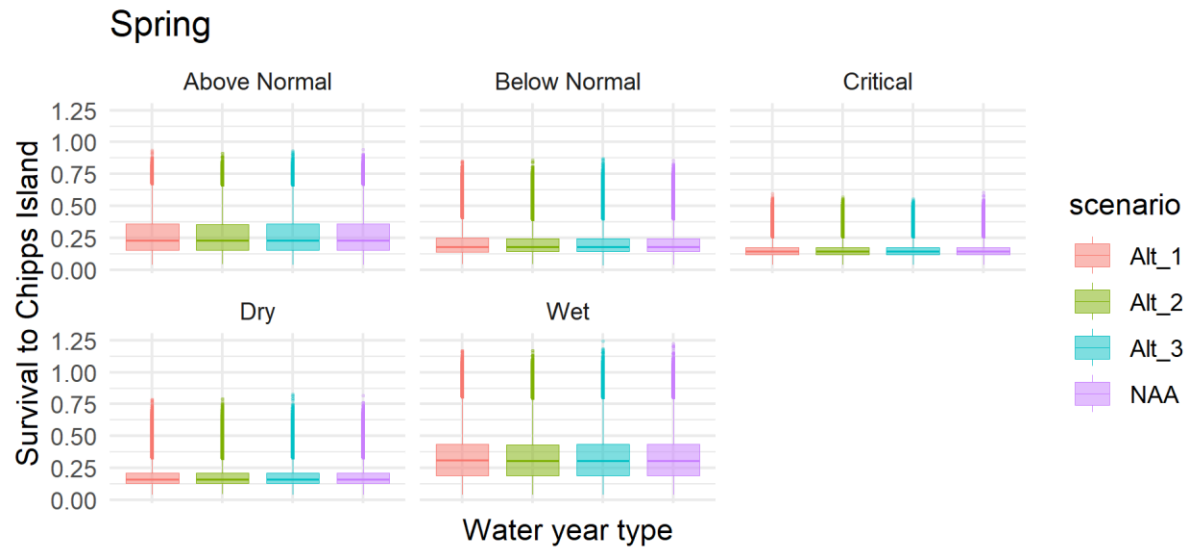


Figure I.4-11. Spring-Run Chinook Salmon Survival to Chipps Island under Initial Alternatives 1, 2, and 3, and the No Action Alternative (NAA)

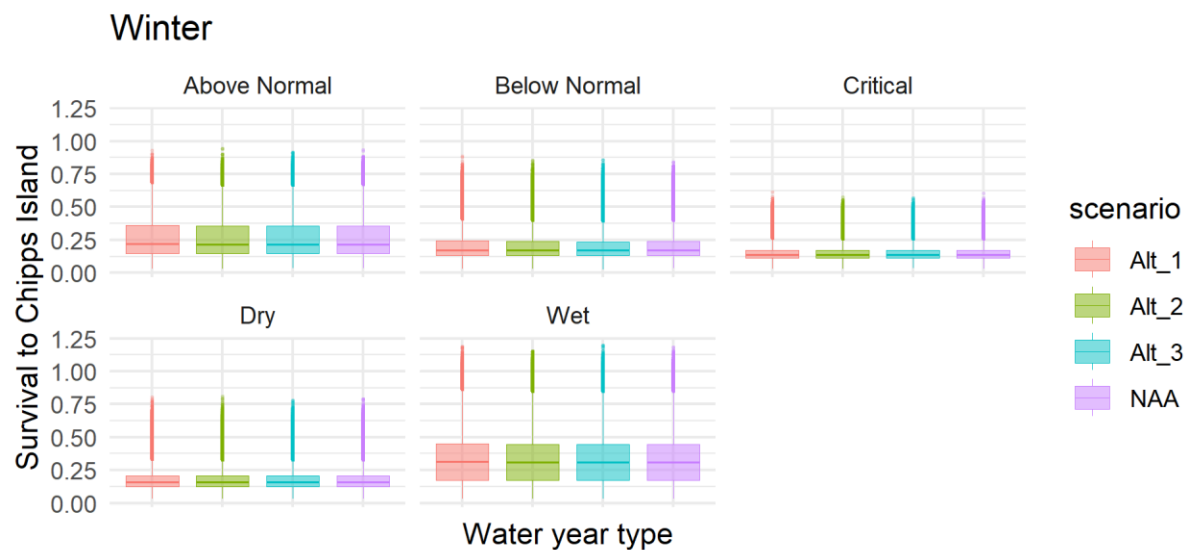


Figure I.4-12. Winter-Run Chinook Salmon Survival to Chipps Island under 3 CalSim Alternatives and NAA.



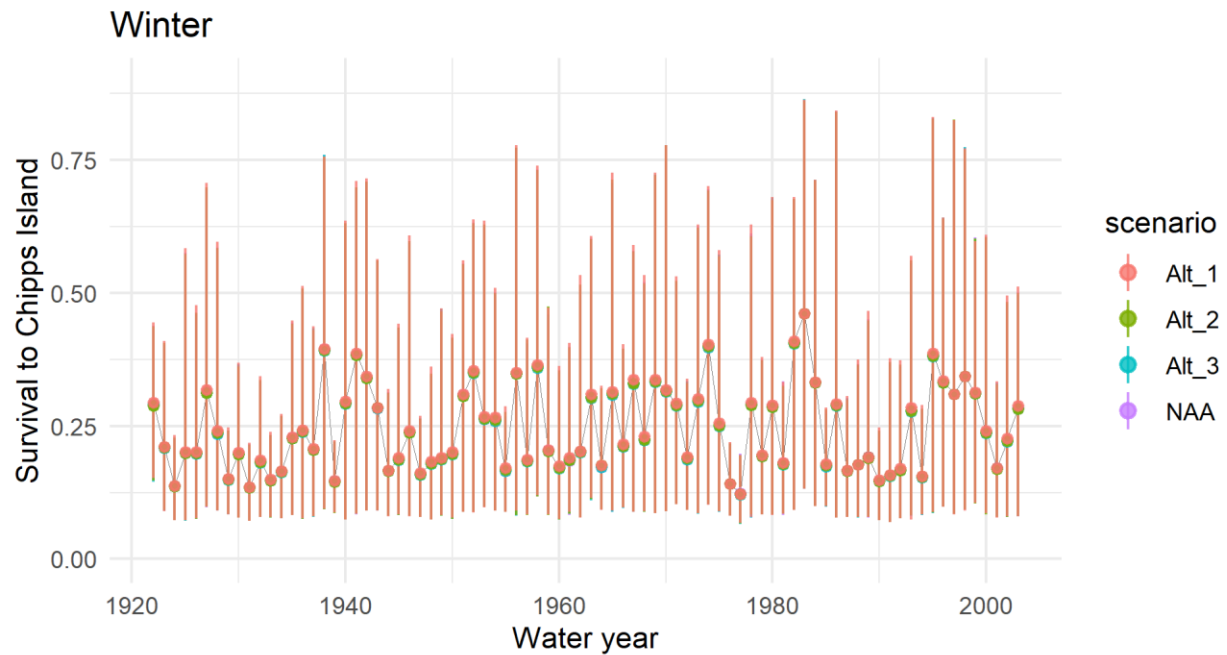


Figure I.4-13. Winter-Run Chinook Salmon Survival to Chipps Island under 3 CalSim Alternatives and NAA.

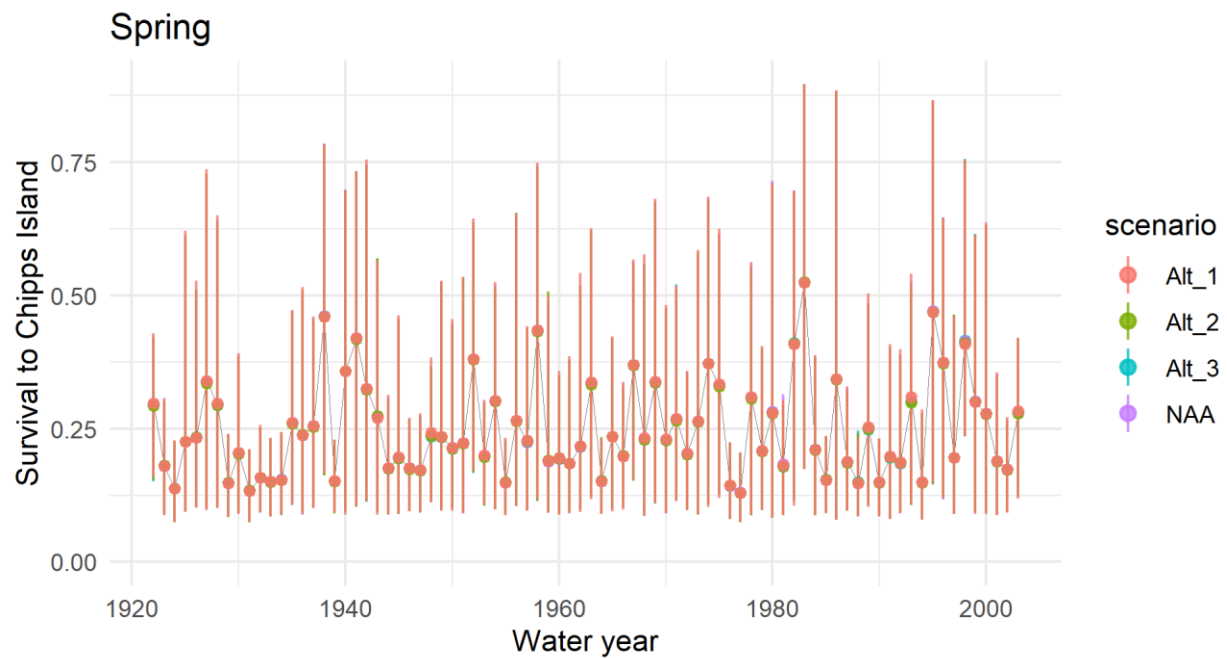


Figure I.4-14. Spring-Run Chinook Salmon Survival to Chipps Island under 3 CalSim Alternatives and NAA.

## I.4.6 Acknowledgements

This update would not have been possible without the generous cooperation of multiple researchers that allowed us to analyze their JSAT tag detections. Specifically, Arnold Ammann, Cyril Michel, Jeremy Notch, and Flora Cordoleani provided access to their transmitter and receiver data.

## I.4.7 Literature cited

- Berggren, T. J., and M. J. Filardo. 1993. An Analysis of Variables Influencing the Migration of Juvenile Salmonids in the Columbia River Basin. *North American Journal of Fisheries Management* 13(1):48–63.
- Blake, A., and M. J. Horn. 2003. *Acoustic Tracking of Juvenile Chinook Salmon Movement in the Vicinity of the Delta Cross Channel, Sacramento River, California – 2001 Study Results*. Prepared for U.S. Geological Survey and SRI International.
- Cavallo, B., P. Gaskill, J. Melgo, and S. C. Zeug. 2015. Predicting Juvenile Chinook Salmon Routing in Riverine and Tidal Channels of a Freshwater Estuary. *Environmental Biology of Fishes* 98(6):1571–1582.
- Newman, K. B., and P. L. Brandes. 2010. Hierarchical Modeling of Juvenile Chinook Salmon Survival as a Function of Sacramento–San Joaquin Delta Water Exports. *North American Journal of Fisheries Management* 30:157–169.
- Perry, R. W. 2010. *Survival and Migration Dynamics of Juvenile Chinook Salmon (Oncorhynchus tshawytscha) in the Sacramento–San Joaquin River Delta*. Ph.D. Dissertation. University of Washington, Seattle, WA.
- Plumb, J. M., N. S. Adams, R. W. Perry, C. M. Holbrook, J. G. Romine, A. R. Blake, and J. R. Burau. 2015. *Diel Activity Patterns of Juvenile Late Fall–Run Chinook Salmon with Implications for Operation of a Gated Water Diversion in the Sacramento–San Joaquin River Delta*. River Research and Applications. DOI: 10.1002/rra.2885.
- R Core Team. 2012. *R: A Language and Environment for Statistical Computing*. Vienna, Austria: R Foundation for Statistical Computing. Available: <http://www.R-project.org>. Accessed: DATE 6/1/2012
- Raymond, H. L. 1968. Migration Rates of Yearling Chinook Salmon in Relation to Flows and Impoundments in the Columbia and Snake Rivers. *Transactions of the American Fisheries Society* 97:356–359.
- Schreck, C. B., J. C. Snelling, R. E. Ewing, C. S. Bradford, L. E. Davis, and C. H. Slater. 1994. *Migratory Characteristics of Juvenile Spring Chinook Salmon in the Willamette River*. Completion Report. Bonneville Power Administration.

Sommer, T. R., W. C. Harrell, and M. L. Nobriga. 2005. Habitat Use and Stranding Risk of Juvenile Chinook Salmon on a Seasonal Floodplain. *North American Journal of Fisheries Management* 25:1493–1504.